PCT WORLD INTELLECTUAL PROPERTY ORGANIZATION
International Bureau

INTERNATIONAL APPLICATION PUBLISHED UNDER THE PATENT COOPERATION TREATY (PCT)

(51) **International Patent Classification** 7 : **C12N** | **A2**

(11) **International Publication Number:** **WO 00/22094**

(43) **International Publication Date:** 20 April 2000 (20.04.00)

(21) **International Application Number:** PCT/US99/23702

(22) **International Filing Date:** 8 October 1999 (08.10.99)

(30) **Priority Data:**
60/103,795 9 October 1998 (09.10.98) US

(71) **Applicants** *(for all designated States except US)*: KANSAS UNIVERSITY MEDICAL CENTER [US/US]; 3901 Rainbow Boulevard, Kansas City, KS 66160–7702 (US). UNIVERSITY OF SOUTH CAROLINA [US/US]; Office of Technology Transfer, Columbia, SC 29208 (US).

(72) **Inventors; and**
(75) **Inventors/Applicants** *(for US only)*: BAYNES, John [US/US]; University of South Carolina, Dept. of Chemistry and Biochemistry, Columbia, SC 29208 (US). ONORATO, Joelle [US/US]; University of South Carolina, Dept. of Chemistry and Biochemistry, Columbia, SC 29208 (US). THORPE, Suzanne [US/US]; University of South Carolina, Dept. of Chemistry and Biochemistry, Columbia, SC 29208 (US). KHALIFAH, Raja [US/US]; 5701 West 98th Terrace, Overland Park, KS 66207 (US). HUDSON, Billy [US/US]; 15414 West 94th Street, Lenexa, KS 66219 (US).

(74) **Agent:** HARPER, David, S.; McDonnell, Boehnen, Hulbert & Berghoff, Suite 3200, 300 South Wacker Drive, Chicago, IL 60606 (US).

(81) **Designated States:** AE, AL, AM, AT, AU, AZ, BA, BB, BG, BR, BY, CA, CH, CN, CU, CZ, DE, DK, EE, ES, FI, GB, GD, GE, GH, GM, HR, HU, ID, IL, IN, IS, JP, KE, KG, KP, KR, KZ, LC, LK, LR, LS, LT, LU, LV, MD, MG, MK, MN, MW, MX, NO, NZ, PL, PT, RO, RU, SD, SE, SG, SI, SK, SL, TJ, TM, TR, TT, UA, UG, US, UZ, VN, YU, ZA, ZW, ARIPO patent (GH, GM, KE, LS, MW, SD, SL, SZ, TZ, UG, ZW), Eurasian patent (AM, AZ, BY, KG, KZ, MD, RU, TJ, TM), European patent (AT, BE, CH, CY, DE, DK, ES, FI, FR, GB, GR, IE, IT, LU, MC, NL, PT, SE), OAPI patent (BF, BJ, CF, CG, CI, CM, GA, GN, GW, ML, MR, NE, SN, TD, TG).

Published
Without international search report and to be republished upon receipt of that report.

(54) **Title:** METHODS FOR INHIBITING OXIDATIVE MODIFICATION OF PROTEINS

(57) **Abstract**

The instant invention provides compositions and methods for modeling post–Amadori AGE formation and the identification and characterization of effective inhibitors of post–Amadori AGE formation, and such identified inhibitor compositions. The instant invention also teaches new methods to treat or prevent oxidative modification of proteins, including low density lipoproteins, to treat or prevent lipid peroxidation, and to treat or prevent atherosclerosis, comprising administering an amount effective of one of the compounds of the invention to treat or prevent the disorder.

FOR THE PURPOSES OF INFORMATION ONLY

Codes used to identify States party to the PCT on the front pages of pamphlets publishing international applications under the PCT.

AL	Albania	**ES**	Spain	**LS**	Lesotho	**SI**	Slovenia
AM	Armenia	**FI**	Finland	**LT**	Lithuania	**SK**	Slovakia
AT	Austria	**FR**	France	**LU**	Luxembourg	**SN**	Senegal
AU	Australia	**GA**	Gabon	**LV**	Latvia	**SZ**	Swaziland
AZ	Azerbaijan	**GB**	United Kingdom	**MC**	Monaco	**TD**	Chad
BA	Bosnia and Herzegovina	**GE**	Georgia	**MD**	Republic of Moldova	**TG**	Togo
BB	Barbados	**GH**	Ghana	**MG**	Madagascar	**TJ**	Tajikistan
BE	Belgium	**GN**	Guinea	**MK**	The former Yugoslav Republic of Macedonia	**TM**	Turkmenistan
BF	Burkina Faso	**GR**	Greece			**TR**	Turkey
BG	Bulgaria	**HU**	Hungary	**ML**	Mali	**TT**	Trinidad and Tobago
BJ	Benin	**IE**	Ireland	**MN**	Mongolia	**UA**	Ukraine
BR	Brazil	**IL**	Israel	**MR**	Mauritania	**UG**	Uganda
BY	Belarus	**IS**	Iceland	**MW**	Malawi	**US**	United States of America
CA	Canada	**IT**	Italy	**MX**	Mexico	**UZ**	Uzbekistan
CF	Central African Republic	**JP**	Japan	**NE**	Niger	**VN**	Viet Nam
CG	Congo	**KE**	Kenya	**NL**	Netherlands	**YU**	Yugoslavia
CH	Switzerland	**KG**	Kyrgyzstan	**NO**	Norway	**ZW**	Zimbabwe
CI	Côte d'Ivoire	**KP**	Democratic People's Republic of Korea	**NZ**	New Zealand		
CM	Cameroon			**PL**	Poland		
CN	China	**KR**	Republic of Korea	**PT**	Portugal		
CU	Cuba	**KZ**	Kazakstan	**RO**	Romania		
CZ	Czech Republic	**LC**	Saint Lucia	**RU**	Russian Federation		
DE	Germany	**LI**	Liechtenstein	**SD**	Sudan		
DK	Denmark	**LK**	Sri Lanka	**SE**	Sweden		
EE	Estonia	**LR**	Liberia	**SG**	Singapore		

Methods for Inhibiting Oxidative Modification of Proteins

Cross Reference

This application is a continuation-in-part of U.S. Patent Applications, serial numbers 60/103,795 filed October 9, 1998; 08/971,285 filed November 17, 1997 and 08/711,555, filed September 10, 1996, and claims priority to U.S. Provisional Application for Patent serial number 60/003,268, filed September 12, 1995, the contents of each of which are hereby incorporated by reference in their entirety.

Statement of Government Rights

Some of the work disclosed has been supported in part by NIH Grant DK 43507 and NIH grant DK-19971, therefore, the United States Government may have certain rights in the invention.

BACKGROUND OF THE INVENTION

The instant invention is in the field of Advanced Glycation End-products (AGEs), their formation, detection, identification, inhibition, and inhibitors thereof.

Protein Aging and Advanced Glycosylation End-products

Nonenzymatic glycation by glucose and other reducing sugars is an important post-translational modification of proteins that has been increasingly implicated in diverse pathologies. Irreversible nonenzymatic glycation and crosslinking through a slow, glucose-induced process may mediate many of the complications associated with diabetes. Chronic hyperglycemia associated with diabetes can cause chronic tissue damage which can lead to complications such as retinopathy, nephropathy, and atherosclerotic disease. (Cohen and Ziyadeh, 1996, *J. Amer. Soc. Nephrol.* **7**:183-190). It has been shown that the resulting chronic tissue damage associated with long-term diabetes mellitus arise in part from *in situ* immune complex formation by accumulated immunoglobulins and/or antigens bound to long-lived structural proteins that have undergone Advanced Glycosylation End-product (AGE) formation, via non-enzymatic glycosylation (Brownlee et al., 1983, *J. Exp. Med.* **158**:1739-1744). The primary

protein target is thought to be extra-cellular matrix associated collagen. Nonenzymatic glycation of proteins, lipids, and nucleic acids may play an important role in the natural processes of aging. Recently protein advanced glycation has been associated with ß-amyloid deposits and formation of neurofibrillary tangles in Alzheimer disease, and possibly other neurodegenerative diseases involving amyloidosis (Colaco and Harrington, 1994, *NeuroReport* **5**: 859-861). Glycated proteins have also been shown to be toxic, antigenic, and capable of triggering cellular injury responses after uptake by specific cellular receptors (see for example, Vlassara, Bucala & Striker, 1994, *Lab. Invest.* **70**:138-151; Vlassara et al., 1994, *PNAS(USA)* **91**:11704-11708; Daniels & Hauser, 1992, *Diabetes* **41**:1415-1421; Brownlee, 1994, *Diabetes* **43**:836-841; Cohen et al., 1994, *Kidney Int.* **45**:1673-1679; Brett et al., 1993, *Am. J. Path.* **143**:1699-1712; and Yan et al., 1994, *PNAS(USA)* **91**:7787-7791).

The appearance of brown pigments during the cooking of food is a universally recognized phenomenon, the chemistry of which was first described by Maillard in 1912, and which has subsequently led to research into the concept of protein aging. It is known that stored and heat-treated foods undergo nonenzymatic browning that is characterized by crosslinked proteins which decreases their bioavailibility. It was found that this Maillard reaction occurred *in vivo* as well, when it was found that a glucose was attached via an Amadori rearrangement to the amino-terminal of the α-chain of hemoglobin.

The instant disclosure teaches previously unknown, and unpredicted mechanism of formation of post-Amadori advanced glycation end products (Maillard products; AGEs) and methods for identifying and characterizing effective inhibitors of post-Amadori AGE formation. The instant disclosure demonstrates the unique isolation and kinetic characterization of a reactive protein intermediate competent in forming post-Amadori AGEs, and for the first time teaching methods which allow for the specific elucidation and rapid quantitative kinetic study of "late" stages of the protein glycation reaction.

In contrast to such "late" AGE formation, the "early" steps of the glycation reaction have been relatively well characterized and identified for several proteins (Harding, 1985, *Adv. Protein Chem.* **37**:248-334; Monnier & Baynes eds., 1989, *The Maillard Reaction in Aging, Diabetes, and Nutrition* (Alan R. Liss, New York); Finot

et al., 1990, eds. *The Maillard Reaction in Food Processing, Human Nutrition and Physiology* (Birkhauser Verlag, Basel)). Glycation reactions are known to be initiated by reversible Schiff-base (aldimine or ketimine) addition reactions with lysine side-chain ε-amino and terminal α-amino groups, followed by essentially irreversible Amadori rearrangements to yield ketoamine products e.g. 1-amino-1-deoxy-ketoses from the reaction of aldoses (Baynes et al., 1989, in The Maillard Reaction in Aging, Diabetes, and Nutrition, ed. Monnier and Baynes, (Alan R. Liss, New York, pp 43-67). Typically, sugars initially react in their open-chain (not the predominant pyranose and furanose structures) aldehydo or keto forms with lysine side chain ε-amino and terminal α-amino groups through reversible Schiff base condensation (Scheme I). The resulting aldimine or ketimine products then undergo Amadori rearrangements to give ketoamine Amadori products, i.e. 1-amino-1-deoxy-ketoses from the reaction of aldoses (Means & Chang, 1982, *Diabetes* **31, Suppl. 3**:1-4; Harding, 1985, *Adv. Protein Chem.* **37**:248-334). These Amadori products then undergo, over a period of weeks and months, slow and irreversible Maillard "browning" reactions, forming fluorescent and other products via rearrangement, dehydration, oxidative fragmentation, and cross-linking reactions. These post-Amadori reactions, (slow Maillard "browning" reactions), lead to poorly characterized Advanced Glycation End-products (AGEs).

As with Amadori and other glycation intermediaries, free glucose itself can undergo oxidative reactions that lead to the production of peroxide and highly reactive fragments like the dicarbonyls glyoxal and glycoaldehyde. Thus the elucidation of the mechanism of formation of a variety of AGEs has been extremely complex since most *in vitro* studies have been carried out at extremely high sugar concentrations.

In contrast to the relatively well characterized formation of these "early" products, there has been a clear lack of understanding of the mechanisms of forming the "late" Maillard products produced in post-Amadori reactions, because of their heterogeneity, long reaction times, and complexity. The lack of detailed information about the chemistry of the "late" Maillard reaction stimulated research to identify fluorescent AGE chromophores derived from the reaction of glucose with amino groups of polypeptides. One such chromophore, 2-(2-furoyl)-4(5)-(2-furanyl)-1*H*-imidazole (FFI) was identified after nonenzymatic browning of bovine serum albumin

and polylysine with glucose, and postulated to be representative of the chromophore present in the intact polypeptides. (Pongor et al., 1984, *PNAS(USA)* **81**:2684-2688). Later studies established FFI to be an artifact formed during acid hydrolysis for analysis.

A series of U.S. Patents have issued in the area of inhibition of protein glycosylation and cross-linking of protein sugar amines based upon the premise that the mechanism of such glycosylation and cross-linking occurs via saturated glycosylation and subsequent cross-linking of protein sugar amines via a single basic, and repeating reaction. These patents include U.S. Patents 4,665,192; 5,017,696; 4,758,853; 4,908,446; 4,983,604; 5,140,048; 5,130,337; 5,262,152; 5,130,324; 5,272,165; 5,221,683; 5,258,381; 5,106,877; 5,128,360; 5,100,919; 5,254,593; 5,137,916; 5,272,176; 5,175,192; 5,218,001; 5,238,963; 5,358,960; 5,318,982; and 5,334,617. (All U.S. Patents cited are hereby incorporated by reference in their entirety).

The focus of these U.S. Patents, are a method for inhibition of AGE formation focused on the carbonyl moiety of the early glycosylation Amadori product, and in particular the most effective inhibition demonstrated teaches the use of exogenously administered aminoguanidine. The effectiveness of aminoguanidine as an inhibitor of AGE formation is currently being tested in clinical trials.

Inhibition of AGE formation has utility in the areas of, for example, food spoilage, animal protein aging, and personal hygiene such as combating the browning of teeth. Some notable, though quantitatively minor, advanced glycation end-products are pentosidine and N^{ε} -carboxymethyllysine (Sell and Monnier, 1989, *J. Biol. Chem.* **264**:21597-21602; Ahmed et al., 1986, *J. Biol. Chem.* **261**:4889-4894).

The Amadori intermediary product and subsequent post-Amadori AGE formation, as taught by the instant invention, is not fully inhibited by reaction with aminoguanidine. Thus, the formation of post-Amadori AGEs as taught by the instant disclosure occurs via an important and unique reaction pathway that has not been previously shown, or even previously been possible to demonstrate in isolation. It is a highly desirable goal to have an efficient and effective method for identifying and characterizing effective post-Amadori AGE inhibitors of this "late" reaction. By providing efficient screening methods and model systems, combinatorial chemistry can be employed to screen candidate compounds effectively, and thereby greatly reducing

time, cost, and effort in the eventual validation of inhibitor compounds. It would be very useful to have *in vivo* methods for modeling and studying the effects of post-Amadori AGE formation which would then allow for the efficient characterization of effective inhibitors.

Inhibitory compounds that are biodegradeble and/or naturally metabolized are more desirable for use as therapeutics than highly reactive compounds which may have toxic side effects, such as aminoguanidine.

SUMMARY OF THE INVENTION

In accordance with the present invention, a stable post-Amadori advanced glycation end-product (AGE) precursor has been identified which can then be used to rapidly complete the post-Amadori conversion into post-Amadori AGEs. This stable product is a presumed sugar saturated Amadori/Schiff base product produced by the further reaction of the early stage protein/sugar Amadori product with more sugar. In a preferred embodiment, this post-Amadori/Schiff base intermediary has been generated by the reaction of target protein with ribose sugar.

The instant invention provides for a method of generating stable protein-sugar AGE formation intermediary precursors via a novel method of high sugar inhibition. In a preferred embodiment the sugar used is ribose.

The instant invention provides for a method for identifying an effective inhibitor of the formation of late Maillard products comprising: generating stable protein-sugar post-Amadori advanced glycation end-product intermediates by incubating a protein with sugar at a sufficient concentration and for sufficient length of time to generate stable post-Amadori AGE intermediates; contacting said stable protein-sugar post-Amadori advanced glycation end-product intermediates with an inhibitor candidate; identifying effective inhibition by monitoring the formation of post-Amadori AGEs after release of the stable protein-sugar post-Amadori advanced glycation end-product intermediates from sugar induced equilibrium. Appropriate sugars include, and are not limited to ribose, lyxose, xylose, and arabinose. It is believed that certain conditions will also allow for use of glucose and other sugars. In a preferred embodiment the sugar used is ribose.

The instant invention teaches that an effective inhibitor of post-Amadori AGE formation via "late" reactions can be identified and characterized by the ability to

inhibit the formation of post-Amadori AGE endproducts in an assay comprising; generating stable protein-sugar post-Amadori advanced glycation end-product intermediates by incubating a protein with sugar at a sufficient concentration and for sufficient length of time to generate stable post-Amadori AGE intermediates; contacting said stable protein-sugar post-Amadori advanced glycation end-product intermediates with an inhibitor candidate; identifying effective inhibition by monitoring the formation of post-Amadori AGEs after release of the stable protein-sugar post-Amadori advanced glycation end-product intermediates from sugar induced equilibrium. In a preferred embodiment the assay uses ribose.

Thus the methods of the instant invention allow for the rapid screening of candidate post-Amadori AGE formation inhibitors for effectiveness, greatly reducing the cost and amount of work required for the development of effective small molecule inhibitors of post-Amadori AGE formation. The instant invention teaches that effective inhibitors of post-Amadori "late" reactions of AGE formation include derivatives of vitamin B_6 and vitamin B_1, in the preferred embodiment the specific species being pyridoxamine and thiamine pyrophosphate.

The instant invention teaches new methods for rapidly inducing diabetes like pathologies in rats comprising administering ribose to the subject animal. Further provided for is the use of identified inhibitors pyridoxamine and thiamine pyrophosphate *in vivo* to inhibit post-Amadori AGE induced pathologies.

The present invention encompasses compounds for use in the inhibition of AGE formation and post-Amadori AGE pathologies, and pharmaceutical compositions

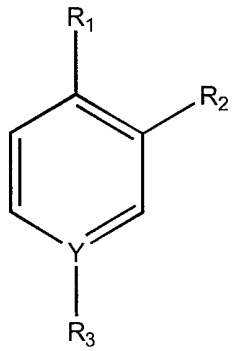

containing such compounds of the general formula:

Formula I

wherein R_1 is CH_2NH_2, CH_2SH, COOH, $CH_2CH_2NH_2$, CH_2CH_2SH, or CH_2COOH;
R_2 is OH, SH or NH_2;
Y is N or C, such that when Y is N R_3 is nothing, and when Y is C, R_3 is NO_2 or another electron withdrawing group; and salts thereof.

The present invention also encompasses compounds of the general formula
Formula II

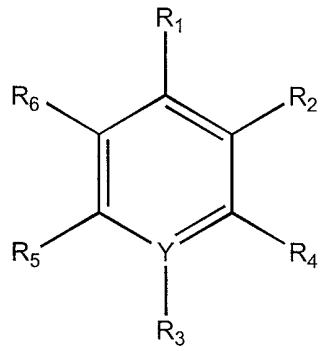

wherein R_1 is CH_2NH_2, CH_2SH, COOH, $CH_2CH_2NH_2$, CH_2CH_2SH, or CH_2COOH;
R_2 and R_6 is H, OH, SH, NH_2, C 1-18 alkyl, alkoxy or alkene;
R_4 and R_5 are H, C 1-18 alkyl, alkoxy or alkene;
Y is N or C, such that when Y is N R_3 is nothing, and when Y is C, R_3 is NO_2 or another electron withdrawing group, and salts thereof.

In a preferred embodiment at least one of R_4, R_5 and R_6 are H.

In addition, the instant invention also envisions compounds of the formulas

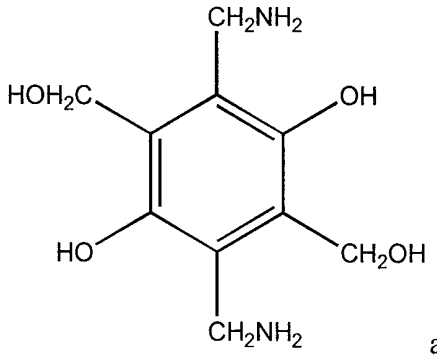

and

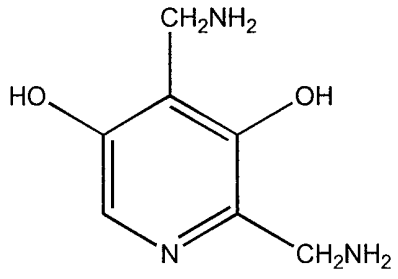

The compounds of the present invention can embody one or more electron withdrawing groups, such as and not limited to $-NH_2$, -NHR, $-NR_2$, -OH, $-OCH_3$, -OCR, and $-NH-COCH_3$ where R is C 1-6 alkyl.

The instant invention encompasses pharmaceutical compositions which comprise one or more of the compounds of the present invention, or salts thereof, in a suitable carrier. The instant invention encompasses methods for administering pharmaceuticals of the present invention for therapeutic intervention of pathologies which are related to AGE formation *in vivo*. In one preferred embodiment of the present invention the AGE related pathology to be treated is related to diabetic nephropathy.

The instant invention also teaches new methods to treat or prevent oxidative modification of proteins, including low density lipoproteins, to treat or prevent lipid peroxidation, and to treat or prevent atherosclerosis, comprising administering an amount effective of one of the compounds of the invention to treat or prevent the disorder.

BRIEF DESCRIPTION OF THE DRAWINGS

Figure 1 is a series of graphs depicting the effect of vitamin B_6 derivatives on AGE formation in bovine serum albumin (BSA). Figure 1A Pyridoxamine (PM); Figure 1B pyridoxal phosphate (PLP); Figure 1C pyridoxal (PL); Figure 1D pyridoxine (PN).

Figure 2 is a series of graphs depicting the effect of vitamin B_1 derivatives and aminoguanidine (AG) on AGE formation in bovine serum albumin. Figure 2A Thiamine pyrophosphate (TPP); Figure 2B thiamine monophosphate (TP); Figure 2C thiamine (T); Figure 2D aminoguanidine (AG).

Figure 3 is a series of graphs depicting the effect of vitamin B_6 derivatives on AGE formation in human methemoglobin (Hb). Figure 3A Pyridoxamine (PM); Figure 3B pyridoxal phosphate (PLP); Figure 3C pyridoxal (PL); Figure 3D pyridoxine (PN).

Figure 4 is a series of graphs depicting the effect of vitamin B_1 derivatives and aminoguanidine (AG) on AGE formation in human methemoglobin. Figure 2A Thiamine pyrophosphate (TPP); Figure 2B thiamine monophosphate (TP); Figure 2C

thiamine (T); Figure 2D aminoguanidine (AG).

Figure 5 is a bar graph comparison of the inhibition of the glycation of ribonuclease A by thiamine pyrophosphate (TPP), pyridoxamine (PM) and aminoguanidine (AG).

Figure 6A is a graph of the kinetics of glycation of RNase A (10 mg/mL) by ribose as monitored by ELISA. Figure 6B is a graph showing the dependence of reciprocal half-times on ribose concentration at pH 7.5.

Figure 7 are two graphs showing a comparison of uninterrupted and interrupted glycation of RNase by glucose (7B) and ribose (7A), as detected by ELISA.

Figure 8 are two graphs showing kinetics of pentosidine fluorescence (arbitrary units) increase during uninterrupted and interrupted ribose glycation of RNase. Figure 8A Uninterrupted glycation in the presence of 0.05 M ribose. Figure 8B Interrupted glycation after 8 and 24 hours of incubation.

Figure 9 is a graph which shows the kinetics of reactive intermediate buildup.

Figure 10 are graphs of Post-Amadori inhibition of AGE formation by ribose. Figure 10A graphs data where aliquots were diluted into inhibitor containing buffers at time 0. Figure 10B graphs data where samples were interrupted at 24h, and then diluted into inhibitor containing buffers.

Figure 11 is a graph showing dependence of the initial rate of formation of antigenic AGE on pH following interruption of glycation.

Figure 12 are two graphs showing the effect of pH jump on ELISA detected AGE formation after interrupted glycation. Interrupted samples left 12 days at 37°C in pH 5.0 buffer produced substantial AGEs (33%; Figure 12 B) when pH was changed to 7.5, as compared to the normal control sample not exposed to low pH (Figure 12 A).

Figure 13 is a series of graphs depicting the effect of vitamin B_6 derivatives on AGE formation during uninterrupted glycation of ribonuclease A (RNase A) by ribose. Figure 13A Pyridoxamine (PM); Figure 13B pyridoxal-5'-phosphate (PLP); Figure 13C pyridoxal (PL); Figure 13D pyridoxine (PN).

Figure 14 is a series of graphs depicting the effect of vitamin B_1 derivatives and aminoguanidine (AG) on AGE formation during uninterrupted glycation of ribonuclease A (RNase A) by ribose. Figure 14A Thiamine pyrophosphate (TPP); Figure 14B thiamine monophosphate (TP); Figure 14C thiamine (T); Figure 14D

aminoguanidine (AG).

Figure 15 is a series of graphs depicting the effect of vitamin B_6 derivatives on AGE formation during uninterrupted glycation of bovine serum albumin (BSA) by ribose. Figure 15A Pyridoxamine (PM); Figure 15B pyridoxal-5'-phosphate (PLP); Figure 15C pyridoxal (PL); Figure 15D pyridoxine (PN).

Figure 16 is a series of graphs depicting the effect of vitamin B_1 derivatives and aminoguanidine (AG) on AGE formation during uninterrupted glycation of bovine serum albumin (BSA) by ribose. Figure 16A Thiamine pyrophosphate (TPP); Figure 16B thiamine monophosphate (TP); Figure 16C thiamine (T); Figure 16D aminoguanidine (AG).

Figure 17 is a series of graphs depicting the effect of vitamin B_6 derivatives on AGE formation during uninterrupted glycation of human methemoglobin (Hb) by ribose. Figure 17A Pyridoxamine (PM); Figure 17B pyridoxal-5'-phosphate (PLP); Figure 17C pyridoxal (PL); Figure 17D pyridoxine (PN).

Figure 18 is a series of graphs depicting the effect of vitamin B_6 derivatives on post-Amadori AGE formation after interrupted glycation by ribose. Figure 18A BSA and Pyridoxamine (PM); Figure 18B BSA and pyridoxal-5'-phosphate (PLP); Figure 18C BSA and pyridoxal (PL); Figure 18D RNase and pyridoxamine (PM).

Figure 19 are graphs depicting the effect of thiamine pyrophosphate on post-Amadori AGE formation after interrupted glycation by ribose. Figure 19A RNase, Figure 19B BSA.

Figure 20 are graphs depicting the effect of aminoguanidine on post-Amadori AGE formation after interrupted glycation by ribose. Figure 20A RNase, Figure 20B BSA.

Figure 21 is a graph depicting the effect of N-a c etyl-L-lysine on post-Amadori AGE formation after interrupted glycation by ribose.

Figure 22 are bar graphs showing a comparison of post-Amadori inhibition of AGE formation by thiamine pyrophosphate (TPP), pyridoxamine (PM) and aminoguanidine (AG) after interrupted glycation of RNase (Figure 22A) and BSA (Figure 22B) by ribose.

Figure 23 is a bar graph showing the effects of Ribose treatment *in vivo* alone on rat tail-cuff blood pressure. Treatment was with 0.05 M, 0.30 M, and 1 M Ribose

(R) injected for 1, 2 or 8 Days (D).

Figure 24 is a bar graph showing the effects of Ribose treatment *in vivo* alone on rat creatinine clearance (Clearance per 100 g Body Weight). Treatment was with 0.05 M, 0.30 M, and 1 M Ribose (R) injected for 1, 2 or 8 Days (D).

Figure 25 is a bar graph showing the effects of Ribose treatment *in vivo* alone on rat Albuminuria (Albumin effusion rate). Treatment was with 0.30 M, and 1 M Ribose (R) injected for 1, 2 or 8 Days (D).

Figure 26 is a bar graph showing the effects of inhibitor treatment *in vivo*, with or without ribose, on rat tail-cuff blood pressure. Treatment groups were: 25 mg/kg body weight aminoguanidine (AG); 25 or 250 mg/kg body weight Pyridoxamine (P); 250 mg/kg body weight Thiamine pyrophosphate (T), or with 1 M Ribose (R).

Figure 27 is a bar graph showing the effects of inhibitor treatment *in vivo*, with or without ribose, on rat creatinine clearance (Clearance per 100 g body weight). Treatment groups were: 25 mg/kg body weight aminoguanidine (AG); 25 or 250 mg/kg body weight Pyridoxamine (P); 250 mg/kg body weight Thiamine pyrophosphate (T), or with 1 M Ribose (R).

Figure 28 is a bar graph showing the effects of inhibitor treatment *in vivo* without ribose, and ribose alone on rat Albuminuria (Albumin effusion rate). Treatment groups were: 25 mg/kg body weight aminoguanidine (AG); 250 mg/kg body weight Pyridoxamine (P); 250 mg/kg body weight Thiamine pyrophosphate (T), or treatment with 1 M Ribose (R) for 8 days (D). Control group had no treatment.

Figure 29 is a bar graph showing the effects of inhibitor treatment *in vivo*, with 1 M ribose , on rat Albuminuria (Albumin effusion rate). Treatment groups were: 25 mg/kg body weight aminoguanidine (AG); 25 and 250 mg/kg body weight Pyridoxamine (P); 250 mg/kg body weight Thiamine pyrophosphate (T), or treatment with 1 M Ribose (R) for 8 days (D) alone. Control group had no treatment.

Figure 30A depicts Scheme 1 showing a diagram of AGE formation from protein. Figure 30B depicts Scheme 2, a chemical structure of aminoguanidine. Figure 30C depicts Scheme 3, chemical structures for thiamine, thiamine-5'-phosphate, and thiamine pyrophosphate. Figure 30D depicts Scheme 4, chemical structures of pyridoxine, pyridoxamine, pyridoxal-5'-phosphate, and pyridoxal. Figure 30E depicts Scheme 5, kinetics representation of AGE formation. Figure 30F depicts Scheme 6,

kinetics representation of AGE formation and intermediate formation.

Figure 31 shows a 125 MHz C-13 NMR Resonance spectrum of Riobonuclease Amadori Intermediate prepared by 24 HR reaction with 99% [2-C13]Ribose.

Figure 32 are graphs which show AGE intermediary formation using the pentoses Xylose, Lyxose, Arabinose and Ribose.

Figure 33 is a graph showing the results of glomeruli staining at pH 2.5 with Alcian blue.

Figure 34 is a graph showing the results of glomeruli staining at pH 1.0 with Alcian blue.

Figure 35 is a graph showing the results of immunofluroescent glomeruli staining for RSA.

Figure 36 is a graph showing the results of immunofluroescent glomeruli staining for Heparan Sulfate Proteoglycan Core protein.

Figure 37 is a graph showing the results of immunofluroescent glomeruli staining for Heparan Sulfate Proteoglycan side-chain.

Figure 38 is a graph showing the results of analysis of glomeruli sections for average glomerular volume.

Figure 39. Structure and mass spectrum of the TFAME derivative of lysine. Lysine was derivatized to its methyl ester using methanolic-HCl then converted to its TFAME derivative with trifluoroacetic anhydride. The 180 ion (base peak) was used for quantification of lysine by GC/MS.

Figure 40. Structure of derivatized CML and CEL. CML and CEL were derivatized to TFAMEs as described for lysine. Ions 392 and 379 were used for quantification of CML and CEL, respectively.

Figure 41. Mass Spectrum of derivatized CML and CEL. CML and CEL were derivatized to TFAMEs as described for lysine. Ions 392 and 379 were used for quantification of CML and CEL, respectively.

Figure 42. Structure of MDA-lysine (A) and HNE-lysine (B). MDA-lysine and HNE-lysine were derivatized to TFAMEs as described for lysine. Ions 474 and 323 were used for quantification of MDA-lysine and HNE-lysine, respectively.

Figure 43. Mass Spectrum of MDA-lysine (A) and HNE-lysine (B). MDA-lysine and HNE-lysine were derivatized to TFAMEs as described for lysine. Ions 474 and 323 were used for quantification of MDA-lysine and HNE-lysine, respectively.

Figure 44. Loss of free amino groups during reaction of PM with PUFAs. PM (1 mM) was incubated alone (τ) or in the presence of oleate (λ), linoleate (σ), or arachidonate (ν) (5 mM) in 0.2 M sodium phosphate buffer pH 7.4 for 6 days at 37°C. Aliquots were withdrawn at various time intervals and analyzed for free amino groups using the TNBS assay. Data shown are the mean and standard deviation of 3 independent experiments.

Figure 45. LC-MS analysis of a PM/linoleate reaction at day 6. PM (1 mM) was reacted with linoleate (5 mM). The day 6 sample was analyzed by LC-MS as described in Materials and Methods. Panel A and panel B represent the mass spectra taken from the major products.

Figure 46. Kinetics of formation of products 267, 339, and 305. PM (1 mM) was reacted with linoleate (5 mM) as described previously. The samples were analyzed by RP-HPLC using absorbance detection at 294 nm. Panel A shows a chromatogram of a day 6 reaction and the formation of products 339, 267 and 305. The products were quantified (Panel B) based on their area ratios to the internal standard PL (267 (λ), 339 (ν), and 305 (σ)). The data shown are the mean and standard deviation from 3 independent experiments.

Figure 47. Proposed structure of products 267 and 339. Products 267 and 339 were hypothesized to be hexamide and nonanedioic acid amide derivatives of PM.

Figure 48. TNBS reactivity of synthetic 339. An estimated 80 nmoles of synthetic 339 was analyzed by the TNBS assay. An equivalent amount of PM standard was analyzed for comparison.

Figure 49. Proposed mechanism to the formation of 267 and 339. Oxidation of linoleic acid proceeds through formation of linoleic acid 9- and 13- lipid hydroperoxides. These may then dehydrate to form ketoacids. Nucleophilic attack of PM on the ketoacids could lead to formation of the amide derivatives via oxidative cleavage of the Schiff base.

Figure 50. Preferential cleavage of the Schiff base to form the amide derivatives may be driven by radical stabilization within the conjugated system. The

carbinolamine, precursor of the Schiff base adduct, would then undergo hydrogen abstraction. The resulting radical might be stabilized by the conjugated carbon system, directing the cleavage reaction to form the 6-carbon amide derivative. The same mechanism would apply to formation of the nonanedioic acid amide derivative.

Figure 51. Proposed structure for product 305. Though complete characterization of 305 was not accomplished, a molecular formula obtained by high resolution FAB-MS suggests the product is either a pyrrole or furan derivative of PM.

Figure 52. Inhibition of CML and CEL formation by PM during reactions of RNase with arachidonate. RNase (1 mM (10 mM lysine)) was reacted with arachidonate (100 mM) alone (❑) or in the presence of 1 mM PM (■) in 200 mM sodium phosphate buffer, pH 7.4 at 37°C for 6 days. At various time points 1 mg of protein was removed and prepared for GC/MS analysis. CML and CEL were analyzed by GC/MS as their trifluoroacetyl methyl esters. Data shown is the average and range of two independent experiments.

Figure 53. Inhibition of MDA-lysine and HNE-lysine by PM during reactions of RNase with arachidonate. RNase (1 mM) was reacted with arachidonate (100 mM) alone (❑) or in the presence of 1 mM PM (■) in 200 mM sodium phosphate buffer, pH 7.4 at 37°C for 6 days. At various time intervals 1 mg of protein was removed and prepared for GC/MS analysis. MDA-lysine and HNE-lysine were analyzed by GC/MS as their trifluoroacetyl methyl esters. Data shown is the average and range of two independent experiments.

Figure 54. Prolongation of conjugated diene formation by PM during copper catalyzed oxidation of LDL. LDL (50 μg/ml) was incubated alone (■) or oxidized in the presence of 5 μM Cu^{2+} (●) or with 5 μM Cu^{2+} in the presence of 100 μM (▲) or 250 μM (Δ) PM. Conjugated diene formation was monitored at an absorbance of 234 nm. Results are shown for two independent pools of LDL (A and B).

Figure 55. PM inhibits formation of CML and CEL during copper-catalyzed oxidation of LDL. LDL (50 μg/ml) was incubated for 3 hours alone or oxidized with 5 μM Cu^{2+} in the presence of 10 or 100 μM PM in PBS. Approximately 1 mg of protein was removed at 3 hours and reduced with 500 mM $NaBH_4$ (Requena, 1997). Following reduction, the samples were dialyzed, delipidated and hydrolyzed in 6N HCl. CML and

CEL were analyzed as their trifluoroacetyl methyl esters. Results shown represent the average and range of two independent pools of LDL.

Figure 56. PM inhibits formation of MDA-lysine and HNE-lysine during copper catalyzed oxidation of LDL. LDL (50 μg/ml) was incubated for 3 hours alone or oxidized with 5 μM Cu^{2+} in the presence of 10 or 100 μM PM in PBS. Approximately 1 mg of protein was removed at 3 hours and reduced with 500 mM $NaBH_4$. Following reduction, the samples were dialyzed, delipidated and hydrolyzed in 6N HCl. MDA-lysine and HNE-lysine were analyzed as their trifluoroacetyl methyl esters. Results represent the average and range of two independent pools of LDL.

Figure 57. PM prevents lysine modification during copper catalyzed oxidation of LDL. LDL (50 μg/ml) was incubated for 3 hours alone or oxidized with 5 μM Cu^{2+} in the presence of 100 or 250 μM PM in PBS. Approximately 150 μg of protein was removed at 3 hours and immediately hydrolyzed, or reduced with $NaBH_4$ then hydrolyzed, in 6N HCl for 24 hours at 110°C. Following hydrolysis the samples were reconstituted in Pickering buffer A and analyzed by cation-exchange HPLC. The results shown for both non-reduced and reduced lysine are the average values +/- the range from two independent pools of LDL.

Figure 58. Effect of PM on TBARs formation during oxidation of linoleate. Linoleate was oxidized alone (5 mM) (■) or in the presence of PM (1 mM) (●) for 6 days at 37°C in sodium phosphate buffer, pH 7.4. Aliquots were removed at various time intervals and analyzed for TBARs as described above. Data shown represents the mean +/- standard deviation of 3 independent experiments.

Figure 59. Effect of PM on the rate of linoleate oxidation. Linoleate (5 mM) was oxidized alone (■) or in the presence of PM (1 mM) (●) for 6 days. Linoleate was extracted using acidified chloroform:methanol (Folch, 1957). Following addition of the internal standard, palmitate, the samples were derivatized with borontrichloride-methanol and the fatty acids analyzed as their methyl esters by GC/MS. Quantification was based on standard curves generated from linoleate and palmitate standards. Data shown is the mean +/- standard deviation of 3 independent experiments.

Figure 60. Mechanism by which PM may act as an antioxidant. PM (A) may donate a hydrogen to radicals produced either during the initiation or propagation

phases of lipid peroxidation. The resulting PM radical (B) is stabilized by the aromatic ring system (C).

DETAILED DESCRIPTION

Animal Models for Protein Aging

Alloxan induced diabetic Lewis rats have been used as a model for protein aging to demonstrate the *in vivo* effectiveness of inhibitors of AGE formation. The correlation being demonstrated is between inhibition of late diabetes related pathology and effective inhibition of AGE formation (Brownlee, Cerami, and Vlassara, 1988, *New Eng. J. Med.* **318(20)**:1315-1321). Streptozotocin induction of diabetes in Lewis rats, New Zealand White rabbits with induced diabetes, and genetically diabetic BB/Worcester rats have also been utilized, as described in, for example, U.S. Patent 5,334,617 (incorporated by reference). A major problem with these model systems is the long time period required to demonstrate AGE related injury, and thus to test compounds for AGE inhibition. For example, 16 weeks of treatment was required for the rat studies described in U.S. Patent 5,334,617, and 12 weeks for the rabbit studies. Thus it would be highly desirable and useful to have a model system for AGE related diabetic pathology that will manifest in a shorter time period, allowing for more efficient and expeditious determination of AGE related injury and the effectiveness of inhibitors of post-Amadori AGE formation.

Antibodies to AGEs

An important tool for studying AGE formation is the use of polyclonal and monoclonal antibodies that are specific for AGEs elicited by the reaction of several sugars with a variety of target proteins. The antibodies are screened for resultant specificity for AGEs that is independent of the nature of the protein component of the AGE (Nakayama et al., 1989, *Biochem. Biophys. Res. Comm.* **162**: 740-745; Nakayama et al., 1991, *J. Immunol. Methods* **140**: 119-125; Horiuchi et al., 1991, *J. Biol. Chem.* **266**: 7329-7332; Araki et al., 1992, *J. Biol. Chem.* **267**: 10211-10214; Makita et al., 1992, *J. Biol. Chem.* **267**: 5133-5138). Such antibodies have been used to monitor AGE formation *in vivo* and *in vitro*.

Thiamine - Vitamin B_1

The first member of the Vitamin B complex to be identified, thiamine is practically devoid of pharmacodynamic actions when given in usual therapeutic doses; and even large doses were not known to have any effects. Thiamine pyrophosphate is the physiologically active form of thiamine, and it functions mainly in carbohydrate metabolism as a coenzyme in the decarboxylation of α-keto acids. Tablets of thiamine hydrochloride are available in amounts ranging from 5 to 500 mg each. Thiamine hydrochloride injection solutions are available which contain 100 to 200 mg/ml.

For treating thiamine deficiency, intravenous doses of as high as 100 mg/L of parenteral fluid are commonly used, with the typical dose of 50 to 100 mg being administered. GI absorption of thiamine is believed to be limited to 8 to 15 mg per day, but may be exceed by oral administration in divided doses with food.

Repeated administration of glucose may precipitate thiamine deficiency in under nourished patients, and this has been noted during the correction of hyperglycemia.

Surprisingly, the instant invention has found, as shown by *in vitro* testing, that administration of thiamine pyrophosphate at levels above what is normally found in the human body or administered for dietary therapy, is an effective inhibitor of post-Amadori antigenic AGE formation, and that this inhibition is more complete than that possible by the administration of aminoguanidine.

Pyridoxine - Vitamin B_6

Vitamin B_6 is typically available in the form of pyridoxine hydrochloride in over-the-counter preparations available from many sources. For example Beach pharmaceuticals Beelith Tablets contain 25 mg of pyridoxine hydrochloride that is equivalent to 20 mg of B_6, other preparations include Marlyn Heath Care Marlyn Formula 50 which contain 1 mg of pyridoxine HCl and Marlyn Formula 50 Mega Forte which contains 6 mg of pyridoxine HCl, Wyeth-Ayerst Stuart Prenatal® tablets which contain 2.6 mg pyridoxine HCl, J&J-Merck Corp. Stuart Formula® tablets contain 2 mg of pyridoxine HCl, and the CIBA Consumer Sunkist Children's chewable multivitamins which contain 1.05 mg of pyridoxine HCl, 150% of the U.S. RDA for

children 2 to 4 years of age, and 53% of the U.S. RDA for children over 4 years of age and adults. (Physician's Desk Reference for nonprescription drugs, 14th edition (Medical Economics Data Production Co., Montvale, N.J., 1993).

There are three related forms of pyridoxine, which differ in the nature of the substitution on the carbon atom in position 4 of the pyridine nucleus: pyridoxine is a primary alcohol, pyridoxal is the corresponding aldehyde, and pyridoxamine contains an aminomethyl group at this position. Each of these three forms can be utilized by mammals after conversion by the liver into pyridoxal-5'-phosphate, the active form of the vitamin. It has long been believed that these three forms are equivalent in biological properties, and have been treated as equivalent forms of vitamin B_6 by the art. The Council on Pharmacy and Chemistry has assigned the name pyridoxine to the vitamin.

The most active antimetabolite to pyridoxine is 4-deoxypyridoxine, for which the antimetabolite activity has been attributed to the formation *in vivo* of 4-deoxypyridoxine-5-phosphate, a competitive inhibitor of several pyridoxal phosphate-dependent enzymes. The pharmacological actions of pyridoxine are limited, as it elicits no outstanding pharmacodynamic actions after either oral or intravenous administration, and it has low acute toxicity, being water soluble. It has been suggested that neurotoxicity may develop after prolonged ingestion of as little as 200 mg of pyridoxine per day. Physiologically, as a coenzyme, pyridoxine phosphate is involved in several metabolic transformations of amino acids including decarboxylation, transamination, and racemization, as well as in enzymatic steps in the metabolism of sulfur-containing and hydroxy-amino acids. In the case of transamination, pyridoxal phosphate is aminated to pyridoxamine phosphate by the donor amino acid, and the bound pyridoxamine phosphate is then deaminated to pyridoxal phosphate by the acceptor α-keto acid. Thus vitamin B complex is known to be a necessary dietary supplement involved in specific breakdown of amino acids. For a general review of the vitamin B complex see The Pharmacological Basis of Therapeutics, 8th edition, ed. Gilman, Rall, Nies, and Taylor (Pergamon Press, New York, 1990, pp. 1293-4; pp. 1523-1540).

Surprisingly, the instant invention has discovered that effective dosages of the metabolically transitory pyridoxal amine form of vitamin B_6 (pyridoxamine), at levels above what is normally found in the human body, is an effective inhibitor of post-

Amadori antigenic AGE formation, and that this inhibition may be more complete than that possible by the administration of aminoguanidine.

Formation of Stable Amadori/Schiff base Intermediary

The typical study of the reaction of a protein with glucose to form AGEs has been by ELISA using antibodies directed towards antigenic AGEs, and the detection of the production of an acid-stable fluorescent AGE, pentosidine, by HPLC following acid hydrolysis. Glycation of target proteins (i.e. BSA or RNase A) with glucose and ribose were compared by monitoring ELISA reactivity of polyclonal rabbit anti-Glucose-AGE-RNase and anti-Glucose-AGE-BSA antibodies. The antigen was generated by reacting 1 M glucose with RNase for 60 days and BSA for 90 days. The antibodies (R618 and R479) were screened and showed reactivity with only AGEs and not the protein, except for the carrier immunogen BSA.

Example 1

Thiamine Pyrophosphate and Pyridoxamine Inhibit the Formation of Antigenic Advanced Glycation End-Products from Glucose: Comparison with Aminoguanidine

Some B_6 vitamers, especially pyridoxal phosphate (PLP), have been previously proposed to act as "competitive inhibitors" of early glycation, since as aldehydes they themselves can form Schiff bases adducts with protein amino groups (Khatami et al., 1988, *Life Sciences* **43**:1725-1731) and thus limit the amount of amines available for glucose attachment. However, effectiveness in limiting initial sugar attachment is not a predictor of inhibition of the conversion of any Amadori products formed to AGEs. The instant invention describes inhibitors of "late" glycation reactions as indicated by their effects on the *in vitro* formation of *antigenic* AGEs (Booth et al., 1996, *Biochem. Biophys. Res. Com.* **220**:113-119).

Chemicals Bovine pancreatic ribonuclease A (RNase) was chromatographically pure, aggregate-free grade from Worthington Biochemicals. Bovine Serum albumin (BSA; fraction V, fatty-acid free), human methemoglobin (Hb), D-glucose, pyridoxine, pyridoxal, pyridoxal 5'phosphate, pyridoxamine, thiamine, thiamine monophosphate,

thiamine pyrophosphate, and goat alkaline phosphatase-conjugated anti-rabbit IgG were all from Sigma Chemicals. Aminoguanidine hydrochloride was purchased from Aldrich Chemicals.

Uninterrupted Glycation with Glucose Bovine serum albumin, ribonuclease A, and human hemoglobin were incubated with glucose at 37°C in 0.4 M sodium phosphate buffer of pH 7.5 containing 0.02% sodium azide. The protein, glucose (at 1.0 M), and prospective inhibitors (at 0.5, 3, 15 and 50 mM) were introduced into the incubation mixture simultaneously. Solutions were kept in the dark in capped tubes. Aliquots were taken and immediately frozen until analyzed by ELISA at the conclusion of the reaction. The incubations were for 3 weeks (Hb) or 6 weeks (RNase, BSA).

Preparation of polyclonal antibodies to AGE proteins

Immunogen preparation followed earlier protocols (Nakayama et al., 1989, *Biochem. Biophys. Res. Comm.* **162**:740-745; Horiuchi et al., 1991, *J. Biol. Chem.* **266**:7329-7332; Makita et al., 1992, *J. Biol. Chem.* **267**:5133-5138). Briefly, immunogen was prepared by glycation of BSA (R479 antibodies) or RNase (R618 antibodies) at 1.6 g protein in 15 ml for 60-90 days using 1.5 M glucose in 0.4 M sodium phosphate buffer of pH 7.5 containing 0.05% sodium azide at pH 7.4 and 37°C. New Zealand white rabbit males of 8-12 weeks were immunized by subcutaneous administration of a 1 ml solution containing 1 mg/ml of glycated protein in Freund's adjuvant. The primary injection used the complete adjuvant and three boosters were made at three week intervals with Freund's incomplete adjuvant. Rabbits were bled three weeks after the last booster. The serum was collected by centrifugation of clotted whole blood. The antibodies are AGE-specific, being unreactive with either native proteins (except for the carrier) or with Amadori intermediates. The polyclonal anti-AGE antibodies have proven to be a sensitive and valuable analytical tool for the study of "late" AGE formation *in vitro* and *in vivo*. The nature of the dominant antigenic AGE epitope or hapten remains in doubt, although recently it has been proposed that the protein glycoxidation product carboxymethyl lysine (CML) may be a dominant antigen of some antibodies (Reddy et al., 1995, *Biochem.* **34**:10872-10878). Earlier studies have failed to reveal ELISA reactivity with model CmL compounds (Makita et

al., 1992, *J. Biol. Chem.* **267**:5133-5138).

ELISA detection of AGE products The general method of Engvall (1981, *Methods Enzymol.* **70**:419-439) was used to perform the ELISA. Typically, glycated protein samples were diluted to approximately 1.5 ug/ml in 0.1 M sodium carbonate buffer of pH 9.5 to 9.7. The protein was coated overnight at room temperature onto 96-well polystyrene plates by pippetting 200 ul of the protein solution in each well (0.3 ug/well). After coating, the protein was washed from the wells with a saline solution containing 0.05% Tween-20. The wells were then blocked with 200 ul of 1% casein in carbonate buffer for 2 h at 37°C followed by washing. Rabbit anti-AGE antibodies were diluted at a titer of about 1:350 in incubation buffer, and incubated for 1 h at 37°C, followed by washing. In order to minimize background readings, antibodies R479 used to detect glycated RNase were raised against glycated BSA, and antibodies R618 used to detect glycated BSA and glycated Hb were raised against glycated RNase. An alkaline phosphatase-conjugated antibody to rabbit IgG was then added as the secondary antibody at a titer of 1:2000 or 1:2500 (depending on lot) and incubated for 1 h at 37°C, followed by washing. The p-nitrophenylphosphate substrate solution was then added (200 ul/well) to the plates, with the absorbance of the released p-nitrophenolate being monitored at 410 nm with a Dynatech MR 4000 microplate reader.

Controls containing unmodified protein were routinely included, and their readings were subtracted, the corrections usually being negligible. The validity of the use of the ELISA method in quantitatively studying the kinetics of AGE formation depends on the linearity of the assay (Kemeny & Challacombe, 1988, *ELISA and Other Solid Phase Immunoassays*, John Wiley & Sons, Chichester, U.K.). Control experiments were carried out, for example, demonstrating that the linear range for RNase is below a coating concentration of about 0.2-0.3 mg/well.

Results

Figure 1 A-D are graphs which show the effect of vitamin B_6 derivatives on post-Amadori AGE formation in bovine serum albumin glycated with glucose. BSA (10 mg/ml) was incubated with 1.0 M glucose in the presence and absence of the

various indicated derivative in 0.4 M sodium phosphate buffer of pH 7.5 at 37°C for 6 weeks. Aliquots were assayed by ELISA using R618 anti-AGE antibodies. Concentrations of the inhibitors were 3, 15 and 50 mM. Inhibitors used in Figures (1A) Pyridoxamine (PM); (1B) pyridoxal phosphate (PLP); (1C) pyridoxal (PL); (1D) pyridoxine (PN).

Figure 1 (control curves) demonstrates that reaction of BSA with 1.0 M glucose is slow and incomplete after 40 days, even at the high sugar concentration used to accelerate the reaction. The simultaneous inclusion of different concentrations of various B_6 vitamers markedly affects the formation of antigenic AGEs. (Figure 1A-D) Pyridoxamine and pyridoxal phosphate strongly suppressed antigenic AGE formation at even the lowest concentrations tested, while pyridoxal was effective above 15 mM. Pyridoxine was slightly effective at the highest concentrations tested.

Figure 2 A-D are graphs which show the effect of vitamin B_1 derivatives and aminoguanidine (AG) on AGE formation in bovine serum albumin. BSA (10 mg/ml) was incubated with 1.0 M glucose in the presence and absence of the various indicated derivative in 0.4 M sodium phosphate buffer of pH 7.5 at 37°C for 6 weeks. Aliquots were assayed by ELISA using R618 anti-AGE antibodies. Concentrations of the inhibitors were 3, 15 and 50 mM. Inhibitors used in Figures (2A) Thiamine pyrophosphate (TPP); (2B) thiamine monophosphate (TP); (2C) thiamine (T); (2D) aminoguanidine (AG).

Of the various B_1 vitamers similarly tested (Figure 2A-D), thiamine pyrophosphate was effective at all concentrations tested (Figure 2C), whereas thiamine and thiamine monophosphate were not inhibitory. Most significantly it is remarkable to note the decrease in the *final levels* of AGEs formed observed with thiamine pyrophosphate, pyridoxal phosphate and pyridoxamine. Aminoguanidine (Figure 2D) produced some inhibition of AGE formation in BSA, but less so than the above compounds. Similar studies were carried out with human methemaglobin and bovine ribonuclease A.

Figure 3 A-D are graphs which show the effect of vitamin B_6 derivatives on AGE formation in human methemoglobin. Hb (1 mg/ml) was incubated with 1.0 M glucose in the presence and absence of the various indicated derivative in 0.4 M sodium phosphate buffer of pH 7.5 at 37°C for 3 weeks. Aliquots were assayed by ELISA

using R618 anti-AGE antibodies. Concentrations of the inhibitors were 0.5, 3, 15 and 50 mM. Inhibitors used in Figures (3A) Pyridoxamine (PM); (3B) pyridoxal phosphate (PLP); (3C) pyridoxal (PL); (3D) pyridoxine (PN).

It had been previously reported that Hb of a diabetic patient contains a component that binds to anti-AGE antibodies, and it was proposed that this glycated Hb (termed Hb-AGE, not to be confused with Hb_{A1c}) could be useful in measuring long-term exposure to glucose. The *in vitro* incubation of Hb with glucose produces antigenic AGEs at an apparently faster rate than observed with BSA. Nevertheless, the different B_6 (Figure 3A-D) and B_1 (Figure 4A-C) vitamers exhibited the same inhibition trends in Hb, with pyridoxamine and thiamine pyrophosphate being the most effective inhibitors in each of their respective families. Significantly, in Hb, aminoguanidine only inhibited the rate of AGE formation, and not the final levels of AGE formed (Figure 4D).

With RNase the rate of antigenic AGE formation by glucose was intermediate between that of Hb and BSA, but the extent of inhibition within each vitamer series was maintained. Again pyridoxamine and thiamine pyrophosphate were more effective that aminoguanidine (Figure 5).

Figure 4 A-D are graphs which show the effect of vitamin B_1 derivatives and aminoguanidine (AG) on AGE formation in human methemoglobin. Hb (1 mg/ml) was incubated with 1.0 M glucose in the presence and absence of the various indicated derivative in 0.4 M sodium phosphate buffer of pH 7.5 at 37°C for 3 weeks. Aliquots were assayed by ELISA using R618 anti-AGE antibodies. Concentrations of the inhibitors were 0.5, 3, 15 and 50 mM. Inhibitors used in Figures (4A) Thiamine pyrophosphate (TPP); (4B) thiamine monophosphate (TP); (4C) thiamine (T); (4D) aminoguanidine (AG).

Figure 5 is a bar graph which shows a comparison of the inhibition of the glycation of ribonuclease A by thiamine pyrophosphate (TPP), pyridoxamine (PM) and aminoguanidine (AG). RNase (1 mg/ml) was incubated with 1.0 M glucose (glc) in the presence and absence of the various indicated derivative in 0.4 M sodium phosphate buffer of pH 7.5 at 37°C for 6 weeks. Aliquots were assayed by ELISA using R479 anti-AGE antibodies. The indicated percent inhibition was computed from ELISA readings in the absence and presence of the inhibitors at the 6 week time point.

Concentrations of the inhibitors were 0.5, 3, 15 and 50 mM.

Discussion

These results demonstrate that certain derivatives of B_1 and B_6 vitamins are capable of inhibiting "late" AGE formation. Some of these vitamers successfully inhibited the final levels of AGE produced, in contrast to aminoguanidine, suggesting that they have greater interactions with Amadori or post-Amadori precursors to antigenic AGEs. The Amadori and post-Amadori intermediates represent a crucial juncture where the "classical" pathway of nonenzymatic glycation begins to become essentially irreversible (Scheme I). In earlier inhibition studies "glycation" was usually measured either as Schiff base formed (after reduction with labeled cyanoborohydride) or as Amadori product formed (after acid precipitation using labeled sugar). Such assays do not yield information on inhibition of post-Amadori conversion steps to "late" AGE products, since such steps lead to no change in the amount of labeled sugar that is attached to the proteins. Other "glycation" assays have relied on the sugar-induced increase of non-specific protein fluorescence, but this can also be induced by dicarbonyl oxidative fragments of free sugar, such as glycoaldehyde or glyoxal (Hunt et al., 1988, *Biochem.* **256**:205-212), independently of Amadori product formation.

In the case of pyridoxal (PL) and pyridoxal phosphate (PLP), the data support the simple mechanism of inhibition involving competitive Schiff-base condensation of these aldehydes with protein amino groups at glycation sites. Due to internal hemiacetal formation in pyridoxal but not pyridoxal phosphate, stronger inhibition of post-Amadori AGE formation by PLP is expected by this competitive mechanism. This indeed is observed in the data (Figure 1B, 1C, Figure 3B, 3C). The inhibition by pyridoxamine is necessarily different, as pyridoxamine lacks an aldehyde group. However, pyridoxamine is a candidate amine potentially capable of forming a Schiff-base linkage with the carbonyls of open-chain sugars, with dicarbonyl fragments, with Amadori products, or with post-Amadori intermediates. The mechanism of inhibition of B_1 compounds is not obvious. All the forms contain an amino functionality, so that the marked efficiency of only the pyrophosphate form suggests an important requirement for a strong negative charge.

A significant unexpected observation is that the extent of inhibition by

aminoguanidine, and some of the other compounds, is considerably less at late stages of the reaction, than during the early initial phase. This suggests a different mechanism of action than that of pyridoxamine and thiamine pyrophosphate, suggesting that the therapeutic potential of these compounds will be enhanced by co-administration with aminoguanidine.

Example 2

Kinetics of Non-enzymatic glycation: Paradoxical Inhibition by Ribose and Facile Isolation of Protein Intermediate for Rapid Post-Amadori AGE Formation

While high concentrations of glucose are used to cause the non-enzymatic glycation of proteins, paradoxically, it was found that ribose at high concentrations is *inhibitory* to post-Amadori AGE formation in ribonuclease by acting on the post-Amadori "late" stages of the glycation reaction. This unexpectedly inhibitory effect suggests that the "early" reactive intermediates, presumably Amadori products, can be accumulated with little formation of "late" post-Amadori AGE products (AGEs; Maillard products). Investigation into this phenomenon has demonstrated: (1) ability to define conditions for the kinetic isolation of Amadori (or post-Amadori) glycated intermediate(s); (2) the ability study the fast kinetics of buildup of such an intermediate; (3) the ability to study the surprisingly rapid kinetics of conversion of such intermediates to AGE products *in the absence of free or reversibly bound sugar*; (4) the ability to use these intermediates to study and characterize inhibition of post-Amadori steps of AGE formation thus providing a novel system to investigate the mechanism of reaction and the efficacy of potential agents that could block AGE formation; and (5) with this knowledge it is also further possible to use ^{13}C NMR to study the reactive intermediates and monitor their conversion to various candidate AGEs (Khalifah et al., 1996, *Biochemistry* **35(15)**:4645-4654).

Chemicals and Materials As in Example 1 above.

Preparation of polyclonal antibodies to AGEs

As in Example 1 above.

ELISA detection of AGE products As in Example 1 above.

Amino Acid Analysis Amino acid analyses were carried out at the Biotechnology Support Facility of the Kansas University Medical Center. Analyses were performed after hydrolysis of glycated protein (reduced with sodium cyanoborohydride) with 6 N HCl at 110°C for 18-24 h. Phenyl isothiocyanate was used for derivatization, and PTH derivatives were analyzed by reverse-phase HPLC on an Applied Biosystems amino acid analyzer (420A derivatizer, 130A separation system, 920A data analysis system).

Pentosidine Reverse-Phase HPLC Analysis Pentosidine production in RNase was quantitated by HPLC (Sell & Monnier, 1989, *J. Biol. Chem.* **264**:21597-21602; Odetti et al., 1992, *Diabetes* **41**:153-159). Ribose-modified protein samples were hydrolyzed in 6 N HCl for 18 h at 100°C and then dried in a Speed Vac. The samples were then redissolved, and aliquots were taken into 0.1% trifluoroacetic acid and analyzed by HPLC on a Shimadzu system using a Vydac C-18 column equilibrated with 0.1% TFA. A gradient of 0-6% acetonitrile (0.1% in TFA) was run in 30 min at a flow rate of about 1 ml/min. Pentosidine was detected by 335 nm excitation/385 nm emission fluorescence, and its elution time was determined by running a synthesized standard. Due to the extremely small levels of pentosidine expected (Grandhee & Monnier, 1991, *J. Biol. Chem.* **266**:11649-11653; Dyer et al., 1991, *J. Biol. Chem.* **266**:11654-11660), no attempt was made to quantitate the absolute concentrations. Only relative concentrations were determined from peak areas.

Glycation Modifications Modification with ribose or glucose was generally done at 37°C in 0.4 M phosphate buffer of pH 7.5 containing 0.02% sodium azide. The high buffer concentration was always used with 0.5 M ribose modifications. The solutions were kept in capped tubes and opened only to remove timed aliquots that were immediately frozen for later carrying out the various analyses. "Interrupted glycation" experiments were carried out by first incubating protein with the ribose at 37°C for 8 or 24 h, followed by immediate and extensive dialysis against frequent cold buffer changes at 4°C. The samples were then reincubated by quickly warming to 37°C

in the absence of external ribose. Aliquots were taken and frozen at various intervals for later analysis. Due to the low molecular weight of RNase, protein concentrations were remeasured after dialysis even when low molecular weight cut-off dialysis tubing was used. An alternative procedure was also devised (see below) in which interruption was achieved by simple 100-fold dilution from reaction mixtures containing 0.5 M ribose. Protein concentrations were estimated from UV spectra. The difference in molar extinction between the peak (278 nm) and trough (250 nm) was used for RNase concentration determinations in order to compensate for the general increase in UV absorbance that accompanies glycation. Time-dependent UV-difference spectral studies were carried out to characterize the glycation contributions of the UV spectrum.

Data Analysis and Numerical Simulations of Kinetics Kinetic data were routinely fit to monoexponential or biexponential functions using nonlinear least-squares methods. The kinetic mechanisms of Schemes 5-6 have been examined by numerical simulations of the differential equations of the reaction. Both simulations and fitting to observed kinetics data were carried out with the SCIENTIST 2.0 software package (Micromath, Inc.). Determination of apparent half-times (Figure 6B) from kinetic data fit to two-exponential functions (Figure 6A) was carried out with the "solve" function of MathCAD 4.0 software (MathSoft, Inc.).

RESULTS

Comparison of Glycation by Glucose and Ribose

The reaction of RNase A with ribose and glucose has been followed primarily with ELISA assays, using R479 rabbit AGE-specific antibodies developed against glucose-modified BSA. To a lesser extent, the production of pentosidine, the only known acid-stable fluorescent AGE, was quantiated by HPLC following acid hydrolysis. Preliminary studies using 0.05 M ribose at 37°C showed that the rate of antigenic AGE formation appears to be modestly increased (roughly 2-3 fold as measured by the apparent half-time) as the pH is increased from 5.0 to 7.5, with an apparent small induction period at the beginning of the kinetics in all cases. The glycation of RNase with 0.05 M ribose at pH 7.5 (half-time near 6.5 days) appears to be almost an order of magnitude faster than that of glycation with 1.0 M glucose (half-

time in excess of 30 days; see Figure 7B, solid line). The latter kinetics also displayed a small induction period but incomplete leveling off even after 60 days, making it difficult to estimate a true half-time.

When the dependence of the kinetics on ribose concentration was examined at pH 7.5, a most unexpected result was obtained. The rate of reaction initially increased with increasing ribose concentration, but at concentrations above 0.15 M the rate of reaction leveled off and then significantly decreased (Figure 6A). A plot of the dependence of the reciprocal half-time on the concentration of ribose (Figure 6B) shows that high ribose concentrations are paradoxically inhibitory to post-Amadori antigenic AGE formation. This unusual but consistent effect was found to be independent of changes in the concentration of either buffer (2-fold) or RNase (10-fold), and it was not changed by affinity purification of the R479 antibody on a column of immobilized AGE-RNase. It is also not due to effects of ribose on the ELISA assay itself. The measured inhibitory effect by ribose on post-Amadori AGE formation is not likely due to ribose interference with antibody recognition of the AGE antigenic sites on protein in the ELISA assay. Prior to the first contact with the primary anti-AGE antibody on the ELISA plates, glycated protein has been diluted over 1000-fold, washed extensively with Tween-20 after adsorption, and blocked with a 1% casein coating followed by further washing with Tween-20.

Kinetics of Formation of post-Amadori Antigenic AGEs by "Interrupted Glycation"

In view of the small induction period seen, an attempt was made to determine whether there was some accumulation during the reaction, of an early precursor such as an Amadori intermediate, capable of producing the ELISA-detectable post-Amadori antigenic AGEs. RNase was glycated at pH 7.5 and 37°C with a high ribose concentration of 0.5 M, and the reaction was interrupted after 24 h by immediate cooling to 4°C and dialysis against several changes of cold buffer over a period of 24 h to remove free and reversibly bound (Schiff base) ribose. Such a ribose-free sample was then rapidly warmed to 37°C *without re-adding any ribose*, and was sampled for post-Amadori AGE formation over several days. The AGE antigen production of this 24 h "interrupted glycation" sample is shown by the dashed line and open triangles in Figure 7A, the time spent in the cold dialysis is not included. An uninterrupted control

(solid line and filled circles) is also shown for comparison. Dramatically different kinetics of post-Amadori antigenic AGE formation are evident in the two samples. The kinetics of AGE antigen production of the ribose-free interrupted sample now show (1) monoexponential kinetics with no induction period, (2) a greatly enhanced rate of antigenic AGE formation, with remarkable half-times of the order of 10 h, and (3) production of levels of antigen comparable to those seen in long incubations in the continued presence of ribose (see Figure 6A). Equally significant, the data also demonstrate that negligible AGE antigen was formed during the cold dialysis period, as shown by the small difference between the open triangle and filled circle points at time 1 day in Figure 7A. Very little, if any, AGE was formed by the "interruption" procedure itself. These observations show that a fully competent isolatable intermediate or precursor to antigenic AGE has been generated during the 24 h contact with ribose prior to the removal of the free and reversibly bound sugar.

Samples interrupted after only 8 h produced a final amount of AGE antigen that was about 72% of the 24 h interrupted sample. Samples of RNase glycated with only 0.05 M ribose and interrupted at 8 h by cold dialysis and reincubation at 37°C revealed less than 5% production of ELISA-reactive antigen after 9 days. Interruption at 24 h, however, produced a rapid rise of ELISA antigen (similar to Figure 7A) to a level roughly 50% of that produced in the uninterrupted presence of 0.05 M ribose.

The same general interruption effects were also seen with other proteins (BSA and Hemoglobin). Except for a somewhat different absolute value of the rate constants, and the amount of antigenic AGEs formed during the 24 h 0.5 M ribose incubation, the same dramatic increase in the rate of AGE antigen formation was observed after removal of 0.5 M ribose.

Glycation is much slower with glucose than with ribose (note the difference in time scales between Figure 7A and Figure 7B). However, unlike the case with ribose, interruption after 3 days of glycation by 1.0 M glucose produced negligible buildup of precursor to ELISA-reactive AGE antigens (Figure 7B, dashed curve).

Kinetics of Pentosidine Formation

The samples subjected to ELISA testing were also assayed for the production of pentosidine, an acid-stable AGE. The content of pentosidine was measured for the

same RNase samples analyzed for antibody reactivity by ELISA. Glycation by ribose in 0.4 M phosphate buffer at pH 7.5 produced pentosidine in RNase A that was quantitated by fluroescence after acid hydrolysis. Figure 8A shows that under uninterrupted conditions, 0.05 M ribose produces a progressive increase in pentosidine. However, when glycation is carried out under "interrupted" conditions using 0.5 M ribose, a dramatic increase in the rate of pentosidine formation is seen immediately after removal of excess ribose (Figure 8B), which is similar to, but slightly more rapid than, the kinetics of the appearance of antigenic AGEs (Figure 7A). A greater amount of pentosidine was also produced with 24 h interruption as compared with 8 h. Reproducible differences between the kinetics of formation of pentosidine and antigenic AGEs can also be noted. A significant amount of pentosidine is formed during the 24 h incubation and also during the cold dialysis, resulting in a jump of the dashed vertical line in Figure 8B. Our observations thus demonstrate that a pentosidine precursor accumulates during ribose glycation that can rapidly produce pentosidine after ribose removal (cf. Odetti et al., 1992, *Diabetes* **41**:153-159).

Rate of Buildup of the Reactive Intermediate(s)

The "interrupted glycation" experiments described above demonstrate that a precursor or precursors to both post-Amadori antigenic AGEs and pentosidine can be accumulated during glycation with ribose. The kinetics of formation of this intermediate can be independently followed and quantitated by a variation of the experiments described above. The amount of intermediate generated in RNase at different contact times with ribose can be assayed by the maximal extent to which it can produce antigenic AGE after interruption. At variable times after initiating glycation, the free and reversibly-bound ribose is removed by dialysis in the cold or by rapid dilution (see below). Sufficient time (5 days, which represents several half-lives according to Figure 7A) is then allowed after warming to 37°C for maximal development of post-Amadori antigenic AGEs. The ELISA readings 5 days after each interruption point, representing maximal AGE development, would then be proportional to the intermediate concentration present at the time of interruption.

Figure 9 shows such an experiment where the kinetics of intermediate buildup are measured for RNase A in the presence of 0.5 M ribose (solid symbols and curve).

For comparison, the amount of AGE present before ribose removal at each interruption point is also shown (open symbols and dashed lines). As expected (cf. Figure 7A), little AGE is formed prior to removal (or dilution) of ribose, so that ELISA readings after the 5 day secondary incubation periods are mostly a measure of AGE formed after ribose removal. The results in Figure 9 show that the rate of buildup of intermediate in 0.5 M ribose is exponential and very fast, with a half-time of about 3.3 h. This is about 3-fold more rapid than the observed rate of conversion of the intermediate to antigenic AGEs after interruption (open symbols and dashed curve Figure 7A).

In these experiments the removal of ribose at each interruption time was achieved by 100-fold dilution, and not by dialysis. Simple dilution reduced the concentration of ribose from 0.05 M to 0.005 M. It was independently determined (Figure 6A) that little AGE is produced in this time scale with the residual 5 mM ribose. This dilution approach was primarily dictated by the need for quantitative point-to-point accuracy. Such accuracy would not have been achieved by the dialysis procedure that would be carried out independently for each sample at each interruption point. Our results show that dilution was equivalent to dialysis.

A separate control experiment (see Figure 10 below) demonstrated that the instantaneous 100-fold dilution gave nearly identical results to the dialysis procedure. These control experiments demonstrate that the reversible ribose-protein binding (Schiff base) equilibrium is quite rapid on this time scale. This is consistent with data of Bunn and Higgins (1981, *Science* **213**: 222-224) that indicated that the half-time of Schiff base formation with 0.5 M ribose should be on the order of a few minutes. The 100-fold rapid dilution method to reduce ribose is a valid method where quantitative accuracy is essential and cannot be achieved by multiple dialysis of many samples.

Direct Inhibition of Post-Amadori AGE Formation from the Intermediate by Ribose and Glucose

The increase in the rate of AGE formation after interruption and sugar dilution suggests, but does not prove, that high concentrations of ribose are inhibiting the reaction at or beyond the first "stable" intermediate, presumably the Amadori derivative (boxed in Scheme I). A test of this was then carried out by studying the effect of directly adding ribose, on the post-Amadori reaction. RNase was first incubated for 24

h in 0.5 M ribose in order to prepare the intermediate. Two protocols were then carried out to measure possible inhibition of the post-Amadori formation of antigenic AGEs by different concentrations of ribose. In the first experiment, the 24 h ribated sample was simply diluted 100-fold into solutions containing varying final concentrations of ribose ranging from 0.005 M to 0.505 M (Figure 10A). The rate and extent of AGE formation are clearly seen to be diminished by increasing ribose concentrations. Significantly, up to the highest concentration of 0.5 M ribose, the kinetics appear exponential and do not show the induction period that occurs with uninterrupted glycation (Figures 6A and 7A) in high ribose concentrations.

A second experiment (Figure 10B) was also conducted in which the 24 h interrupted sample was extensively dialyzed in the cold to release free and reversibly bound ribose as well as any inhibitory products that may have formed during the 24 h incubation with ribose. Following this, aliquots were diluted 100-fold into varying concentrations of freshly made ribose, and the formation of antigenic AGE products was monitored as above. There results were nearly identical to the experiment of Figure 10A where the dialysis step was omitted. In both cases, the rate and extent of AGE formation were diminished by increasing concentrations of ribose, and the kinetics appeared exponential with no induction period.

The question of whether glucose or other sugars can also inhibit the formation of AGEs from the reactive intermediate obtained by interrupted glycation in 0.5 M ribose was also investigated. The effects of glucose at concentrations of 1.0-2.0 M were tested (data not shown). Glucose was clearly not as inhibitory as ribose. When the 24 h ribose interrupted sample was diluted 100-fold into these glucose solutions, the amount of antigenic AGE formed was diminished by about 30%, but there was little decrease in the apparent rate constant. Again, the kinetics appeared exponential.

Effect of pH on Post-Amadori Kinetics of AGE Formation

The interrupted glycation method was used to investigate the pH dependence of the post-Amadori kinetics of AGE formation from the reactive intermediate. In these experiments, RNase A was first reacted for 24 h with 0.5 M ribose at pH 7.5 to generate the reactive intermediate. The kinetics of the decay of the intermediate to AGEs were then measured by ELISA. Figure 11 shows that an extremely wide pH range of 5.0-9.5

was achievable when the kinetics were measured by initial rates. A remarkable bell-shaped dependence was observed, showing that the kinetics of antigenic AGEs formation are decreased at both acidic and alkaline pH ranges, with an optimum near pH 8.

A single "pH jump" experiment was also carried out on the pH 5.0 sample studied above which had the slowest rate of antigenic AGE formation. After 12 days at 37°C in pH 5.0 buffer, the pH was adjusted quickly to 7.5, and antigenic AGE formation was monitored by ELISA. Within experimental error, the sample showed identical kinetics (same first order rate constant) of AGE formation to interrupted glycation samples that had been studied directly at pH 7.5 (Figure 12). In this experiment, the relative amounts of antigenic AGE could not be directly compared on the same ELISA plate, but the pH-jumped sample appeared to have formed substantial though somehow diminished levels of antigenic AGEs. These results demonstrate that intermediate can be prepared free of AGE and stored at pH 5 for later studies of conversion to AGEs.

Inhibition of Post-Amadori AGE formation by Aminoguanidine

The efficacy of aminoguanidine was tested by this interrupted glycation method, i.e., by testing its effect on post-Amadori formation of antigenic AGEs after removal of excess and reversibly bound ribose. Figure 20A demonstrates that aminoguanidine has modest effects on blocking the formation of antigenic AGEs in RNase under these conditions, with little inhibition below 50 mM. Approximately 50% inhibition is achieved only at or above 100-250 mM. Note again that in these experiments, the protein was exposed to aminoguanidine only after interruption and removal of free and reversibly bound ribose. Comparable results were also obtained with the interrupted glycation of BSA (Figure 20B).

Amino acid analysis of Interrupted Glycation Samples

Amino acid analysis was carried out on RNase after 24 h contact with 0.5 M ribose (undialyzed), after extensive dialysis of the 24 h glycated sample, and after 5 days of incubation of the latter sample at 37°C. These determinations were made after sodium cyanoborohydride reduction, which reduces Schiff base present on lysines or

the terminal amino group. All three samples, normalized to alanine (12 residues), showed the same residual lysine content (4.0 ± 0.5 out of the original 10 in RNase). This indicates that after 24 h contact with 0.5 M ribose, most of the formed Schiff base adducts had been converted to Amadori or subsequent products. No arginine or histidine residues were lost by modification.

Discussion

The use of rapidly reacting ribose and the discovery of its reversible inhibition of post-Amadori steps have permitted the dissection and determination of the kinetics of different steps of protein glycation in RNase. Most previous kinetic studies of protein "glycation" have actually been restricted to the "early" steps of Schiff base formation and subsequent Amadori rearrangement. Some kinetic studies have been carried out starting with synthesized fructosylamines, i.e. small model Amadori compounds of glucose (Smith and Thornalley, 1992, *Eur. J. Biochem.* **210**:729-739, and references cited therein), but such studies, with few exceptions, have hitherto not been possible with proteins. One notable exception is the demonstration by Monnier (Odetti et al., 1992, *supra*) that BSA partially glycated with ribose can rapidly produce pentosidine after ribose removal. The greater reactivity of ribose has also proven a distinct advantage in quantitatively defining the time course of AGE formation. It is noted that glucose and ribose are both capable of producing similar AGE products, such as pentosidine (Grandhee & Monnier, 1991, *supra*; Dyer et al. 1991, *supra*), and some ^{13}C NMR model compound work has been done with ADP-ribose (Cervantes-Laurean et al., 1993, *Biochemistry* **32**:1528-1534). The present work shows that antigenic AGE products of ribose fully cross-react with anti-AGE antibodies directed against glucose-modified proteins, suggesting that ribose and glucose produce similar antigenic AGEs. The primary kinetic differences observed between these two sugars are probably due to relative differences in the rate constants of steps leading to post-Amadori AGE formation, rather than in the mechanism.

The results presented reveal a marked and paradoxical inhibition of overall AGE formation by high concentrations of ribose (Figure 6) that has not been anticipated by earlier studies. This inhibition is rapidly reversible in the sense that it is removed by dialysis of initially modified protein (Figure 7A) or by simple 100-fold

dilution (as used in Figure 11). The experiments of Figure 10 demonstrate that it is not due to the accumulation of dialyzable inhibitory intermediates during the initial glycation, since dialysis of 24 h modified protein followed by addition of different concentrations of fresh ribose induces the same inhibition. The data of Figure 10A,B show that the inhibition occurs by reversible and rapid interaction of ribose with protein intermediate containing reactive Amadori products. The inhibition is unlikely to apply to the early step of formation of Amadori product due to the rapid rate of formation of the presumed Amadori intermediate that was determined in the experiment of Figure 9. The identification of the reactive intermediate as an Amadori product is well supported by the amino acid analysis carried out (after sodium cyanoborohydrate reduction) before and after dialysis at the 24 h interruption point. The unchanged residual lysine content indicates that any dischageable Schiff bases have already been irreversibly converted (presumably by Amadori rearrangement) by the 24 h time.

The secondary ribose suppression of "late" but not "early" glycation steps significantly enhances the accumulation of a fully-competent reactive Amadori intermediate containing little AGE. Its isolation by the interruption procedure is of importance for kinetic and structural studies, since it allows one to make studies in the absence of free or Schiff base bound sugar and their attendant reactions and complications. For example, the post-Amadori conversion rates to antigenic AGE and pentosidine AGE products have been measured (Figure 7A, open symbols, and Figure 8B), and demonstrated to be much faster (t 1/2 ~ 10 h) than reflected in the overall kinetics under uninterrupted conditions (Figure 6A and Figure 8A). The rapid formation of pentosidine that was measured appears consistent with an earlier interrupted ribose experiment on BSA by Odetti et al. (1992, *supra*). Since ribose and derivatives such as ADP-ribose are normal metabolites, the very high rates of AGE formation seen here suggest that they should be considered more seriously as sources of potential glycation in various cellular compartments (Cervantes-Laurean et al., 1993, *supra*), even though their concentrations are well below those of the less reactive glucose.

Another new application of the isolation of intermediate is in studying the pH dependence of this complex reaction. The unusual bell-shaped pH profile seen for the post-Amadori AGE formation (Figure 11) is in striking contrast to the mild pH

dependence of the overall reaction. The latter kinetics reflect a composite effect of pH on all steps in the reaction, including Schiff base and Amadori product formation, each of which may have a unique pH dependence. This complexity is especially well illustrated by studies of hemoglobin glycation (Lowery et al., 1985, *J. Biol. Chem.* **260**:11611-11618). The bell-shaped pH profile suggests, but does not prove, the involvement of two ionizing groups. If true, the data may imply the participation of a second amino group, such as from a neighboring lysine, in the formation of dominant antigenic AGEs. The observed pH profile and the pH-jump observations described suggest that a useful route to isolating and maintaining the reactive intermediate would be by the rapid lowering of the pH to near 5.0 after 24 h interruption.

The kinetic studies provide new insights into the mechanisms of action of aminoguanidine (guanylhydrazine), an AGE inhibitor proposed by Cerami and co-workers to combine with Amadori intermediates (Brownlee et al., 1986, *supra*). This proposed pharmacological agent is now in Phase III clinical trials for possible therapeutic effects in treating diabetes (Vlassara et al., 1994, *supra*). However, its mechanism of AGE inhibition is likely to be quite complex, since it is multifunctional. As a nucelophilic hydrazine, it can reversibly add to active carbonyls, including aldehydo carbonyls of open-chain glucose and ribose (Khatami et al., 1988, *Life Sci.* **43**:1725-1731; Hirsch et al., 1995, *Carbohyd. Res.* **267**:17-25), as well as keto carbonyls of Amadori compounds. It is also a guanidinium compound that can scavange highly reactive dicarbonyl glycation intermediates such as glyoxal and glucosones (Chen & Cerami, 1993, *J. Carbohyd. Chem.* **12**:731-742; Hirsch et al., 1992, *Carbohyd. Res.* **232**:125-130; Ou & Wolff, 1993, *Biochem. Pharmacol.* **46**:1139-1144). The interrupted glycation method allowed examination of aminoguanidine efficacy on only post-Amadori steps of AGE formation. Equally important, it allowed studies in the absence of free sugar or dicarbonyl-reactive fragments from free sugar (Wolff & Dean, 1987, *Biochem. J.* **245**:243-250; Wells-Knecht et al., 1995, *Biochemistry* **34**:3702-3709) that can combine with aminoguanidine. The results of Figure 20 demonstrate that aminoguanidine has, at best, only a modest effect on post-Amadori AGE formation reactions, achieving 50% inhibition at concentrations above 100-250 mM. The efficacy of aminoguanidine thus predominantly arises either from inhibiting early steps of glycation (Schiff base formation) or from scavenging highly

reactive dicarbonyls generated during glycation. Contrary to the original claims, it does not appear to inhibit AGE formation by complexing the Amadori intermediate.

The use of interrupted glycation is not limited for kinetic studies. Interrupted glycation can simplify structural studies of glycated proteins and identifying unknown AGEs using techniques such as ^{13}C NMR that has been used to detect Amadori adducts of RNase (Neglia et al., 1983, *J. Biol. Chem.* **258**:14279-14283; 1985, *J. Biol. Chem.* **260**:5406-5410). The combined use of structural and kinetic approaches should also be of special interest. For example, although the identity of the dominant antigenic AGEs reacting with the polyclonal antibodies remains uncertain, candidate AGEs, such as the recently proposed (carboxymethyl)lysine (Reddy et al., 1995, *Biochemistry* **34**:10872-10878; cf. Makita et al., 1992, *J. Biol. Chem.* **267**:5133-5138) should display the same kinetics of formation from the reactive intermediate that we have observed. The availability of the interrupted kinetics approach will also help to determine the importance of the Amadori pathway to the formation of this AGE. Similarly, monitoring of the interrupted glycation reaction by techniques such as ^{13}C NMR should identify resonances of other candidate antigenic AGEs as being those displaying similar kinetics of appearance. Table I lists the ^{13}C NMR peaks of the Amadori intermediate of RNase prepared by reaction with C-2 enriched ribose. The downfield peak near 205 ppm is probably due to the carbonyl of the Amadori product. In all cases, the ability to remove excess free and Schiff base sugars through interrupted glycation will considerably simplify isolation, identification, and structural characterization.

Table I lists the peaks that were assigned to the Post-Amadori Intermediate due to their invariant or decreasing intensity with time. Peak positions are listed in ppm downfield from TMS.

Table I 125MHz C-13 NMR Resonances of Ribonuclease Amadori Intermediate Prepared by 24 HR Reaction with 99% [2-C13]Ribose

216.5	ppm	108.5	ppm
211.7		105.9	
208		103.9	
		103	
172		95.8	
165			

163.9	73.65
162.1	70.2
	69.7

Ribonuclease A was reacted for 24 hr with 0.5 M ribose 99% enriched at C-2, following which excess and Schiff base bound ribose was removed by extensive dialysis in the cold. The sample was then warmed back to 37°C immediately before taking a 2 hr NMR scan. The signals from RNase reacted with natural abundance ribose under identical conditions were then subtracted from the NMR spectrum. Thus all peaks shown are due to enriched C-13 that originated at the C-2 position. Some of the peaks arise from degradation products of the intermediate, and these can be identified by the increase in the peak intensity over time. Figure 31 shows the NMR spectrum obtained.

Example 3

***In Vitro* Inhibition of the Formation of Antigenic Advanced Glycation End-Products (AGEs) by Derivatives of Vitamins B_1 and B_6 and Aminoguanidine. Inhibition of Post-Amadori Kinetics Differs from that of Overall Glycation**

The interrupted glycation method for following post-Amadori kinetics of AGE formation allows for the rapid quantitative study of "late" stages of the glycation reaction. Importantly, this method allows for inhibition studies that are free of pathways of AGE formation which arise from glycoxidative products of free sugar or Schiff base (Namiki pathway) as illustrated in Scheme I. Thus the interrupted glycation method allows for the rapid and unique identification and characterization of inhibitors of "late" stages of glycation which lead to antigenic AGE formation.

Among the vitamin B_1 and B_6 derivatives examined, pyridoxamine and thiamine pyrophosphate are unique inhibitors of the post-Amadori pathway of AGE formation. Importantly, it was found that efficacy of inhibition of overall glycation of protein, in the presence of high concentrations of sugar, is not predictive of the ability to inhibit the post-Amadori steps of AGE formation where free sugar is removed. Thus while pyridoxamine, thiamine pyrophosphate and aminoguanidine are potent inhibitors of AGE formation in the overall glycation of protein by glucose, aminoguanidine differs from the other two in that it is not an effective inhibitor of post-Amadori AGE

formation. Aminoguanidine markedly slows the initial rate of AGE formation by ribose under uninterrupted conditions, but has no effect on the final levels of antigenic AGEs produced. Examination of different proteins (RNase, BSA and hemoglobin), confirmed that the inhibition results are generally non-specific as to the protein used, even though there are individual variations in the rates of AGE formation and inhibition.

Chemicals and Materials As in Example 1 above.

Preparation of polyclonal antibodies to AGEs

As in Example 1 above.

ELISA detection of AGE products As in Example 1 above.

Uninterrupted ribose glycation assays Bovine serum albumin, ribonuclease A, and human hemoglobin were incubated with ribose at 37°C in 0.4 M sodium phosphate buffer of pH 7.5 containing 0.02% sodium azide. The protein (10 mg/ml or 1 mg/ml), 0.05 M ribose, and prospective inhibitors (at 0.5, 3, 15 and 50 mM) were introduced into the incubation mixture simultaneously. Solutions were kept in the dark in capped tubes. Aliquots were taken and immediately frozen until analyzed by ELISA at the conclusion of the reaction. The incubations were for 3 weeks (Hb) or 6 weeks (RNase, BSA). Glycation reactions were monitored for constant pH throughout the duration of the experiments.

Interrupted (post-Amadori) ribose glycation assays

Glycation was first carried out by incubating protein (10 mg/ml) with 0.5 M ribose at 37°C in 0.4 M phosphate buffer at pH 7.5 containing 0.2% sodium azide for 24 h in the absence of inhibitors. Glycation was then interrupted to remove excess and reversibly bound (Schiff base) sugar by extensive dialysis against frequent cold buffer changes at 4°C. The glycated intermediate samples containing maximal amount of Amadori product and little AGE (depending on protein) were then quickly warmed to 37°C without re-addition of ribose. This initiated conversion of Amadori intermediates to AGE products in the absence or presence of various concentrations (typically 3, 15 and 50 mM) of prospective inhibitors. Aliquots were taken and frozen at various

intervals for later analysis. The solutions were kept in capped tubes and opened only to remove timed aliquots that were immediately frozen for later carrying out the various analyses.

Numerical Analysis of kinetics data Kinetics data (time progress curves) was routinely fit to mono- or bi-exponential functions using non-linear least squares methods utilizing either SCIENTIST 2.0 (MicroMath, Inc.) or ORIGIN (Microcal, Inc.) software that permit user-defined functions and control of parameters to iterate on. Standard deviations of the parameters of the fitted functions (initial and final ordinate values and rate constants) were returned as measures of the precision of the fits. Apparent half-times for bi-exponential kinetics fits were determined with the "solve" function of MathCad software (MathSoft, Inc.).

RESULTS

Inhibition by vitamin B_6 derivatives of the overall kinetics of AGE formation from Ribose.

The inhibitory effects of vitamin B_1 and B_6 derivatives on the kinetics of antigenic AGE formation were evaluated by polyclonal antibodies specific for AGEs. Initial inhibition studies were carried out on the glycation of bovine ribonuclease A (RNase) in the continuous presence of 0.05 M ribose, which is the concentration of ribose where the rate of AGE formation is near maximal. Figure 13 (control curves, filled rectangles) demonstrates that the formation of antigenic AGEs on RNase when incubated with 0.05 M ribose is relatively rapid, with a half-time of approximately 6 days under these conditions. Pyridoxal-5'-phosphate (Figure 13B) and pyridoxal (Figure 13C) significantly inhibited the rate of AGE formation on RNase at concentrations of 50 mM and 15 mM. Surprisingly, pyridoxine, the alcohol form of vitamin B_6, also moderately inhibited AGE formation on RNase (Figure 13D). Of the B_6 derivatives examined, pyridoxamine at 50 mM was the best inhibitor of the "final" levels of AGE formed on RNase over the 6-week time period monitored (Figure 13A).

Inhibition by vitamin B_1 derivatives of the overall kinetics of AGE formation from Ribose.

All of the B_1 vitamers inhibited antigenic AGE formation on RNase at high concentrations, but the inhibition appeared more complex than for the B_6 derivatives (Figure 14A-C). In the case of thiamine pyrophosphate as the inhibitor (Figure 14A), both the rate of AGE formation and the final levels of AGE produced at the plateau appeared diminished. In the case of thiamine phosphate as the inhibitor (Figure 14B), and thiamine (Figure 14C), there appeared to be little effect on the rate of AGE formation, but a substantial decrease in the final level of AGE formed in the presence of the highest concentration of inhibitor. In general, thiamine pyrophosphate demonstrated greater inhibition than the other two compounds, at the lower concentrations examined.

Inhibition by aminoguanidine of the overall kinetics of AGE formation from Ribose

Inhibition of AGE formation by aminoguanidine (Figure 14D) was distinctly different from that seen in the B_1 and B_6 experiments. Increasing concentration of aminoguanidine decreased the rate of AGE formation on RNase, but did not reduce the final level of AGE formed. The final level of AGE formed after the 6-weeks was nearly identical to that of the control for all tested concentrations of aminoguanidine.

Inhibition of the overall kinetics of AGE formation in serum albumin and hemoglobin from Ribose

Comparative studies were carried out with BSA and human methemoglobin (Hb) to determine whether the observed inhibition was protein-specific. The different derivatives of vitamin B_6 (Figure 15A-D) and vitamin B_1 (Figure 16A-C) exhibited similar inhibition trends when incubated with BSA as with RNase, pyridoxamine and thiamine pyrophosphate being the most effective inhibitors or each family. Pyridoxine failed to inhibit AGE formation on BSA (Figure 15D). Pyridoxal phosphate and pyridoxal (Figure 15B-C) mostly inhibited the rate of AGE formation, but not the final levels of AGE formed. Pyridoxamine (Figure 15A) exhibited some inhibition at lower concentrations, and at the highest concentration tested appeared to inhibit the final levels of AGE formed more effectively than any of the other B_6 derivatives. In the case of B_1 derivatives, the overall extent of inhibition of AGE formation with BSA (Figure 16A-C), was less than that observed with RNase (Figure 14A-C). Higher

concentrations of thiamine and thiamine pyrophosphate inhibited the final levels of AGEs formed, without greatly affecting the rate of AGE formation (Figure 16C). Aminoguanidine again displayed the same inhibition effects with BSA as seen with RNase (Figure 16D), appearing to slow the rate of AGE formation without significantly affecting the final levels of AGE formed.

The kinetics of AGE formation was also examined using Hb in the presence of the B_6 and B_1 vitamin derivatives, and aminoguanidine. The apparent absolute rates of AGE formation were significantly higher with Hb than with either RNase or BSA. However, the tested inhibitors showed essentially similar behavior. The effects of the vitamin B_6 derivatives are shown in Figure 17. Pyridoxamine showed the greatest inhibition at concentrations of 3 mM and above (Figure 17A), and was most effective when compared to pyridoxal phosphate (Figure 17B), pyridoxal (Figure 17C), and pyridoxine (Figure 17D). In the case of the B_1 vitamin derivatives (data not shown), the inhibitory effects were more similar to the BSA inhibition trends than to RNase. The inhibition was only modest at the highest concentrations tested (50 mM), being nearly 30-50% for all three B_1 derivatives. The primary manifestation of inhibition was in the reduction of the final levels of AGE formed.

Inhibition by vitamin B_6 derivatives of the kinetics of post-Amadori ribose AGE formation

Using the interrupted glycation model to assay for inhibition of the "late" post-Amadori AGE formation, kinetics were examined by incubating isolated Amadori intermediates of either RNase or BSA at 37°C in the absence of free or reversibly bound ribose. Ribose sugar that was initially used to prepare the intermediates was removed by cold dialysis after an initial glycation reaction period of 24 h. After AGE formation is allowed to resume, formation of AGE is quite rapid (half-times of about 10 h) in the absence of any inhibitors. Figure 18 shows the effects of pyridoxamine (Figure 18A), pyridoxal phosphate (Figure 18B), and pyridoxal (Figure 18C) on the post-Amadori kinetics of BSA. Pyridoxine did not produce any inhibition (data not shown). Similar experiments were carried out on RNase. Pyridoxamine caused nearly complete inhibition of AGE formation with RNase at 15 mM and 50 mM (Figure 18D).

Pyridoxal did not show any significant inhibition at 15 mM (the highest tested), but pyridoxal phosphate showed significant inhibition at 15 mM. Pyridoxal phosphate is known to be able to affinity label the active site of RNase (Raetz and Auld, 1972, *Biochemistry* **11**:2229-2236).

With BSA, unlike RNase, a significant amount of antigenic AGE formed during the 24 h initial incubation with RNase (25-30%), as evidenced by the higher ELISA readings after removal of ribose at time zero for Figures 18A-C. For both BSA and RNase, the inhibition, when seen, appears to manifest as a decrease in the final levels of AGE formed rather than as a decrease in the rate of formation of AGE.

Inhibition by vitamin B_1 derivatives of the kinetics of post-Amadori ribose AGE formation

Thiamine pyrophosphate inhibited AGE formation more effectively than the other B_1 derivatives with both RNase and BSA (Figure 19). Thiamine showed no effect, while thiamine phosphate showed some intermediate effect. As with the B_6 assays, the post-Amadori inhibition was most apparently manifested as a decrease in the final levels of AGE formed.

Effects of aminoguanidine and N^{α}-acetyl-L-lysine on the kinetics of post-Amadori ribose AGE formation

Figure 20 shows the results of testing aminoguanidine for inhibition of post-Amadori AGE formation kinetics with both BSA and RNase. At 50 mM, inhibition was about 20% in the case of BSA (Figure 20B), and less than 15% with RNase (Figure 20A). The possibility of inhibition by simple amino-containing functionalities was also tested using N^{α}-acetyl-L-lysine (Figure 21), which contains only a free N^{ε}-amino group. N^{α}-acetyl-L-lysine at up to 50 mM failed to exhibit any significant inhibition of AGE formation.

Discussion

Numerous studies have demonstrated that aminoguanidine is an apparently potent inhibitor of many manifestations of nonenzymatic glycation (Brownlee et al.,

1986; Brownlee, 1992,1994, 1995). The inhibitory effects of aminoguanidine on various phenomena that are induced by reducing sugars are widely considered as proof of the involvement of glycation in many such phenomena. Aminoguanidine has recently entered into a second round of Phase III clinical trials for ameliorating the complications of diabetes thought to be caused by glycation of connective tissue proteins due to high levels of sugar.

Data from the kinetic study of uninterrupted "slow" AGE formation with RNase induced by glucose (Example 1) confirmed that aminoguanidine is an effective inhibitor, and further identified a number of derivatives of vitamins B_1 and B_6 as equally or slightly more effective inhibitors. However, the inhibition by aminoguanidine unexpectedly appeared to diminish in effect at the later stages of the AGE formation reaction. Due to the slowness of the glycation of protein with glucose, this surprising observation could not be fully examined. Furthermore, it has been suggested that there may be questions about the long-term stability of aminoguanidine (Ou and Wolff, 1993, *supra*).

Analysis using the much more rapid glycation by ribose allowed for the entire time-course of AGE formation to be completely observed and quantitated during uninterrupted glycation of protein. The use of interrupted glycation uniquely allowed further isolation and examination of only post-Amadori antigenic AGE formation in the absence of free and reversibly bound (Schiff base) ribose. Comparison of the data from these two approaches with the earlier glucose glycation kinetics has provided novel insights into the mechanisms and effectiveness of various inhibitors. Figure 22 are bar graphs which depict summarized comparative data of percent inhibition at defined time points using various concentrations of inhibitor. Figure 22A graphs the data for inhibition after interrupted glycation of RNase AGE formation in ribose. Figure 22B graphs the data for inhibition after interrupted glycation of BSA AGE formation by ribose.

The overall results unambiguously demonstrate that aminoguanidine slows the rate of antigenic AGE formation in the presence of sugar but has little effect on the final amount of post-Amadori AGE formed. Thus observations limited to only the initial "early" stages of AGE formation which indicate efficacy as an inhibitor may in fact be misleading as to the true efficacy of inhibition of post-Amadori AGE formation.

Thus the ability to observe a full-course of reaction using ribose and interrupted glycation gives a more complete picture of the efficacy of inhibition of post-Amadori AGE formation.

Example 4

Animal model & testing of in vivo effects of AGE formation/inhibitors

Hyperglycemia can be rapidly induced (within one or two days) in rats by administration of streptozocin (aka. streptozotocin, STZ) or alloxan. This has become a common model for diabetes melitus. However, these rats manifest nephropathy only after many months of hyperglycemia, and usually just prior to death from end-stage renal disease (ESRD). It is believed that this pathology is caused by the irreversible glucose chemical modification of long-lived proteins such as collagen of the basement membrane. STZ-diabetic rats show albuminuria very late after induction of hyperglycemia, at about 40 weeks usually only just prior to death.

Because of the dramatic rapid effects of ribose demonstrated *in vitro* in the examples above, it was undertaken to examine the effects of ribose administration to rats, and the possible induction of AGEs by the rapid ribose glycation. From this study, a rat model for accelerated ribose induced pathology has been developed.

Effects of very short-term ribose administration in vivo

Phase I Protocol

Two groups of six rats each were given in one day either:

a. 300 mM ribose (two intraperitoneal infusions 6-8 hours apart, each 5% of body weight as ml); or

b. 50 mM ribose (one infusion)

Rats were then kept for 4 days with no further ribose administration, at which time they were sacrificed and the following physiological measurements were determined: (i) initial and final body weight; (ii) final stage kidney weight; (iii) initial and final tail-cuff blood pressure; (iv) creatinine clearance per 100 g body weight.

Albumin filtration rates were not measured, since no rapid changes were initially anticipated. Past experience with STZ-diabetic rats shows that albuminuria develops very late (perhaps 40 weeks) after the induction of hyperglycemia and just

before animals expire.

Renal Physiology Results

a. Final body weight and final single kidney weight was same for low and high ribose treatment groups.

b. Tail-cuff blood pressure increased from 66 ± 4 to 83 ± 3 to rats treated with low ribose (1 x 50 mM), and from 66 ± 4 to 106 ± 5 for rats treated with high ribose (2 x 300 mM). These results are shown in the bar graph of Figure 23.

c. Creatinine clearance, as cc per 100 g body weight, was decreased (normal range expected about 1.0-1.2) in a dose-dependent fashion to 0.87 ± 0.15 for the low ribose group, and decreased still further 30% to 0.62 ± 0.13 for the high ribose group. These results are shown in the bar graph of Figure 24.

Phase I Conclusion

A single day's ribose treatment caused a dose-dependent hypertension and a dose-dependent decrease in glomerular clearance function manifest 4 days later. These are significant metabolic changes of diabetes seen only much later in STZ-diabetic rats. These phenomenon can be hypothesized to be due to ribose irreversible chemical modification (glycation) of protein *in vivo*.

Effect of exposure to higher ribose concentrations for longer time

Phase II Protocol

Groups of rats (3-6) were intraperitoneally given 0.3 M "low ribose dose" (LR) or 1.0 M "high ribose dose" (HR) by twice-daily injections for either (i) 1 day, (ii) a "short-term" (S) of 4 days, or (iii) a "long-term" (L) of 8 days. Additionally, these concentrations of ribose were included in drinking water.

Renal Physiology Results

a. Tail-cuff blood pressure increased in all groups of ribose-treated rats, confirming Phase I results. (Figure 23).

b. Creatinine clearance decreased in all groups in a ribose dose-dependent and time-dependent manner (Figure 24).

c. Albumin Effusion Rate (AER) increased significantly in a ribose-dependent manner at 1-day and 4-day exposures. However, it showed some recovery at 8 day relative to 4 day in the high-dose group but not in the low-dose group. These results are shown in the bar graph of Figure 25.

d. Creatinine clearance per 100 g body weight decreased for both low- and high-ribose groups to about the same extent in a time-dependent manner (Figure 24).

Phase II Conclusion

Exposure to ribose for as little as 4 days leads to hypertension and renal dysfunction, as manifest by both decreased creatinine clearance and increased albumin filtration. These changes are typical of diabetes and are seen at much later times in STZ-diabetic rats.

Intervention by two new therapeutic compounds and aminoguanidine

Phase III Protocol

Sixty rats were randomized into 9 different groups, including those exposed to 1 M ribose for 8 days in the presence and absence of aminoguanidine, pyridoxamine, and thiamine pyrophosphate as follows:

Control Groups:

(i) no treatment;

(ii) high dose (250 mg/kg body weight) of pyridoxamine ("compound-P");

(iii) high dose (250 mg/kg body weight of thiamine pyrophosphate ("compound-T" or "TPP"); and

(iv) low dose (25 mg/kg body weight) of aminoguanidine ("AG").

Test Groups:

(i) only 1 M ribose-saline (2 x 9 cc daily IP for 8 days);

(ii) ribose plus low dose ("LP") of pyridoxamine (25 mg/kg body weight injected as 0.5 ml with 9 cc ribose);

(iii) ribose plus high dose ("HP") of pyridoxamine (250 mg/kg body weight injected as 0.5 ml with 9 cc ribose);

(iv) ribose plus high dose ("HT") of thiamine pyrophosphate (250 mg/kg body weight injected as 0.5 ml with 9 cc ribose); and

(v) ribose plus low dose of amino guanidine (25 mg/kg body weight injected as 0.5 ml with 9 cc ribose).

Unlike Phase II, no ribose was administered in drinking water. Intervention compounds were pre-administered for one day prior to introducing them with ribose.

Renal physiology Results

a. Blood pressure was very slightly increased by the three compounds alone (control group); ribose-elevated BP was not ameliorated by the co-administration of compounds. These results are shown in the bar graph of Figure 26.

b. Creatinine clearance in controls was unchanged, except for TPP which diminished it.

c. Creatinine clearance was normalized when ribose was co-administerd with low dose (25 mg/kg) of either aminoguanidine or pyridoxamine. These results are shown in the bar graph of Figure 27.

d. High concentrations (250 mg/kg) or pyridoxamine and TPP showed only partial protection against the ribose-induced decrease in creatinine clearance (Figure 27).

e. Albumin effusion rate (AER) was elevated by ribose, as well as by high dose of pyridoxamine and TPP, and low dose of aminoguanidine in the absence of ribose. These results are shown in the bar graph of Figure 28.

f. Albumin effusion rate was restored to normal by the co-administration of low dose of both aminoguanidine and pyridoxamine. These results are shown in the bar graph of Figure 29.

Phase III Conclusions

As measured by two indicies of renal function, pyridoxamine and aminoguanidine, both at 25 mg/kg, were apparently effective, and equally so, in preventing the ribose-induced decrease in creatinine clearance and ribose-induced mild increase in albuminuria.

(i) Thiamine pyrophosphate was not tested at 25 mg/kg; (ii) thiamine pyrophosphate and pyridoxamine at 250 mg/kg were partially effective in preventing creatinine clearance decreases but possibly not in preventing mild proteinuria; (iii) at

these very high concentrations and in the absence of ribose, thiamine pyrophosphate alone produced a decrease in creatinine clearance, and both produced mild increases in albuminuria.

Summary

Renal Function and Diabetes

Persistent hyperglycemia in diabetes mellitus leads to diabetic nephropathy in perhaps one third of human patients. Clinically, diabetic nephropathy is defined by the presence of:

1. decrease in renal function (impaired glomerular clearance)
2. an increase in urinary protein (impaired filtration)
3. the simultaneous presence of hypertension

Renal function depends on blood flow (not measured) and the glomerular clearance, which can be measured by either inulin clearance (not measured) or creatinine clearance. Glomerular permeability is measured by albumin filtration rate, but this parameter is quite variable. It is also a log-distribution function: a hundred-fold increase in albumin excretion represents only a two-fold decrease in filtration capacity.

Ribose Diabetic Rat Model

By the above criteria, ribose appears to very rapidly induce manifestations of diabetic nephropathy, as reflected in hypertension, creatinine clearance and albuminuria, even though the latter is not large. In the established STZ diabetic rat, hyperglycemia is rapidly established in 1-2 days, but clinical manifestations of diabetic nephropathy arise very late, perhaps as much as 40 weeks for albuminuria. In general, albuminuria is highly variable from day to day and from animal to animal, although unlike humans, most STZ rats do eventually develop nephropathy.

Intervention by Compounds

Using the ribose-treated animals, pyridoxamine at 25 mg/kg body weight appears to effectively prevent two of the three manifestations usually attributed to diabetes, namely the impairment of creatinine clearance and albumin filtration. It did so as effectively as aminoguanidine. The effectiveness of thiamine pyrophosphate was not

manifest, but it should be emphasized that this may be due to its use at elevated concentrations of 250 mg/kg body weight. Pyridoxamine would have appeared much less effective if only the results at 250 mg/kg body weight are considered.

Effect of Compounds Alone

Overall, the rats appeared to tolerate the compounds well. Kidney weights were not remarkable and little hypertension developed. The physiological effects of the compounds were only tested at 250 mg/kg. Thiamine pyrophosphate, but not pyridoxamine, appeared to decrease creatinine clearance at this concentration. Both appeared to slightly increase albuminuria, but these measurements were perhaps the least reliable.

Human Administration

A typical adult human being of average size weighs between 66 - 77 Kg. Typically, diabetic patients may tend to be overweight and can be over 112 Kg. The Recommended dietary allowances for an adult male of between 66 - 77 Kg, as revised in 1989, called for 1.5 mg per day of thiamine, and 2.0 mg per day of Vitamin B_6 (Merck Manual of Diagnosis and Therapy, 16th edition (Merck & Co., Rathaway, N.J., 1992) pp 938-939).

Based upon the rat model approach, a range of doses for administration of pyridoxamine or thiamine pyrophosphate that is predicted to be effective for inhibiting post-Amadori AGE formation and thus inhibiting related pathologies would fall in the range of 1 mg/100 g body weight to 200 mg/100 g body weight. The appropriate range when co-administered with aminoguanidine will be similar. Calculated for an average adult of 75 Kg, the range (at 10 mg/1 Kg body weight) can be approximately 750 mg to upwards of 150 g (at 2 g/1 Kg body weight). This will naturally vary according to the particular patient.

Example 5

***In Vivo* Inhibition of the Formation of Advanced Glycation End-Products (AGEs) by Derivatives of Vitamins B_1 and B_6 and Aminoguanidine. Inhibition of diabetic nephropathy.**

The interrupted glycation method, as described in the examples above, allows for the rapid generation of stable well-defined protein Amadori intermediates from ribose and other pentose sugars for use in *in vivo* studies.

The effects of 25 mg/kg/day pyridoxamine (PM) and aminoguanidine (AG) on renal pathology induced by injecting Sprague-Dawley rats daily with 50 mg/kg/day of ribose-glycated Amadori-rat serum albumin (RSA), AGE-RSA, and unmodified RSA for 6 weeks. Hyperfiltration (increased creatinine clearance) was transiently seen with rats receiving Amadori-RSA and AGE-RSA, regardless of the presence of PM and AG.

Individuals from each group receiving Amadori-RSA and AGE-RSA exhibited microalbuminuria, but none was seen if PM was co-administered. Immunostaining with anti-RSA revealed glomerular staining in rats treated with AGE-RSA and with Amadori-RSA; and this staining was decreased by treatment with PM but not by AG treatment. A decrease in glomerular sulfated glycosaminoglycans (Alcian blue pH 1.0 stain) was also found in rats treated with glycated (Amadori and AGE) RSA. This appears to be due to reduced heparan sulfate proteoglycans (HSPG), as evidenced by diminished staining with mAb JM-403 that is specific for HSPG side-chain. These HSPG changes were ameliorated by treatment with PM, but not by AG treatment.

Thus we conclude that pyridoxamine can prevent both diabetic-like glomerular loss of heparan sulfate and glomerular deposition of glycated albumin in SD rats chronically treated with ribose-glycated albumin.

Materials and methods

Chemicals

Rat serum albumin (RSA) (fraction V, essentially fatty acid-free 0.005%; A2018), D-ribose, pyridoxamine, and goat alkaline phosphatase-conjugated anti-rabbit IgG were all from Sigma Chemicals. Aminoguanidine hydrochloride was purchased from Aldrich Chemicals.

Preparation of ribated RSA

Rat serum albumin was passed down an Affi-Gel Blue column (Bio-Rad), a heparin-Sepharose CL-6B column (Pharmacia) and an endotoxin-binding affinity column (Detoxigel, Pierce Scientific) to remove any possible contaminants. The purified rat serum albumin (RSA) was then dialyzed in 0.2 M phosphate buffer (pH 7.5). A portion of the RSA (20 mg/ml) was then incubated with 0.5 M ribose for 12 hours at 37°C in the dark. After the 12 hour incubation the reaction mixture was dialyzed in cold 0.2 M sodium phosphate buffer over a 36 hour period at 4°C (this dialysis removes not only the free ribose, but also the Schiff-base intermediaries). At this stage of the glycation process, the ribated protein is classified as Amadori-RSA and is negative for antigenic AGEs, as determined by antibodies reactive with AGE protein (as described previously; R618, antigen:glucose modified AGE-Rnase). The ribated protein is then divided into portions that will be injected either as: a)Amadori-RSA, b)$NaBH_4$-reduced Amadori-RSA, c)AGE-RSA.

The ribated protein to be injected as Amadori-RSA is simply dialyzed against cold PBS at 4°C for 24 hours. A portion of the Amadori-RSA in 0.2 M sodium phosphate is reduced with $NaBH_4$ to form $NaBH_4$-reduced Amadori-RSA. Briefly, aliquots were reduced by adding 5 uL of $NaBH_4$ stock solution (100 mg/ml in 0.1 M NaOH) per mg of protein, incubated for 1 hour at 37°C, treated with HCl to discharge excess $NaBH_4$, and then dialyzed extensively in cold PBS at 4°C for 36 hours. The AGE-RSA was formed by reincubating the Amadori-RSA in the absence of sugar for 3 days. The mixture was then dialyzed against cold PBS at 4°C for 24 hours. All solutions were filtered (22 um filter) sterilized and monitored for endotoxins by a limulus amoebocyte lysate assay (E-Toxate, Sigma Chemical) and contained <0.2 ng/ml before being frozen (-70°C) down into individual aliquots until it was time for injection.

Animal Studies

Male Sprague-Dawley rats (Sasco, 100g) were used. After a 1 week adaptation period, rats were placed in metabolic cages to obtain a 24 hour urine specimen for 2 days before administration of injections. Rats were then divided into experimental and

control groups and given tail vein injections with either saline, unmodified RSA (50 mg/kg), Amadori-RSA (50 mg/kg), $NaBH_4$-reduced Amadori-RSA (50 mg/kg), or AGE-RSA (50 mg/kg).

Rats injected with Amadori-RSA and AGE-RSA were then either left untreated, or futher treated by the administration of either aminoguanidine (AG; 25 mg/kg), pyridoxamine (PM; 25 mg/kg), or a combination of AG and PM (10 mg/kg each) through the drinking water. Body weight and water intake of the rats were monitored weekly in order to adjust dosages. At the conclusion of the experimental study the rats were placed in metabolic cages to obtain 24 hour urine specimen for 2 days prior to sacrificing the animals.

Total protein in the urine samples was determined by Bio-Rad assay. Albumin in urine was determined by competitive ELISA using rabbit anti-rat serum albumin (Cappell) as primary antibody (1/2000) and goat anti-rabbit IgG (Sigma Chemical) as a secondary antibody (1/2000). Urine was tested with Multistix 8 SG (Miles Laboratories) for glucose, ketone, specific gravity, blook, pH, protein, nitrite, and leukocytes. Nothing remarkable was detected other than some protein.

Creatinine measurements were performed with a Beckman creatinine analyzer II. Blood samples were collected by heart puncture before termination and were used in the determination of creatinine clearance, blood glucose (glucose oxidase, Sigma chemical), fructosamine (nitroblue tetrazolium, Sigma chemical), and glycated Hb (columns, Pierce chemicals). Aorta, heart, both kidneys and the rat tail were visually inspected and then quickley removed after perfusing with saline through the right ventricle of the heart. One kidney, aorta, rat tail, and the lower 2/3 of the heart were snap-frozen and then permanently stored at -70°C. The other kidney was sectioned by removing both ends (cortex) to be snap-frozen, with the remaining portions of the kidney being sectioned into thirds with two portions being placed into neutral buffered formalin and the remaining third minced and placed in 2.5% glutaraldehyde/2% paraformaldehyde.

Light Microscopy

After perfusion with saline, kidney sections were fixed in ice-cold 10% neutral buffered formalin. Paraffin-embedded tissue sections from all rat groups (n = 4 per

group) were processed for staining with Harris' alum hematoxylin and eosin (H&E), perodic acid/Schiff reagent (PAS), and alcian blue (pH 1.0 and pH 2.5) stains for histological examination. The alcian blue sections were scored by two investigators in a blinded fashion.

Electron Microscopy

Tissues were fixed in 2.5% glutaraldehyde/2% paraformaldehyde (0.1 M sodium cacodylate, pH 7.4), post-fixed for 1 hour in buffered osmium tetroxide (1.0%), prestained in 0.5% uranyl acetate for 1 hour and embedded in Effapoxy resin. Ultrathin sections were examined by electron microscopy.

Immunofluorescence

Parrafin-embedded sections were deparaffinized and then blocked with 10% goat serum in PBS for 30 min at room temperature. The sections were then incubated for 2 hour at 37°C with primary antibody, either affinity purified polyclonal rabbit anti-AGE antibody, or a polyclonal sheep anti-rat serum albumin antibody (Cappell). The sections were then rinsed for 30 min with PBS and incubated with secondary antibody, either affinity purified FITC-goat anti-rabbit IgG (H+L) double stain grade (Zymed) or a Rhodamine-rabbit anti-sheep IgG (whole) (Cappell) for 1 hour at 37°C. The sections were then rinsed for 30 min with PBS in the dark, mounted in aqueous mounting media for immunocytochemistry (Biomeda), and cover slipped. Sections were scored in a blinded fashion. Kidney sections were evaluated by the number and intensity of glomerular staining in 5 regions around the periphery of the kidney. Scores were normalized for the immunofluorescent score per 100 glomeruli with a scoring system of 0-3.

Preparation of Polyclonal Antibodies to AGE-Proteins

Immunogen was prepared by glycation of BSA (R479 antibodies) or Rnase (R618 antibodies) at 1.6 g protein in 15 ml for 60 – 90 days using 1.5 M glucose in 0.4 M phosphate containing 0.05% sodium azide at pH 7.4 and 37°C. New Zealand white rabbit males of 8-12 weeks were immunized by subcutaneous administration of a 1 ml solution containing 1 mg/ml of glycated protein in Freund's adjuvant. The primary

injection used the complete adjuvant and three boosters were made at three week intervals with Freund's incomplete adjuvant. The rabbits were bled three weeks after the last booster. The serum was collected by centrifugation of clotted whole blood. The antibodies are AGE-specific, being unreactive with either native proteins or with Amadori intermediates.

ELISA Detection of AGE Products

The general method of Engvall (21) was used to perform the ELISA. Glycated protein samples were diluted to approximately 1.5 ug/ml in 0.1 M sodium carbonate buffer of pH 9.5 to 9.7. The protein was coated overnight at room temperature onto a 96-well polystyrene plate by pippetting 200 ul of protein solution into each well (about .3 ug/well). After coating, the excess protein was washed from the wells with a saline solution containing 0.05% Tween-20. The wells were then blocked with 200 ul of 1% casein in carbonate buffer for 2 hours at 37°C followed by washing. Rabbit anti-AGE antibodies were diluted at a titer of 1:350 in incubation buffer and incubated for 1 hour at 37°C, followed by washing. In order to minimize background readings, antibody R618 used to detect glycated RSA was generated by immunization against glycated Rnase. An alkaline phosphatase-conjugated antibody to rabbit IgG was then added as the secondary antibody at a titer of 1:2000 and incubated for 1 hour at 37°C, followed by washing. The *p*-nitrophenolate being monitored at 410 nm with a Dynatech MR4000 microplate reader.

Results

The rats in this study survived the treatments and showed no outward signs of any gross pathology. Some of the rats showed some small weight changes and tail scabbing.

Initial screening of kidney sections with PAS and H&E stains did not reveal any obvious changes, and some EM sections did not reveal any gross changes in the glomerular basement membrane (GBM). However, upon Alcian Blue staining, striking differences were discovered. Alcian blue staining is directed towards negatively charged groups in tissues and can be made selective via changes in the pH of staining. At pH 1.0 Alcian blue is selective for mucopolysaccharides, and at pH 2.5 detects

glucoronic groups. Thus negative charges are detected depending upon the pH of the stain.

At pH 2.5 Alcian blue staining showed that Amadori-RSA ($p<0.05$) and AGE-RSA ($p<0.01$) induced increased staining for acidic glycosaminoglycans (GAG) over control levels (Figure 33). For both AGE-RSA and Amadori-RSA, treatment with pyridoxamine (PM) prevented the increase in staining ($p<0.05$ as compared with controls). In contrast, treatment with aminoguanidine (AG) or combined PM and AG at 10 mg/kg each, did not prevent the increase.

At pH 1.0 Alcian blue staining was significantly decreased by AGE-RSA ($p<0.001$) (Figure 34). However, no significant difference was seen with Amadori-RSA. Due to faint staining, treatment with PM, AG and combined could not be quantitated.

Immunofluorescent glomerular staining for RSA showed elevated staining with Amadori-RSA and AGE-RSA injected animals (Figure 35). Significant reduction of this effect was seen in the rats treated with PM, and not with AG or combined AG & PM.

Immunofluorescent glomerular staining for Heparan Sulfate Proteoglycan Core protein showed slightly reduced staining with Amadori-RSA and AGE-RSA injected animals but were not statistically significant(Figure 36). A reduction of this effect was seen in the rats treated with PM, and not with AG or combined AG & PM. However, immunofluorescent glomerular staining for Heparan Sulfate Proteoglycan side-chain showed highly reduced staining with Amadori-RSA and AGE-RSA injected animals (Figure 37) A significant reduction of this effect was seen in the rats treated with PM, and not with AG or combined AG & PM.

Analysis of average glomerular volume by blinded scoring showed that Amadori-RSA and AGE-RSA caused significant increase in average glomeruli volume (Figure 38). A significant reduction of this effect was seen with treatment of the rats with PM. No effect was seen with treatment with AG or combined AG and PM at 10 mg/kg each.

Example 6 Identification of PM-adducts Formed During Oxidation of Linoleate

Introduction

Modification of the lysine residues of low density lipoprotein (LDL) is thought to be an initiating event in the development of atherosclerosis. Analysis of copper-oxidized LDL ($NaBH_4$ treated protein) leads to modification of approximately 32% of the lysine residues. Analysis of non-reduced oxidized LDL shows that approximately one-half of the modifications are labile to conditions of acid hydrolysis (Steinbrecher, 1987). The majority of the lysine modifications present on oxidized LDL have not been identified. The only characterized and chemically measurable lipoxidation products are N^{ε}-(carboxymethyl)lysine (CML), N^{ε}-(carboxyethyl)lysine (CEL), MDA-lysine and HNE-lysine. These products, however, account for less than 1% of the reducible lysine modifications formed during LDL oxidation. To better understand the changes that occur to LDL *in vivo*, other, more prevalent lipoxidation products need to be identified.

Information on the nature of lysine modifications formed during modification of proteins by lipid peroxidation reactions is scant. Part of the difficulty in identifying modifications is the extreme complexity of poly-unsaturated fatty acid (PUFA) oxidation reactions. Not only do PUFAs produce a large number of oxidation products (Spiteller, 1998), but the kinetics of PUFA oxidation and the quantities of oxidation products also varies from lab to lab depending on such factors as buffer pH, contaminating metal ions, and temperature. The variations affecting the rate of PUFA oxidation and the types of products produced become even more complicated upon introduction of protein into the system. For this reason, identification of specific and measurable lysine modifications has been an ongoing challenge.

In vitro copper-catalyzed oxidation of LDL is a commonly used model for studying covalent modifications that occur to the lysine residues during oxidation of apoB-100 *in vivo*. Several well-known products of lipid peroxidation have been used to modify LDL *in vitro*. Malondialdehyde-modified LDL is taken up by macrophages *in vitro* if greater than 15% of the lysine residues are modified (Haberland, 1982). The α, β-unsaturated aldehyde 4-HNE has been shown to modify LDL more rapidly than MDA (Jürgens, 1986; Uchida, 1994). We have quantified both MDA- and HNE-adducts to lysine in copper-oxidized LDL (Requena, 1997). Though readily detectable, both products together account for less than 1% of the total lysine modifications in copper-oxidized LDL. We hve also quantified CML and CEL in oxidized LDL (~ 2

and 0.2 mmoles/mole lysine, respectively) but like MDA- and HNE-lysine, these are also present at low levels, (Fu, 1996).

Our initial goal was to trap products of lipid peroxidation using pyridoxamine (PM), which has a nucleophilic primary amino group and could therefore serve as a model for the types of modifications that might occur to lysine residues in proteins. PM was easily monitored because of its fluorescence and absorbance properties, and therefore served as a convenient chemical "tag" with which new product formation could be detected. PM was reacted with linoleate (the primary PUFA in LDL) in phosphate buffer at a ratio of 1:5. The reactions were analyzed by RP-HPLC for new product formation. New products, representing PM-adducts to oxidized linoleate, were then isolated and characterized using a variety of techniques. We have identified 2 major products, and propose that these same modifications may account for a significant number of the unidentified lysine modifications *in vivo*.

EXPERIMENTAL PLAN

First, we sought to characterize the types of lysine modifications that occur during LDL oxidation *in vivo*, using model reactions of pyridoxamine (PM) with linoleic acid (the major PUFA in LDL). We describe experiments showing that the primary amino group of PM covalently traps products of linoleate oxidation, and that the two major products formed are amide derivatives of PM.

Secondly, based on observations discussed above, we hypothesized that PM would inhibit the modification of proteins by lipid peroxidation reactions by acting as a "sacrificial nucleophile" or carbonyl trap. We disclose experiments in which PM was shown to inhibit lipoxidative modification in both a model protein system (reaction of bovine pancreatic ribonuclease with arachidonic acid) and during copper-catalyzed oxidation of LDL. We also report that PM demonstrated minimal anti-oxidant activity, consistent with its proposed primary role in trapping reactive carbonyl intermediates formed during lipid peroxidation reactions. This finding is based on measurements of the kinetics of oxidation of linoleate and formation of thiobarbituric acid reactive substances (TBARs) in the presence and absence of PM.

The results demonstrated two important findings. First, the formation of PM-amide derivatives during reaction of PM with linoleate can be used as model for the

types of lysine modifications that occur when LDL is oxidized *in vivo*. This finding is important considering that to this date, fewer than 1% of the lysine modifications of oxidized LDL have been described. Secondly, the inhibition of lipoxidation reactions by PM suggests that it may be effective as a therapeutic agent for inhibiting the development of atherosclerosis and diabetic vascular disease.

Materials

Arachidonic acid, linoleic acid, linoleic acid methyl ester, oleic acid, pyridoxamine (dihydrochloride), pyridoxal (hydrochloride), pyridoxine (hydrochloride), ribonuclease A (Type II-A from bovine pancreas), diethylenetriaminepentaacetic acid, phytic acid, sodium borohydride, borontrichloride-methanol, hexanoyl (caproyl) chloride and aminoguanidine (hemisulfate) were purchased from Sigma. Heptafluorobutyric acid, trifluoracetic acid, acetyl chloride and trifluoroacetic anhydride were purchased from Acros. Azelaic (nonanedioic) acid monomethyl ester was purchased from Aldrich. Low-density lipoprotein was a gift from Dr. Alicia Jenkins of the Department of Medicine, Division of Endocrinology, Medical University of South Carolina.

Methods

Analytical Instrumentation

RP-HPLC was performed on a Waters (Waters Associates, Milford, MA) 600S controller, 660 HPLC pump equipped with a Waters WISP model 723 autosampler, photodiode array detector (model 996) and Shimadzu (Kyoto, Japan) fluorescence detector (RF-535 fluorescence HPLC monitor).

Amino acid analysis was performed using a SSI (Scientific Systems Inc., State College, PA) model 22D HPLC pump and model 232D gradient controller, SSI model 50 column oven (maintained at 55°C) equipped with a Waters Ultra-WISP model 715 autosampler and Waters model 420-AC fluorescence detector. Amino acids were separated using a sulfonated divinylbenzene cation-exchange column (3 x 250 mm) (Pickering Labs, Mountain View, CA) and a Pickering buffering system. The buffers used were of the following composition: buffer A (Na315), pH 3.15, 98% water, 2% sodium citrate, 0.6% HCl; buffer B (Na740) pH 7.5, 93% water, 5% sodium chloride,

1.4% sodium acetate; buffer C (Na Reagent), pH 13, 94% water, 0.4% NaCl, 0.6% NaOH. The gradient used is shown in Table 2.1. Amino acids were derivatized post-column using o-phthaldialdehyde (OPA) and detected by fluorescence (Ex = 365 nm and Em = 425 nm).

Table 2.1:

TIME	%A	%B	%C	FLOW
Initial	100	0	0	0.3
10	100	0	0	0.3
40	40	60	0	0.3
60	0	100	0	0.3
84	0	100	0	0.3
84.1	0	0	100	0.3
86	0	0	100	0.3
86.1	100	0	0	0.3
115	100	0	0	0.3

Gas chromatography/mass spectrometry was performed on a Hewlett-Packard (Palo Alto, CA) model 5890 gas chromatograph/5970 mass selective detector equipped with a Hewlett-Packard model 7673A autosampler. A 30 meter HP-5MS (5% phenyl methyl siloxane) capillary column (Restek, Bellefonte, PA) was used for GC separation.ESI-MS and LC-ESI-MS were performed on a VG-70 triple quadropole mass spectrometer (Analytica ion source) interfaced to a Hewlett Packard series 1100 HPLC pump and degasser. Absorbance was monitored with an ISCO (Lincoln, NE) μLC-10 absorbance detector. Separations were done on an ODS Aquasil column (Keystone Scientific, Bellefonte, PA) using a solvent system of 0.1% HFBA (Buffer A) and acetonitrile (Buffer B). Gradient conditions are shown in Table 2.2.

Table 2.2:

TIME	%A	%B	FLOW (ml/min)
Initial	100	0	0.05
2	100	0	0.05
8	40	60	0.05
12	40	60	0.05
15	25	75	0.05
25	25	75	0.05

Spectrophotometry and Fluorescence

Absorbance measurements were performed on a Hewlett-Packard 8452A photodiode array spectrophotometer. Fluorescence measurements were done on a Shimadzu RF5000U spectrofluorometer. Protein hydrolysates were dried in a Savant (Savant Instruments, Farmingdale, NY) speed-vac concentrator. An N-evap (Organomation, Berlin, MA) was used to dry samples under nitrogen.

Reactions of pyridoxamine with PUFAs

PM (1 mM) was reacted with arachidonate, linoleate or oleate (5 mM) at 37°C in 200 mM sodium phosphate buffer, pH 7.4 for 6 days. Aliquots were removed at days 0, 1, 3 and 6, quenched with 1 mM DTPA and stored at –20°C until analysis. Modification of the amino group of PM was determined by the trinitrobenzenesulfonic acid (TNBS) assay (Spadaro, 1979). Reactions were analyzed by RP-HPLC using a Supelco (Bellefonte, PA) C-18 column (25 mm x 4.6 cm) with the gradient described in Table 2.3 (solvent A = 0.1% HFBA, solvent B = acetonitrile).

Table 2.3:

TIME	%A	%B	FLOW (ml/min)
Initial	100	0	1
2	100	0	1
20	40	60	1
30	40	60	1
31	25	75	1
41	25	75	1
42	100	0	1
55	100	0	1

Products were monitored by fluorescence (Ex = 328nm and Em = 393nm) or absorbance at 294 nm. For some analyses, pyridoxal was added as an internal standard prior to injection.

PM-adducts were isolated on a Beckman (Berkeley, CA) semi-preparative RP-HPLC column using the gradient described in Table 2.4 at a flow of 2 ml/min (solvent A = 0.1% HFBA and solvent B = acetonitrile).

Table 2.4:

TIME	%A	%B	FLOW (ml/min)
Initial	75	25	2
30	75	25	2
40	70	30	2
60	70	30	2
61	30	70	2
80	30	70	2
85	75	25	2
100	75	25	2

Reactions of ribonuclease with arachidonate in the presence of pyridoxamine

RNase (1 mM, 13.7 mg/ml) was reacted with arachidonate (100 mM) alone or in the presence of PM (1 mM) in 200 mM sodium phosphate buffer, pH 7.4. The reactions were done in glass scintillation vials in a 37°C shaking water bath for 6 days, and were prepared using sterile technique to prevent bacterial growth. Aliquots were taken at 0, 1, 3 and 6 days and frozen at –20°C after addition of 1 mM DTPA/phytic acid to quench all metal catalyzed oxidation chemistry.

For GC/MS analysis of lipoxidation products, approximately 1 mg of protein was delipidated according to the method of Folch *et al.* (Folch, 1957). The lower organic phase was discarded and the aqueous phase reduced with 500 mM $NaBH_4$ (in 0.1 N NaOH) in 0.1 M borate buffer, pH 9 for 4 hours at room temperature. The samples were transferred to dialysis tubing (molecular weight cut-off 6,000-8,000) and dialyzed against deionized water for 24 hours at 4°C with 4 water changes. The dialysates were dried *in vacuo,* internal standards (d_8-lysine, d_4-CML, d_4- or d_8-CEL, d_8-MDA-lysine and d_4-HNE-lysine) were added, then hydrolyzed in 6 N HCl at 110°C for 24 hours following. The hydrolysates were reconstituted in 1 ml of 0.1% TFA and applied to a 1-ml Sep-Pak (Waters Corporation, Milford, MA), eluted with 3 ml of 0.1% TFA containing 20% methanol, then dried *in vacuo.* Lysine **(Figure 39)** CML, CEL **(Figures 40 and 41)**, MDA-lysine and HNE-lysine **(Figures 42 and 43)** were derivatized to their trifluoroacetyl methyl esters for GC/MS analysis (Knecht, 1991). Methyl esters were prepared by addition of 1 ml of methanolic-HCl (18.7 ml of anhydrous MeOH + 1.3 ml acetyl chloride) followed by heating at 65°C for 1 hour. The methyl esters were dried under nitrogen then converted to trifluoracetyl derivatives by addition of 1 ml *N,O-* trifluoroacetic acid anhydride and reaction at room

temperature for 1 hour. The derivatized samples were dried under nitrogen and reconstituted in 150 µl methylene chloride for GC/MS analysis.

For GC/MS analysis, the injection port was maintained at 275°C and the temperature program was: 4 min at 140°C, 5°C/min ramp to 220°C, 25°C/min ramp to 300°C, then hold at 300°C for 5 min. Quantification was based on standard curves constructed from mixtures of deuterated and non-deuterated standards. Analyses were performed using selected ion monitoring GC/MS; the following ions were used: lysine and [$^2H_8$]lysine, *m/z* 180 and 187, respectively; CML and [$^2H_4$]CML, *m/z* 392 and 396; CEL and [$^2H_4$]CEL, *m/z* 379 and 383; MDA-lysine and [$^2H_8$]MDA-lysine, *m/z* 474 and 482; HNE-lysine and [$^2H_4$]HNE-lysine, *m/z* 323 and 331.

LDL Oxidations in the presence of PM

LDL was isolated by density centrifugation, then passed through PD-10 (Pharmacia, Sweden) columns pre-equilibrated with 30 ml of PBS (1.5 ml of LDL per column) to remove salts and EDTA, then passed through a Costar 0.4 µm syringe filter (Cambridge, MA) to remove aggregates. The filtered LDL (50 µg/ml) was oxidized in PBS with 5 µM Cu^{2+} for 4-5 hours. Conjugated diene formation was measured at 294 nm at 10-15 minute intervals. For measurements of lipoxidation products, 1 mg (20 ml) of protein was removed at various time intervals and reduced immediately with 500 mM $NaBH_4$ (added dry weight) in 0.1 M borate buffer pH 9 in the presence of 1 mM DTPA overnight at 4°C. The reduced samples were dialyzed against dionized (DI) water for 2 days at 4°C then dried *in vacuo*. The dialysates were reconstituted in 0.5 ml of DI water and delipidated with MeOH:ether (3:1, v/v). Briefly, 3 ml of MeOH:ether was added to the samples with vortexing and the samples were iced for 10 minutes to allow protein precipitation. Following centrifugation in refrigerated centrifuge, the supernatant was removed and discarded. One ml of ether was added to the pellets, the samples were vortexed, iced for 10 minutes, centrifuged, and the supernatant discarded. The ether wash was repeated once more.

Following delipidation, deuterated internal standards were added and the samples were hydrolyzed in 6 N HCl for 24 hours at 110°C and dried *in vacuo*. The hydrolysates were reconstituted in 1 ml of 1% TFA and applied to 1 ml Sep-Pak (Waters, Milford, MA) cartridges pre-washed and equilibrated with 4 ml of MeOH and

4 ml of 1% TFA. Lipoxidation products were eluted with 3 ml of 1% TFA in 20% MeOH. After drying *in vacuo*, the samples were derivatized to trifluoroacetyl methyl esters and analyzed by GC/MS as described above.

For measurement of lysine modification during lipid peroxidation of LDL, 100-150 µg of protein were removed at various time intervals and delipidated according to the method of Folch (1957). The samples were hydrolyzed in 6 N HCl at 110°C for 24 hours, dried *in vacuo* then analyzed by cation-exchange HPLC.

Analysis of thiobarbituric reactive substances (TBARs)

PM (1 mM) was reacted with linoleate (5 mM) in 200 mM sodium phosphate buffer for 6 days at 37°C. Aliquots were removed at 0, 1, 3 and 6 days, quenched with 1 mM DTPA and frozen at –20°C until analysis. TBARs were analyzed according to the method of Sawicki (1963).

Analysis of linoleate by GC/MS

PM was reacted with linoleate as described above, except each time-point was prepared as an independent incubation that was quenched with DTPA and frozen at –20°C until analysis. Linoleate was extracted directly from the reaction vial according to the method of Folch (1957). Briefly, 1 ml of chloroform:methanol (2:1, v/v) was added to the aqueous sample, made 20% in 2N HCl, with vortexing. Following centrifugation, the upper aqueous layer was removed and discarded. Extraction of the organic layer was repeated once more by adding 1 ml of DI water, vortexing, discarding the aqueous phase, then drying the organic phase under nitrogen. Palmitate, the internal standard, was added to all samples, followed by derivatization using boron trichloride-methanol in the presence of 1mM butylated hydroxy toluene (BHT). Boron trichloride-methanol (0.5 ml) was added to the dried linoleate samples and heated at 80°C for 1 hour. Following derivatization, the samples were dried under nitrogen and the nonpolar methyl esters extracted twice with hexane:water (2:1 v/v). The hexane layers were pooled and dried under nitrogen. The methyl esters were reconstituted in 150 µl of methylene chloride then analyzed by GC/MS using single ion monitoring (SIM) of m/z fragments 294 (linoleate) and 220 (palmitate). The temperature program was as follows: 150°C, hold for 3 minutes; 5°C/minute ramp to 180°C; 8°C/minute

ramp to 300°C, hold for 5 minutes. Linoleate was quantified based on standard curves generated from linoleate and palmitate standards.

Characterization of PM-linoleate adducts

Synthesis of *N*-hexanoyl-pyridoxamine (product 267)

N-hexanoyl-pyridoxamine was synthesized from pyridoxamine dihydrochloride and hexanoyl (caproyl) chloride. PM (20 mg) was dissolved in 50 ml of 2N NaOH in a 250 ml round bottomed flask. Hexanoyl chloride (in 30 ml ether) was added drop-wise over an hour to the PM solution; the reaction was kept on ice and stirred vigorously. Following addition of hexanoyl chloride, the reaction was allowed to proceed for 1-2 hours. The ether layer was then removed and dried under nitrogen. The resulting product appeared as a white residue and was fully soluble in water:acetonitrile (50:50 v/v).

Acetylation of PM for GC/MS analysis

PM was acetylated by reaction at room temperature for 2 hours with acetic anhydride/pyridine (1:1, v/v). The solvent was evaporated *in vacuo* and the acetylated PM was reconstituted in methylene chloride and analyzed by GC/MS.

Hydrolysis of product 267

Product 267 was hydrolyzed in 2 N HCl for 4 hours at 95°C. The hydrolysate was then dried *in vacuo*. The resulting free hexanoic acid was analyzed by GC/MS as its propyl ester. Briefly, 1 ml of HCl in dry propanol was added to hexanoic acid and allowed to react at 65°C for 1 hour. Following esterification, the hexanoic acid propyl esters were extracted with 2 ml hexane:water (2:1, v/v). After vortexing, the samples were centrifuged and the upper organic layer removed. Concentration of the hexane layer was performed under nitrogen and on ice to avoid loss of the volatile propyl esters. The temperature program for GC/MS analysis was as follows: initial temperature 75°C, 6°C/min ramp to 110°C, 10°C/min ramp to 180°C hold 5 minutes, 12°C/min ramp to 270°C/min hold 5 minutes.

The aqueous phase containing PM was dried *in vacuo* and PM was either derivatized and analyzed by GC/MS or analyzed by RP-HPLC as described above.

Synthesis of product 339

Synthesis of product 339 was loosely based on the method of D'Alelio et al. (1937). Briefly, 0.3 grams of PM in 0.3 ml of deionized water was combined with 0.3 grams of azelaic acid monomethyl ester and heated at 140°C for 10 hours. The brown reaction mixture was then dried *in vacuo* and reconstituted in deionized water:acetonitrile (1:1, v/v). The reaction mixture was diluted with 0.1% HFBA and analyzed by LC-ESI-MS. After purification by RP-HPLC, product 339 was hydrolyzed in 2N HCl at 95°C for 4 hours. The hydrolysates were analyzed for free PM and nonanedioic acid. PM was analyzed as described above, azelaic acid was analyzed by GC/MS as its dimethyl ester.

Preparation of hexanoylated-BSA

To BSA (5 mg/ml) in 0.1 M sodium borate buffer, pH 9 was added hexanoyl chloride drop-wise over a period of one hour. The reaction was kept on ice with vigorous stirring. Following addition of the acyl chloride, the reaction was continued for at least 2 hours. The samples were then dialyzed against DI water for 24 hours at 4°C with 4 water changes. The dialysates were dried *in vacuo* and reconstituted in DI water. Protein recovery was determined using the Lowry (1951) assay, and amino group modification was determined by the TNBS assay.

Results

Reaction of PM with linoleate

PM, when reacted alone, or when reacted with oleate (a monounsaturated fatty acid), remained stable. However, in the presence of arachidonate and linoleate, approximately 60% of PM was consumed by the end of 6 days. These results suggested that PM was reacting with products of PUFA oxidation.

To determine if the primary amino group of PM was modified during reaction with PUFAs, the incubations were analyzed using the TNBS assay as shown in **Figure 44.** The amino group of PM was not modified when PM was incubated alone or in the presence of oleate, the monounsaturated control. In contrast, approximately 60% of amino groups were modified when PM was reacted with the PUFAs linoleate and

arachidonate. From these results we concluded that the primary amino group of PM was trapping products of PUFA oxidation.

For the characterization of products, PM was reacted with linoleate for 6 days at a molar ratio of 1:5 (linoleate was chosen because it is the primary fatty acid in LDL). In these experiments we were looking for the time-dependent formation of new products eluting downstream from PM that would represent PM-adducts to oxidized linoleate. Two new products were observed that eluted around 24 minutes. Based on fluorescence, the two products accounted for less than 5% of the PM consumed. Considering that almost 60% of PM was consumed overall, it was surprising that no other products were observed. To verify that some products were not binding irreversibly to the reverse-phase C-18 column because of their hydrophobicity, a total fluorescence scan was taken of the PM/linoleate reaction at time 0 and 6 days. The loss of fluorescence determined by these scans was identical to the loss of PM fluorescence determined by RP-HPLC, indicating that the loss in fluorescence was real and not a function of irreversible binding of hydrophobic products to the column.

Because the fluorescent products represented a small fraction of the PM loss, the reactions were analyzed again using absorbance detection at 294 nm. The products eluting between 27 and 28 minutes represent products of linoleate oxidation. However, most of the products eluting between 20 and 25 minutes had an extracted absorbance maximum of 294 nm, suggesting that they contained the PM nucleus. The area containing the potential PM-adducts was collected by semi-preparative RP-HPLC and subjected to LC-ESI-MS. The extracted mass spectrum of the major electrospray active products is shown in **Figure 45**. The major products had m/z values of 267, 305, 479, and 339; 323 was assumed to be the hydrated form of 305. None of these products were present in reactions of linoleate or PM alone. The kinetics of formation of the 3 most abundant products (267, 339 and 305) were determined by RP-HPLC using pyridoxal as an internal standard (**Figure 46**). All three compounds increased with time, with products 267 and 339 consistently forming in the highest yields. For this reason, 267 and 339 were chosen for characterization.

To investigate the chemical properties of 267 and 339, both products were isolated by RP-HPLC from a semi-preparative column, then hydrolyzed 6 N HCl for 24 hours at 110°C, conditions normally used for amino acid analysis. We later learned that

hydrolysis was complete in 4 hours at 95°C. Both 267 and 339 were labile to conditions of acid hydrolysis. Two important observations were made from this experiment. First, hydrolysis of the two compounds confirmed that each contained PM. The recovery of PM was quantitative (based on RP-HPLC analysis using absorbance detection), indicating one PM molecule per molecule of PM-adduct. Additionally, the quantitative recovery of PM allowed us to quantify 267 and 339 using the same extinction coefficient used for PM. Secondly, the linkage between PM and the rest of the compound was acid labile, indicating that it may be either a Schiff base or amide linkage. To distinguish between the two, both 267 and 339 were reduced with sodium borohydride and analyzed by ESI-MS (direct injection). Reduction of a Schiff base would result in an increase of two molecular weight units. After reduction, no change in molecular weight was observed, indicating that neither compound was reducible, which eliminated the presence of a Schiff base linkage. Based on the acid lability and non-reducible properties of 267 and 339, two amide derivatives of PM were proposed, and are shown in **Figure 47**.

Characterization of product 267

Our proposed structure for product 267 was a hexamide derivative of PM. The hexamide derivative was prepared synthetically using PM and caproyl (hexanoyl) chloride (see Materials and Methods). The synthetic reaction mixture was analyzed by LC-ESI-MS to confirm formation of the PM-hexamide derivative. The TIC from the LC-MS shows that 267 was the major product formed during the reaction. The extracted ion chromatogram of m/z 267 showed that only one product having a molecular weight of 267 was formed during the reaction. To verify that the primary amino group of PM participated in an amide linkage (a PM-hexanoate ester derivative would also have a molecular weight of 267), synthetic product 267 was isolated by RP-HPLC then analyzed by the TNBS assay. An equivalent amount of PM standard was analyzed in parallel with product 267 for comparison. No TNBS reactivity was seen in the synthetic 267 compared to the PM standard, indicating that the primary amino group of PM participated in an amide linkage. Next, the synthetic reaction mixture was analyzed by RP-HPLC and compared to authentic 267 isolated from a PM/linoleate

reaction. A mixing experiment between the authentic and synthetic 267 confirmed that the two compounds co-eluted. Final structural verification of 267 (both synthetic and authentic) involved hydrolysis of the compound into free hexanoic acid and PM, followed by derivatization of each for GC/MS analysis. Hydrolysis of synthetic 267 yielded PM and of hexanoic acid in a 1:1 ratio. Identical results were obtained following hydrolysis of authentic 267 isolated from a PM/linoleate reaction. From the results described above we concluded that PM-hexamide is one of the major products formed during reaction of linoleate with PM.

Characterization of product 339

The proposed structure for product 339 corresponds to a PM-nonanedioic acid-amide derivative. To test this hypothesis, synthetic 339 was made by reaction of PM with nonanedioic acid monomethyl ester. The reaction mixture was then analyzed by LC-MS, and the resulting extracted ion chromatogram and mass spectrum confirmed the formation of 339.

Synthetic 339 was isolated by RP-HPLC and analyzed by the TNBS assay to verify covalent attachment of the nonanedioic acid to the primary amino group of PM. The TNBS reactivity was compared to an equivalent amount of PM standard and the results are shown in **Figure 48**. No TNBS reactivity was present in 339, verifying that the amino group of PM participated in the amide bond. For further confirmation of structure, synthetic 339 was hydrolyzed in 2N HCl at 95°C for 4 hours to release free PM and nonanedioic acid. The hydrolysates were derivatized and analyzed by GC/MS for acetylated PM and nonanedioic dimethyl ester. Hydrolysis of 339 yielded complete recovery of PM and of nonanedioic acid in a 1:1 ratio.

Summary

Modification of the lysine residues of apoB-100, the apoprotein associated with LDL, is a hypothesized early event in the development of atherosclerosis. During copper oxidation of LDL, approximately 25% of the lysine residues are modified. However, less than 1% of these lysine modifications have been characterized. The overall purpose of this research project was to identify modifications of lysine residues of protein that form during lipid peroxidation reactions. To do this, PM was used to

trap products of linoleate oxidation, *in vitro*, thereby inhibiting the modification of lysine residues in LDL. From these experiments, the two major PM-adducts were identified as *N*-hexanoyl-PM and *N*-nonanedioyl-PM. Identification of these two products suggest that amide derivatives of lysine may represent a significant fraction of the lysine modifications that occur during the oxidation of LDL, both *in vitro* and *in vivo*. This would explain the observations of Steinbrecher (1987) that a major fraction of lysine modifications in oxidized LDL are resistant to sodium borohydride reduction and are labile to acid hydrolysis.

Discussion

The decrease of free amino groups during reaction of PM with linoleate and arachidonate indicated that PM was trapping products of lipid peroxidation. The amount of TNBS loss agreed well with total PM consumption determined by RP-HPLC, suggesting that the major interaction between PM and PUFAs involves modification of the primary amino group. One of the original reasons for using PM as a trapping agent was to utilize its fluorescence properties for product identification and isolation. Interestingly, the fluorescence response of 267 and 339 is quenched by about a factor of 4 compared to the absorbance response. Fluorescence response also varies among the different B_6 derivatives. For example, pyridoxal is about half as fluorescent as PM, while pyridoxic acid is twice as fluorescent as PM. From these observations it is apparent that slight variations in the structure of PM cause significant changes in its fluorescence. For this reason, when quantifying products 267 and 339 we used absorbance at 294 nm.

As determined by RP-HPLC, of the 50-60% of PM that was consumed during reaction with linoleate, products 267 and 339 accounted for 10% and 5% of the consumed PM, respectively (product 305 accounts for about 2%). Considering the low levels of other lipoxidation markers, products 267 and 339 may constitute major adducts on lipoxidized protein. Only four lipoxidation products have been characterized to date, and each of these has various limitations. For example, CML and CEL are both carbohydrate and lipid derived products, complicating conclusions regarding the origin of protein damage *in vivo*. MDA-lysine and HNE-lysine, while both purely lipid derived products, are subject to rearrangement to other products,

including formation of crosslinks. Furthermore, all four markers represent less than 1% of the lysine modifications formed during lipoxidation reactions. Consequently, the need for additional markers of lipid-derived damage to proteins is evident, and the identification of amide derivatives of lysine may provide a convenient and sensitive tool for assessing protein oxidation. In fact, Kato and colleagues (1999) recently identified the hexamide derivative of *N*-benzoyl-glycyl-L-lysine following reaction with the 13-hydroperoxide of linoleic acid. Also supportive is that approximately half of the lysine modifications formed during oxidation of LDL are acid labile. The structure of the labile products are not known, but hexanoic acid-, nonanedioic acid- or other amide derivatives of lysine may represent a large portion of such lysine modifications *in vivo*. Based on studies of 267 and 339, these types of derivatives can be hydrolyzed under relatively mild conditions of acid hydrolysis, namely 2N HCl at 95°C for 2 hours. Once hydrolyzed, the released carboxylic acid derivatives could be esterified and measured by GC/MS.

While this aspect of the present invention is not limited to a specific method of formation of PM adducts of linoleate oxidation, a proposed mechanism of formation of 267 and 339 is shown in **Figure 49**. The hydroperoxides produced upon oxidation of linoleic acid are known to dehydrate to form ketoacids (Spiteller, 1998). Nucleophilic attack on the keto acid by PM would form a Schiff base, which could then undergo oxidative cleavage to form the corresponding amide derivative. Theoretically, oxidative cleavage could occur on either side of the imine carbon. However, formation of the alternate cleavage products was not observed during reactions of PM with linoleate. The preference for cleavage and release of the vinyl group is probably driven by stabilization of an intermediate radical by the conjugated hydrocarbon system **(Figure 50)**.

Clearly, lipid peroxidation is an extremely complicated series of reactions that is sensitive to variations in reaction conditions. From our model system of PM and linoleate, we propose that amide derivatives of lysine may constitute a significant fraction of the lysine modification formed *in vivo*. Thus, these derivatives can serve as diagnostic markers for in vivo oxidative protein damage. Preferably, the presence and/or concentration of amide derivatives of lysine, including but not limited to hexanoic acid and nonanedioic acid, are determined from urine, blood, or skin biopsy

samples. In a most preferred embodiment, both blood plasma protein and skin biopsy samples are used. The levels of amide derivatives in blood plasma and/or urine serves as an indicator of current exposure, since the half-life of plasma proteins is approximately 2-3 weeks. Conversely, the half life of skin proteins such as collagen and elastin is approximately 35 years, and thus determination of amide derivatives of lysine in skin collagen serves as a diagnostic marker for accumulated chemical damage. Such determinations could utilize the chemical methods detailed herein, or could involve quantitative immunochemical techniques, which would require antibodies specific for the derivative form of the protein to be analyzed (for example, lipoprotein). The immunochemical method (and kits for practicing the method) could also utilize protein standards, (such as modified lipoprotein, where the extent of modification is known) and control samples (for example, the appropriate body fluid from someone with chronic atherosclerosis and/or from someone free of atherosclerosis.

As an additional note, the trapping properties of PM suggest that it may be an effective inhibitor of the oxidative modification of lysine residues on protein during lipid peroxidation reactions.

Example 7 Pyridoxamine Inhibits Lipoxidation Reactions, *In Vitro*

Introduction

Clearance of native LDL from the circulation is dependent on recognition of LDL by the LDL receptor in liver and peripheral tissues. Interactions between this receptor and the apoB-100 component of LDL occur between a region of acidic amino acids on the receptor and a lysine-rich region on the protein (Goldstein, 1974). Covalent modification of the lysine residues (by acetylation, or by reaction with MDA, HNE and other lipid peroxidation products) in the receptor binding region of apoB-100 prevents recognition of LDL by the receptor (Steinbrecher, 1987). Consequently, the modified LDL is taken up the scavenger receptor of macrophages leading to foam cell formation, a hypothesized initiating event in the pathogenesis of atherosclerosis.

Oxidative modification of LDL *in vitro* interferes with its recognition by the LDL receptor and promotes its recognition by the macrophage scavenger receptor. Transition metal ions accelerate the oxidation of LDL, and for this reason, copper-catalyzed oxidation of LDL *in vitro* is a commonly used model for studying chemical

modifications of LDL *in vivo*. Characteristic changes that occur to copper oxidized LDL include increased fluorescence (Ex. 350nm, Em. 433nm), increased conjugated diene formation (absorbance at 234 nm), increased anodic electrophoretic mobility, increased uptake by macrophages, and chemical modification of the lysine residues of apoB protein (Esterbauer, 1992). The majority of lysine modifications that occur during oxidation of LDL are uncharacterized. However, it is generally accepted that the modifications arise from reaction of carbonyl and dicarbonyl compounds with the primary, ε-amino group of lysine residues. As a result, a number of nucleophilic compounds have been evaluated as traps for reactive carbonyls and inhibitors of oxidative modifications of LDL and other proteins.

Experimental Design

The reactive carbonyl and dicarbonyl compounds produced during oxidation of sugars are also produced during oxidation of PUFAs. Because PM was an effective AGE inhibitor during glycation reactions (presumably by trapping carbonyls) we hypothesized that PM would also act as an effective lipoxidation inhibitor.

This example describes the experiments used to test PM's effectiveness as an inhibitor of lipoxidation reactions. We began with a model protein system of RNase incubated with arachidonate in the presence and absence of PM. Arachidonate was chosen for these studies because of its rapid rate of oxidation (the initial biphasic reaction mixtures become monophasic within 2 days). The formation of CML, CEL, MDA-lysine, HNE-lysine and loss of free lysine residues was monitored during the oxidation of arachidonate. In these experiments the RNase concentration was 1 mM (10 mM lysine), PM was 1 mM, and arachidonate was 100 mM.

Experiments with model protein were followed by experiments with the biologically relevant protein, LDL. Copper-catalyzed oxidation of LDL was monitored by measurements of conjugated diene (A_{234nm}) formation, changes in electrophoretic mobility, formation of lipoxidation products and modification of lysine residues.

Results

PM inhibition of lipoxidative modification of RNase by arachidonate

As shown in **Figure 52**, CML, CEL, MDA-lysine and HNE-lysine were formed

rapidly in RNase during incubation with arachidonate. MDA-lysine and HNE-lysine are characteristic products of lipoxidation reactions. Formation of CML was consistent with results of Fu et al. (1996) who first showed that CML was a product of lipoxidation as well as glycoxidation reactions. The formation of CEL during reaction of RNase with arachidonate represents the first evidence that CEL, like CML, forms during both glycoxidation and lipoxidation reactions. Interestingly, unlike CML, which is formed from oxidation of both arachidonate ($20:4^{\Delta 5,8,11,14}$) and linoleate ($18:2^{\Delta 9,12}$), CEL was formed in only trace amounts from oxidized linoleate compared to arachidonate, indicating that CML and CEL likely form from different sources in vivo.

Addition of 1 mM PM to the RNase/arachidonate reactions resulted in almost complete inhibition of formation of CML, CEL (Figure 52), MDA-lysine and HNE-lysine (Figure 53). The early plateau phase and decline in MDA-lysine formation resembles that seen during copper oxidation of LDL (Requena, 1997) and is thought to result from further reaction of MDA-lysine to form cross links, such as lysine-MDA-lysine (LML) (Requena, 1997).

To examine PM's effect on total lysine modification, we quantified lysine by cation-exchange HPLC after hydrolysis of the protein. Lipoxidation products such as MDA-lysine and HNE-lysine contain reactive Schiff base and aldehyde functional groups that are not stable to conditions of acid hydrolysis. To stabilize these adducts, the protein was first reduced with $NaBH_4$, converting imines and aldehydes to amines and alcohols, respectively. Amino acid analysis indicated that 58% of lysine residues were modified during reaction of RNase with arachidonate. Lysine loss decreased by approximately one-half in non-reduced samples (data not shown), confirming formation of acid-labile lysine modifications. PM, at 1 mM, decreased lysine loss to approximately 5% at the end of 6 days. It is interesting to note that less than 1% of the 58% modified lysine residues can be accounted for by CML, CEL, MDA-lysine and HNE-lysine.

The measurements of lipoxidation product formation and of free lysine modification discussed above showed that levels of lipoxidation products and of lysine modification began to rise at about 3 days. This led us to suspect that PM was becoming saturated after 3 days of reaction. To test this, we quantified PM consumption during reactions of RNase with AA by RP-HPLC, which showed that

virtually all the PM was consumed after 3 days of reaction with AA, explaining the increase in CML, CEL, MDA-lysine, HNE-lysine, and lysine modification after 3 days.

Based on the results obtained from reaction of RNase with arachidonate, we confirmed our hypothesis that PM was a potent inhibitor of lipoxidative modification of proteins, even when present at a 10-fold lower concentration than lysine (in RNase) and a 100-fold lower concentration than PUFA. During reaction of RNase with AA, the reaction mixture changed from biphasic to monophasic after 2 days. The inclusion of PM during reaction of RNase with AA appeared to prolong the change from a biphasic to a monophasic system to approximately 3-4 days, but by 6 days the PM-containing reactions were also monophasic, indicating complete oxidation of AA. The fact that PM allowed oxidation of AA but inhibited modification of RNase indicated that PM's primary mechanism of action involved trapping of intermediates produced during the lipid peroxidation reactions.

PM inhibits lipoxidative modification of LDL during metal-catalyzed oxidation

Since PM inhibited lipoxidation chemistry in the RNase/arachidonate model protein system, we evaluated its effectiveness as an inhibitor of lipoxidation during copper-catalyzed oxidation of LDL. Because of limited LDL protein availability, the LDL experiments were done in two parts. The first set of LDL oxidations was done in the presence of 10 or 100 μM PM, and the effect of PM on CML, CEL, MDA-lysine and HNE-lysine formation was measured by GC/MS. For the second set, the concentration of PM was increased to 100 and 250 μM, and the effects of PM on conjugated diene formation, electrophoretic mobility, and lysine modification were determined.

At concentrations of 100 and 250 μM PM, in a concentration-dependent manner, prolonged the lag phase of conjugated diene formation during oxidation of LDL (**Figure 54**) and lowered the total amount of conjugated dienes present at the end of the oxidation. As with RNase, oxidation of LDL proceeded in the presence of PM, yielding similar amounts of A_{234nm}. PM, at both concentrations, also decreased the electrophoretic mobility of oxidized LDL in comparison to the copper oxidized control. Copper oxidation of LDL resulted in formation of CML at levels consistent with those

previously reported by Requena *et al* (1997). Similar to the results obtained during reaction of RNase with arachidonate, CEL was formed at concentrations approximately 10-fold lower than CML. PM, at 100 and 250 μM, inhibited CML (70% and 80%, respectively) CEL (43% and 71%) (**Figure 55**), MDA-lysine (8% and 46%) and HNE-lysine (60% and 83%) formation (**Figure 56**). In addition, total lysine modification was decreased by 62% by 100 μM PM and 87% by 250 μM PM in nonreduced and reduced samples (**Figure 57**). CML, CEL, MDA-lysine and HNE-lysine accounted for approximately 1% of the lysine modifications. These results demonstrate that PM not only inhibits formation of CML, CEL, MDA-lysine and HNE-lysine, but also provides protection against total lysine modification during copper-catalyzed oxidation of LDL.

PM has minimal antioxidant activity against lipid peroxidation

The TBARs assay recognizes primarily malondialdehyde, but also reacts with other compounds produced during PUFA oxidation (such as glyoxal). It is likely that some TBA-reactive compounds continue on to form other products, as shown in **Figure 58**. For example, aldehydes that may polymerize via aldol condensation reactions. This would explain the decrease in TBARs. The production of TBARs during oxidation of linoleate increased during the first 3 days of reaction then decreased by day 6 (**Figure 58**). PM slowed the rate of formation of TBARs by approximately 30%, but did not have a significant effect on the final yield of TBARs in the reaction mixture. Overall, the inhibitory effect of PM on the rate of TBARs formation during oxidation of linoleate suggests that PM does have some antioxidant activity, retarding, rather than completely inhibiting, lipid peroxidation.

Oxidation of linoleate (5 mM) in phosphate buffer for 6 days resulted in complete destruction of the PUFA by 3 days. The rate of linoleate oxidation was slowed approximately 10% by 1 mM PM, though the final extent of linoleate oxidation was not affected (**Figure 59**). The results of these experiments are consistent with those on TBARs formation and LDL oxidation, in that PM slowed the kinetics of lipid peroxidation but had little effect on the final extent of oxidation.

Discussion

The trapping of lipid intermediates by PM suggested that it might inhibit the modification of proteins by lipid peroxidation reactions by acting as a sacrificial nucleophile. To test this hypothesis, PM was included in reactions of model protein (RNase) with arachidonic acid. The effect of PM on copper-catalyzed oxidation of LDL was also studied. In both the RNase/arachidonate system and during oxidation of LDL, PM inhibited the formation of the lipoxidation products CML, CEL, MDA-lysine and HNE-lysine. PM also prevented the modification of lysine residues during these reactions. The results of these experiments suggest that PM might be useful therapeutically for inhibiting the oxidative chemical modification of proteins and thereby limiting the progression of chronic diseases such as diabetes and atherosclerosis.

Exposure of RNase to a 100-fold excess of peroxidizing arachidonate over a period of 6 days resulted in rapid oxidation and solubilization (within 2 days) of the arachidonate and a high percentage of lysine modification. Visually, reactions containing PM remained biphasic longer than those without, indicating that PM had some chelating or antioxidant activity. These visual observations were confirmed chemically when PM was shown to inhibit formation of CML, CEL, MDA-lysine and HNE-lysine, despite the large excess of PUFA to PM (100:1) and of lysine to PM (10:1).

The efficiency with which PM protected against total lysine modifications despite the excess of PUFA, further established that PM is an effective inhibitor of lipoxidation reactions. The concentration of reactive carbonyls produced during oxidation of 100 mM arachidonate greatly exceeds the trapping capacity of 1 mM PM (assuming 1 carbonyl trapped per molecule PM), yet PM still was an effective protector of lysine residues. This suggests that only a small fraction of lipid peroxidation products may participate in lysine modification. Alternatively, PM may intercept early lipid peroxidation products, preventing further oxidation of the products into a larger number of short-chain carbonyl compounds that could also modify protein. This is consistent with the observation that PUFA reactions containing PM appeared to become soluble (monophasic) more slowly than PUFAs oxidized alone. The PM-

containing reactions probably contain more long chain, insoluble compounds (presumably covalently attached to PM) in comparison to the reactions without PM. During lipid peroxidation, it is possible that the majority of protein modification occurs by reaction of short chain, water-soluble carbonyl compounds with primary amino groups exposed to the aqueous environment. By preventing the formation of short-chain lipid peroxidation products, PM would protect the protein against "carbonyl stress" and therefore would undergo less modification. The result: an effective degree of protein protection by a minimum concentration of PM, an attractive quality for a potential drug.

The inhibition of lipoxidation in the RNase model system suggested that PM would have similar effects during copper-catalyzed oxidation of LDL. As shown in **Figure 54**, both 100 and 250 μM PM, in a dose-dependent manner, were effective in prolonging the lag phase and lowering the total amount of conjugated dienes formed. If PM was solely a carbonyl trap, it should have no effect on the initiation phase of lipid peroxidation, but would become effective during the propagation phase, when the hydroperoxides break down into smaller products. However, the fact that PM prolongs the lag phase of conjugated diene formation suggests that PM has some radical scavenging or chelating activity. In fact, the structure of PM is not unlike many compounds that function as radical scavengers; most aromatic amines or phenols have antioxidant activity (Halliwell, 1989). It is possible that PM, like Vitamin E, reacts with lipid peroxy and alkoxy radicals, thus slowing the propagation phase of lipid peroxidation.

The increase in electrophoretic mobility observed following LDL oxidation is poorly understood. Several processes are probably responsible for the increase in negative charge. The most logical explanation is modification of positively charged amino groups by either Schiff's base or Michael adduct formation. An additional possibility involves attachment of negatively charged entities to the surface of LDL. Some studies suggest the presence of negatively charged groups formed after copper oxidation of LDL (Brnjas-Kraljevic, 1991). Whatever the cause, PM, at both concentrations, successfully decreased the electrophoretic mobility of copper oxidized LDL. Additionally, and similar to the results seen in the model experiments, PM effectively inhibited CML, CEL, MDA-lysine and HNE-lysine formation during LDL

oxidation, in a dose dependent manner. Finally, and perhaps most importantly, PM protected against total lysine modification during oxidation of LDL. Though PM clearly prevented lipoxidation, levels of each lipoxidation product appeared to begin increasing after approximately 2 hours of oxidation, suggesting consumption of PM during later stages of LDL oxidation. This is not unlikely considering the ratio of PM to reactive intermediates produced during oxidation of 50 μg/ml LDL. The protein concentration of LDL used in our experiments (50 mg/ml) corresponds to a PUFA concentration of 117 μM, and a ratio of PM to linoleate and to arachidonate of 1:1 and 8:1, respectively. Esterbauer (1992) reports that oxidation of a similar concentration of LDL with 1.66 μM copper results in formation of 27 μM total aldehydes, 50 μM peroxides, and 24 μM conjugated dienes. Taken together, the concentration of reactive compounds following oxidation of LDL with 1.66 μM copper is roughly 100 μM. Our experiments contained 3 times as much copper (5 μM) and we would therefore expect a faster rate of oxidation. Esterbauer's estimation also did not include other reactive intermediates such as endo- and exo-peroxides, epoxides, ketoacids and smaller compounds like glyoxal. Nonetheless, using Esterbauer's estimations, the ratio of PM to reactive intermediates in the LDL oxidations analyzed for CML, CEL, MDA-lysine and HNE-lysine was 1:10 (10 μM PM: 100 μM reactive products) and 1:1. Thus, the observation that PM appeared to become saturated (less effective) during the later stages of LDL oxidation is understandable. However, considering the dose-dependent response to PM, it is certain that larger doses of PM would prove more effective in preventing protein modification. In addition, the rate of carbonyl production during *in vitro* copper-catalyzed oxidation of LDL is much faster than what would occur *in vivo*. Also encouraging is that μM concentrations of PM were effective yet nontoxic in a small animal model (as shown above), indicating that larger doses should be tolerable *in vivo*.

That PM retarded but did not prevent lipid peroxidation (as demonstrated by measurement of TBARs formation and rate of linoleate oxidation) suggests that the antioxidant activity of PM is a minor contributor to its mechanism of action. The mild antioxidant effects of PM were not completely unexpected. In fact, PM contains two functional groups common to many antioxidants; most antioxidants are aromatic amines or phenols. These types of antioxidants inhibit the propagation phase of lipid

peroxidation by donation of a hydrogen atom to a peroxy or alkoxy radical. The resulting antioxidant radical delocalizes into the aromatic ring structure and is not reactive enough itself to perform hydrogen abstraction and further propagate the reaction. **Figure 60** represents a possible mechanism for the antioxidant activity of PM. The ratio of PM to Cu^{2+} in the LDL oxidation experiments was 50:1, yet oxidation of LDL still took place. From the results shown herein it is clear that the major mechanism of inhibition of PM, at least during reaction with linoleate, probably does not involve radical scavenging. For example, during oxidation of LDL, PM slowed conjugated diene formation (an index of PUFA oxidation) but did not prevent it. In contrast, PM virtually prevented lysine modification in the same experiment. This implies that PM acted primarily as a trapping agent (by protecting lysine from modification) and secondly as an antioxidant (by slowing, but not preventing, lipid peroxidation).

The finding that PM, *in vitro*, appears to interrupt lipid peroxidation via two mechanisms (carbonyl trapping and antioxidant) is encouraging. PM may prove to be a powerful and multifunctional drug for the treatment of diabetes, atherosclerosis, and other chronic and inflammatory diseases in which chronic oxidative modifications of proteins is considered to be part of the pathogenic process.

Identification of amide-derivatives of PM: implication for lysine modifications *in vivo*.

During copper-catalyzed oxidation of LDL, approximately half of the lysine modifications that form are labile to conditions of acid hydrolysis (Steinbrecher, 1987). The identification of *N*-hexanoyl-PM and *N*-nonanedioyl-PM from reactions of PM with linoleic acid suggests that amide derivatives may constitute a significant portion of the acid-labile lysine modifications formed during LDL oxidation. Formation of amide derivatives of lysine would also contribute to the increased electrophoretic mobility that occurs during LDL oxidation. Kato and colleagues (1999) have identified the hexamide derivative of hippuryllysine as a product formed during incubation of hippuryllysine with the hydroperoxide of linoleic acid. They went on to show immunohistochemical evidence for the existence of N-hexanoyl-lysine in human atherosclerotic lesions.

Linoleate is the major PUFA in LDL; therefore, the formation of *N*-hexanoyl- and *N*-nonanedioyl-lysine would be expected during LDL oxidation based on our

results from reactions of linoleate with PM. However, LDL also contains arachidonate, albeit at a much lower concentration than linoleate (the ratio of arachidonate to linoleate in LDL is approximately 1:8) (Esterbauer, 1992). However, the oxidation of AA is more facile than that of linoleate because of the presence of 3 *bis*-allylic carbons, but the formation of amide derivatives may be possible from this PUFA as well as from linoleate. Like linoleate, arachidonate is an ω-6 PUFA, and produces a 15-hydroperoxide that, through the mechanism we proposed earlier for formation of 267 (nucleophilic addition of a primary amine on a ketoacid), could conceivably lead to formation of *N*-hexanoyl derivatives of lysine. However, oxidation of arachidonate forms several other hydroperoxides that may lead to several amide derivatives of varying chain lengths, such as a pentadioic-amide derivative (formed from the 5-hydroperoxide) and longer chain unsaturated fatty acid derivatives. As a result, future studies of amide formation during the oxidation of LDL or from other modified proteins should not be limited to 6- and 9- carbon chain-length acids.

Because amide derivatives are not reducible by sodium borohydride and are not stable to acid hydrolysis, their detection in lipoxidatively modified proteins would be indirect. Modified protein, such as LDL, could be hydrolyzed under relatively mild conditions, e.g. 2N HCl at 95°C for 2 hours. This would release the amide derivatives as the free carboxylic acids, which in turn could be separated from the protein (by organic extraction) and analyzed as their ester derivatives by GC/MS. Carboxylic acids containing less than 6 carbons may require either headspace GC analysis or conversion to heavy ester derivatives (such as butyl esters) because of their volatility.

Immunological methods for detection of protein modifications are an alternative approach. For example, antibodies could be raised against hexanoyl-modified proteins then used to detect related derivatives in tissues. Production of both polyclonal and monoclonal antibodies is well known in the art. See, Antibodies: A Laboratory Manual, Harlow et al., eds., Cold Spring Harbor, N.Y. (1988). For polyclonal antibodies, a hexanoyl-modified protein(s), in the presence of an adjuvant, is injected into rabbits with a series of booster shots in a prescribed schedule optimal for high titers of antibody in serum. An extensive description for producing monoclonal antibodies derived from the spleen B cells of an immunized mouse and an immortalized myeloma cell is found in the above reference for polyclonal antisera production. Mice

are immunized with hexanoyl-modified protein(s). Following cell fusion, selection for hybrid cells' and subcloning, hybridomas are screened for a positive antibody against the hexanoyl-modified protein(s) using an indirect ELISA assay

Regardless of the method of analysis, the identification of *N*-hexanoyl and *N*-nonanedioyl derivatives of lysine *in vivo* should prove invaluable. For the first time, a significant marker of lipid-derived modification of protein has been identified that should be useful 1) to assess levels of oxidative damage to protein *in vivo* and 2) to better understand the processes that lead to the development of atherosclerosis.

Inhibition of Lipoxidation by PM: Implications for Drug Therapy

Diabetes is associated with an increased risk of cardiovascular disease and is also accompanied by increased lipid peroxidation that may actually be catalyzed by hyperglycemia (Chisholm, 1992 and Tsai, 1994). The modification of proteins by lipid peroxidation reactions is implicated in the pathology of various complications associated with diabetes and atherosclerosis. Specific modifications of protein that have been identified on lysine residues that occur during lipid peroxidation include, CML, CEL, MDA-lysine and HNE-lysine. These products represent a very small fraction of the lysine modifications that occur during oxidation of LDL, but are the only protein modifications currently characterized. Inhibition of these 4 compounds, and inhibition of total lysine modification, by PM *in vitro* suggests that this B_6 vitamer may provide a useful therapeutic agent for the treatment of complications arising from the chemical modification of proteins *in vivo*.

From our experiments with both model protein and copper-catalyzed oxidation of LDL, PM appears to effectively inhibit lipoxidation by trapping products of lipid peroxidation, although the process of lipid peroxidation itself continues. It is interesting to note that, unlike PM, aminoguanidine (AG), a hydrazine derivative that is also thought to act as a trapping agent, is a potent inhibitor of copper-catalyzed oxidation of LDL (i.e. prevents conjugated diene formation) (Philis-Tsimikas, 1995), though the products formed during AG inhibition of LDL oxidation have not been identified. Although both PM and AG are considered trapping agents, they appear to affect lipid peroxidation at different stages. The prevention of LDL oxidation by AG suggests that it may have chelating activity. PM, on the other hand, does not behave as

if it is chelating metal ions, since it slows the lag phase, but does not prevent, conjugated diene formation. It is also possible that, during LDL oxidation, PM works through multiple mechanisms, for example, by trapping intermediates and, to a lesser extent, by scavenging radicals.

PM will likely function through multiple mechanisms *in vivo* as well. Our studies have shown that PM should prevent lipoxidative damage to protein, thereby impairing the development of atherosclerosis. Previous examples above have demonstrated that PM inhibits both AGE formation from glucose and AGEs from post-Amadori reactions. These findings suggest that PM may also have inhibitory effects on damage to proteins derived from carbohydrates. By inhibiting protein damage occurring from both lipid and carbohydrate sources, PM would be expected to inhibit the development of complications in both atherosclerotic and diabetic animal models.

Example 8

Compounds for inhibiting oxidative protein modification

The present invention encompasses compounds, and pharmaceutical compositions containing compounds having the general formula:

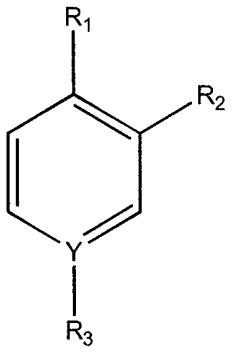

Formula I

wherein R_1 is CH_2NH_2, CH_2SH, COOH, $CH_2CH_2NH_2$, CH_2CH_2SH, or CH_2COOH;

R_2 is OH, SH or NH_2;

Y is N or C, such that when Y is N R_3 is nothing, and when Y is C, R_3 is NO_2 or another electron withdrawing group;

and salts thereof.

The present invention also encompasses compounds of the general formula

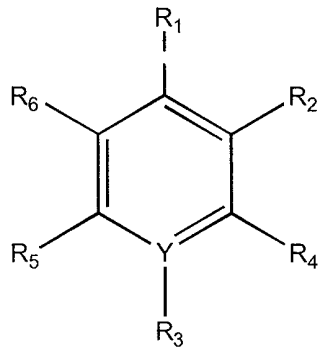

Formula II

wherein R_1 is CH_2NH_2, CH_2SH, COOH, $CH_2CH_2NH_2$, CH_2CH_2SH, or CH_2COOH;

R_2 is OH, SH or NH_2;

Y is N or C, such that when Y is N R_3 is nothing, and when Y is C, R_3 is NO_2 or another electron withdrawing group;

R_4 is H, or C 1-18 alkyl;

R_5 and R_6 are H, C 1-18 alkyl, alkoxy or alkane;

and salts thereof.

In addition, the instant invention also envisions compounds of the formulas

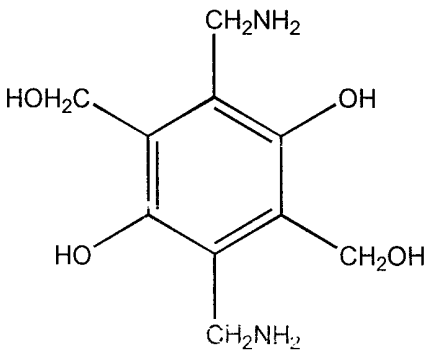

and 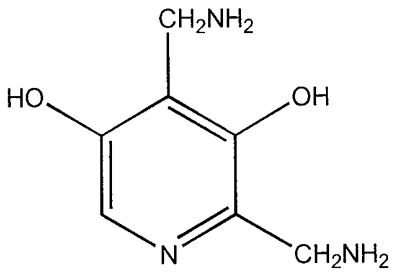

The compounds of the present invention can embody one or more electron withdrawing groups, such as and not limited to $-NH_2$, -NHR, $-NR_2$, -OH, $-OCH_3$, -OCR, and $-NH-COCH_3$ where R is C 1-18 alkyl.

By "alkyl" and "lower alkyl" in the present invention is meant straight or branched chain alkyl groups having from 1-18 carbon atoms, such as, for example, methyl, ethyl, propyl, isopropyl, n-butyl, sec-butyl, tert-butyl, pentyl, 2-pentyl, isopentyl, neopentyl, hexyl, 2-hexyl, 3-hexyl, and 3-methylpentyl. Unless indicated otherwise, the alkyl group substituents herein are optionally substituted with at least one group independently selected from hydroxy, mono- or dialkyl amino, phenyl or pyridyl.

By "alkoxy" and "lower alkoxy" in the present invention is meant straight or branched chain alkoxy groups having 1-18 carbon atoms, such as, for example, methoxy, ethoxy, propoxy, isopropoxy, n-butoxy, sec-butoxy, tert-butoxy, pentoxy, 2-pentyl, isopentoxy, neopentoxy, hexoxy, 2-hexoxy, 3-hexoxy, and 3-methylpentoxy.

By "alkene" and "lower alkene" in the present invention is meant straight and branched chain alkene groups having 1-18 carbon atoms, such as, for example, ethlene, propylene, 1-butene, 1-pentene, 1-hexene, *cis* and *trans* 2-butene or 2-pentene, isobutylene, 3-methyl-1-butene, 2-methyl-2-butene, and 2,3-dimethyl-2-butene.

By "salts thereof" in the present invention is meant compounds of the present invention as salts and metal complexes with said compounds, such as with, and not limited to, Al, Zn, Mg, Cu, and Fe.

One of ordinary skill in the art will be able to make compounds of the present invention using standard methods and techniques.

The instant invention encompasses pharmaceutical compositions which comprise one or more of the compounds of the present invention, or salts thereof, in a

suitable carrier. The instant invention encompasses methods for administering pharmaceuticals of the present invention for therapeutic intervention of pathologies which are related to AGE formation *in vivo*. In one preferred embodiment of the present invention the AGE related pathology to be treated is related to diabetic nephropathy.

The instant invention may be embodied in other forms or carried out in other ways without departing from the spirit or essential characteristics thereof. The present disclosure and enumerated examples are therefore to be considered as in all respects illustrative and not restrictive, the scope of the invention being indicated by the appended claims, and all equivalency are intended to be embraced therein. One of ordinary skill in the art would be able to recognize equivalent embodiments of the instant invention, and be able to practice such embodiments using the teaching of the instant disclosure and only routine experimentation.

We claim:

1. A method for inhibiting oxidative modification of proteins in a non-hyperglycemic mammal, comprising administering to the non-hyperglycemic mammal an amount effective to inhibit protein oxidative modifications of a compound of the general formula:

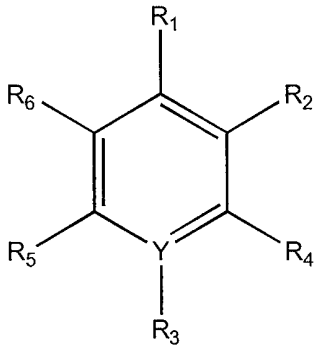

wherein R_1 is CH_2NH_2, CH_2SH, COOH, $CH_2CH_2NH_2$, CH_2CH_2SH, or CH_2COOH;
R_2 and R_6 is H, OH, SH, NH_2, C 1-18 alkyl, alkoxy or alkene;
R_4 and R_5 are H, C 1-18 alkyl, alkoxy or alkene;
Y is N or C, such that when Y is N R_3 is nothing, and when Y is C, R_3 is NO_2 or another electron withdrawing group, and salts thereof.

2. A method for inhibiting oxidative modification of low density lipoproteins in a non-hyperglycemic mammal, comprising administering to the non-hyperglycemic mammal an amount effective to inhibit low density lipoprotein oxidative modifications of a compound of the general formula:

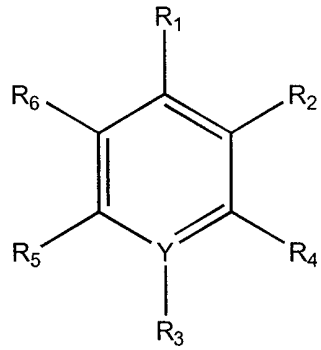

wherein R_1 is CH_2NH_2, CH_2SH, COOH, $CH_2CH_2NH_2$, CH_2CH_2SH, or CH_2COOH;
R_2 and R_6 is H, OH, SH, NH_2, C 1-18 alkyl, alkoxy or alkene;
R_4 and R_5 are H, C 1-18 alkyl, alkoxy or alkene;
Y is N or C, such that when Y is N R_3 is nothing, and when Y is C, R_3 is NO_2 or another electron withdrawing group, and salts thereof.

3. A method for inhibiting lipid peroxidation in a non-hyperglycemic mammal, comprising administering to the non-hyperglycemic mammal an amount effective to inhibit lipid peroxidation of a compound of the general formula:

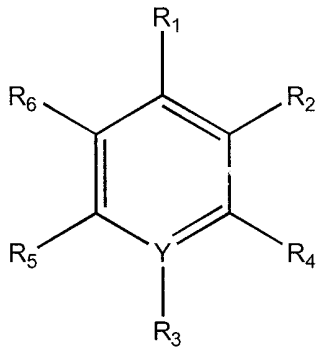

wherein R_1 is CH_2NH_2, CH_2SH, COOH, $CH_2CH_2NH_2$, CH_2CH_2SH, or CH_2COOH;
R_2 and R_6 is H, OH, SH, NH_2, C 1-18 alkyl, alkoxy or alkene;
R_4 and R_5 are H, C 1-18 alkyl, alkoxy or alkene;
Y is N or C, such that when Y is N R_3 is nothing, and when Y is C, R_3 is NO_2 or another electron withdrawing group, and salts thereof.

4. A method for preventing or treating atherosclerosis, comprising administering to a non-hyperglycemic mammal in need thereof an amount effective to prevent or treat atherosclerosis of a compound of the general formula:

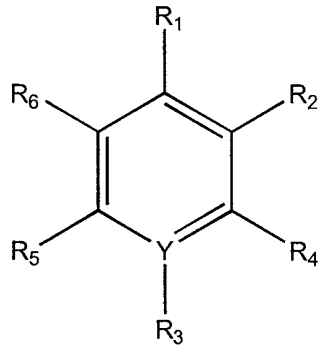

wherein R_1 is CH_2NH_2, CH_2SH, COOH, $CH_2CH_2NH_2$, CH_2CH_2SH, or CH_2COOH;
R_2 and R_6 is H, OH, SH, NH_2, C 1-18 alkyl, alkoxy or alkene;
R_4 and R_5 are H, C 1-18 alkyl, alkoxy or alkene;
Y is N or C, such that when Y is N R_3 is nothing, and when Y is C, R_3 is NO_2 or another electron withdrawing group, and salts thereof.

5. A method to determine the level of in vivo oxidative damage to proteins in a

mammal, comprising determining the level of amide derivatives of lysine or lysine in proteins in a body fluid or tissue of the mammal, wherein the level of the amide derivatives correlates with oxidative damage to proteins.

6. The method of claim 5 wherein the body fluid or tissue is selected from the group consisting of urine, blood plasma, and skin.

7. The method of claim 5 wherein the amide derivatives of lysine are selected from the group consisting of *N*-hexanoyl or *N*-nonanedioyl.

8. A method for inhibiting the oxidative modification of proteins in a non-hyperglycemic mammal, comprising administering to the non-hyperglycemic mammal an amount effective of pyridoxamine to inhibit the oxidative modification of proteins.

9. A method for inhibiting the oxidative modification of low density lipoproteins in a non-hyperglycemic mammal, comprising administering to the non-hyperglycemic mammal an amount effective of pyridoxamine to inhibit the oxidative modification of low density lipoproteins.

10. A method for inhibiting lipid peroxidation in a non-hyperglycemic mammal, comprising administering to the non-hyperglycemic mammal an amount effective of pyridoxamine to inhibit lipid peroxidation

11. A method for preventing or treating atherosclerosis, comprising administering to a non-hyperglycemic mammal in need thereof an amount effective of pyridoxamine to prevent or treat atherosclerosis.

Fig. 1

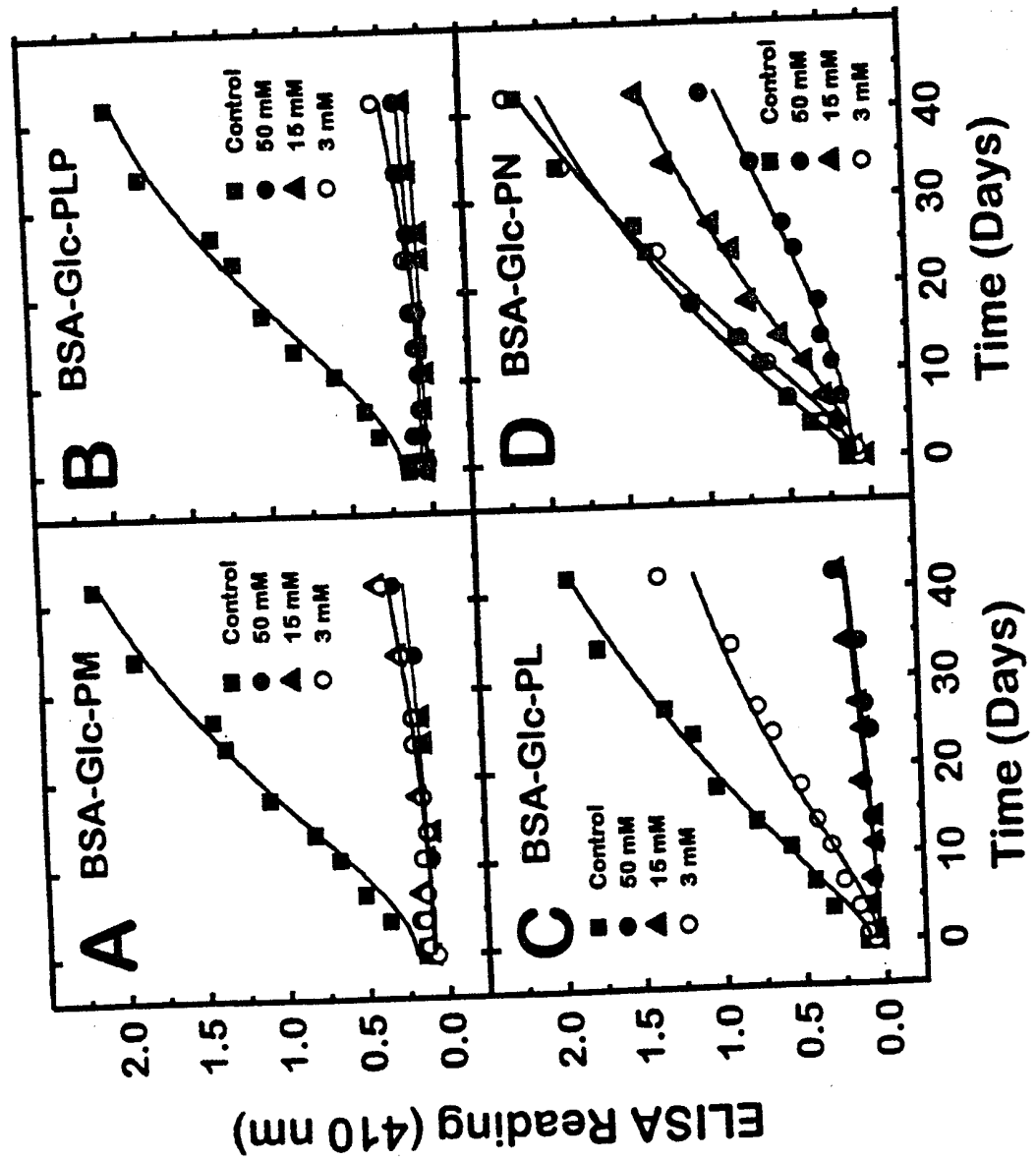
A
BSA-Glc-PM
B
BSA-Glc-PLP
C
BSA-Glc-PL
D
BSA-Glc-PN
Control
50 mM
15 mM
3 mM
ELISA Reading (410 nm)
Time (Days)
0.0
0.5
1.0
1.5
2.0
0
10
20
30
40

Fig. 2

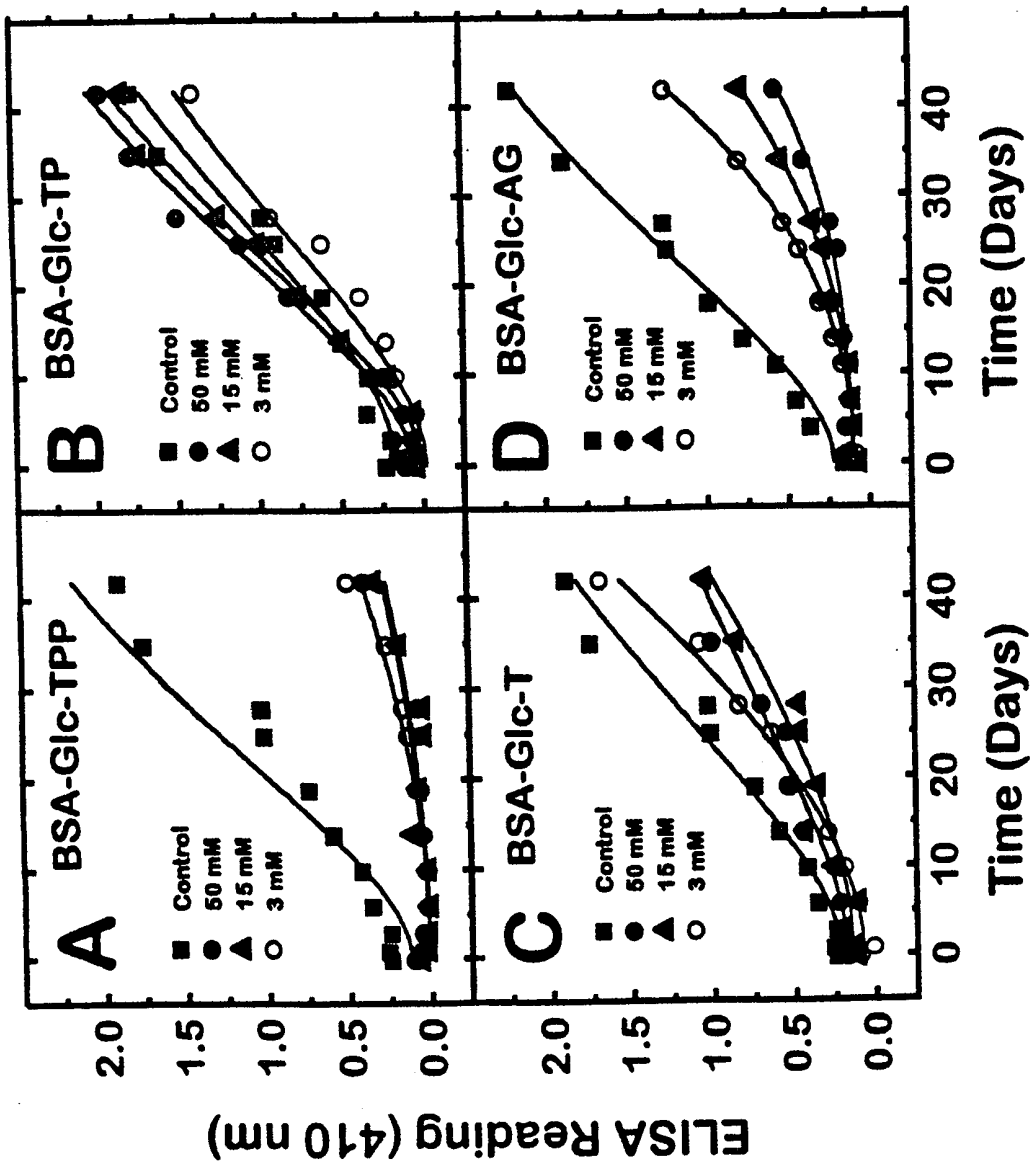
A
BSA-Glc-TPP
B
BSA-Glc-TP
C
BSA-Glc-T
D
BSA-Glc-AG
Control
50 mM
15 mM
3 mM
ELISA Reading (410 nm)
Time (Days)
0.0
0.5
1.0
1.5
2.0
0
10
20
30
40

Fig. 3

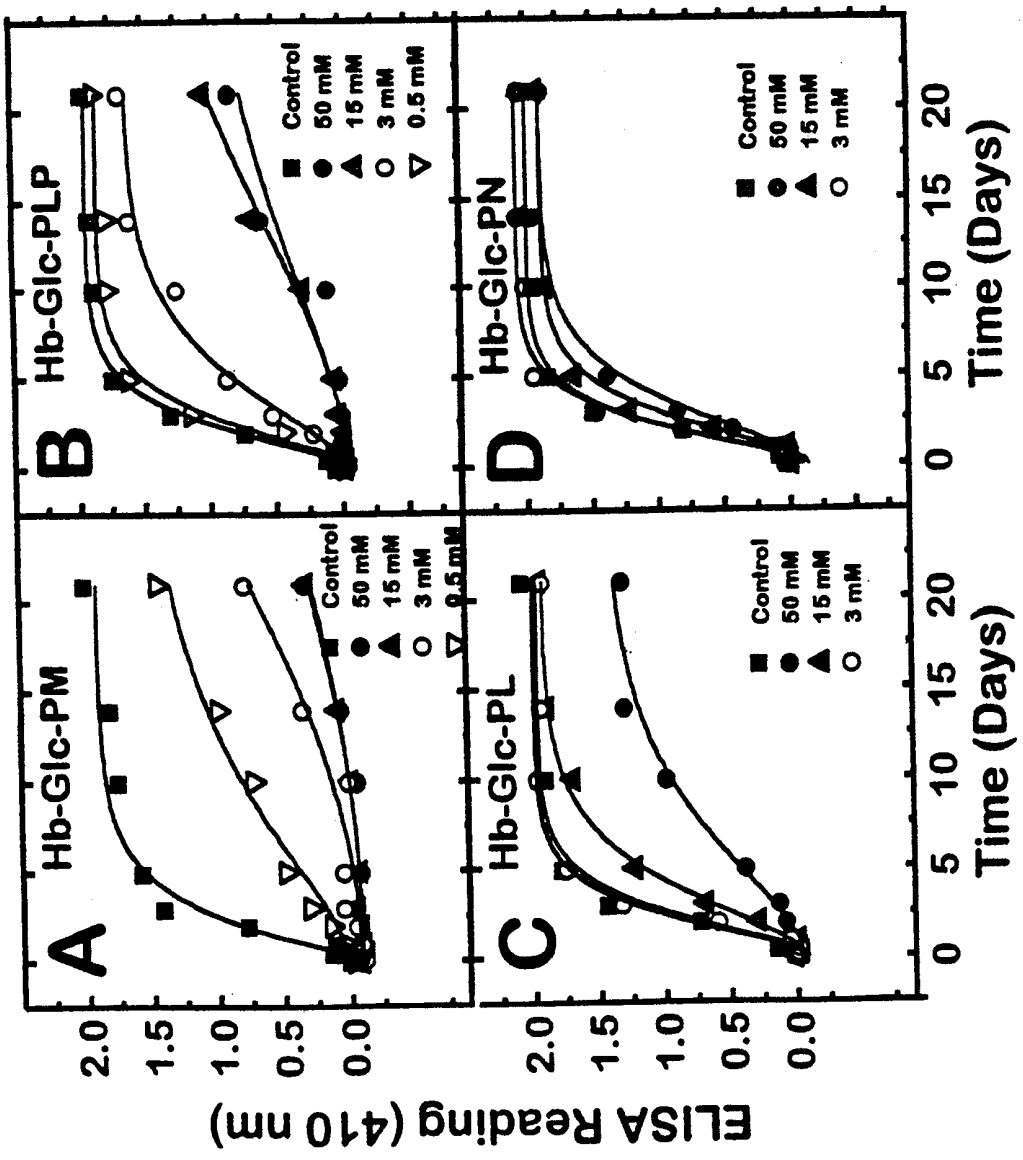
A
Hb-Glc-PM
B
Hb-Glc-PLP
C
Hb-Glc-PL
D
Hb-Glc-PN
Control
50 mM
15 mM
3 mM
0.5 mM
ELISA Reading (410 nm)
Time (Days)
0.0
0.5
1.0
1.5
2.0
0
5
10
15
20

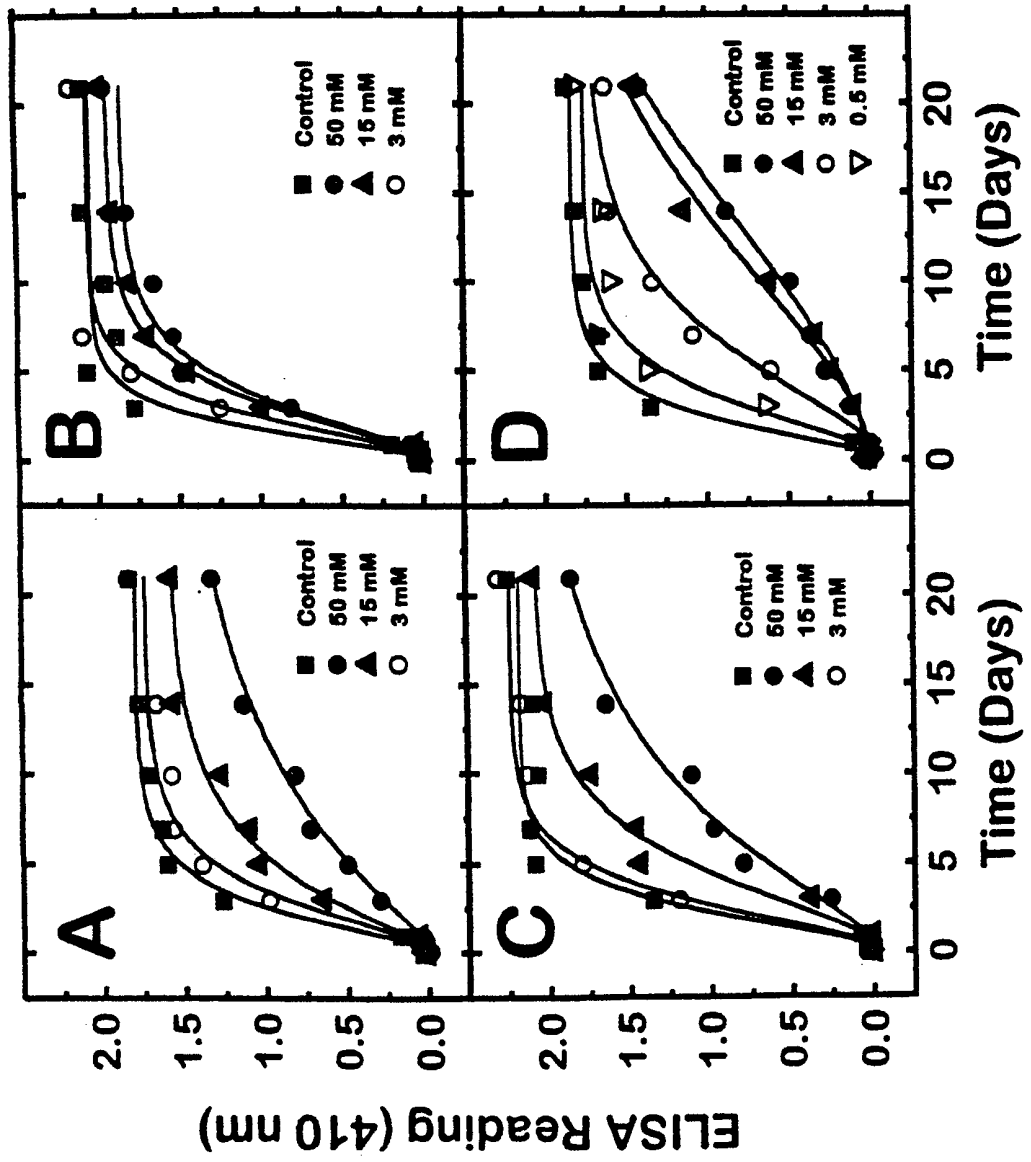
A
B
C
D
Control
50 mM
15 mM
3 mM
0.5 mM
ELISA Reading (410 nm)
Time (Days)
0.0
0.5
1.0
1.5
2.0
0
5
10
15
20

Fig. 4

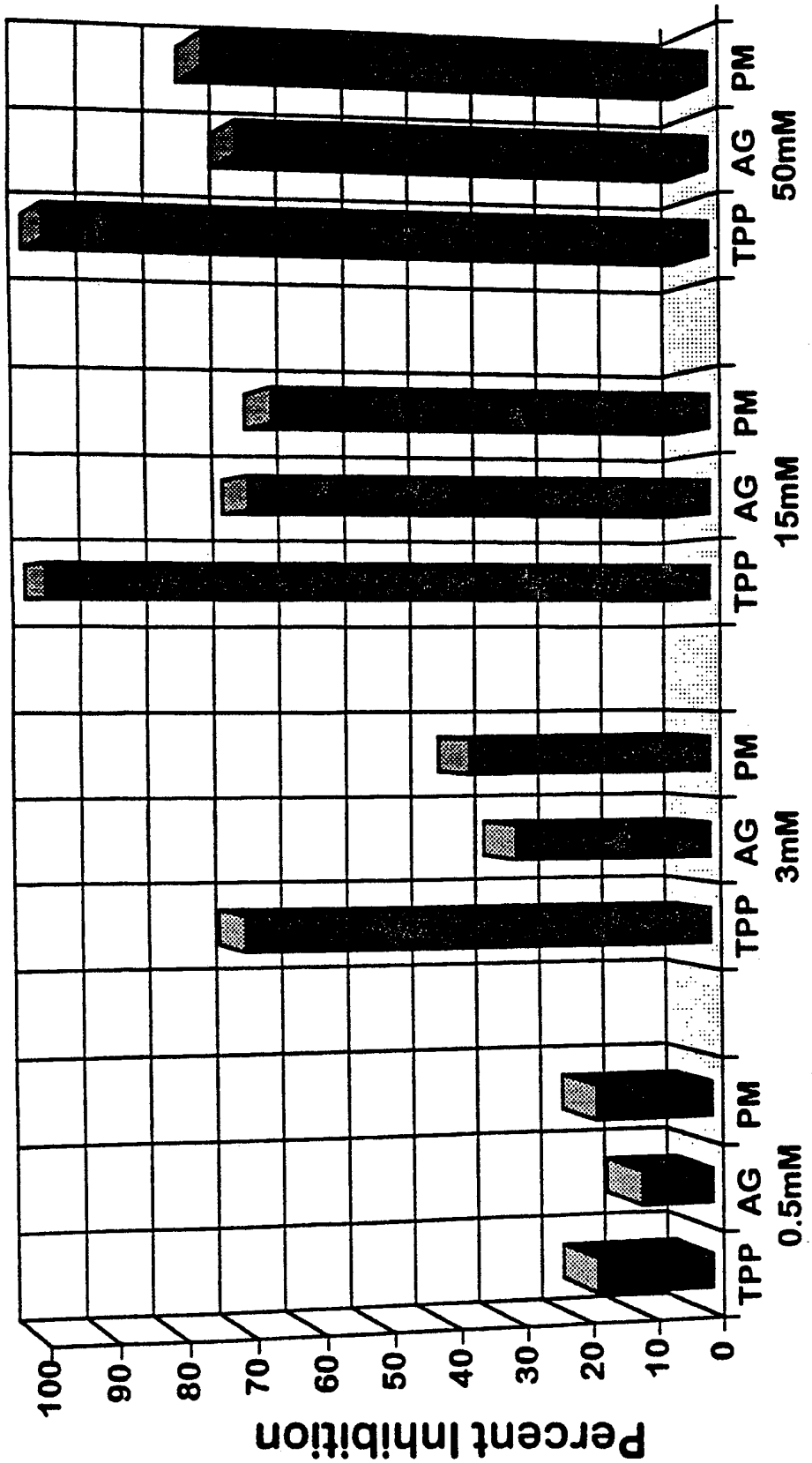
Percent Inhibition
100
90
80
70
60
50
40
30
20
10
0
TPP
AG
PM
0.5mM
3mM
15mM
50mM

Fig. 5

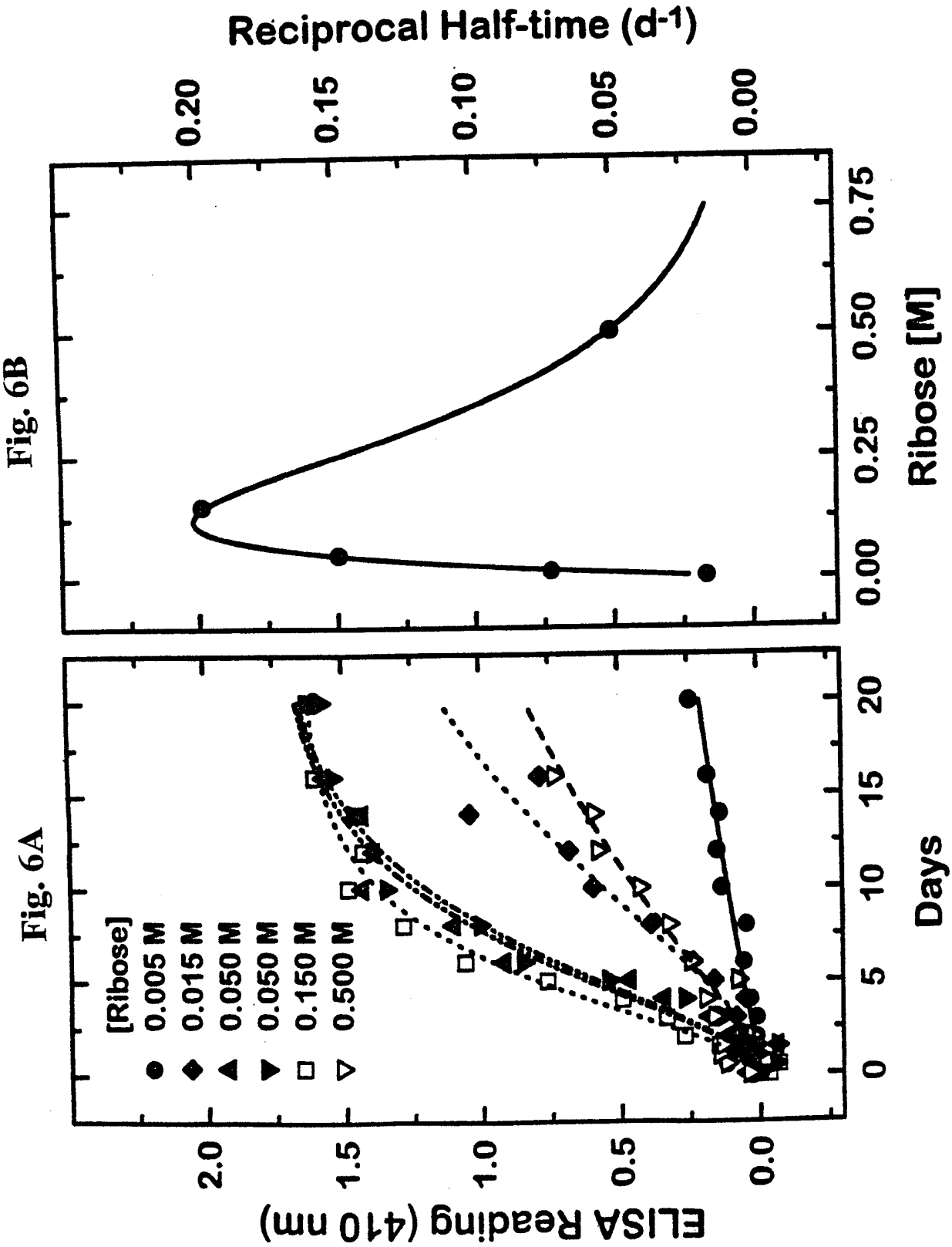
Reciprocal Half-time (d-1)
0.20
0.15
0.10
0.05
0.00
0.00
0.25
0.50
0.75
Ribose [M]
Fig. 6B
ELISA Reading (410 nm)
2.0
1.5
1.0
0.5
0.0
0
5
10
15
20
Days
[Ribose]
0.005 M
0.015 M
0.050 M
0.050 M
0.150 M
0.500 M
Fig. 6A

Fig. 7A

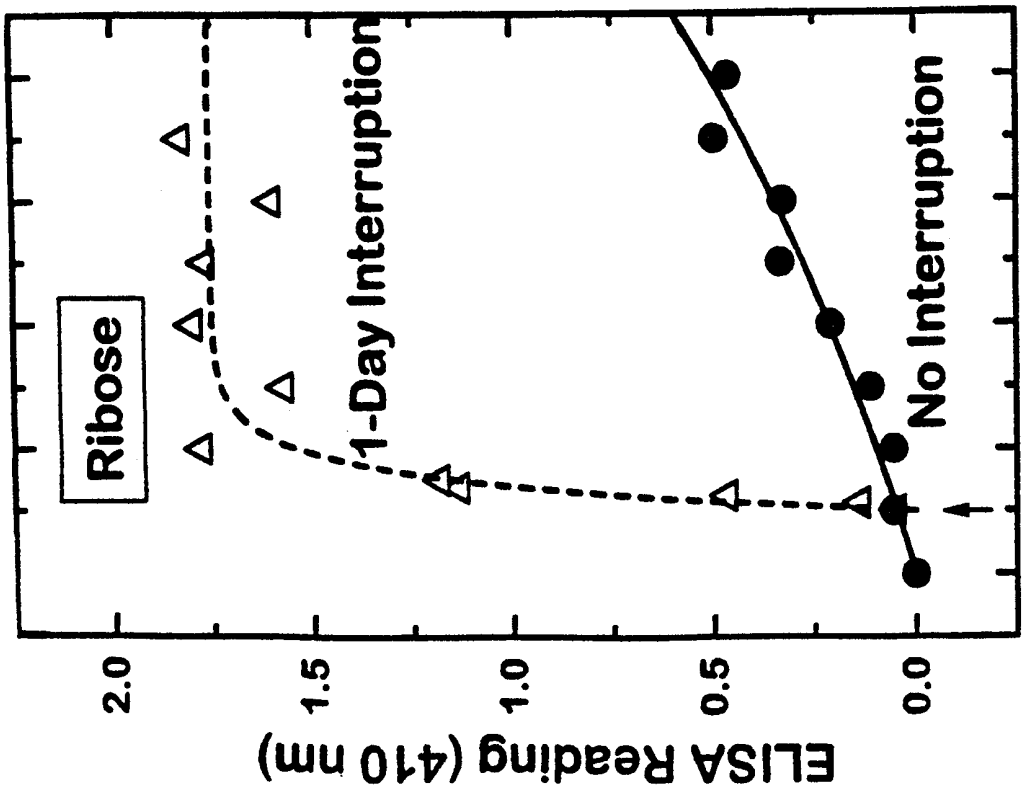
Ribose
1-Day Interruption
No Interruption
ELISA Reading (410 nm)
Time at 37C (days)
0.0
0.5
1.0
1.5
2.0
0
2
4
6
8

Fig. 7B

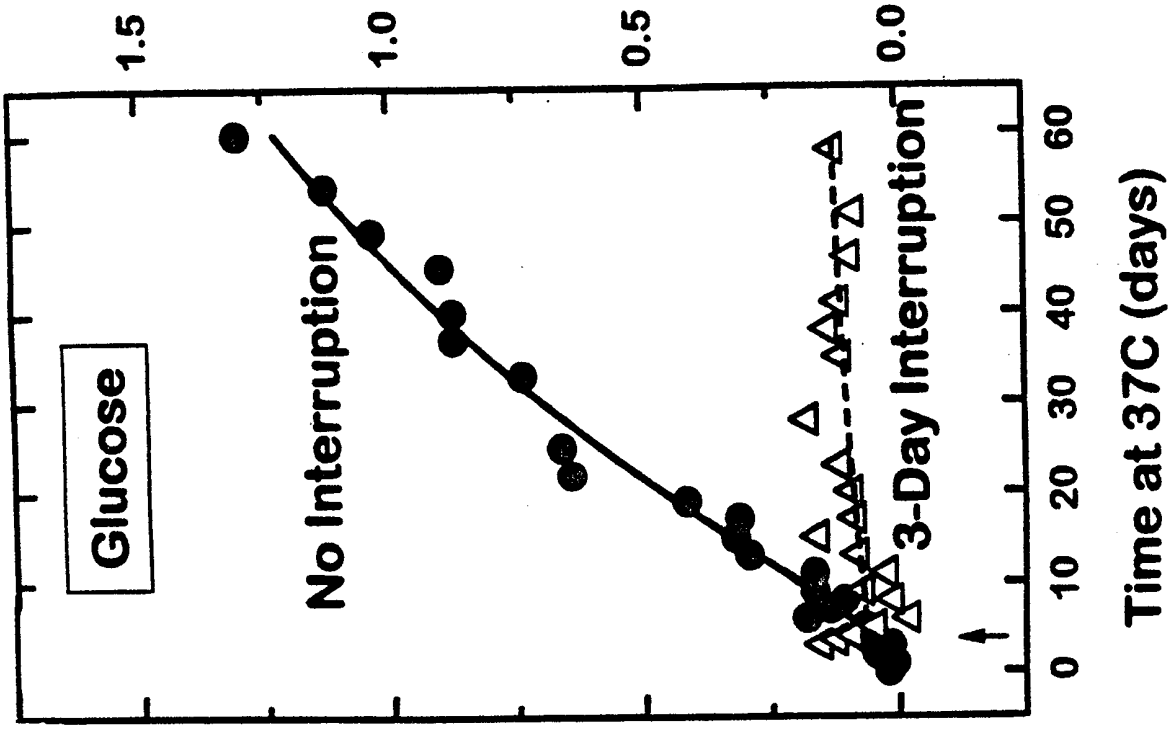
Glucose
No Interruption
3-Day Interruption
Time at 37C (days)
0.0
0.5
1.0
1.5
0
10
20
30
40
50
60

Fig. 8A

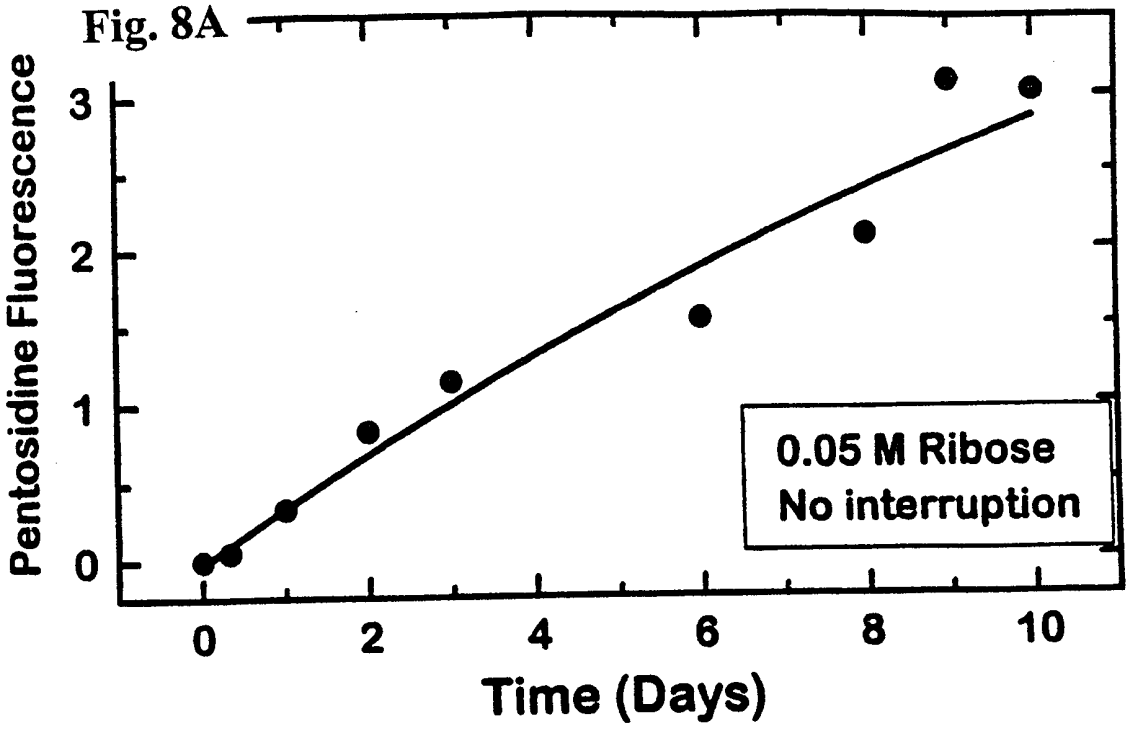
Pentosidine Fluorescence
0
1
2
3
0
2
4
6
8
10
Time (Days)
0.05 M Ribose
No interruption

Fig. 8B

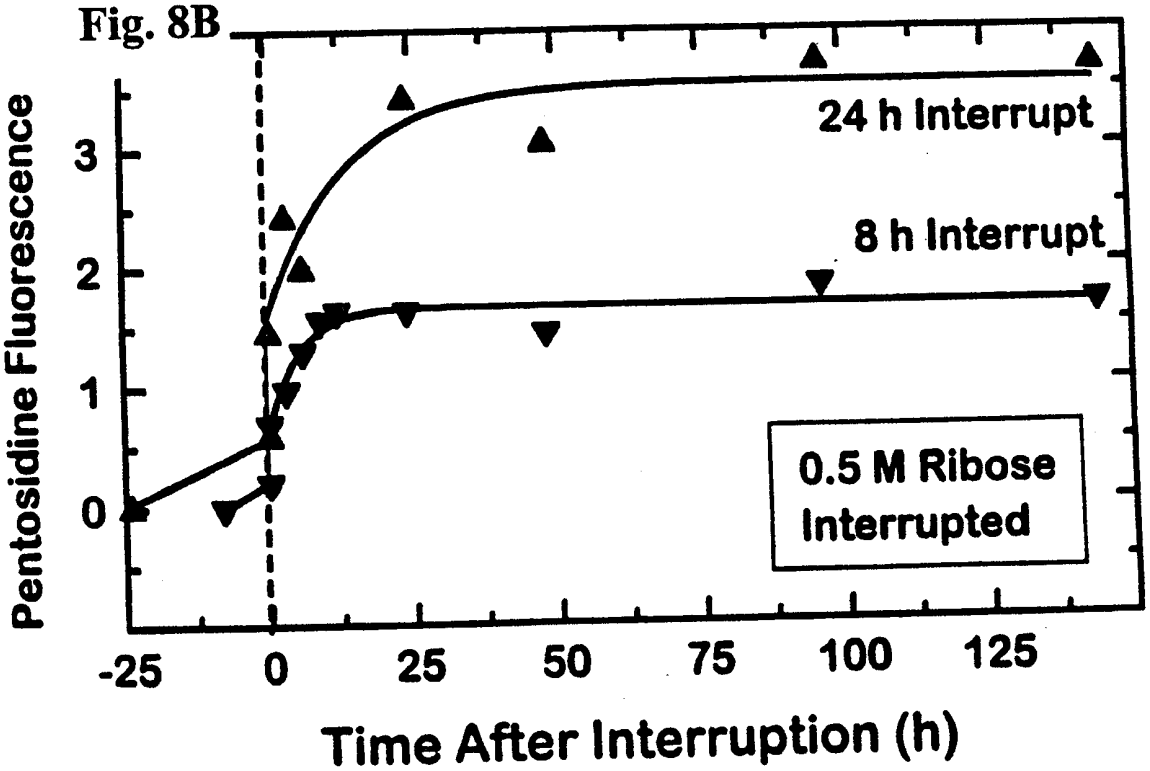
Pentosidine Fluorescence
0
1
2
3
-25
0
25
50
75
100
125
Time After Interruption (h)
24 h Interrupt
8 h Interrupt
0.5 M Ribose
Interrupted

Fig. 9

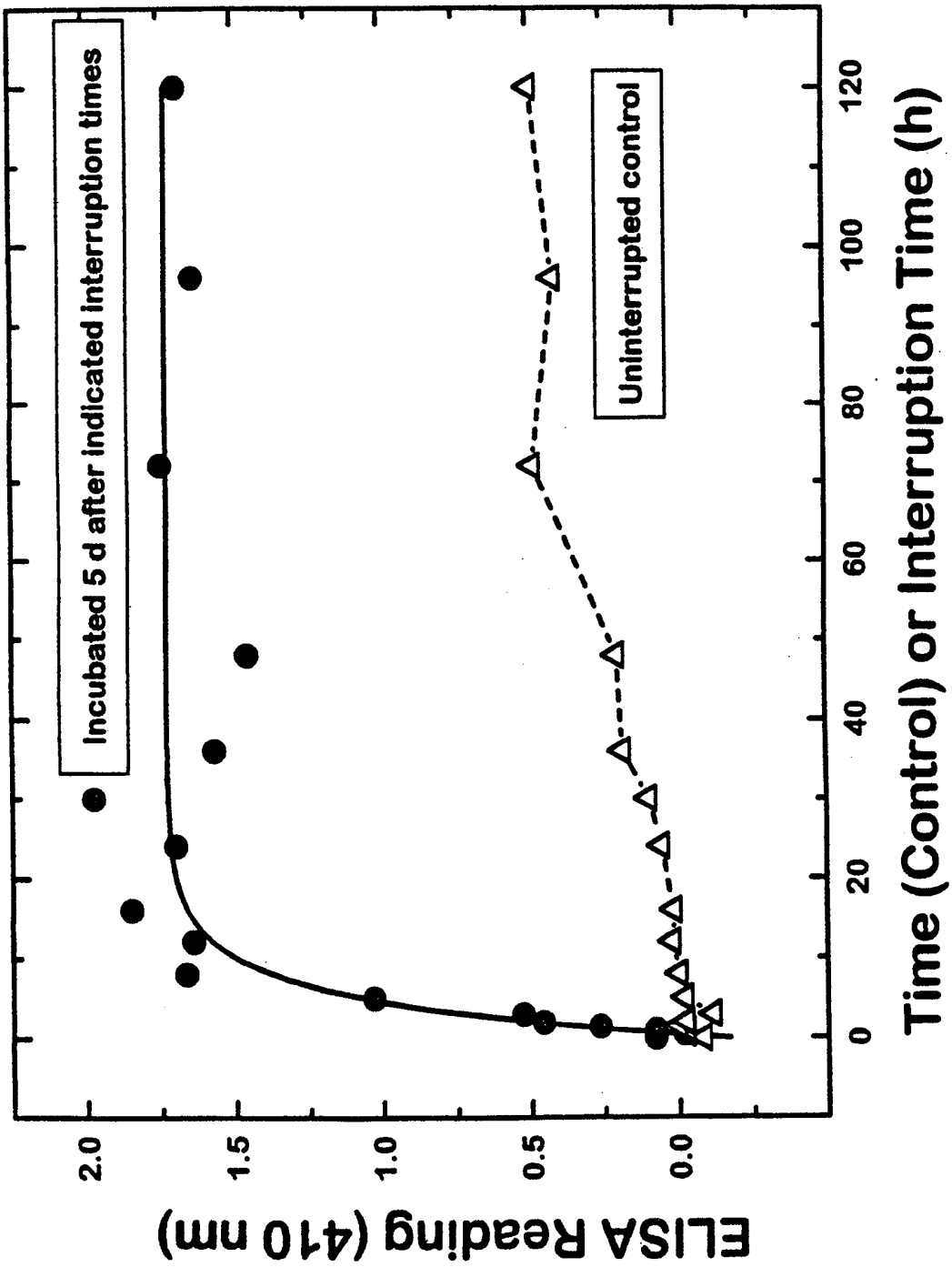
ELISA Reading (410 nm)
2.0
1.5
1.0
0.5
0.0
Time (Control) or Interruption Time (h)
0
20
40
60
80
100
120
Incubated 5 d after indicated interruption times
Uninterrupted control

Fig. 10

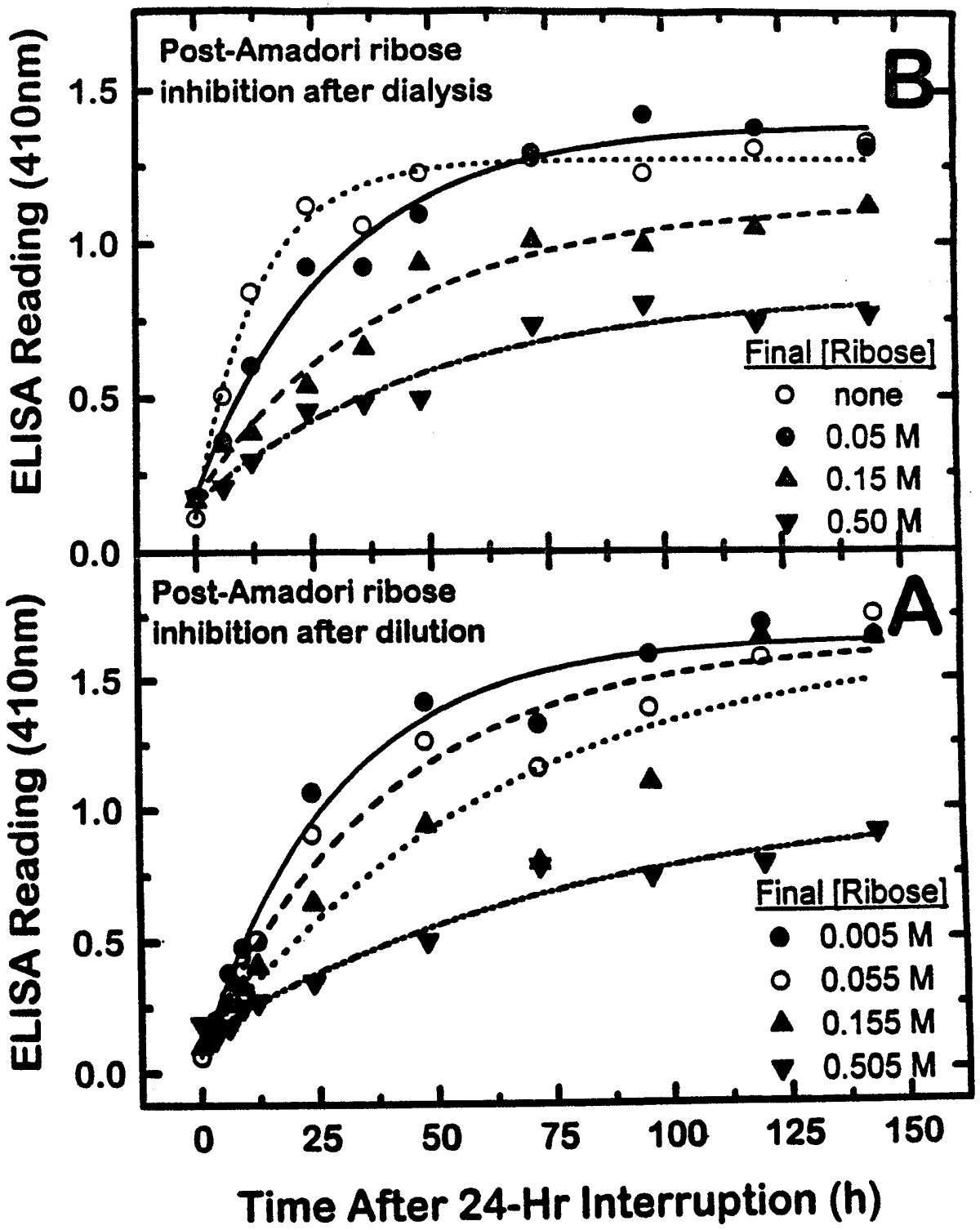
Post-Amadori ribose
inhibition after dialysis
B
Final [Ribose]
none
0.05 M
0.15 M
0.50 M
Post-Amadori ribose
inhibition after dilution
A
Final [Ribose]
0.005 M
0.055 M
0.155 M
0.505 M
ELISA Reading (410nm)
ELISA Reading (410nm)
0.0
0.5
1.0
1.5
0
25
50
75
100
125
150
Time After 24-Hr Interruption (h)

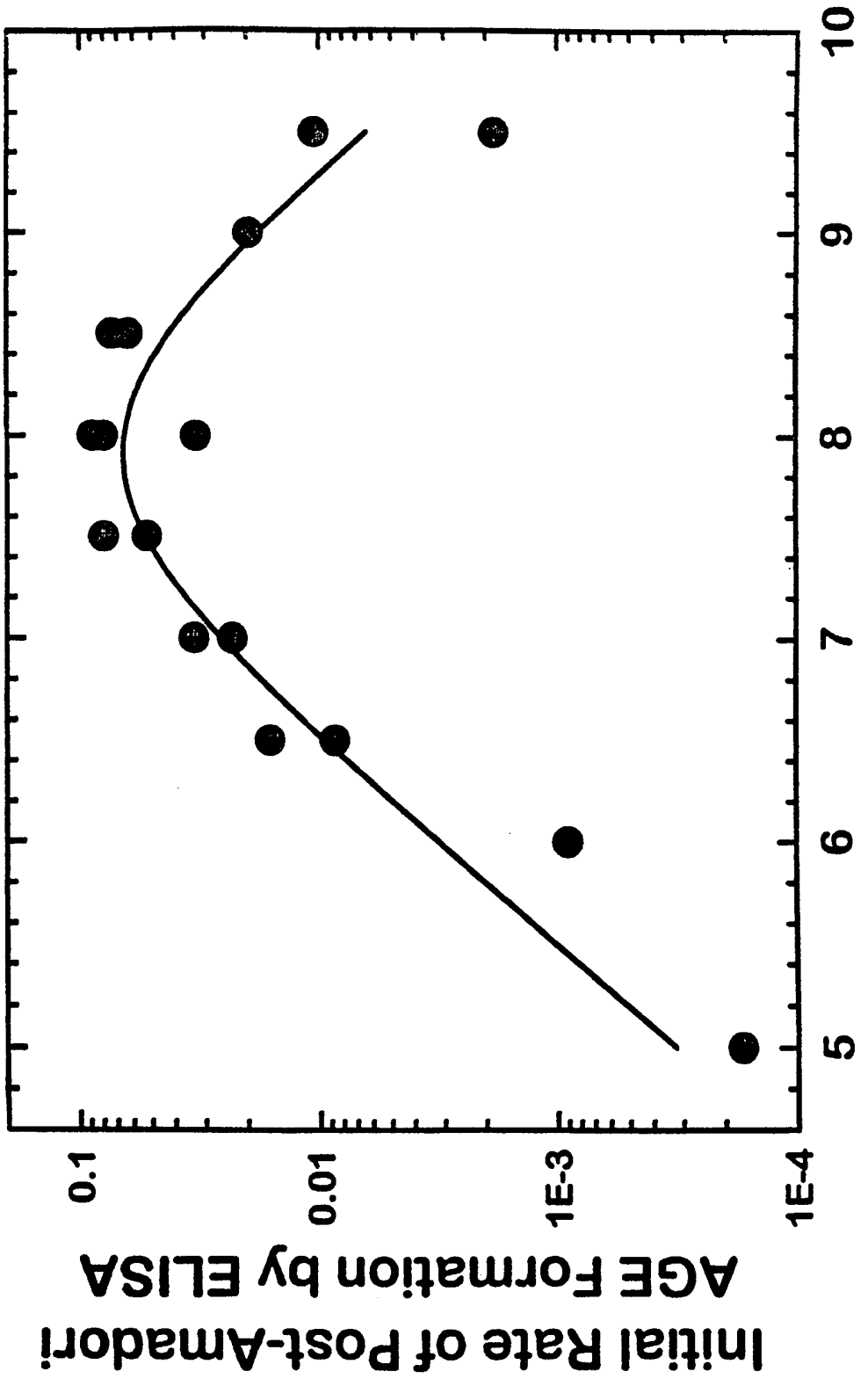
Initial Rate of Post-Amadori
AGE Formation by ELISA
0.1
0.01
1E-3
1E-4
5
6
7
8
9
10
pH

Fig. 11

Fig. 12 A

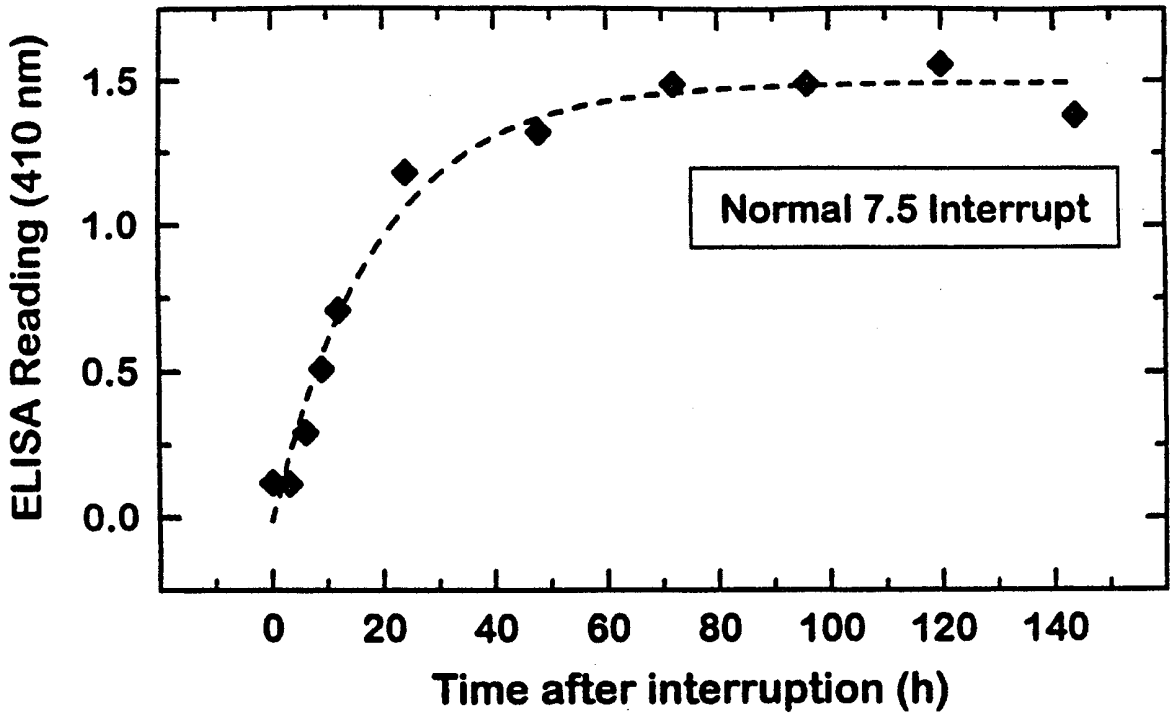

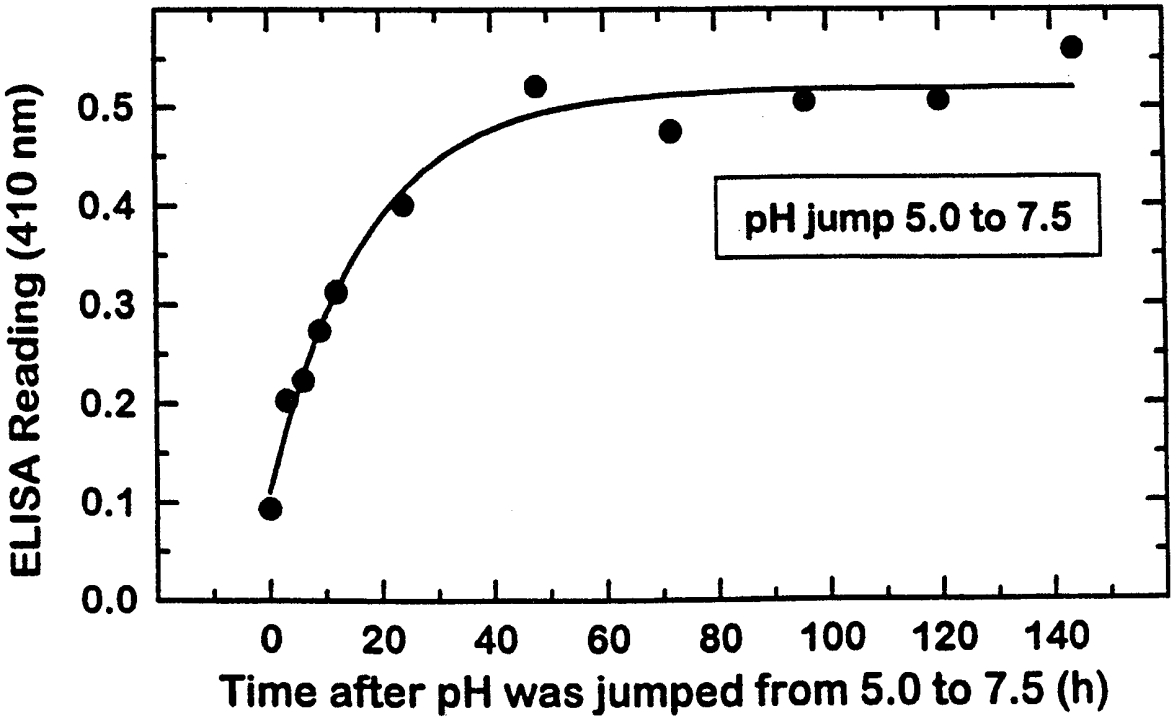

Fig. 12 B

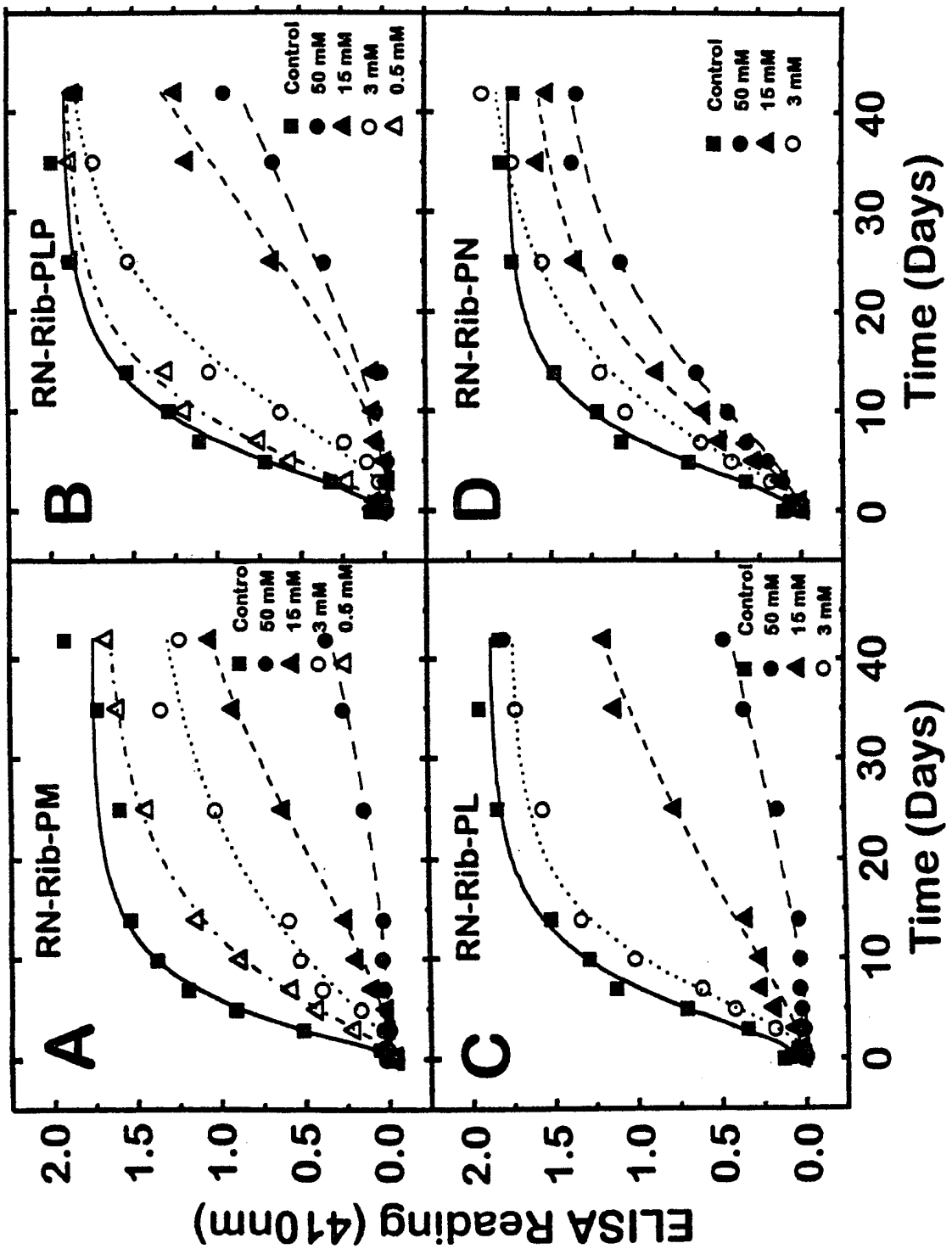
A
RN-Rib-PM
Contro
50 mM
15 mM
3 mM
0.5 mM
B
RN-Rib-PLP
Control
50 mM
15 mM
3 mM
0.5 mM
C
RN-Rib-PL
Control
50 mM
15 mM
3 mM
D
RN-Rib-PN
Control
50 mM
15 mM
3 mM
ELISA Reading (410nm)
2.0
1.5
1.0
0.5
0.0
0
10
20
30
40
Time (Days)

Fig. 13

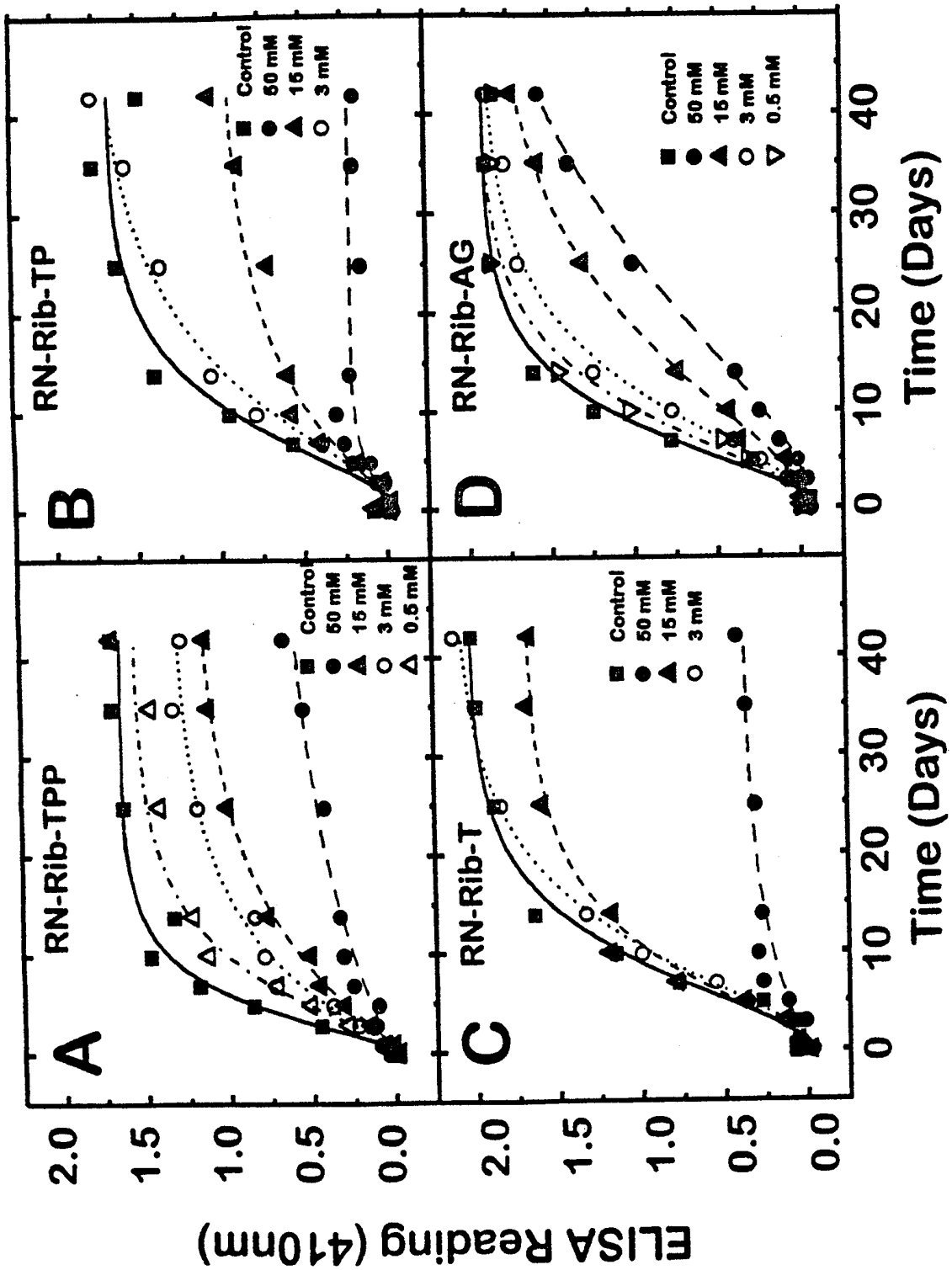
A
RN-Rib-TPP
Control
50 mM
15 mM
3 mM
0.5 mM
B
RN-Rib-TP
Control
50 mM
15 mM
3 mM
C
RN-Rib-T
Control
50 mM
15 mM
3 mM
D
RN-Rib-AG
Control
50 mM
15 mM
3 mM
0.5 mM
ELISA Reading (410nm)
Time (Days)
Time (Days)
0.0
0.5
1.0
1.5
2.0
0
10
20
30
40

Fig. 14

Fig.15

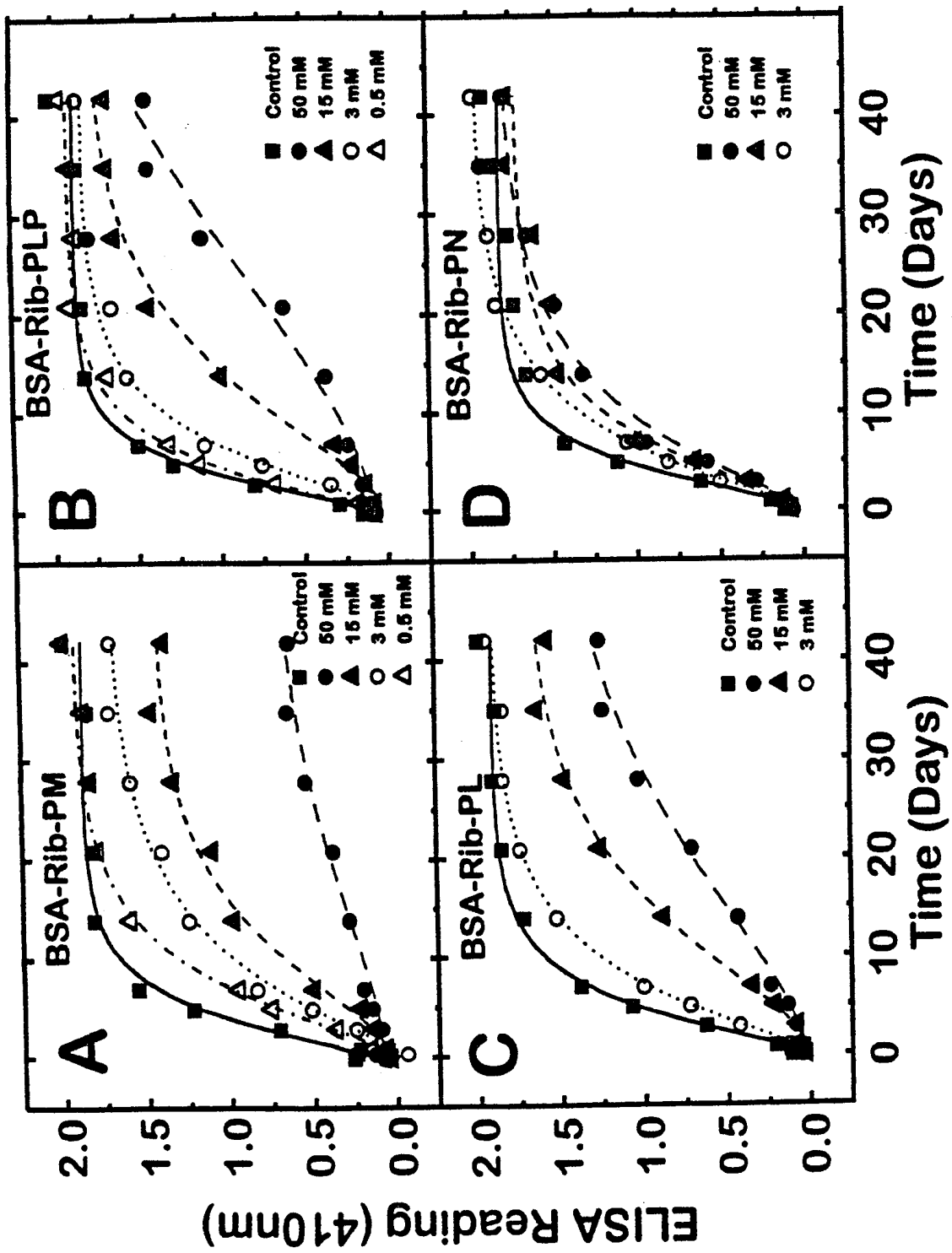
A
BSA-Rib-PM
Control
50 mM
15 mM
3 mM
0.5 mM
B
BSA-Rib-PLP
Control
50 mM
15 mM
3 mM
0.5 mM
C
BSA-Rib-PL
Control
50 mM
15 mM
3 mM
D
BSA-Rib-PN
Control
50 mM
15 mM
3 mM
ELISA Reading (410nm)
0.0
0.5
1.0
1.5
2.0
0
10
20
30
40
Time (Days)

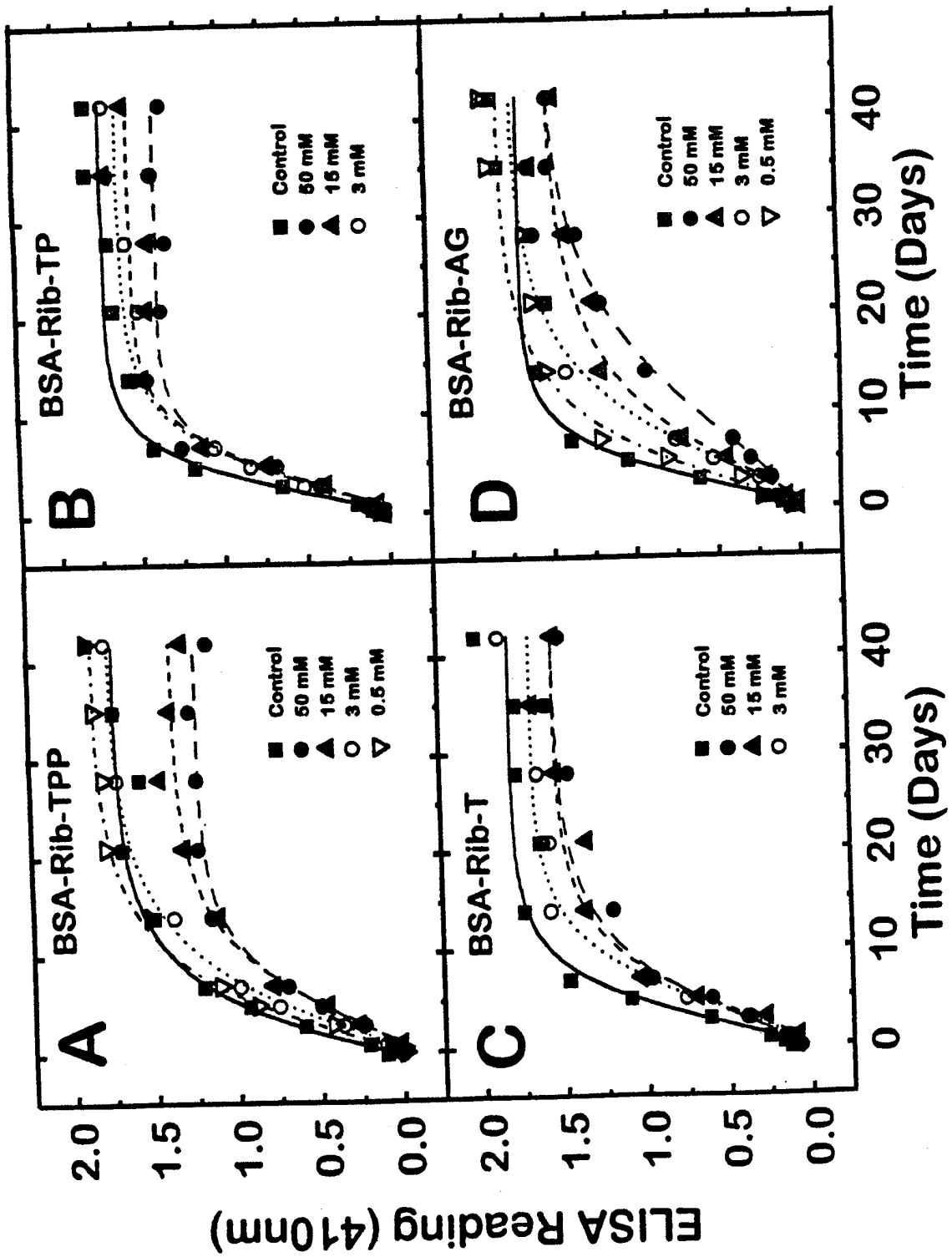
A
BSA-Rib-TPP
Control
50 mM
15 mM
3 mM
0.5 mM
B
BSA-Rib-TP
Control
50 mM
15 mM
3 mM
C
BSA-Rib-T
Control
50 mM
15 mM
3 mM
D
BSA-Rib-AG
Control
50 mM
15 mM
3 mM
0.5 mM
ELISA Reading (410nm)
2.0
1.5
1.0
0.5
0.0
0
10
20
30
40
Time (Days)

Fig. 16

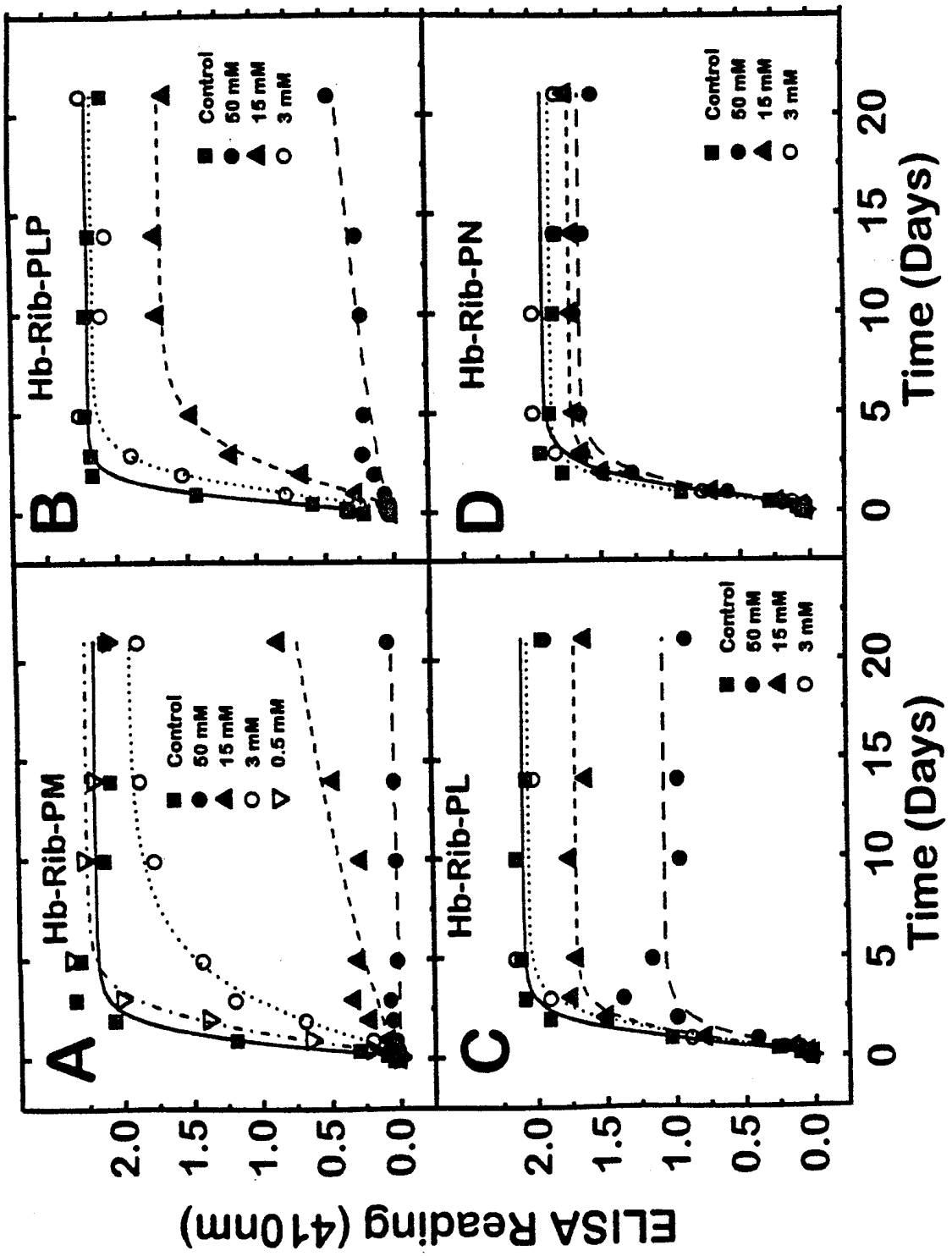
A
Hb-Rib-PM
Control
50 mM
15 mM
3 mM
0.5 mM
B
Hb-Rib-PLP
Control
50 mM
15 mM
3 mM
C
Hb-Rib-PL
Control
50 mM
15 mM
3 mM
D
Hb-Rib-PN
Control
50 mM
15 mM
3 mM
ELISA Reading (410nm)
0.0
0.5
1.0
1.5
2.0
Time (Days)
0
5
10
15
20

Fig. 17

Fig. 18

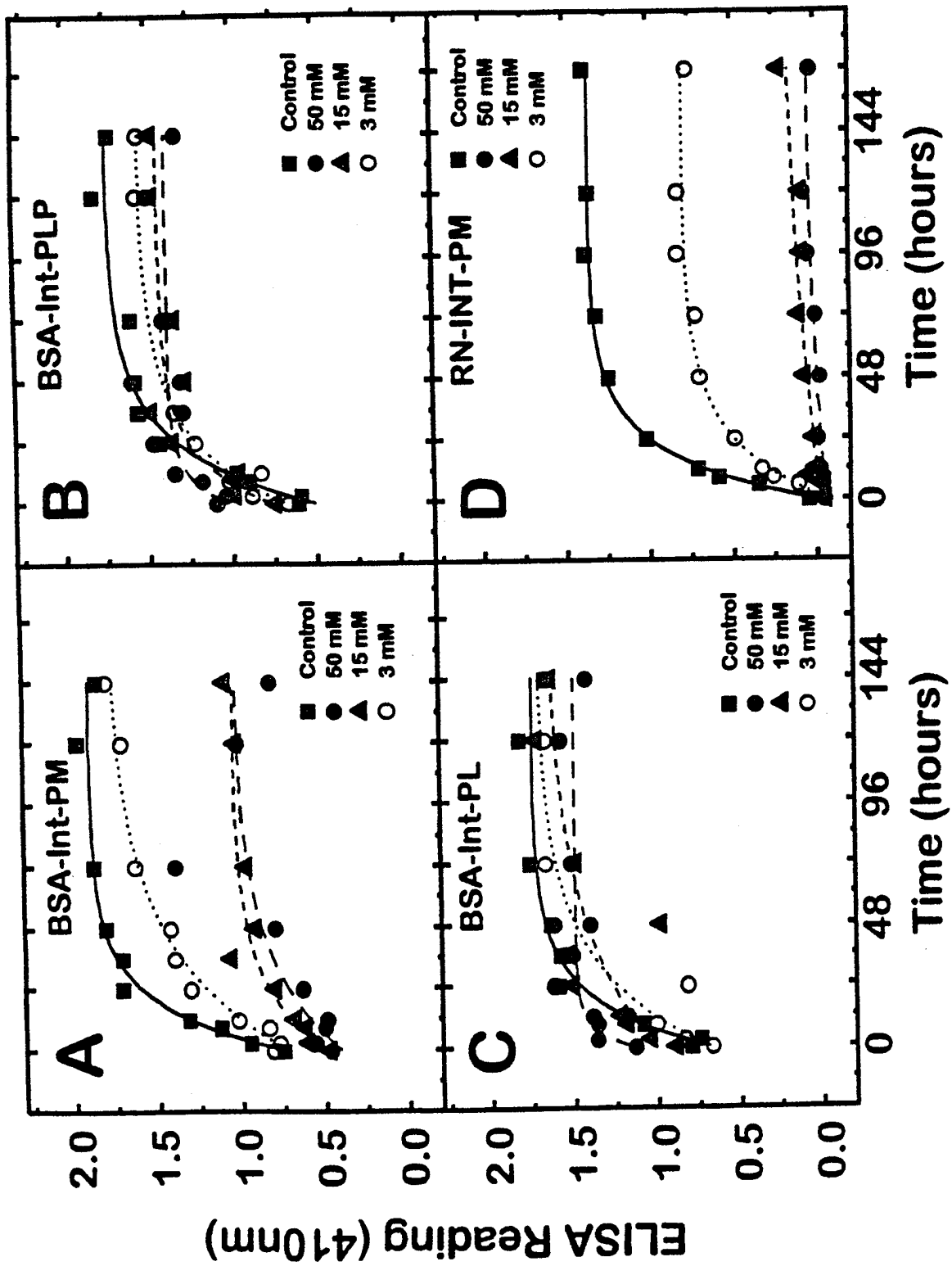
A
BSA-Int-PM
B
BSA-Int-PLP
C
BSA-Int-PL
D
RN-INT-PM
Control
50 mM
15 mM
3 mM
ELISA Reading (410nm)
Time (hours)
0.0
0.5
1.0
1.5
2.0
0
48
96
144

Fig. 19

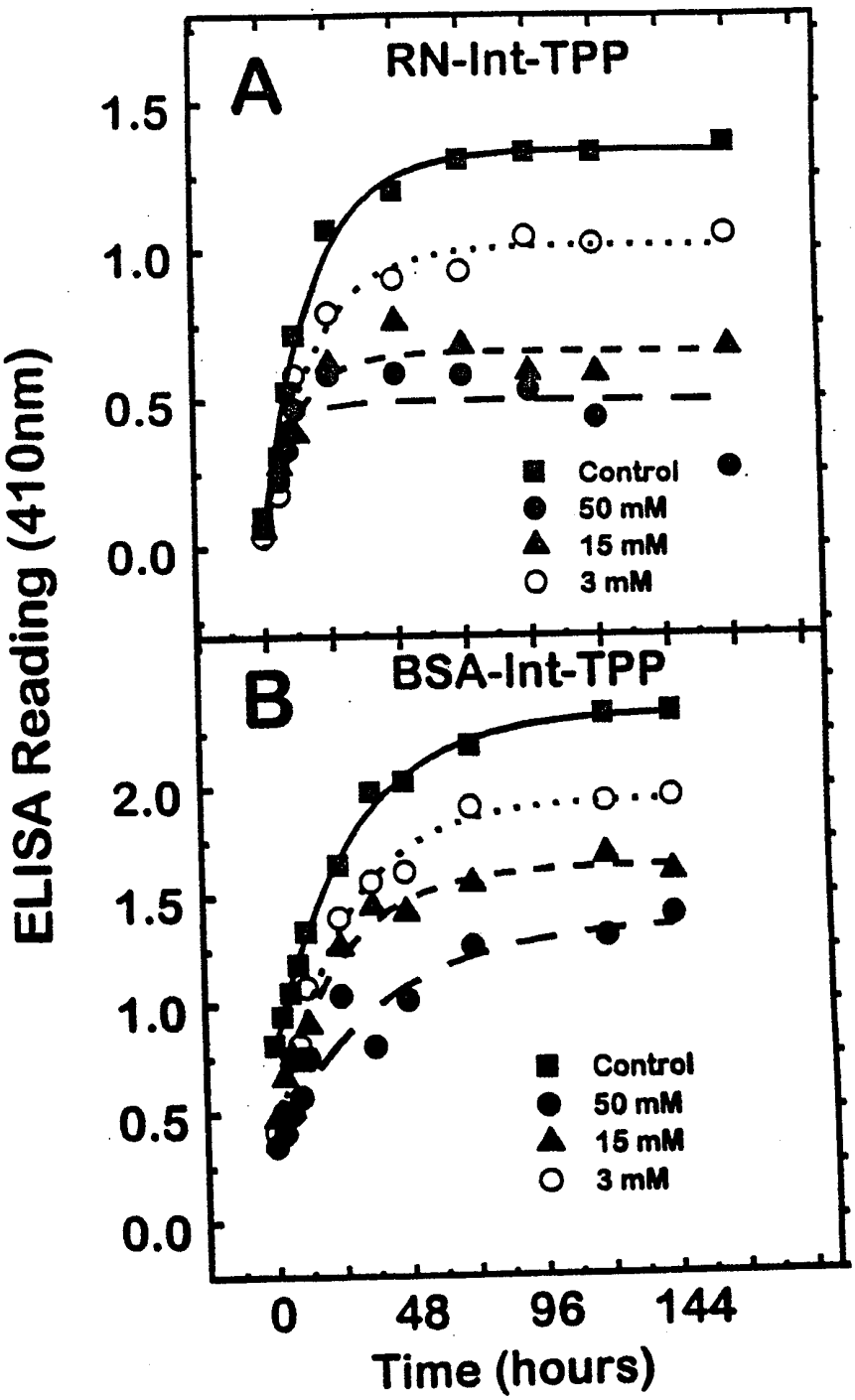
A
RN-Int-TPP
1.5
1.0
0.5
0.0
Control
50 mM
15 mM
3 mM
B
BSA-Int-TPP
2.0
1.5
1.0
0.5
0.0
Control
50 mM
15 mM
3 mM
ELISA Reading (410nm)
0
48
96
144
Time (hours)

Fig. 20

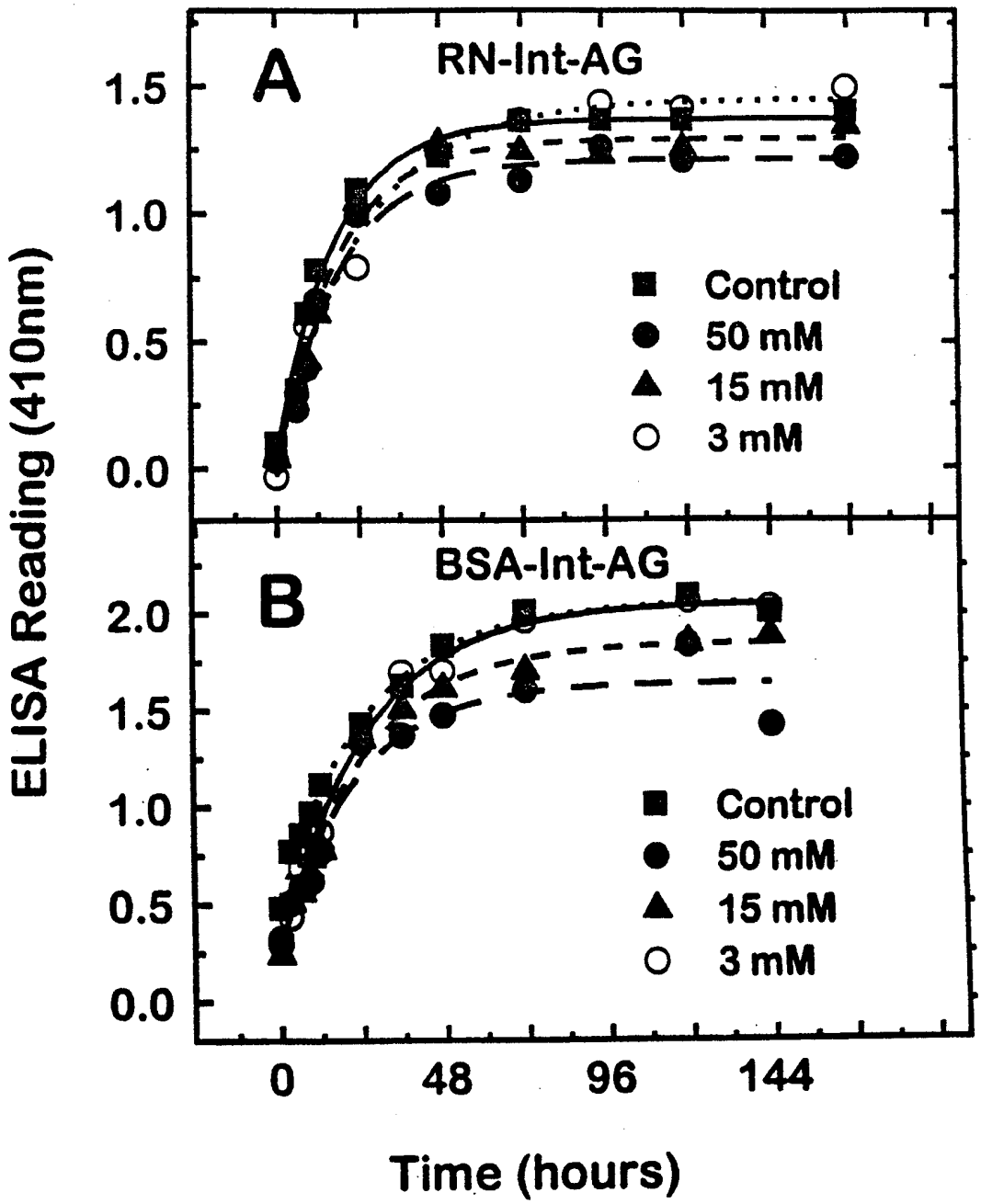
A
RN-Int-AG
B
BSA-Int-AG
Control
50 mM
15 mM
3 mM
ELISA Reading (410nm)
Time (hours)
0.0
0.5
1.0
1.5
2.0
0
48
96
144

Fig. 21

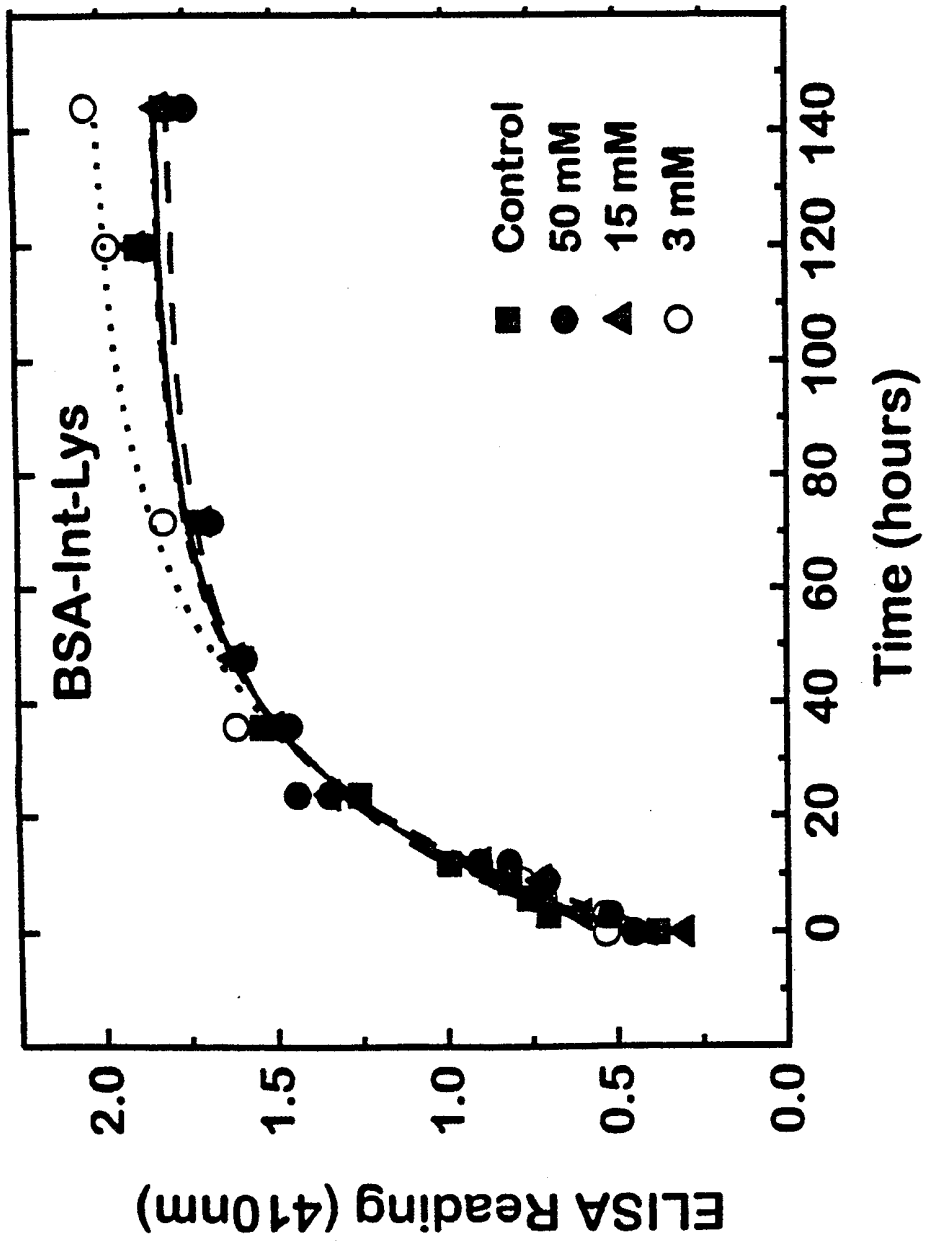
BSA-Int-Lys
Control
50 mM
15 mM
3 mM
ELISA Reading (410nm)
Time (hours)
0.0
0.5
1.0
1.5
2.0
0
20
40
60
80
100
120
140

Fig. 22

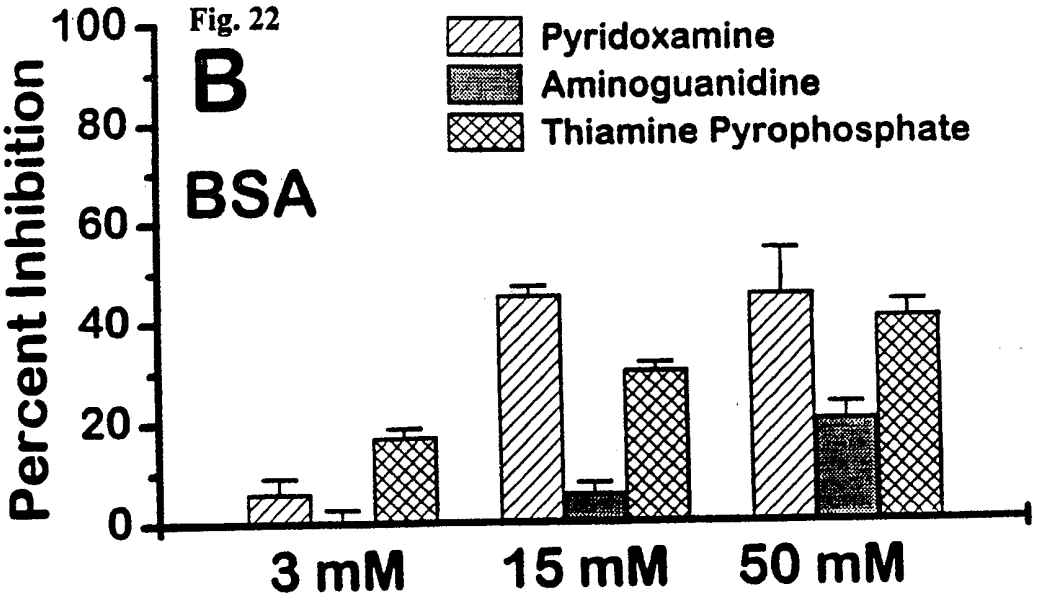
B
BSA
Pyridoxamine
Aminoguanidine
Thiamine Pyrophosphate
Percent Inhibition
100
80
60
40
20
0
3 mM
15 mM
50 mM

Fig. 22

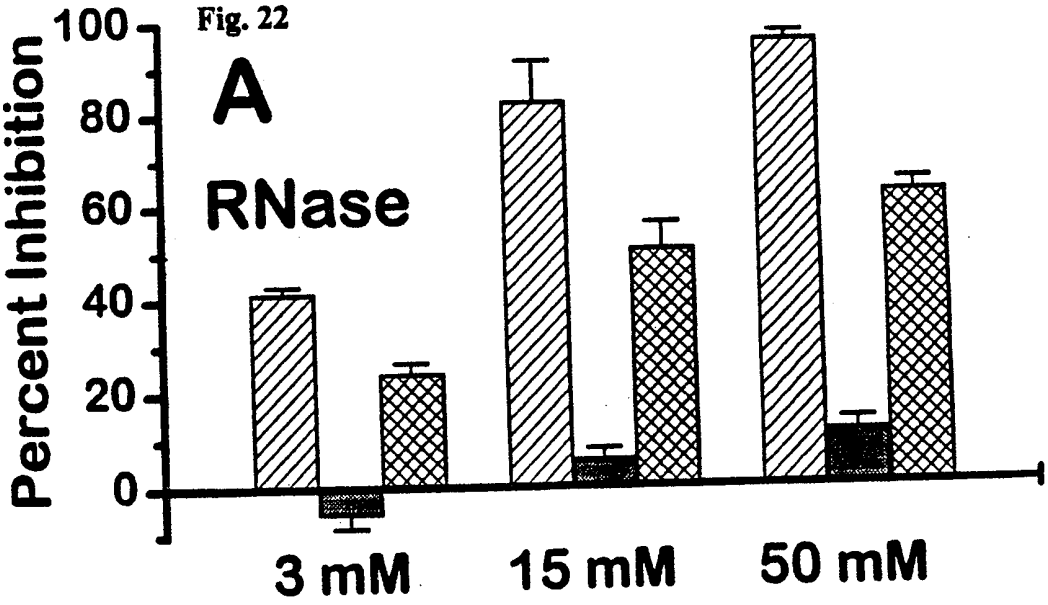
A
RNase
Percent Inhibition
100
80
60
40
20
0
3 mM
15 mM
50 mM

Fig.23

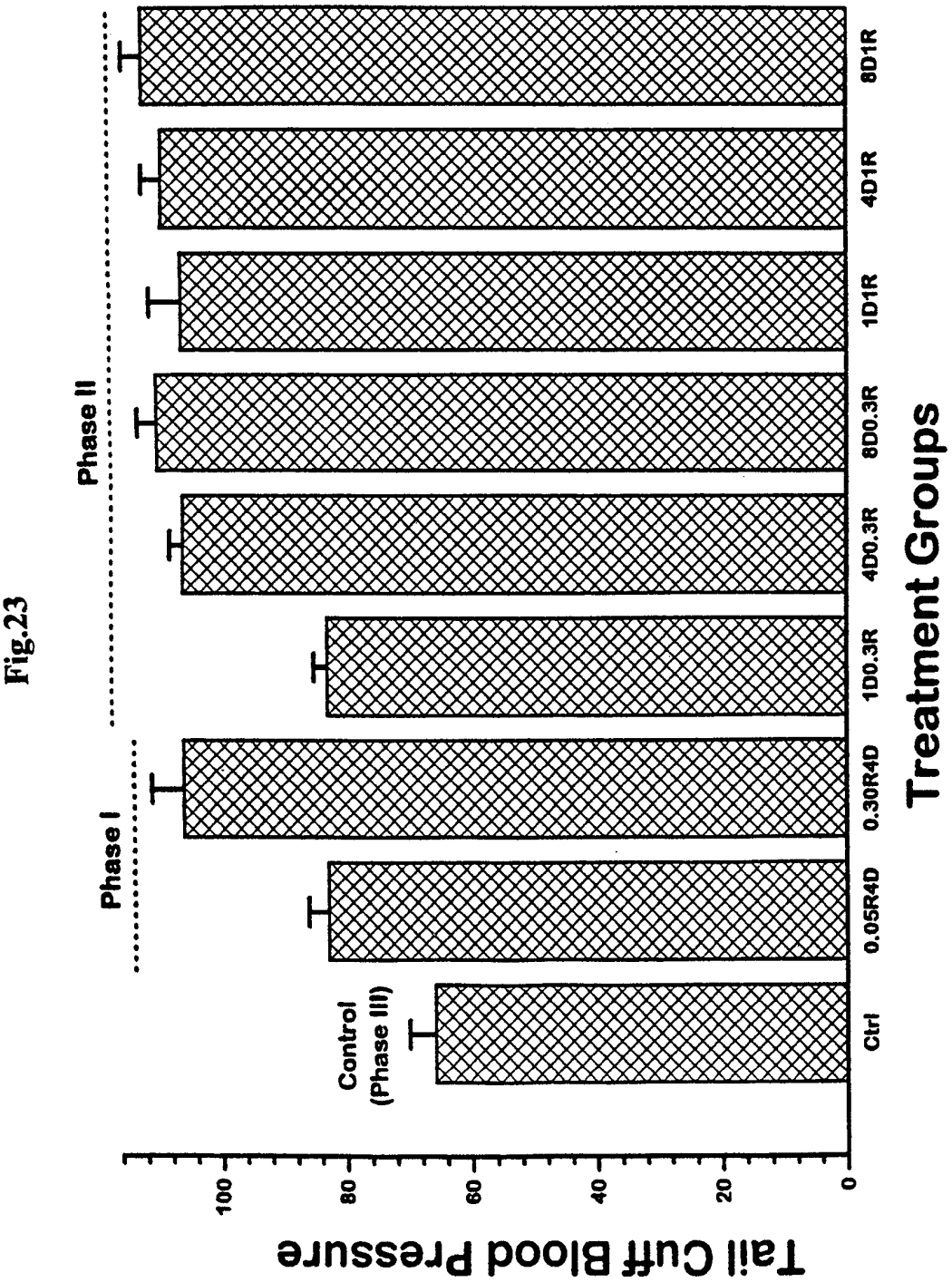
Tail Cuff Blood Pressure
0
20
40
60
80
100
Phase I
Phase II
Control (Phase III)
Ctrl
0.05R4D
0.30R4D
1D0.3R
4D0.3R
8D0.3R
1D1R
4D1R
8D1R
Treatment Groups

Fig. 24

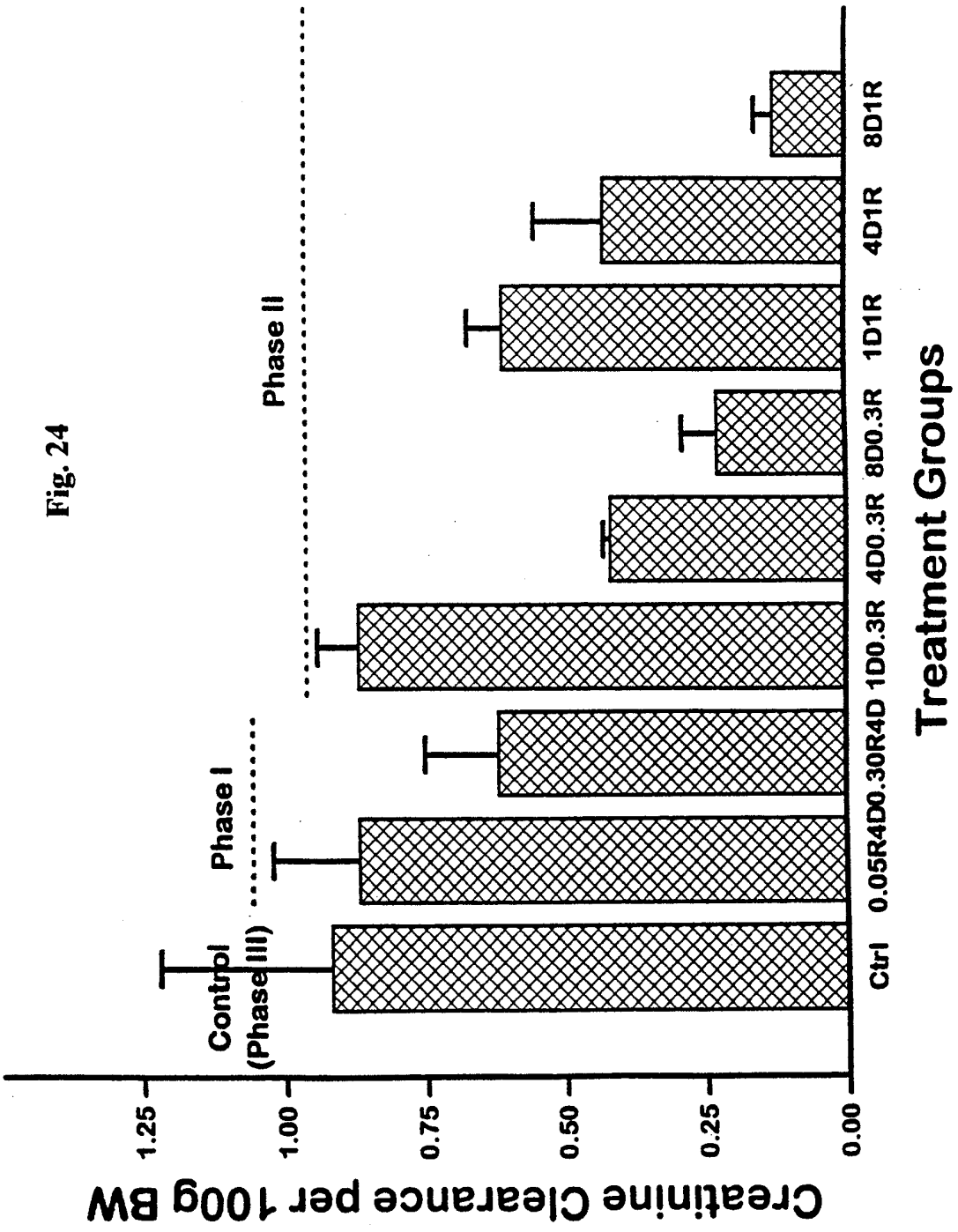
Creatinine Clearance per 100g BW
1.25
1.00
0.75
0.50
0.25
0.00
Control
(Phase III)
Phase I
Phase II
Ctrl
0.05R4D
0.30R4D
1D0.3R
4D0.3R
8D0.3R
1D1R
4D1R
8D1R
Treatment Groups

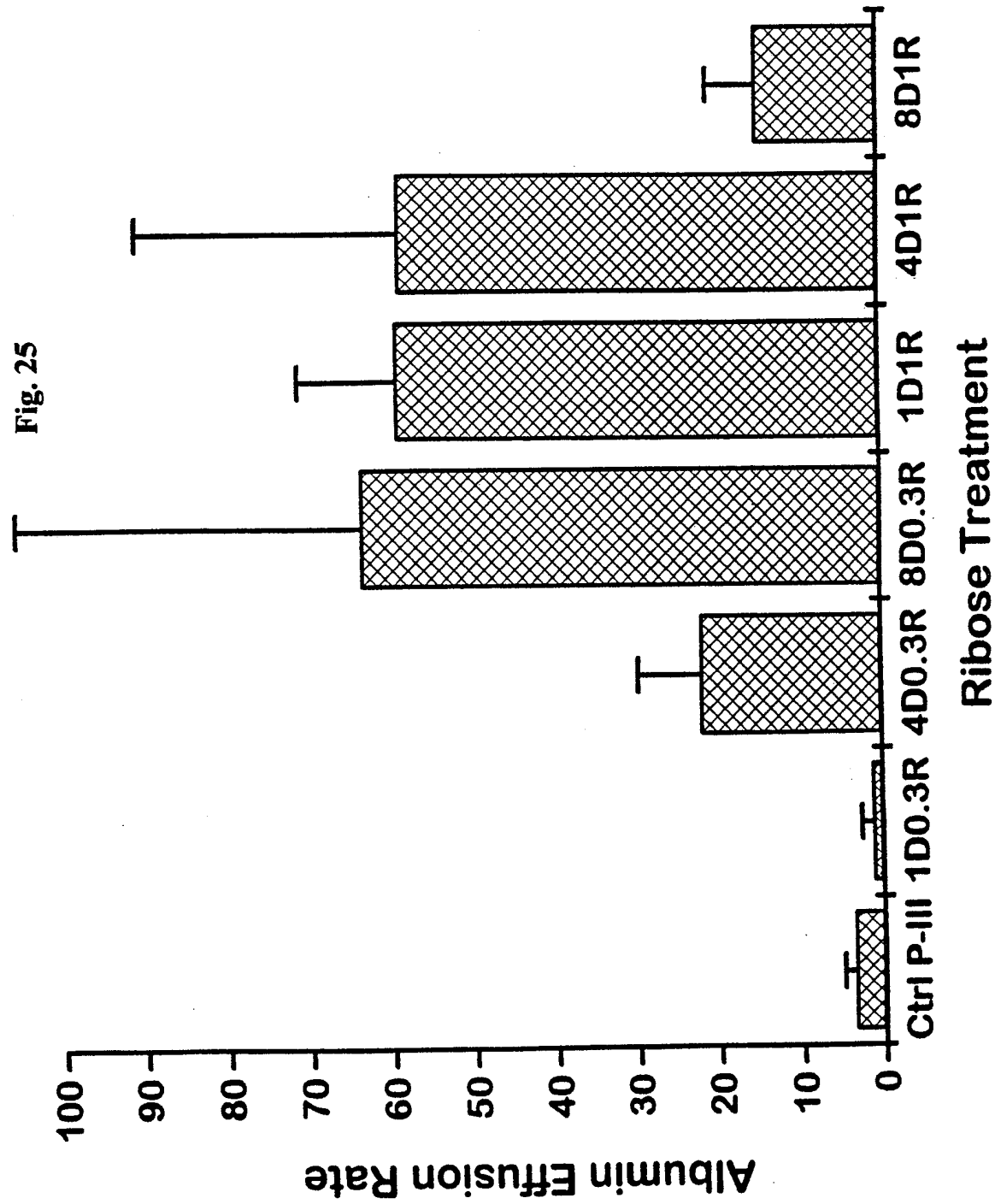
Albumin Effusion Rate
100
90
80
70
60
50
40
30
20
10
0
Ctrl P-III
1D0.3R
4D0.3R
8D0.3R
1D1R
4D1R
8D1R
Ribose Treatment

Fig. 25

Fig. 26

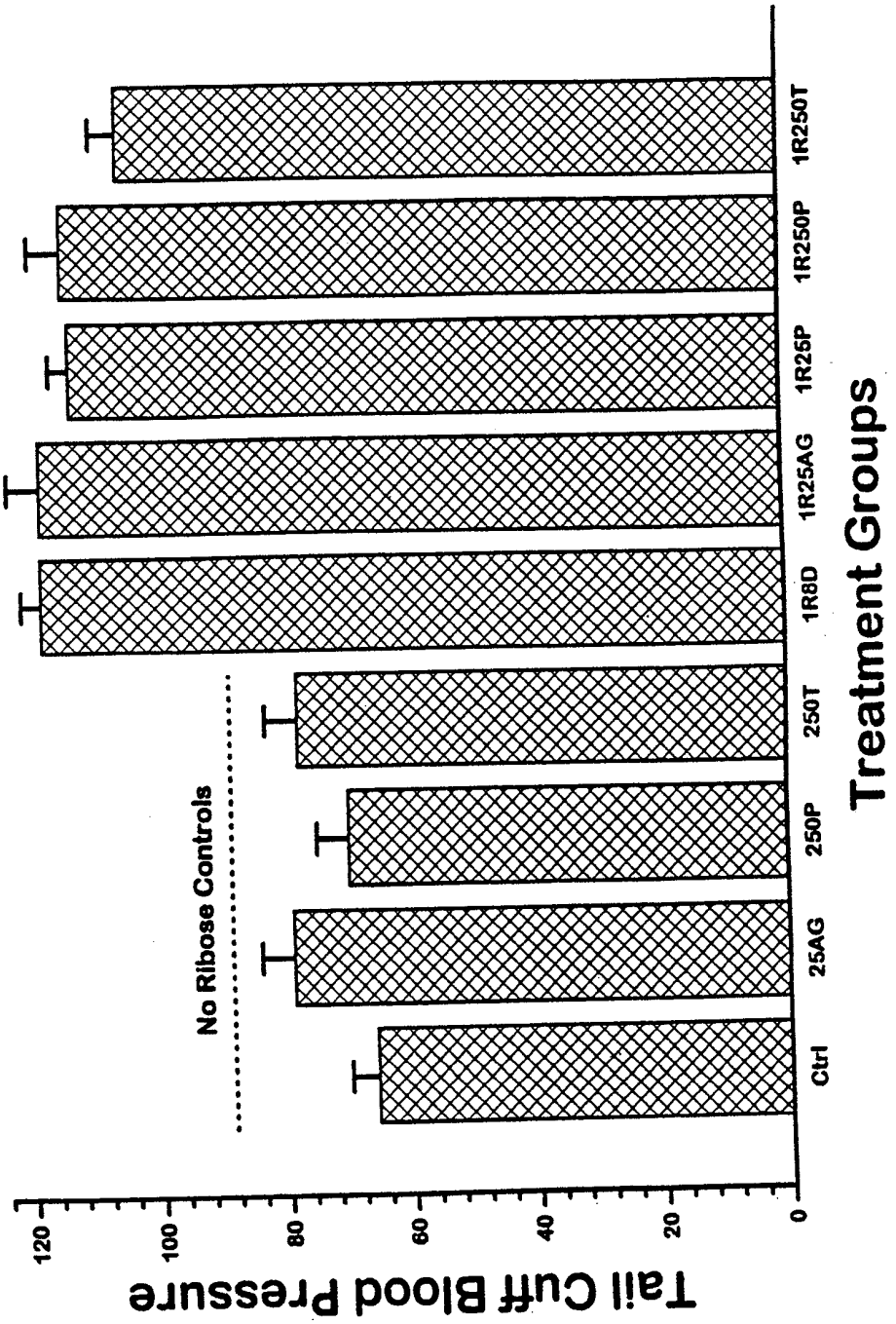
Tail Cuff Blood Pressure
120
100
80
60
40
20
0
No Ribose Controls
1 M Ribose
Ctrl
25AG
250P
250T
1R8D
1R25AG
1R25P
1R250P
1R250T
Treatment Groups

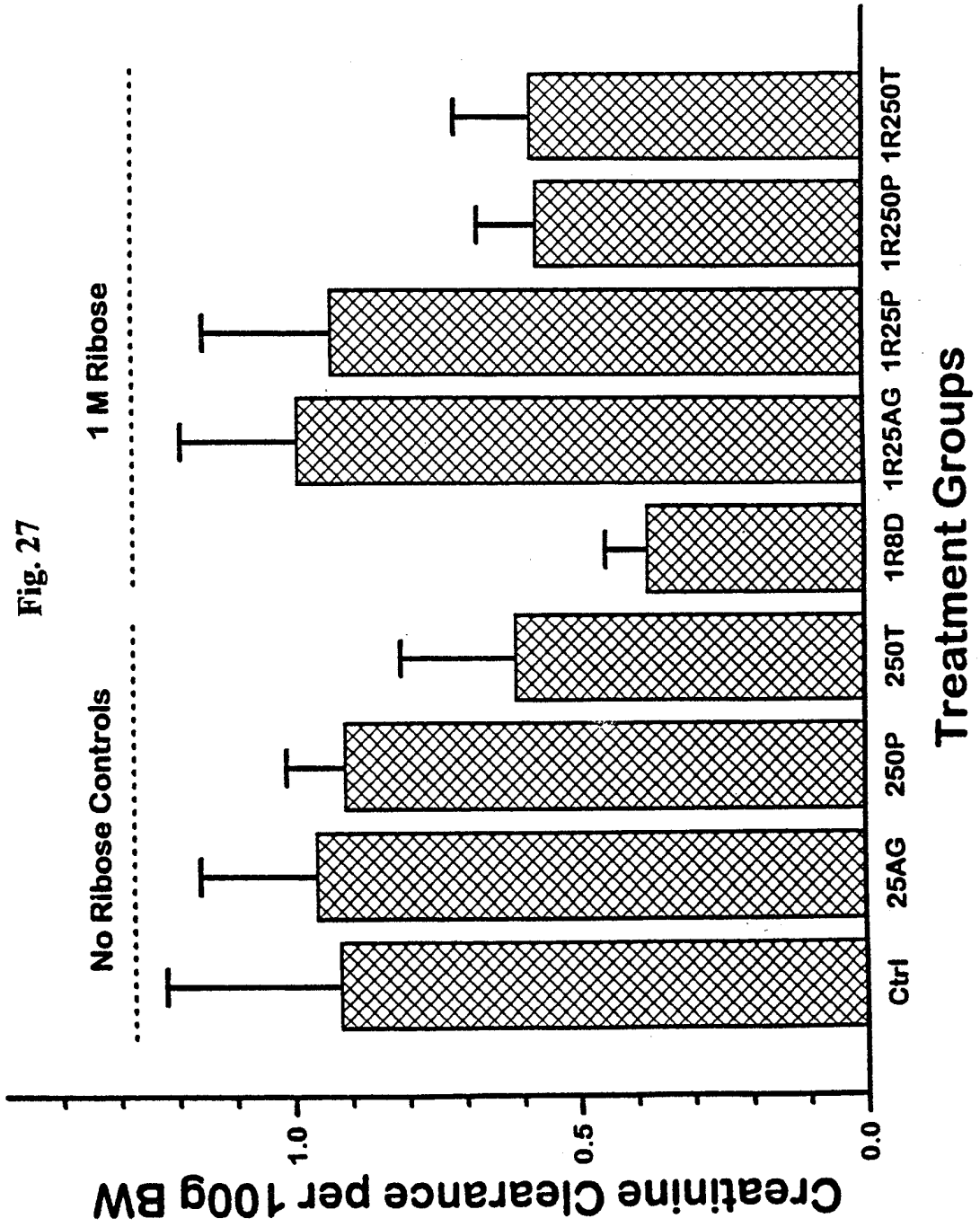
Creatinine Clearance per 100g BW
0.0
0.5
1.0
No Ribose Controls
1 M Ribose
Ctrl
25AG
250P
250T
1R8D
1R25AG
1R25P
1R250P
1R250T
Treatment Groups

Fig. 27

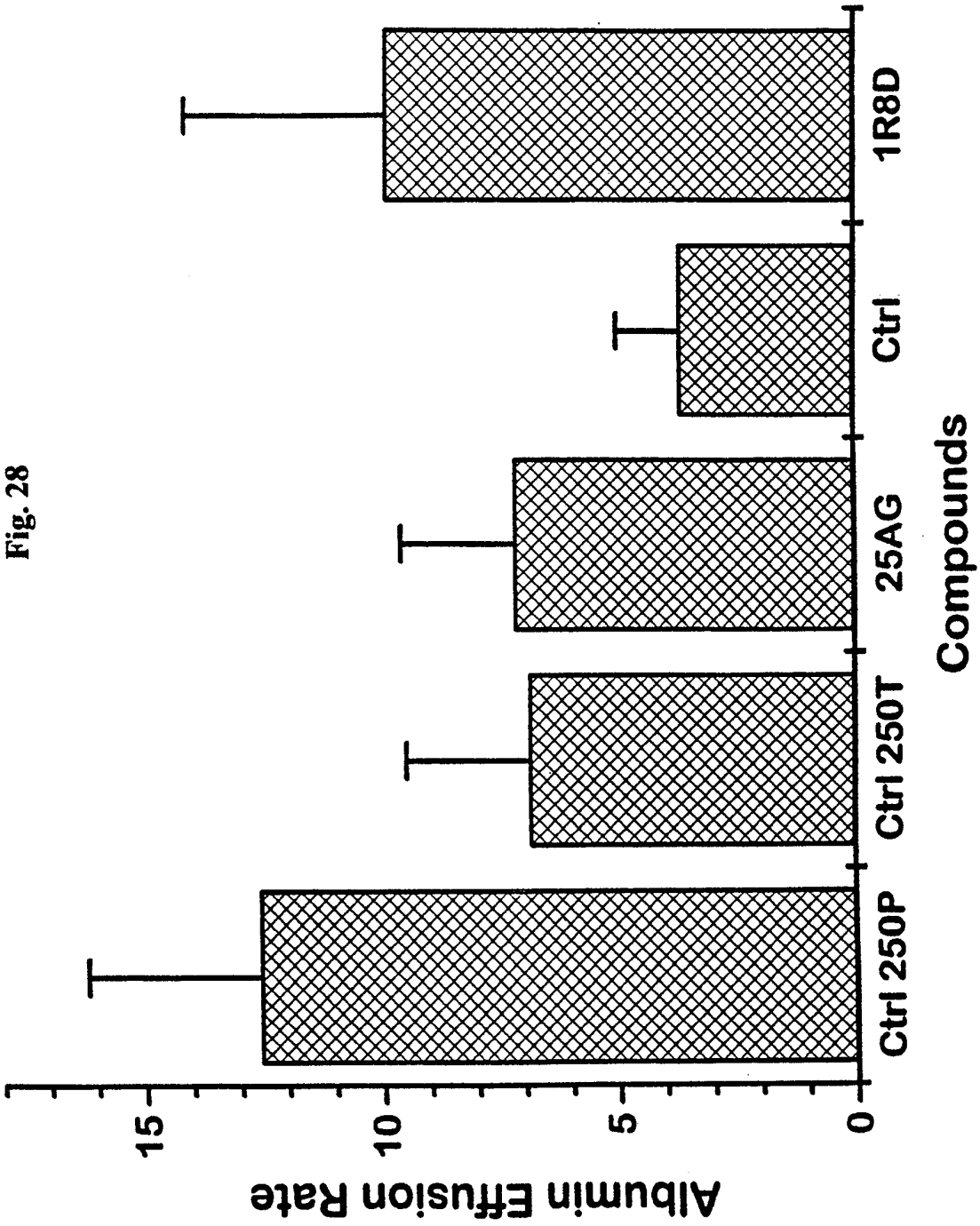
Albumin Effusion Rate
0
5
10
15
Ctrl 250P
Ctrl 250T
25AG
Ctrl
1R8D
Compounds

Fig. 28

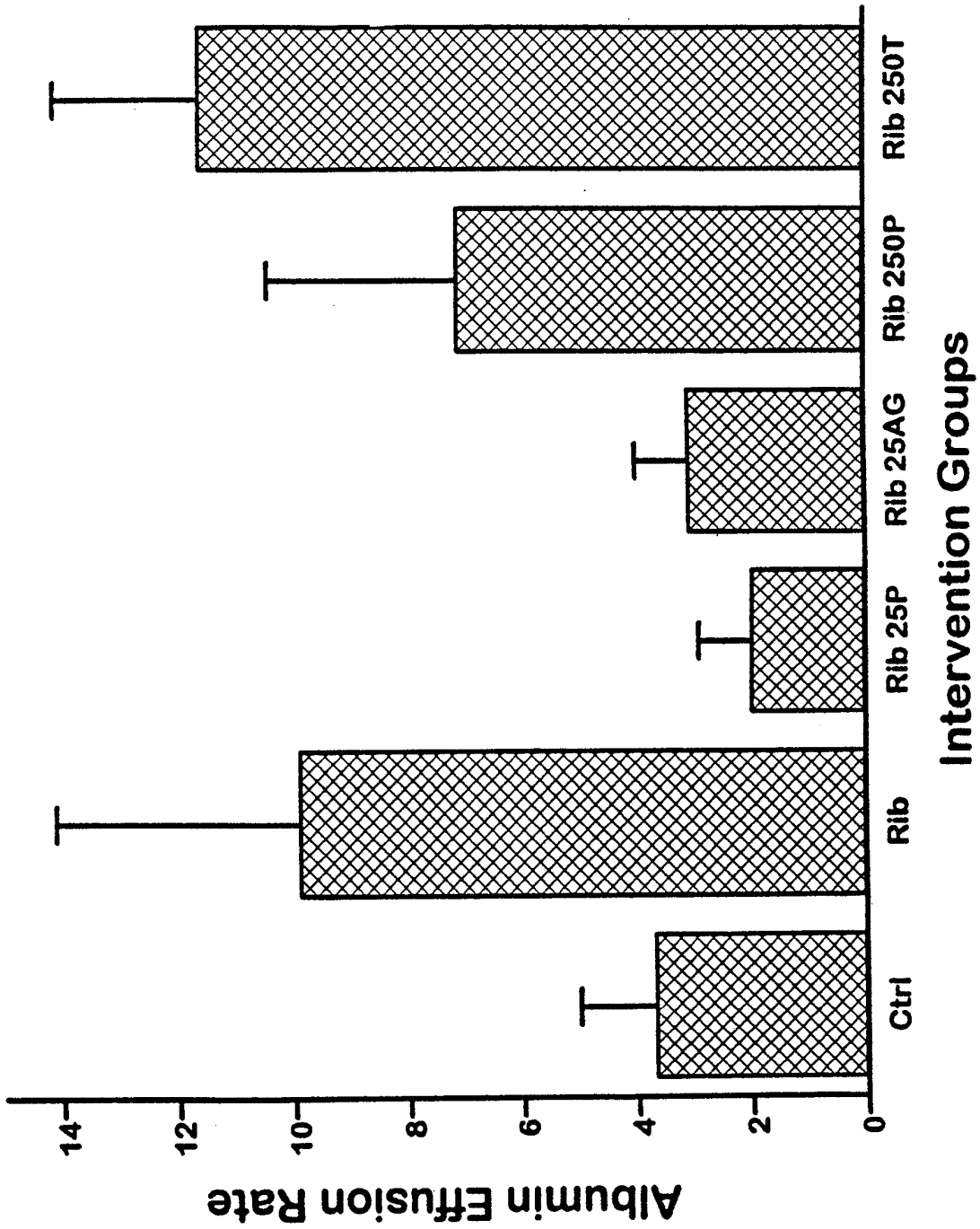
Albumin Effusion Rate
0
2
4
6
8
10
12
14
Ctrl
Rib
Rib 25P
Rib 25AG
Rib 250P
Rib 250T
Intervention Groups

Fig. 29

Fig. 30A

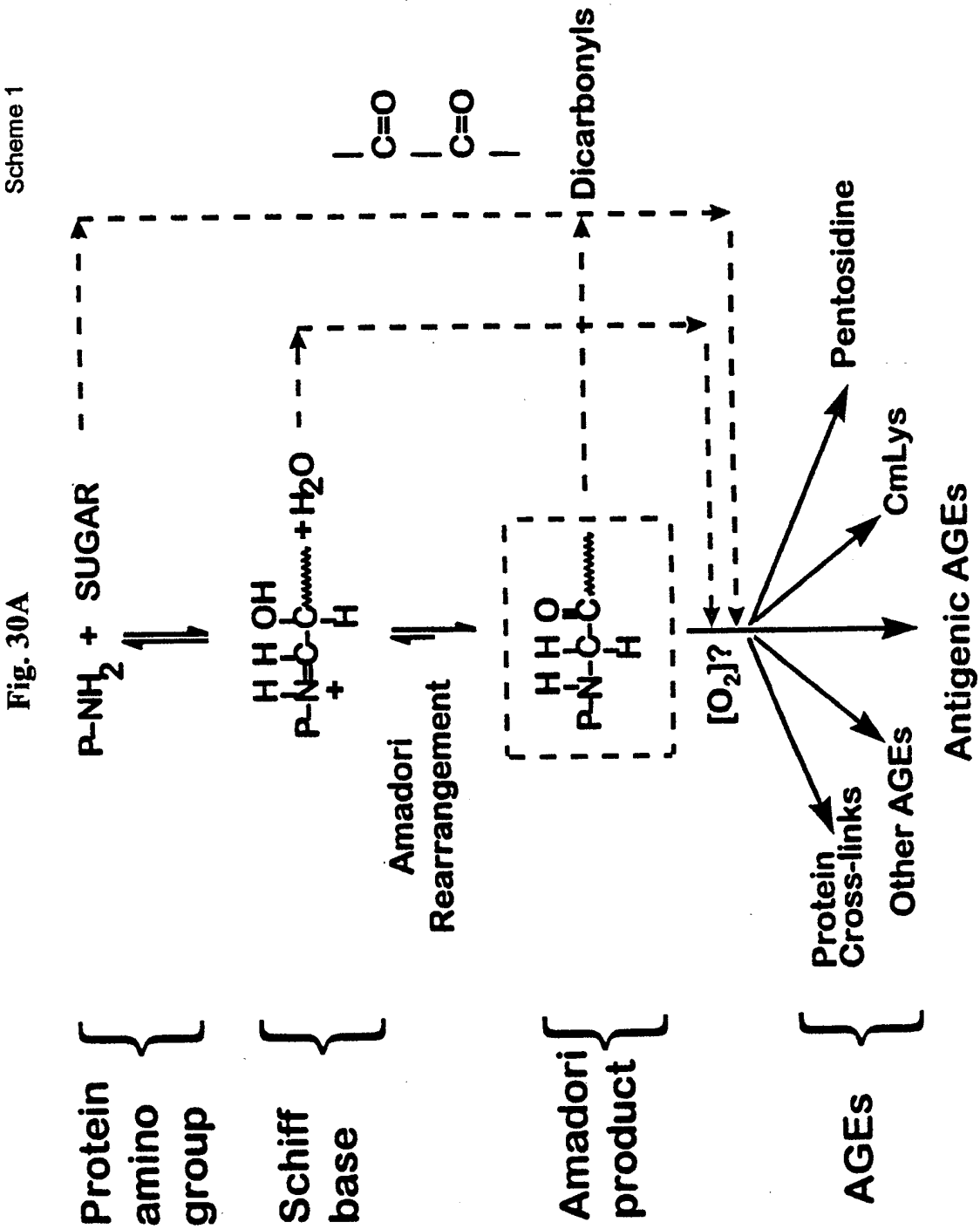
Scheme 1
P-NH2 + SUGAR
H H OH
P-N-C-C + H2O
H H O
P-N-C-C
H
Amadori Rearrangement
C=O
C=O
Dicarbonyls
[O2]?
Pentosidine
CmLys
Antigenic AGEs
Protein Cross-links
Other AGEs
Protein amino group
Schiff base
Amadori product
AGEs

Scheme 2

Fig. 30B

Aminoguanidine

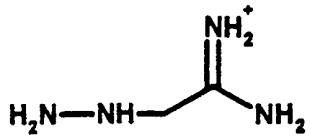

Scheme 3

Fig. 30C

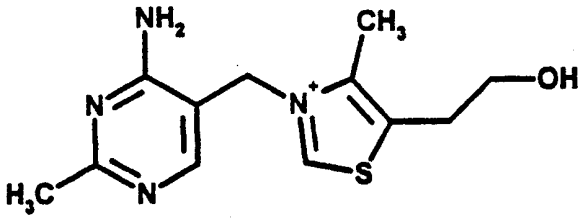

Thiamine

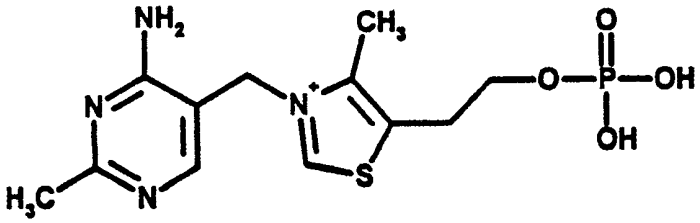

Thiamine-5'-Phosphate

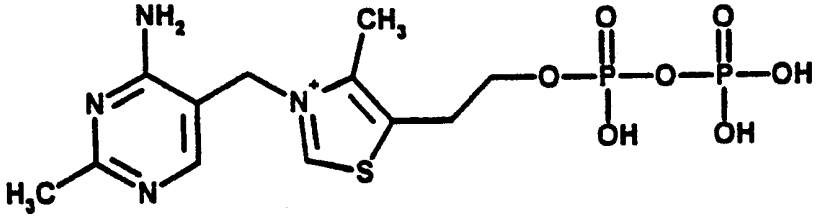

Thiamine Pyrophosphate

Scheme 4

Fig. 30D

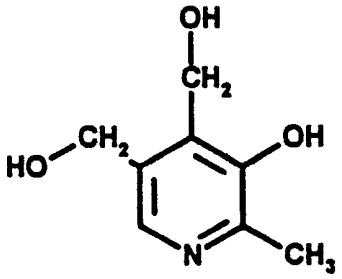

Pyridoxine

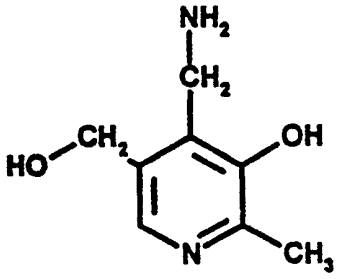

Pyridoxamine

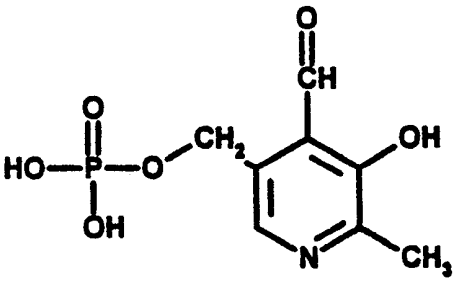

Pyridoxal-5'-Phosphate

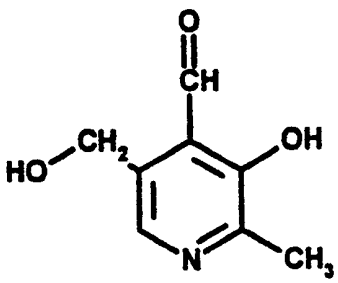

Pyridoxal

Scheme 5

Fig. 30E

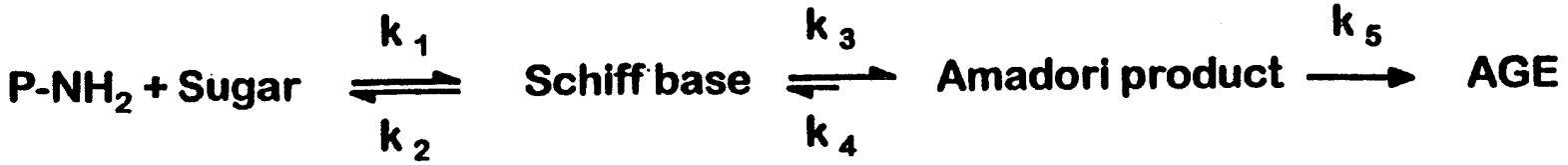

Scheme 6

Fig. 30F

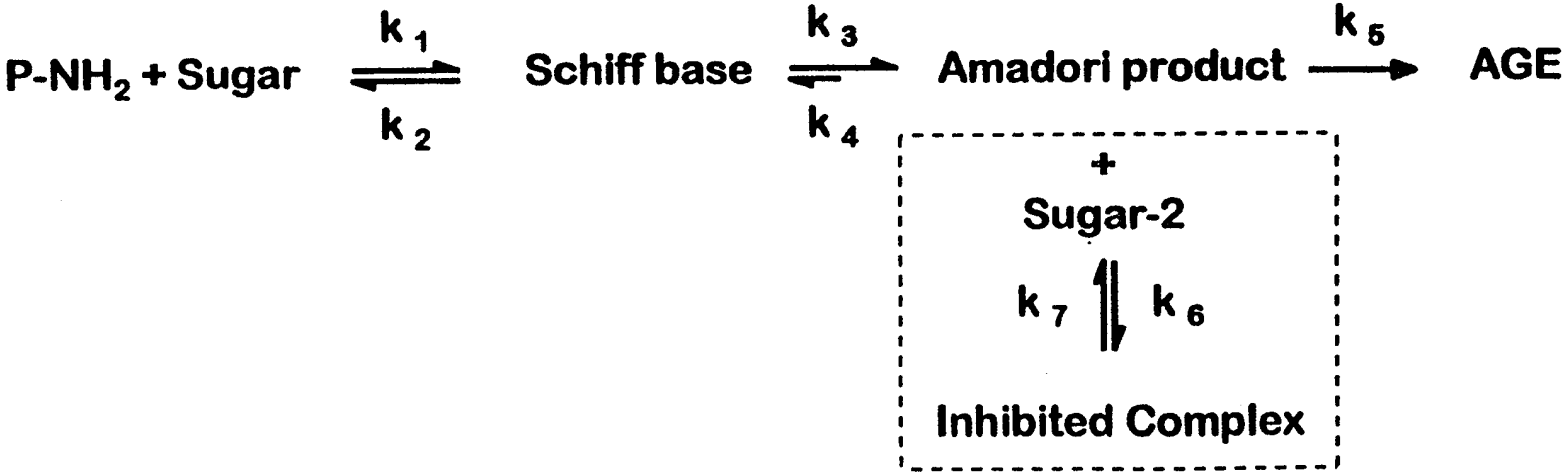

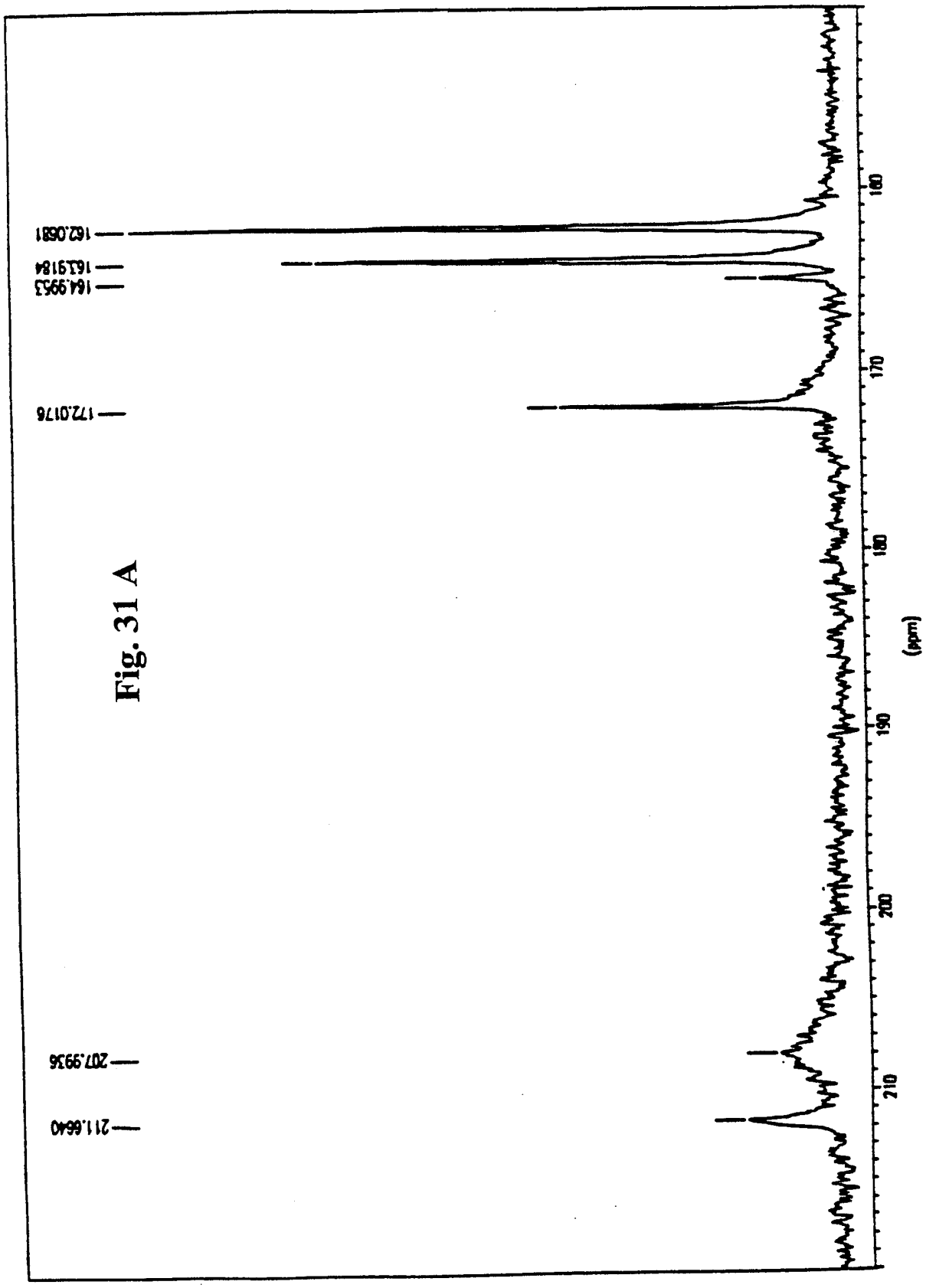
162.0681
163.9184
164.9953
172.0176
207.9936
211.6640
160
170
180
190
200
210
(ppm)

Fig. 31 A

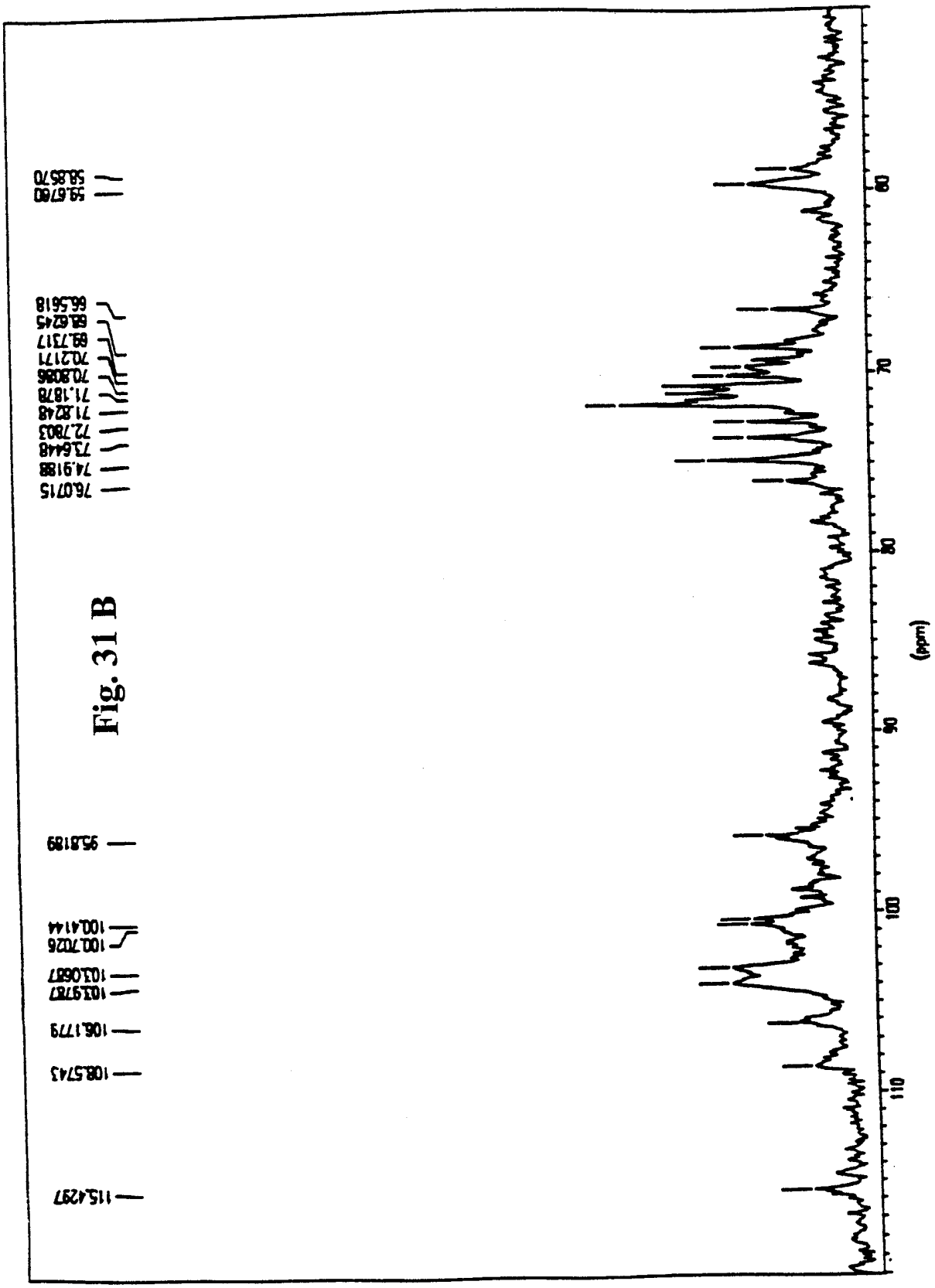
59.6760
58.8570
66.5618
68.6245
69.7317
70.2171
70.8086
71.1878
71.8248
72.7803
73.6448
74.9188
76.0715
95.8189
100.4144
100.7026
103.0687
103.9787
106.1779
108.5743
115.4297
60
70
80
90
100
110
(ppm)

Fig. 31 B

Fig. 32A

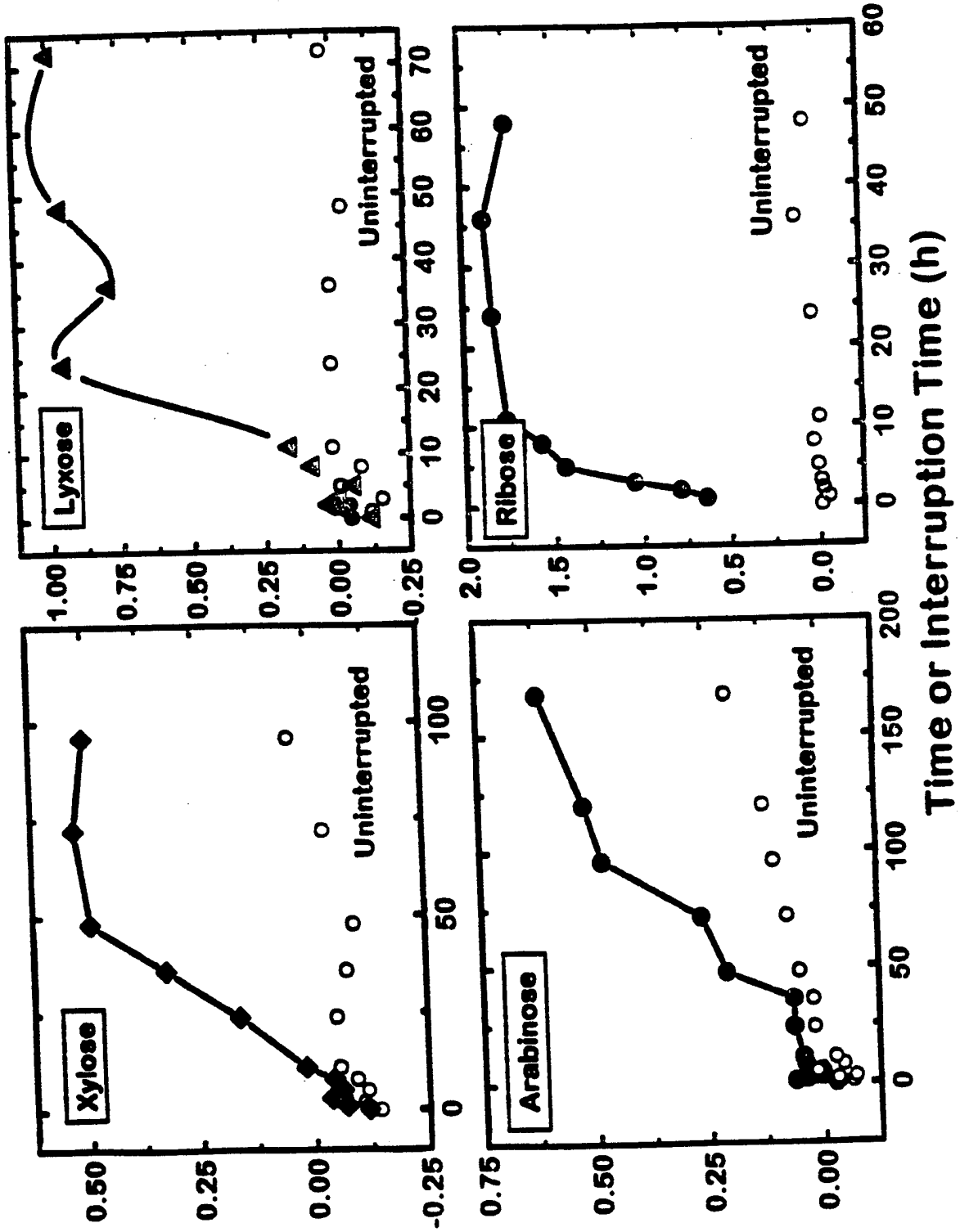
Xylose
Lyxose
Ribose
Arabinose
Uninterrupted
Time or Interruption Time (h)

Fig. 32B

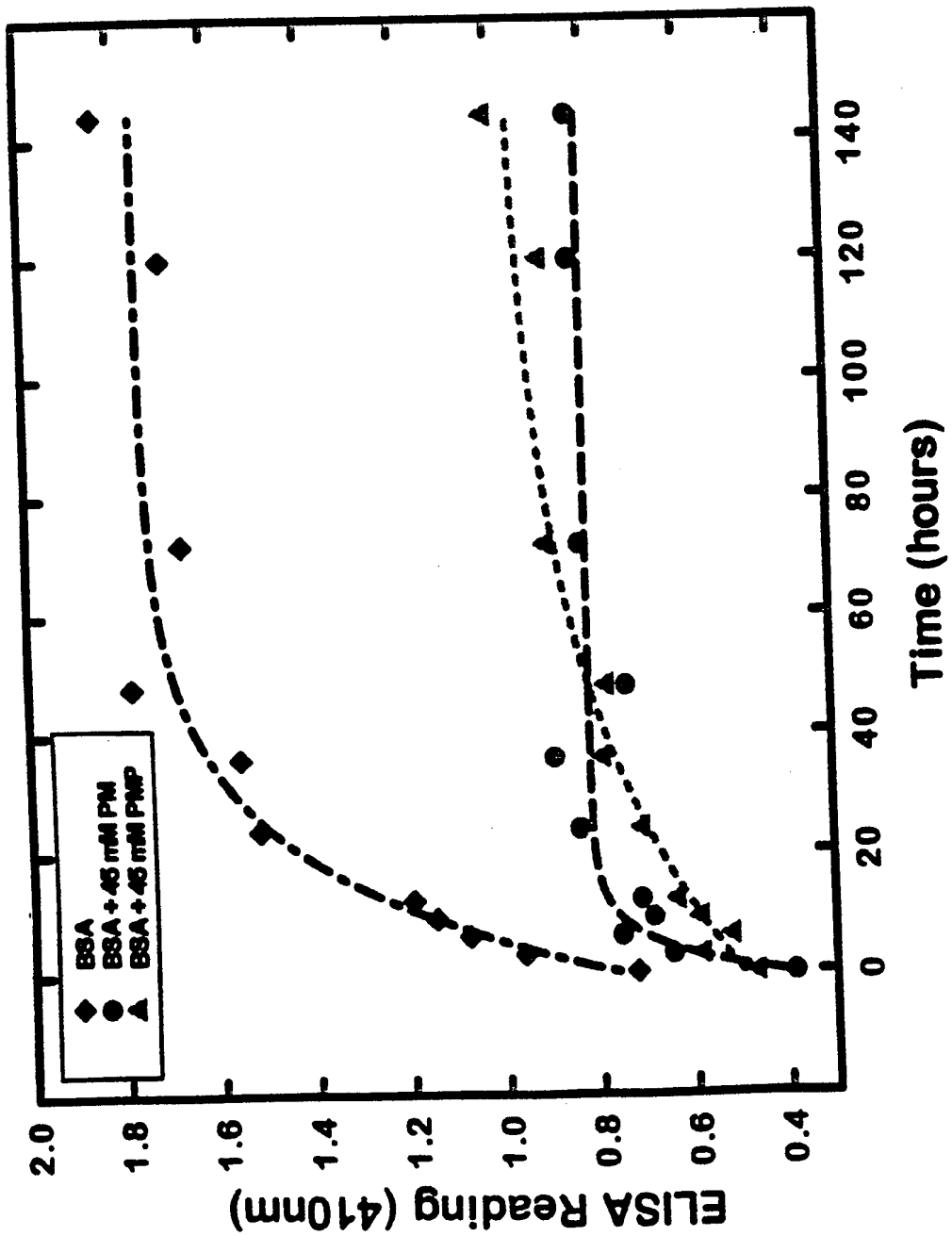
ELISA Reading (410nm)
2.0
1.8
1.6
1.4
1.2
1.0
0.8
0.6
0.4
Time (hours)
0
20
40
60
80
100
120
140
BSA
BSA + 45 mM PM
BSA + 45 mM PMP

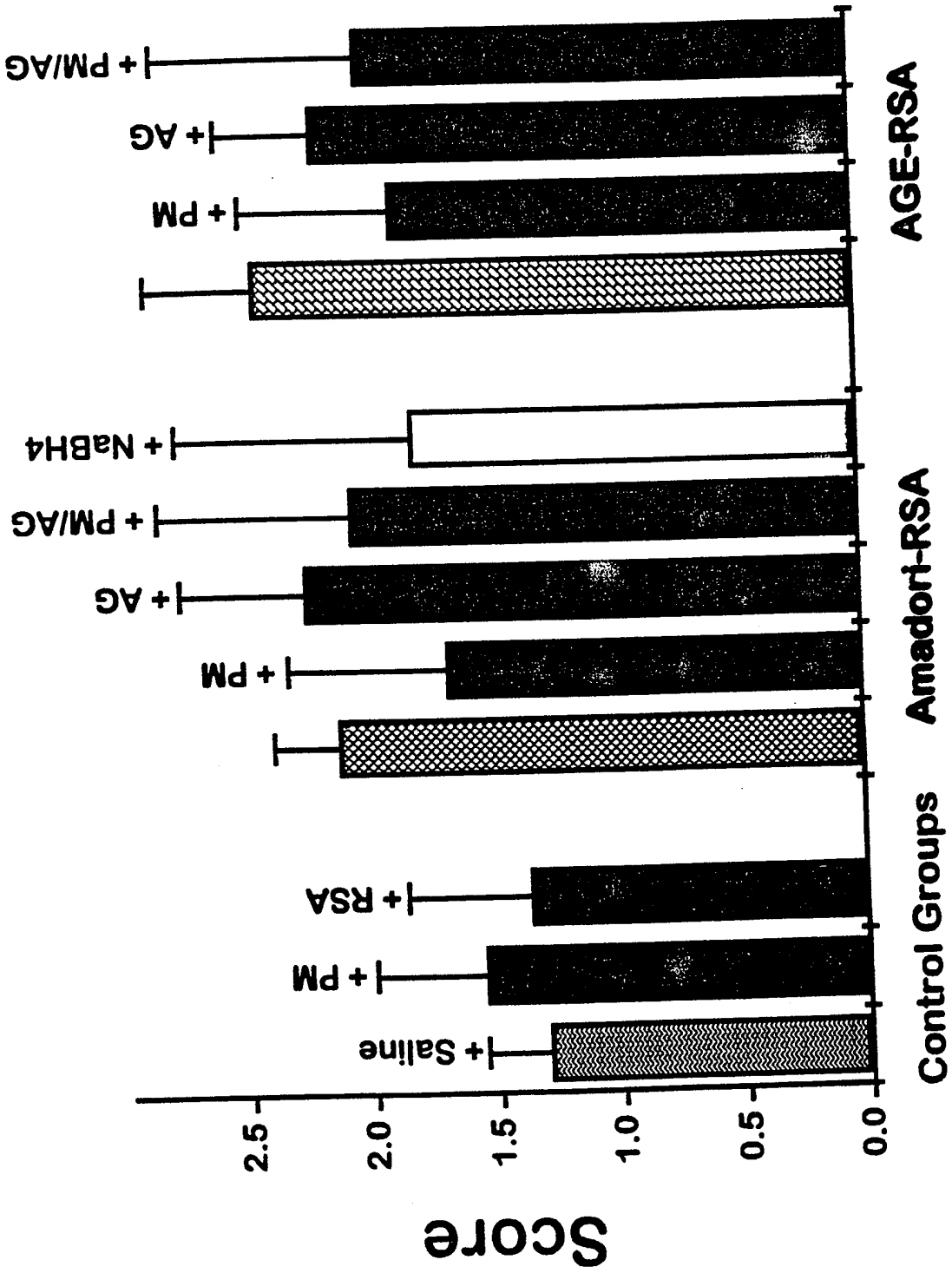
Score
2.5
2.0
1.5
1.0
0.5
0.0
+ Saline
+ PM
+ RSA
+ PM/AG
+ AG
+ PM
+ NaBH4
+ PM/AG
+ AG
+ PM
Control Groups
Amadori-RSA
AGE-RSA

Fig. 33

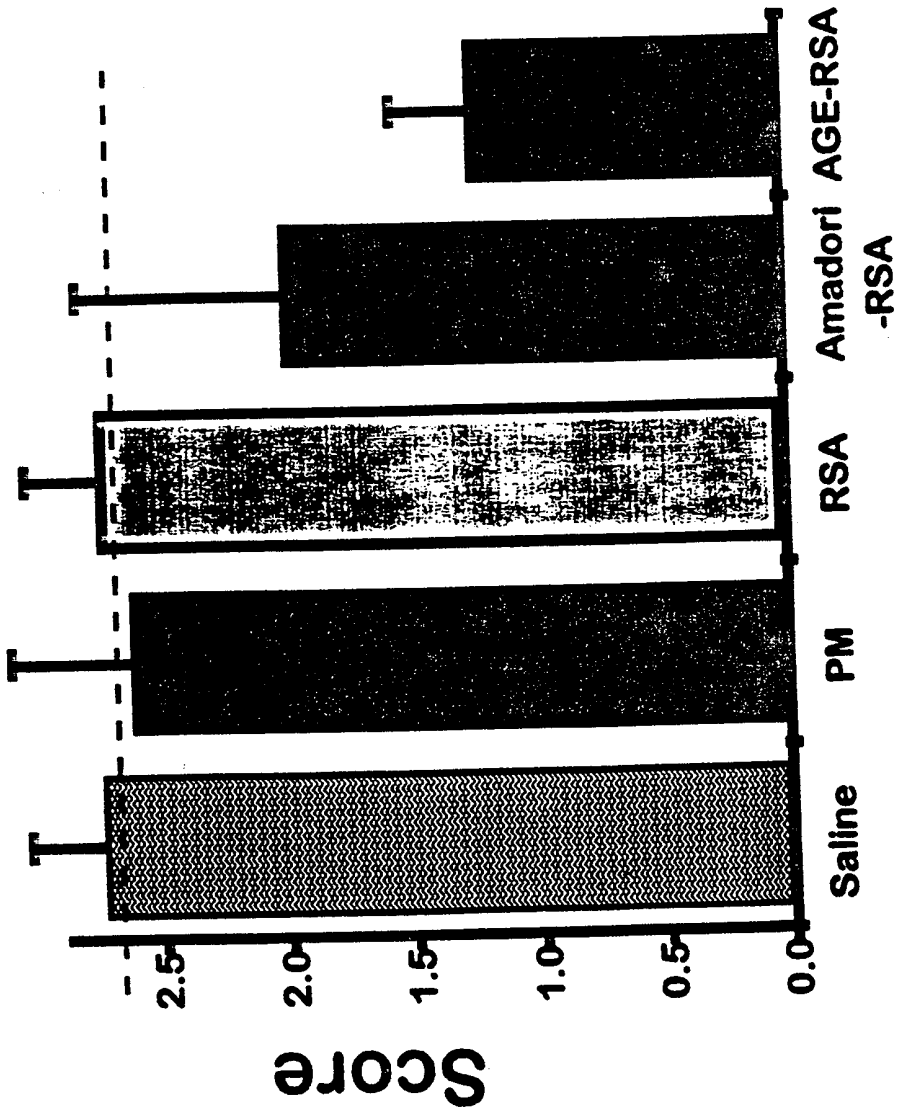

Fig. 34

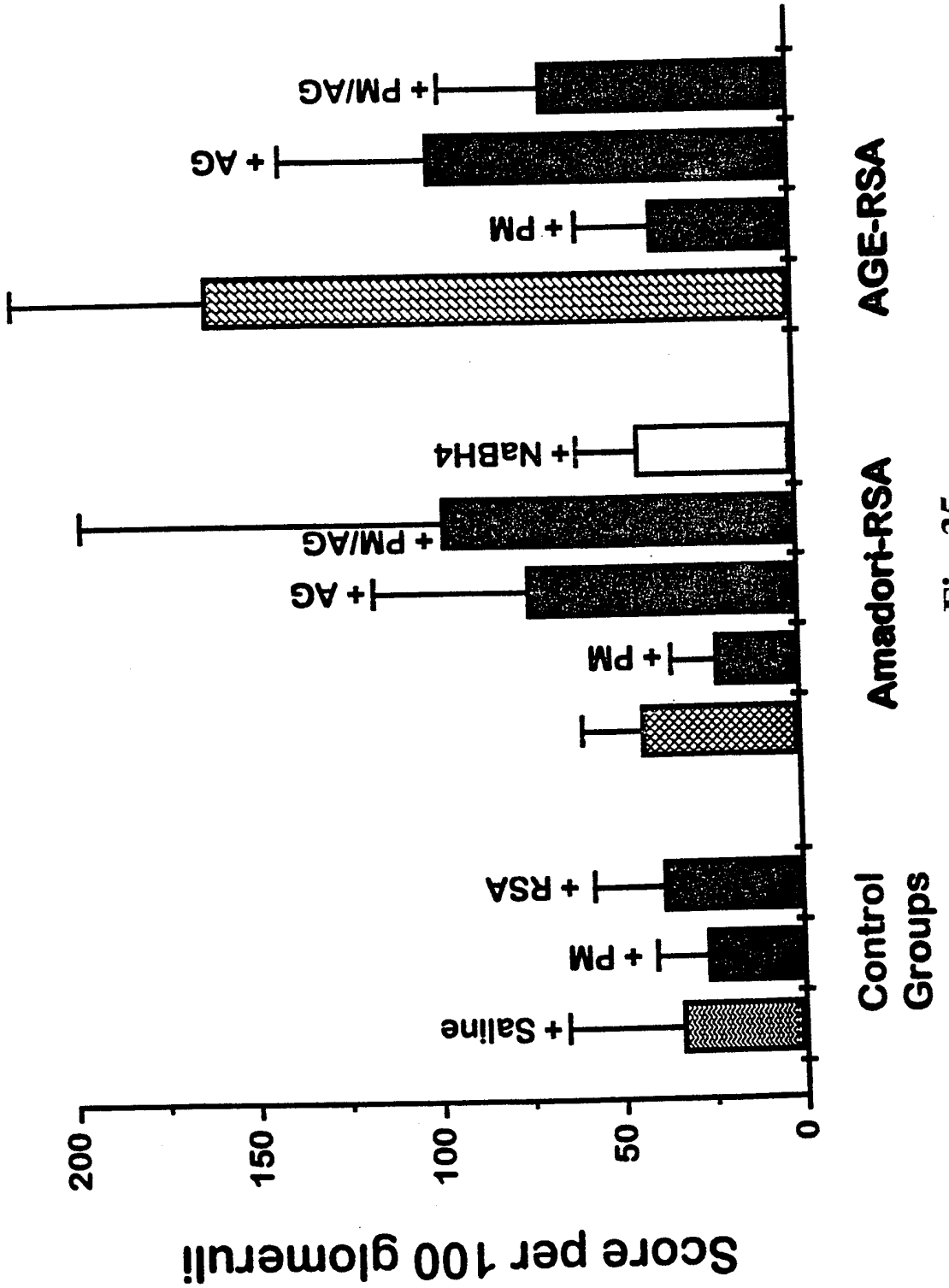
Score per 100 glomeruli
200
150
100
50
0
+ Saline
+ PM
+ RSA
Control Groups
+ PM
+ AG
+ PM/AG
+ NaBH4
Amadori-RSA
+ PM
+ AG
+ PM/AG
AGE-RSA

Fig. 35

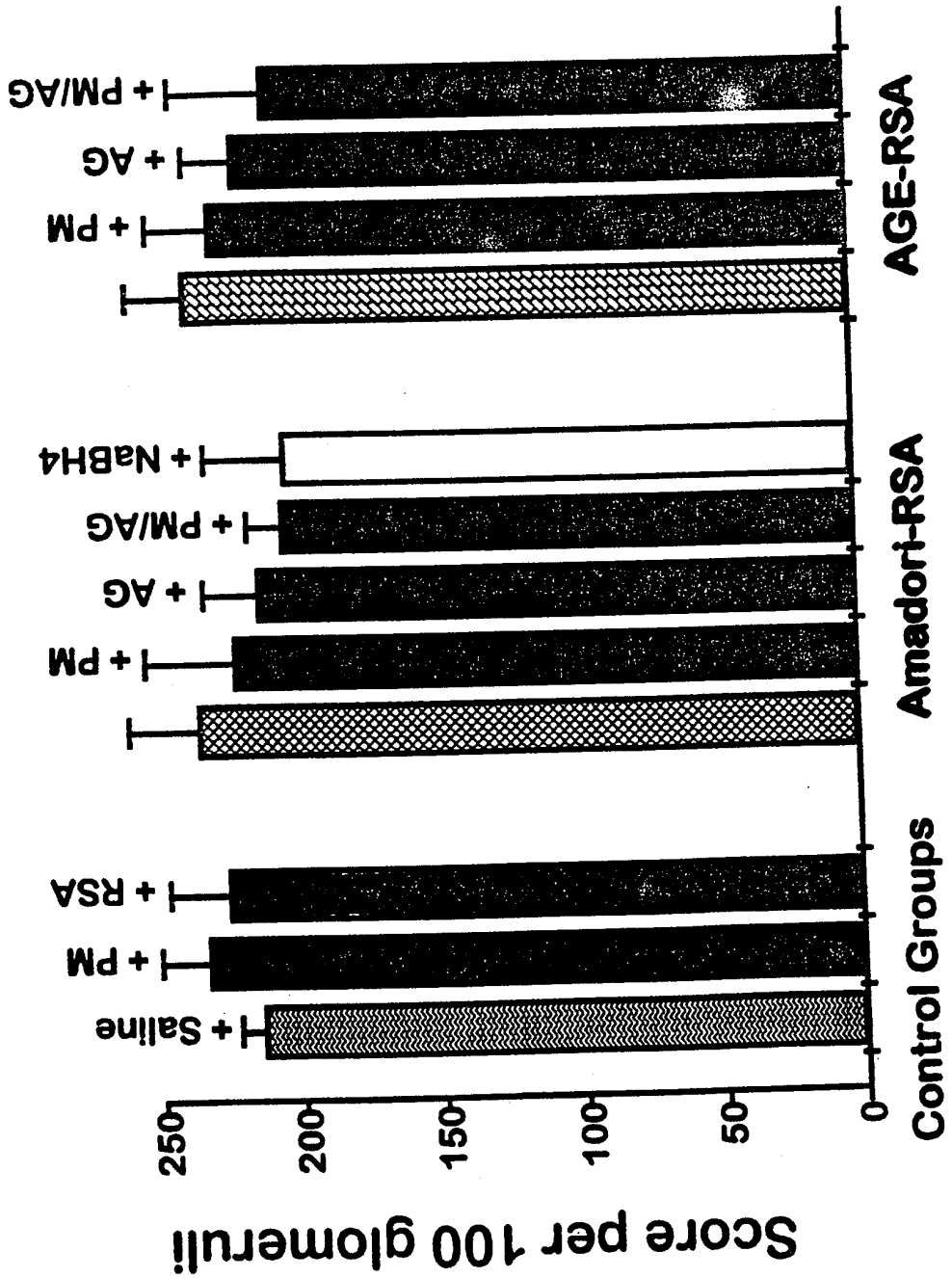
Score per 100 glomeruli
250
200
150
100
50
0
Control Groups
+ Saline
+ PM
+ RSA
Amadori-RSA
+ PM
+ AG
+ PM/AG
+ NaBH4
AGE-RSA
+ PM
+ AG
+ PM/AG

Fig. 36

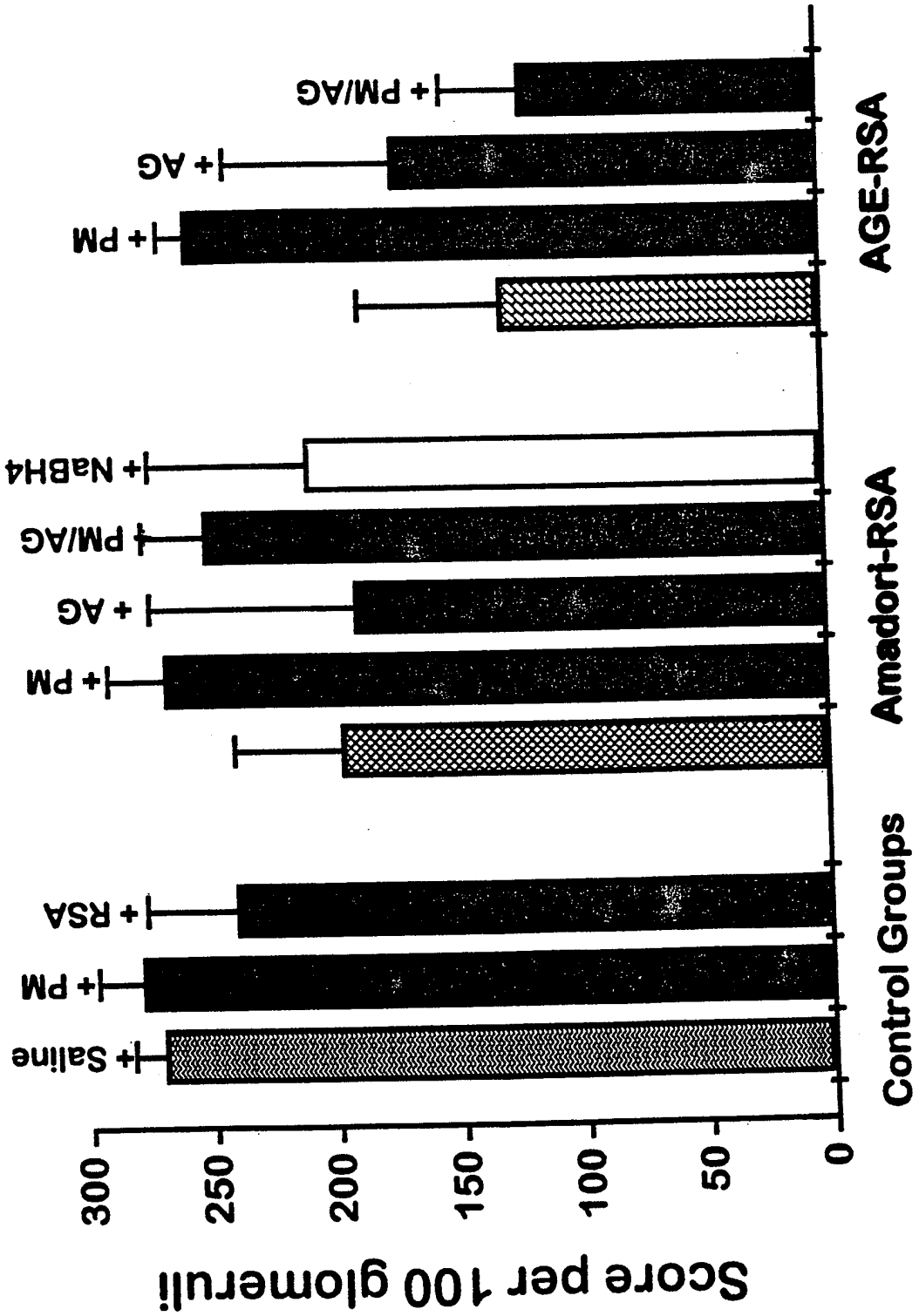
Score per 100 glomeruli
300
250
200
150
100
50
0
Control Groups
Amadori-RSA
AGE-RSA
+ Saline
+ PM
+ RSA
+ PM
+ AG
+ PM/AG
+ NaBH4
+ PM
+ AG
+ PM/AG

Fig. 37

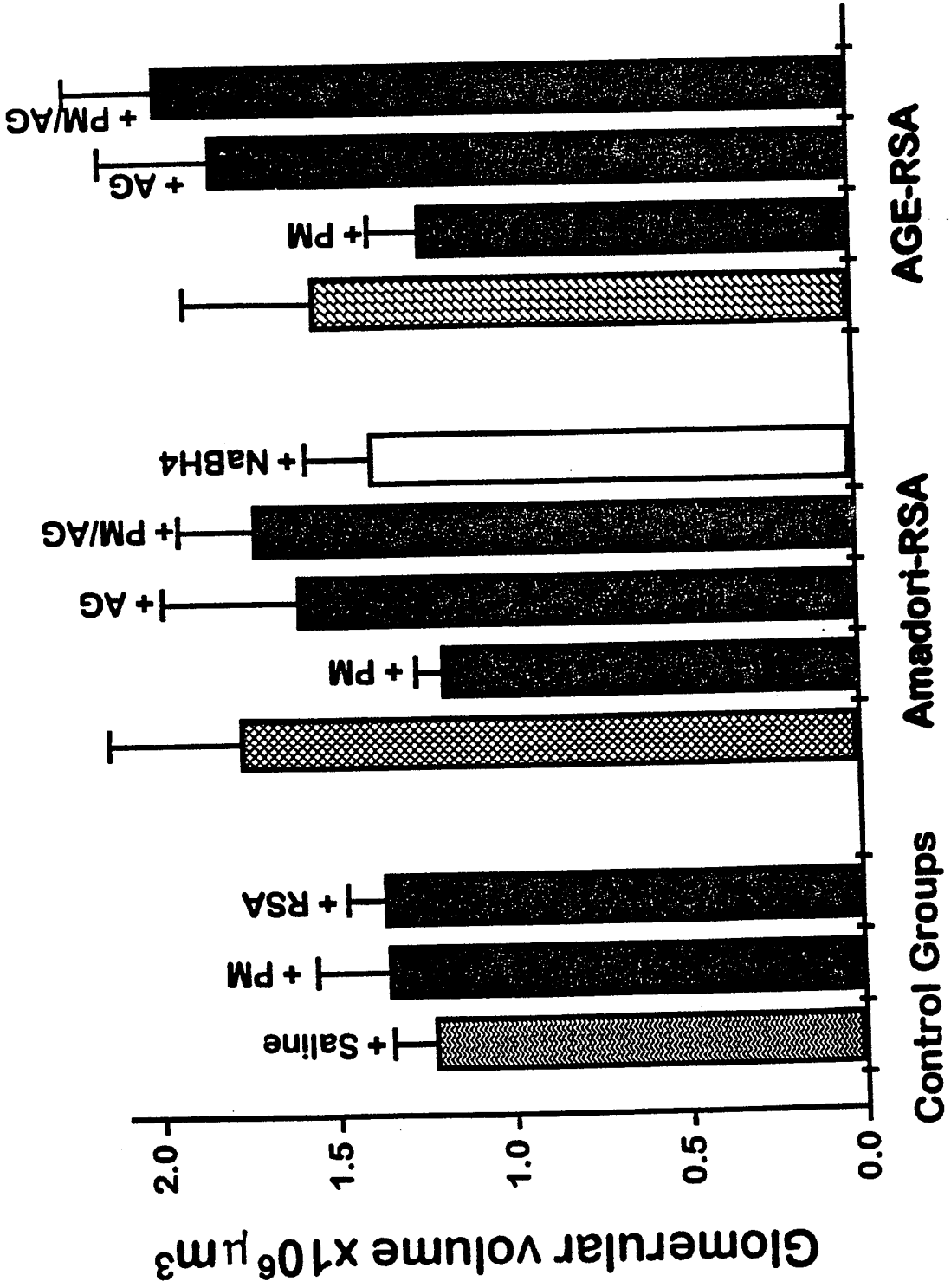
Glomerular volume x10^6 μm^3
2.0
1.5
1.0
0.5
0.0
Control Groups
+ Saline
+ PM
+ RSA
Amadori-RSA
+ PM
+ AG
+ PM/AG
+ NaBH4
AGE-RSA
+ PM
+ AG
+ PM/AG

Fig. 38

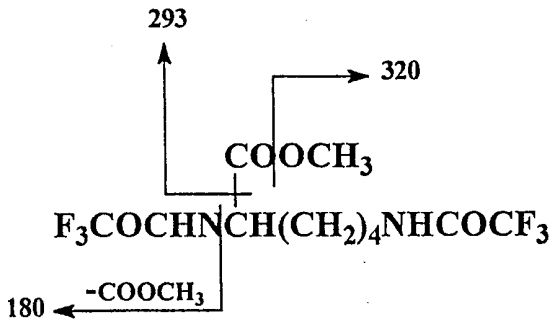
293
320
COOCH3
F3COCHNCH(CH2)4NHCOCF3
180
-COOCH3

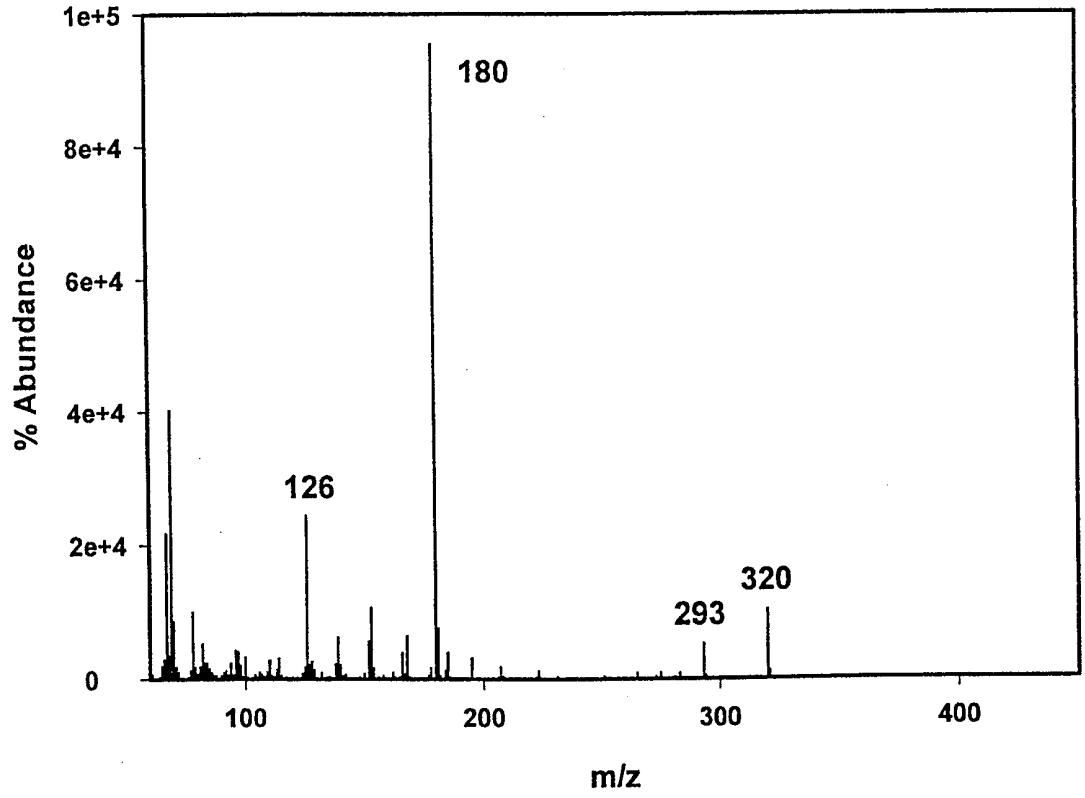
1e+5
8e+4
6e+4
4e+4
2e+4
0
% Abundance
180
126
293
320
100
200
300
400
m/z

CML-TFAME

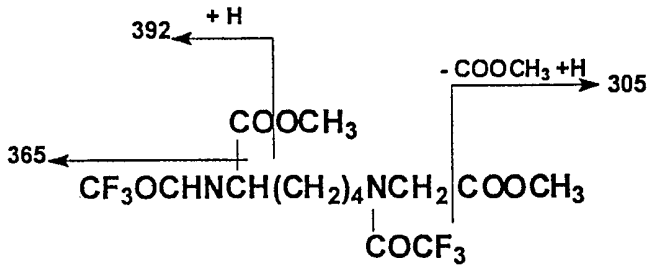

CEL-TFAME

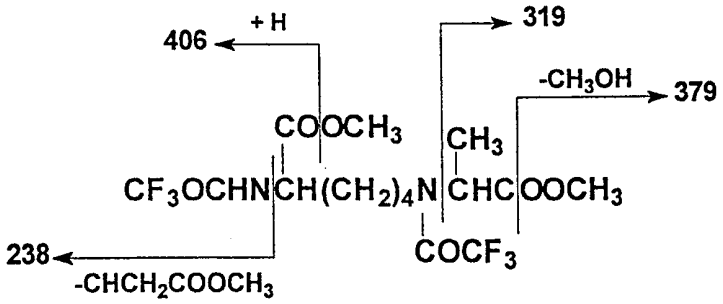

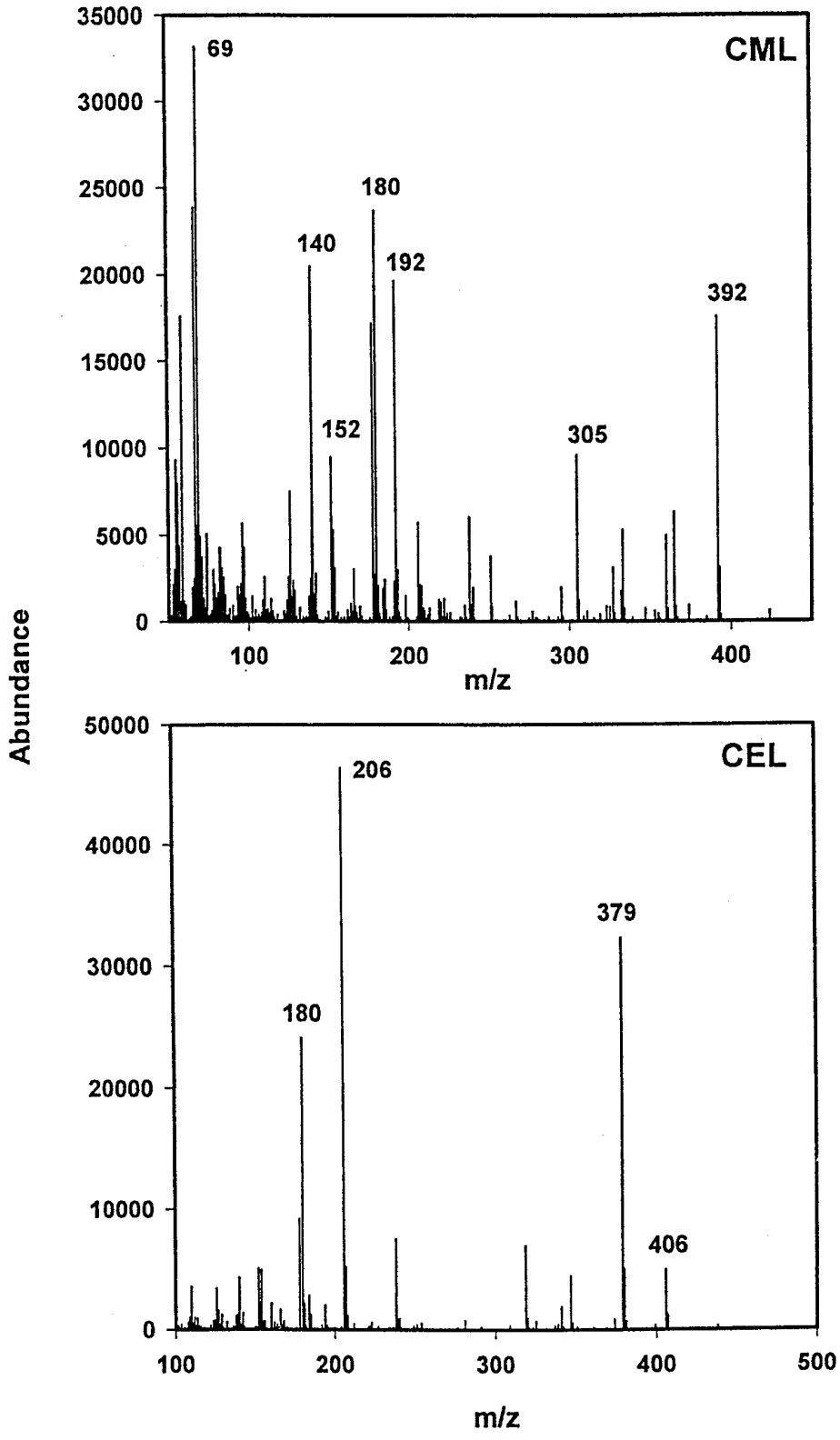
CML
69
180
140
192
392
152
305
35000
30000
25000
20000
15000
10000
5000
0
100
200
300
400
m/z
Abundance
CEL
206
379
180
406
50000
40000
30000
20000
10000
0
100
200
300
400
500
m/z

MDA-Lysine-TFAME

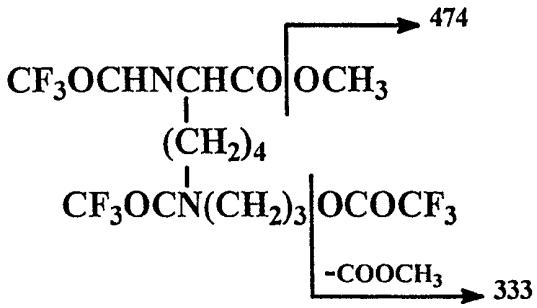

HNE-Lysine-TFAME

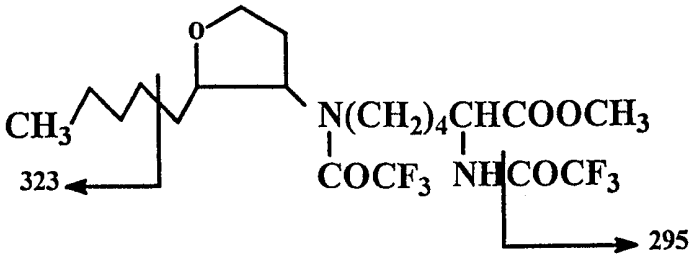

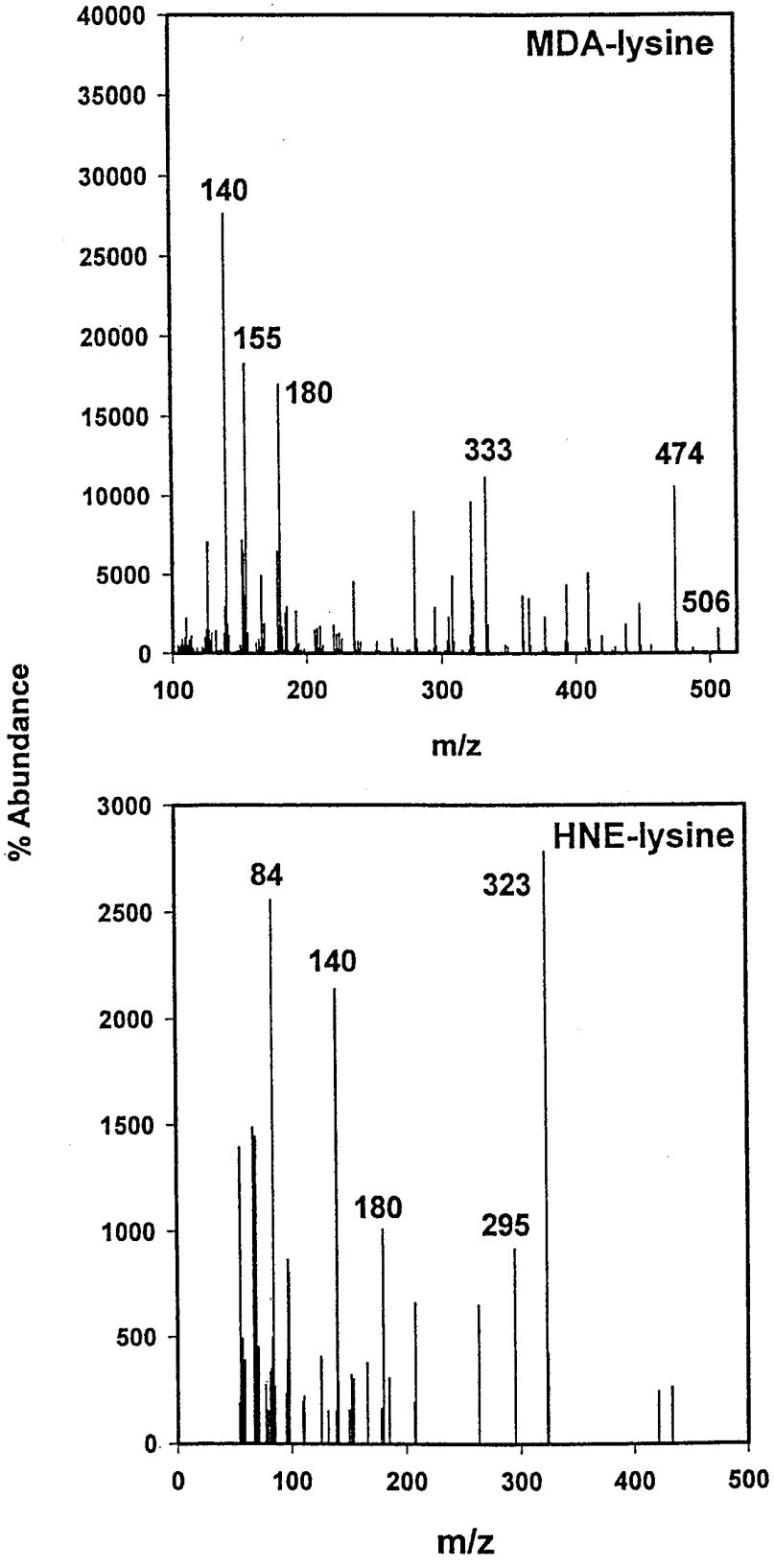
MDA-lysine
140
155
180
333
474
506
HNE-lysine
84
140
180
323
295
% Abundance
m/z
m/z

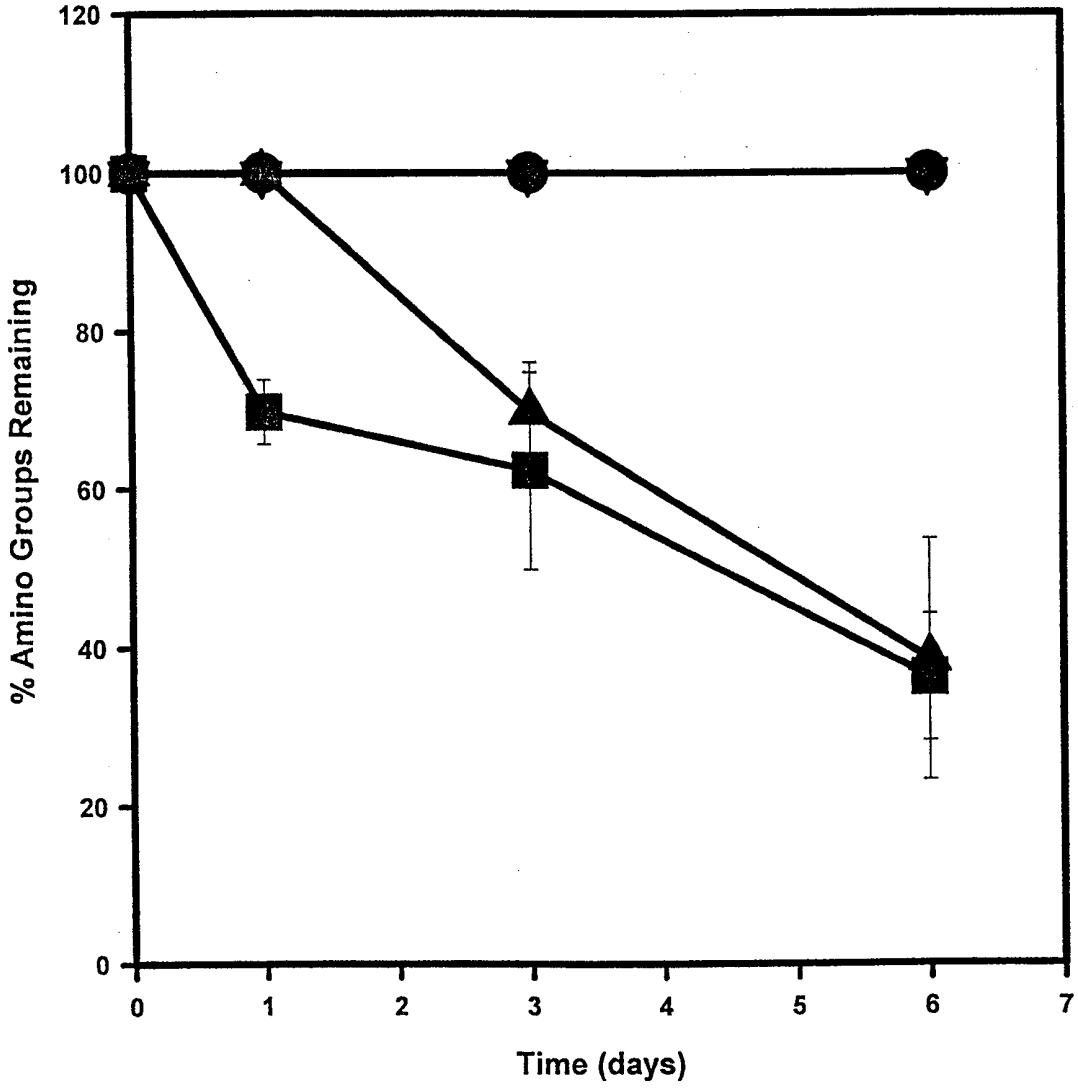
120
100
80
60
40
20
0
% Amino Groups Remaining
0
1
2
3
4
5
6
7
Time (days)

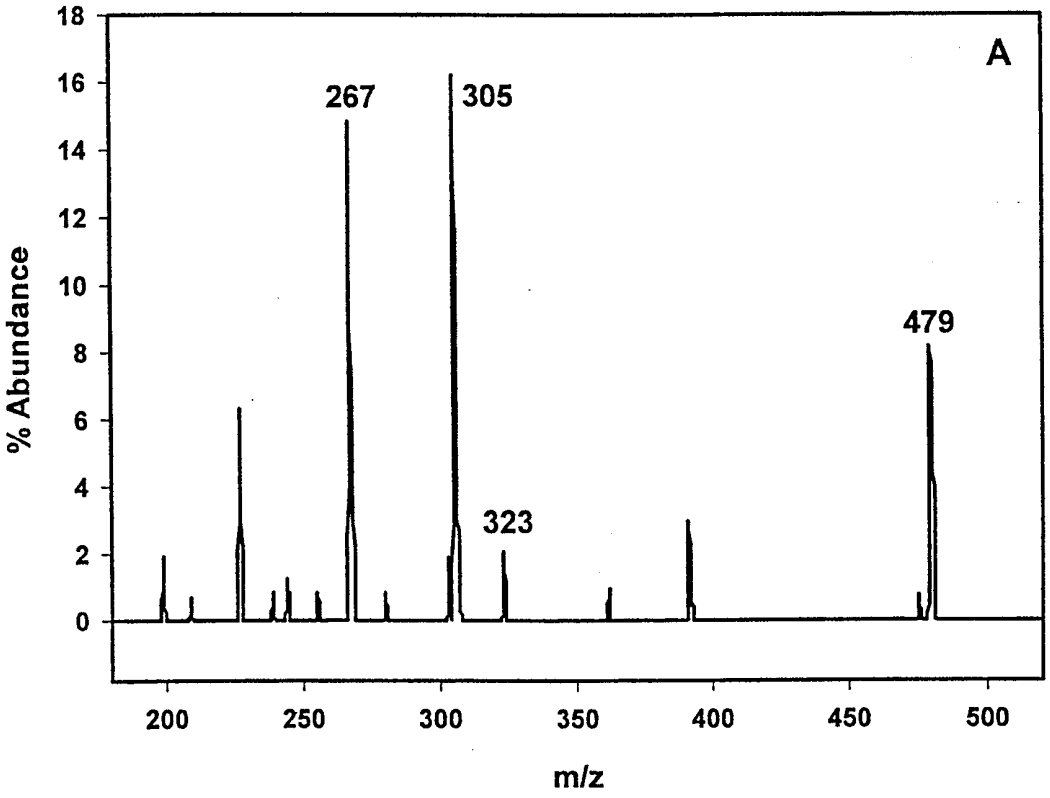
A
267
305
323
479
% Abundance
m/z
0
2
4
6
8
10
12
14
16
18
200
250
300
350
400
450
500

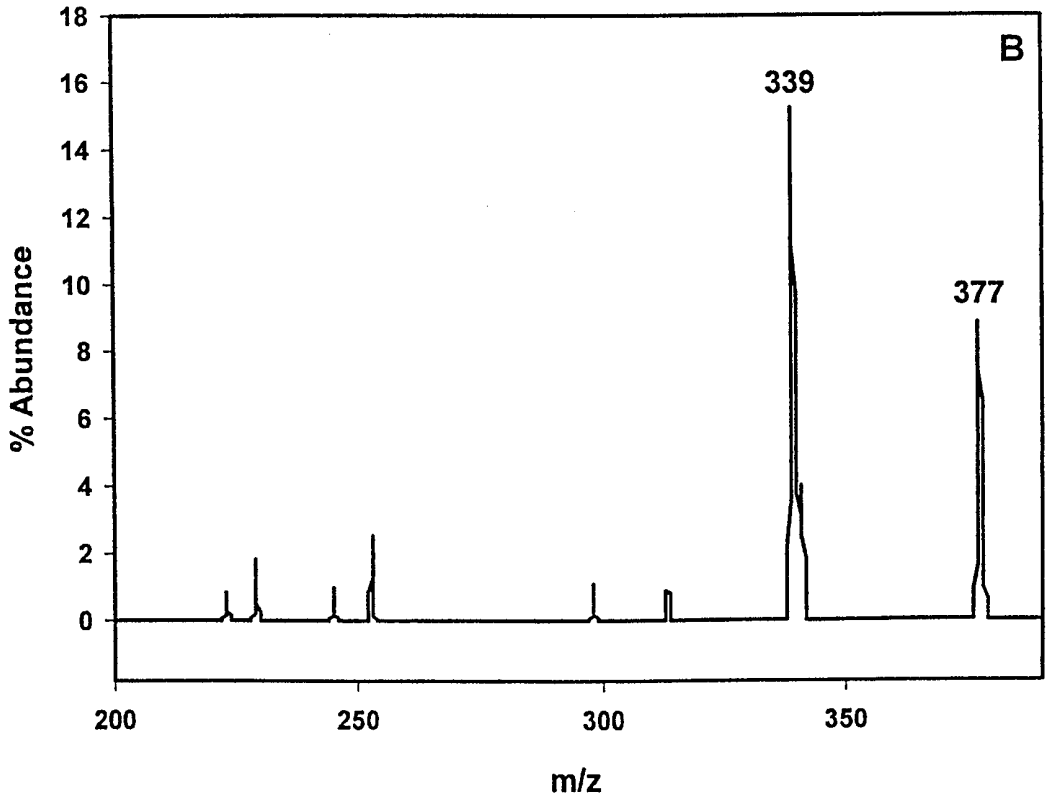
B
339
377
% Abundance
m/z
0
2
4
6
8
10
12
14
16
18
200
250
300
350

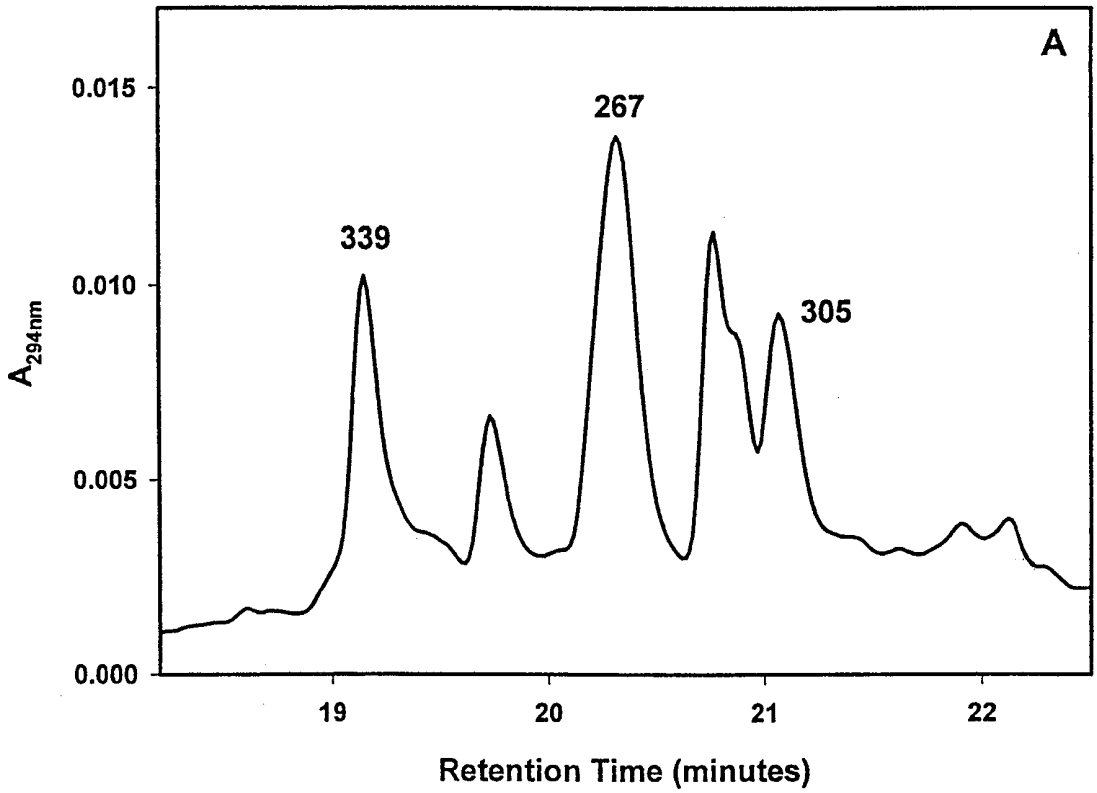
A
0.015
0.010
0.005
0.000
A_{294nm}
339
267
305
19
20
21
22
Retention Time (minutes)

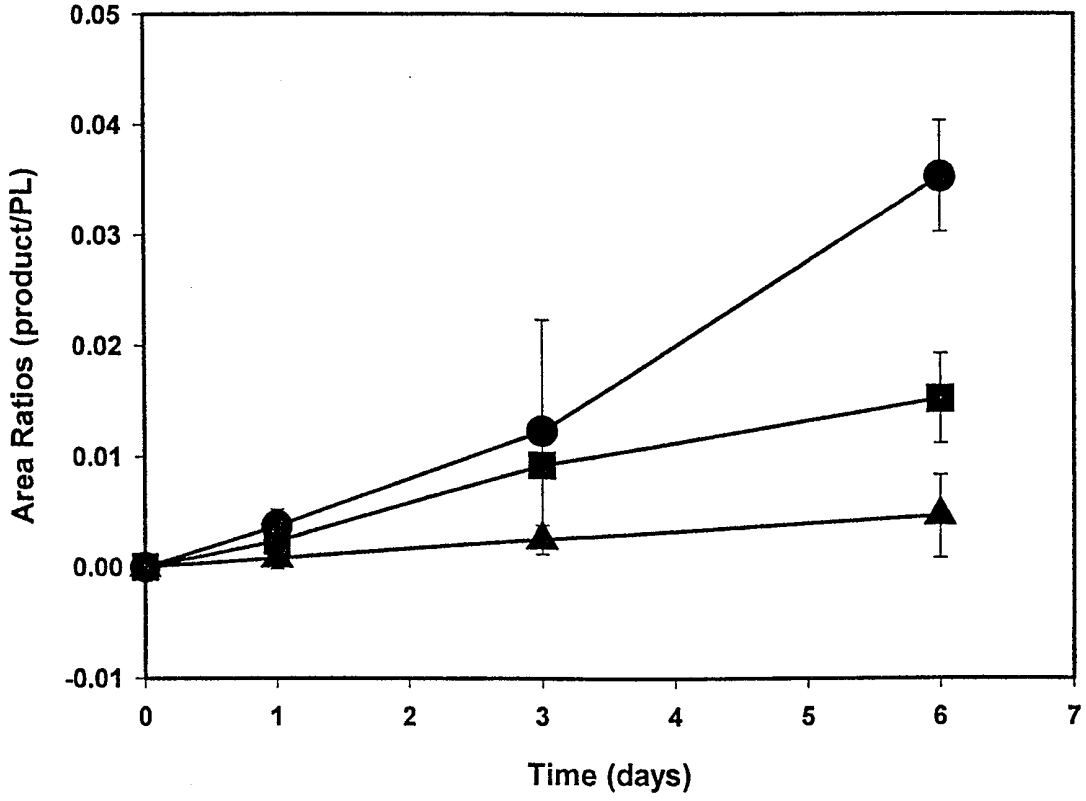
0.05
0.04
0.03
0.02
0.01
0.00
-0.01
Area Ratios (product/PL)
0
1
2
3
4
5
6
7
Time (days)

267

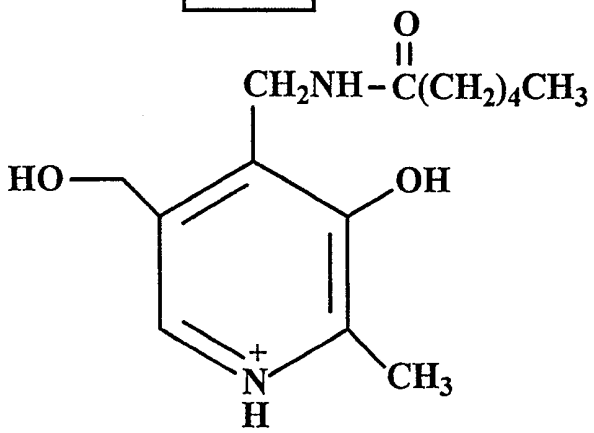

339

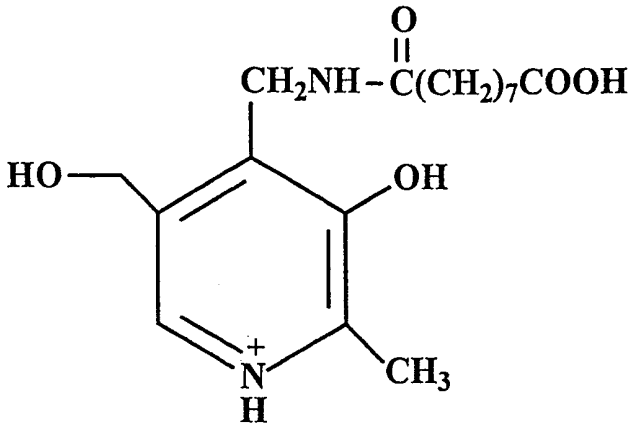

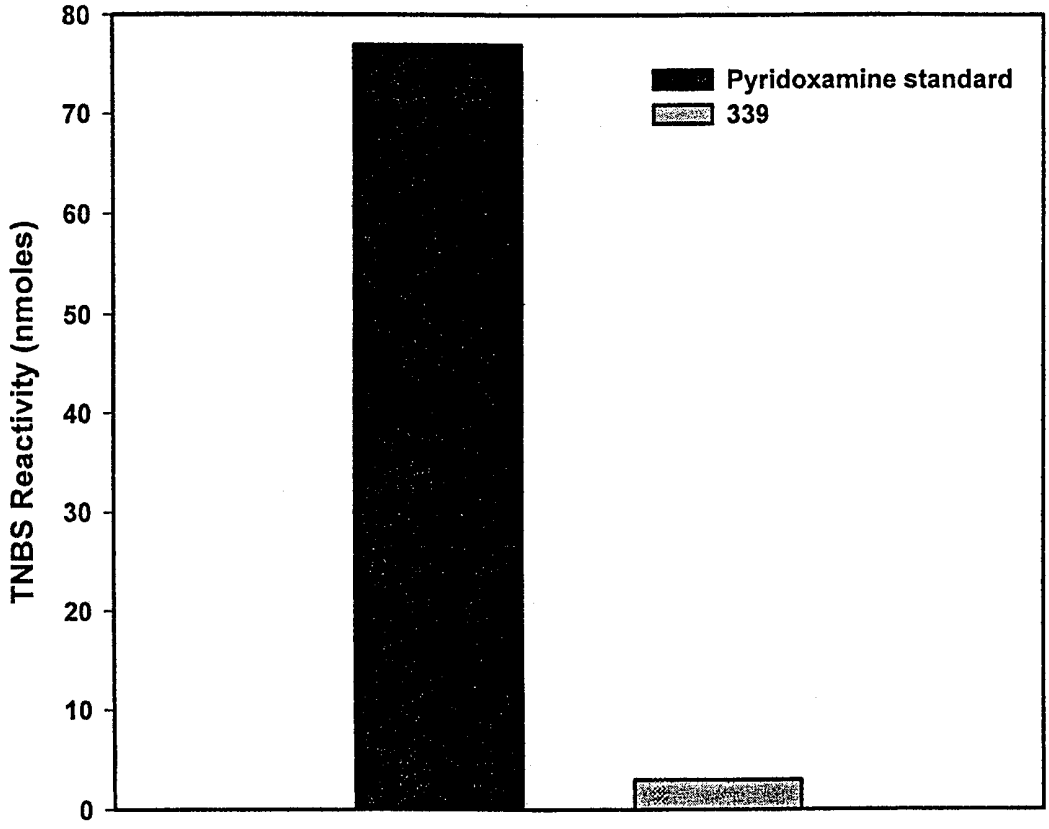
80
70
60
50
40
30
20
10
0
TNBS Reactivity (nmoles)
Pyridoxamine standard
339

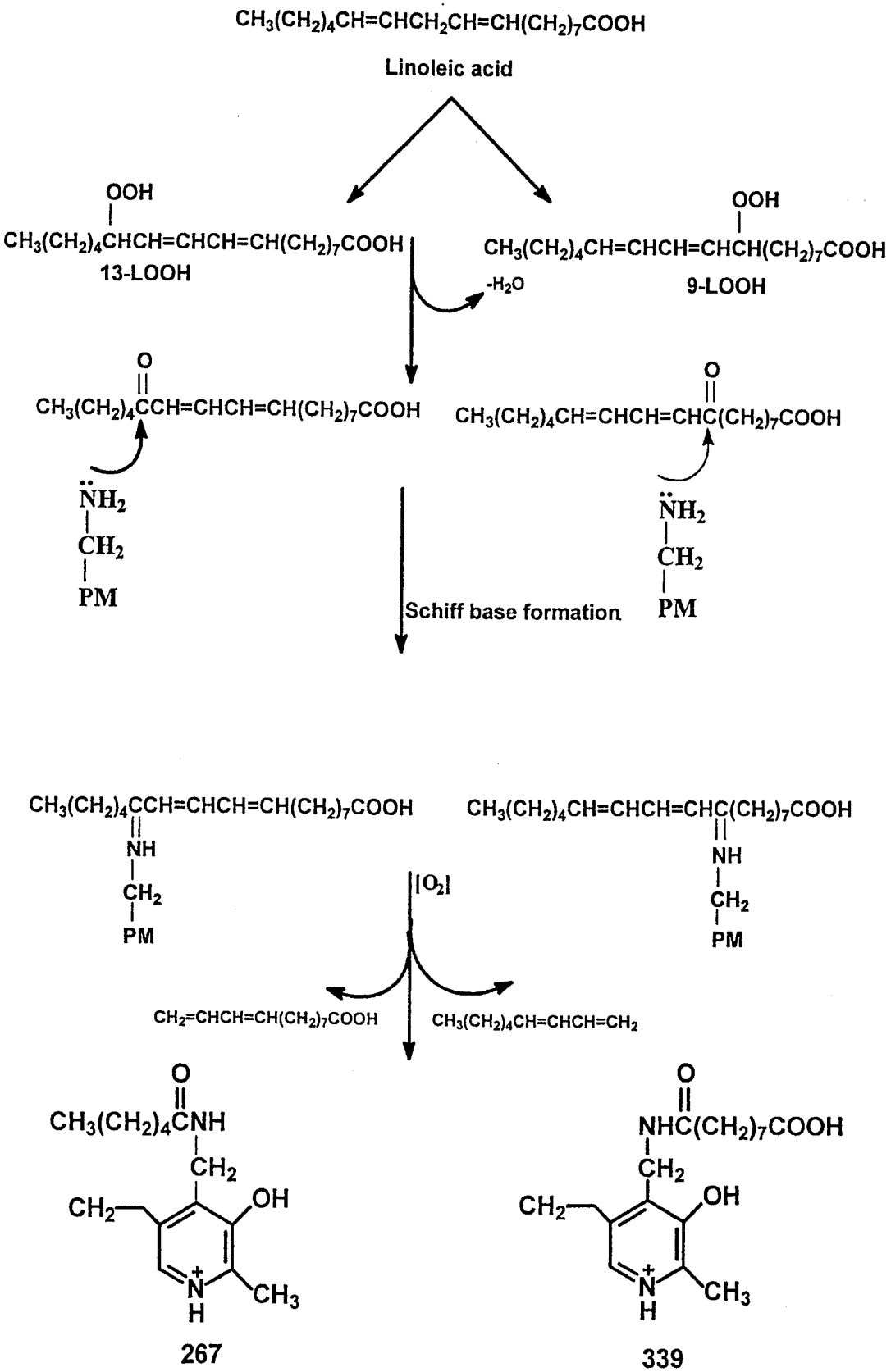
CH3(CH2)4CH=CHCH2CH=CH(CH2)7COOH
Linoleic acid
OOH
CH3(CH2)4CHCH=CHCH=CH(CH2)7COOH
13-LOOH
-H2O
OOH
CH3(CH2)4CH=CHCH=CHCH(CH2)7COOH
9-LOOH
O
CH3(CH2)4CCH=CHCH=CH(CH2)7COOH
O
CH3(CH2)4CH=CHCH=CHC(CH2)7COOH
NH2
CH2
PM
NH2
CH2
PM
Schiff base formation
CH3(CH2)4CCH=CHCH=CH(CH2)7COOH
NH
CH2
PM
CH3(CH2)4CH=CHCH=CHC(CH2)7COOH
NH
CH2
PM
[O2]
CH2=CHCH=CH(CH2)7COOH
CH3(CH2)4CH=CHCH=CH2
O
CH3(CH2)4CNH
CH2
CH2
OH
N+
H
CH3
267
O
NHC(CH2)7COOH
CH2
CH2
OH
N+
H
CH3
339

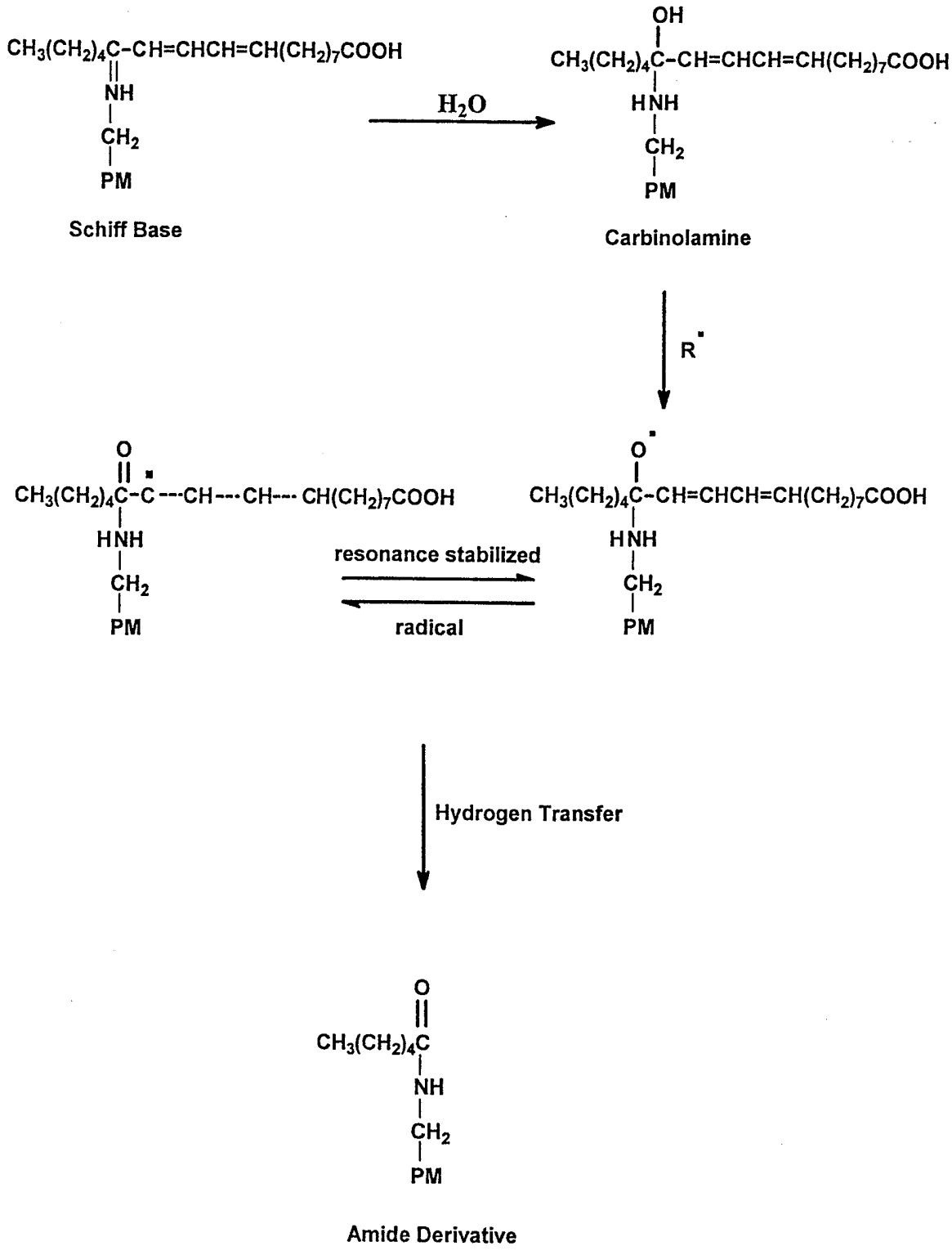
CH3(CH2)4C-CH=CHCH=CH(CH2)7COOH
NH
CH2
PM
Schiff Base
H2O
OH
CH3(CH2)4C-CH=CHCH=CH(CH2)7COOH
HNH
CH2
PM
Carbinolamine
R·
O
CH3(CH2)4C-C---CH---CH--- CH(CH2)7COOH
HNH
CH2
PM
resonance stabilized
radical
O·
CH3(CH2)4C-CH=CHCH=CH(CH2)7COOH
HNH
CH2
PM
Hydrogen Transfer
O
CH3(CH2)4C
NH
CH2
PM
Amide Derivative

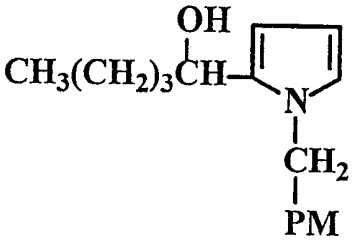
OH
CH3(CH2)3CH
N
CH2
PM

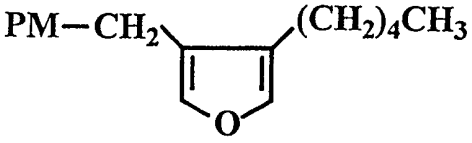
PM—CH2
(CH2)4CH3
O

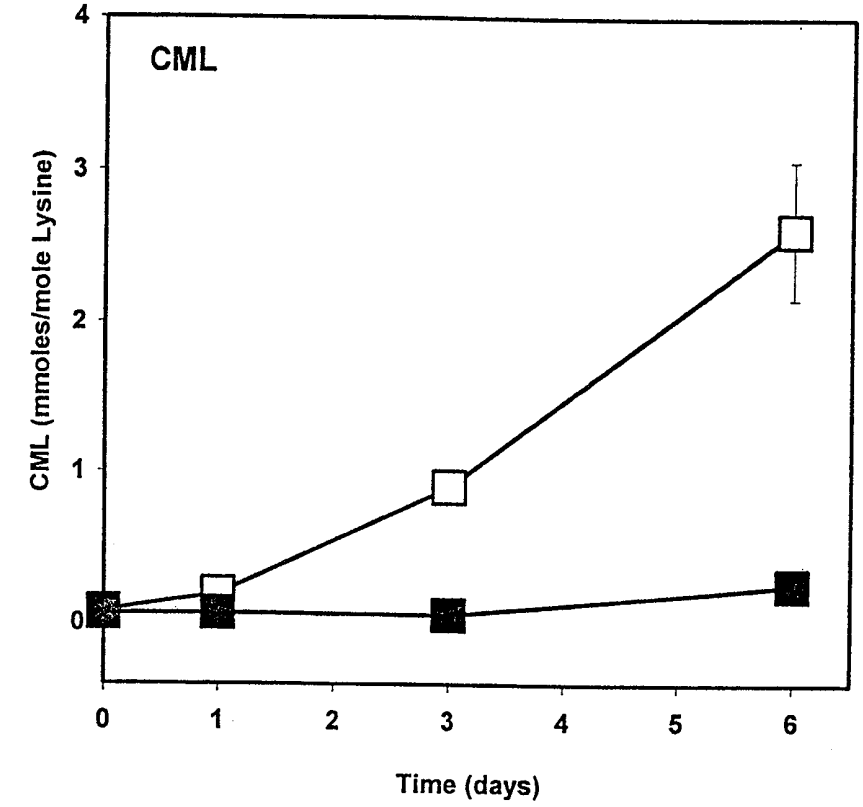
CML
CML (mmoles/mole Lysine)
4
3
2
1
0
0
1
2
3
4
5
6
Time (days)

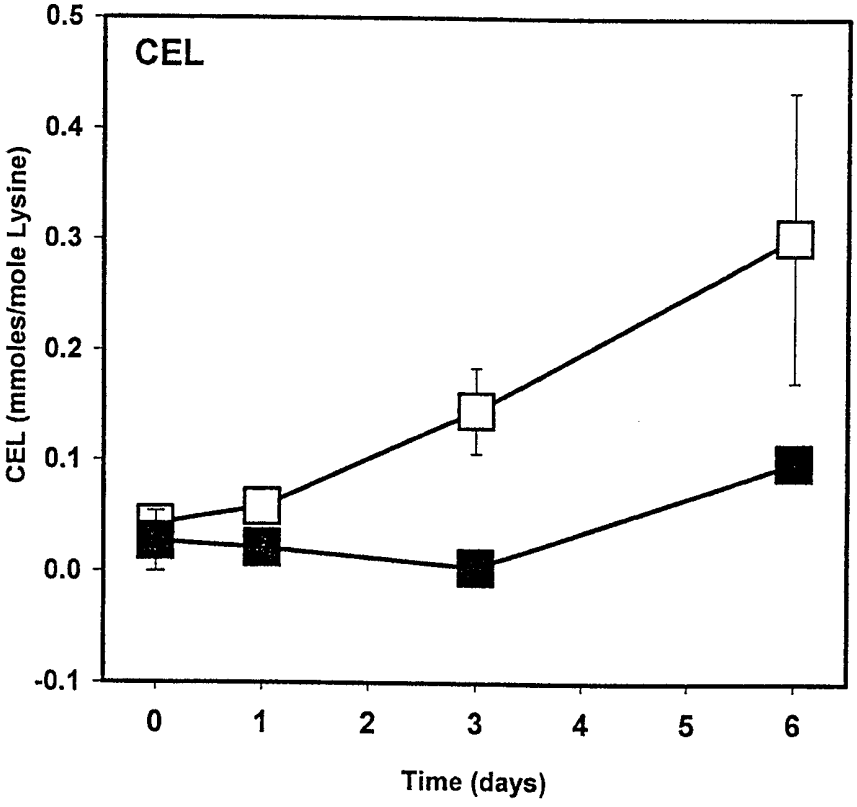
CEL
CEL (mmoles/mole Lysine)
0.5
0.4
0.3
0.2
0.1
0.0
-0.1
0
1
2
3
4
5
6
Time (days)

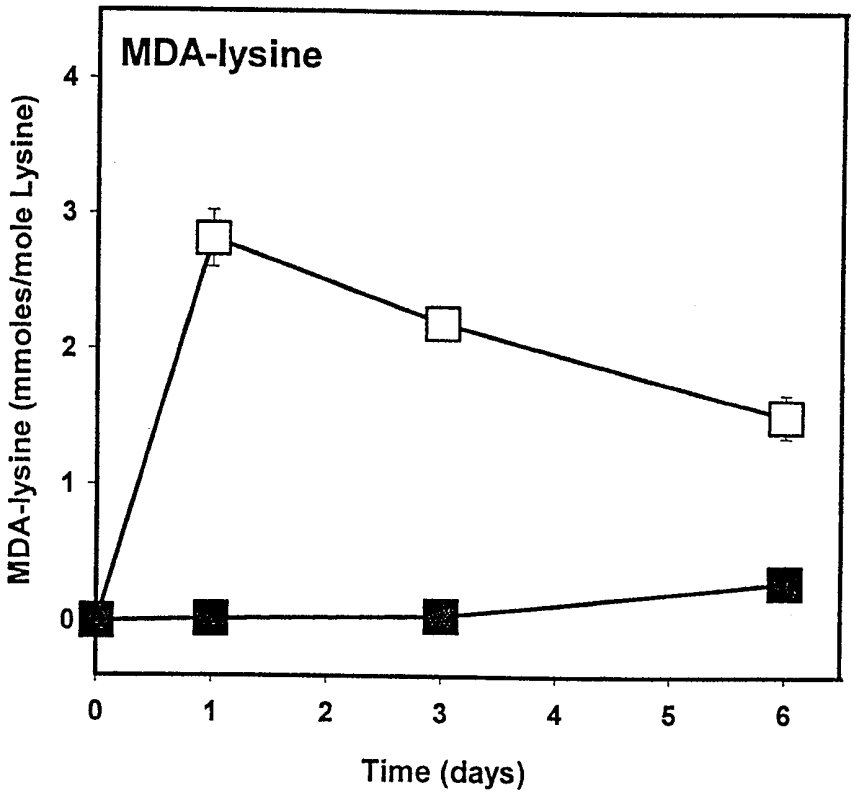
MDA-lysine
MDA-lysine (mmoles/mole Lysine)
0
1
2
3
4
0
1
2
3
4
5
6
Time (days)

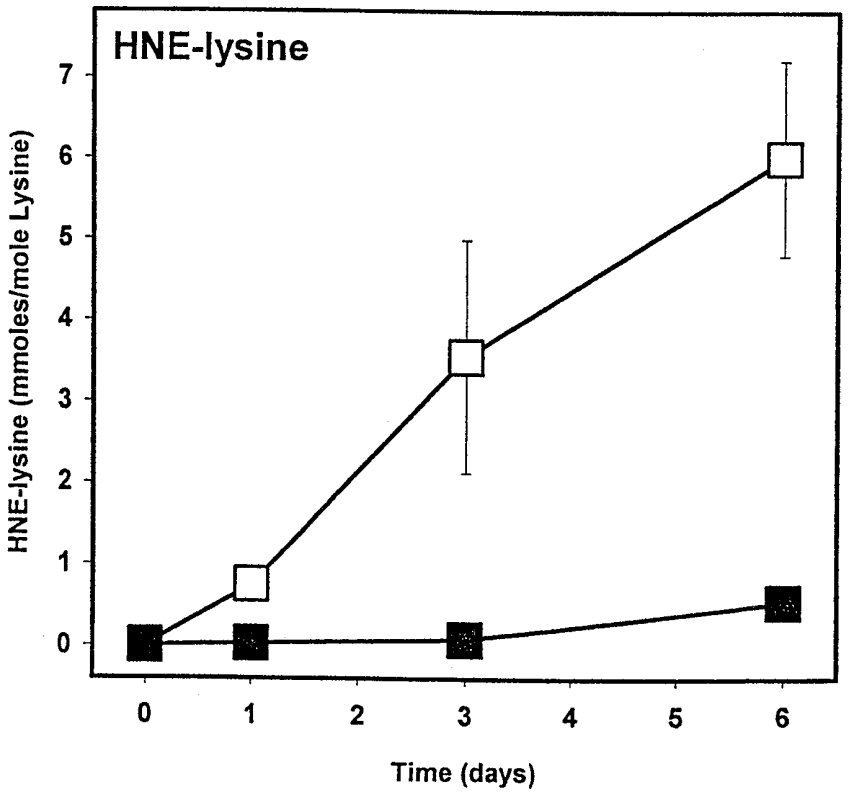
HNE-lysine
HNE-lysine (mmoles/mole Lysine)
0
1
2
3
4
5
6
7
0
1
2
3
4
5
6
Time (days)

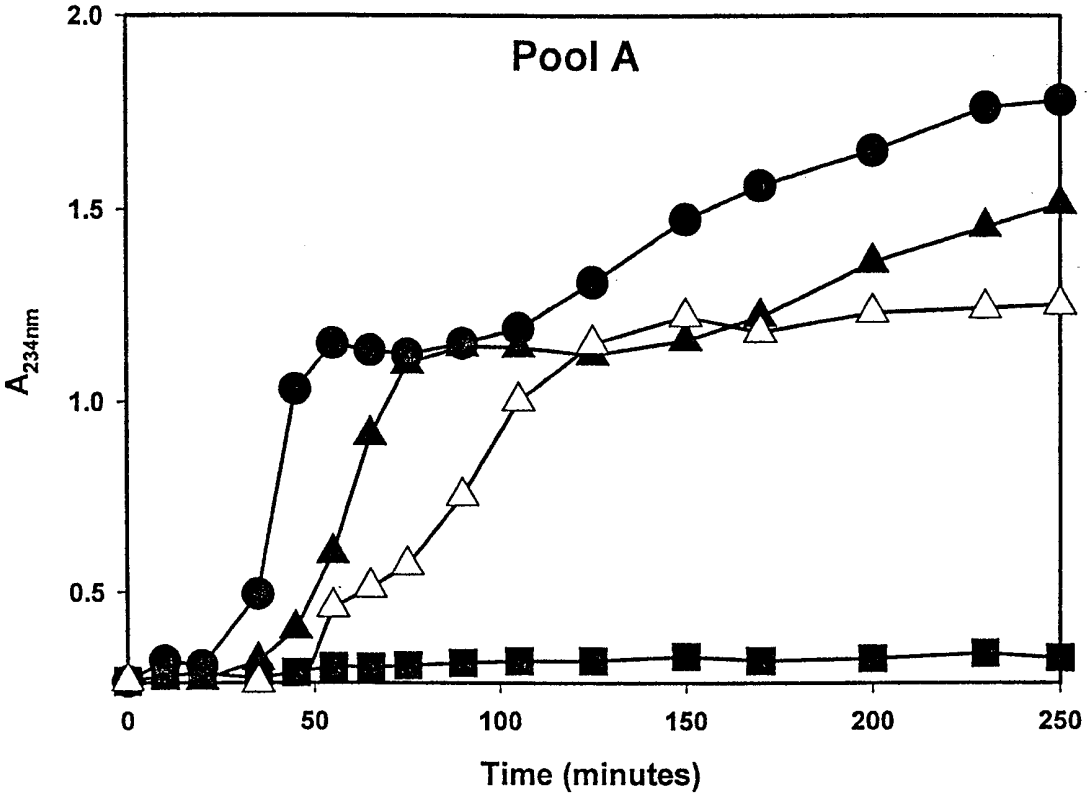
Pool A
2.0
1.5
1.0
0.5
A_{234nm}
0
50
100
150
200
250
Time (minutes)

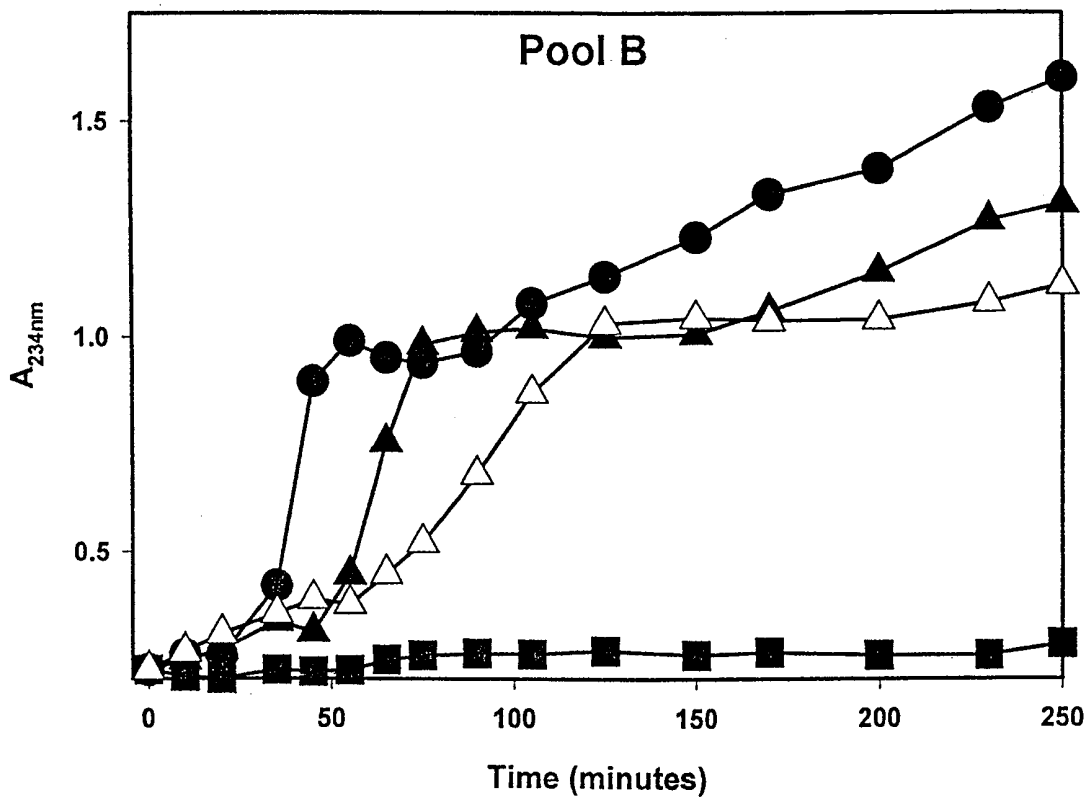
Pool B
1.5
1.0
0.5
A_{234nm}
0
50
100
150
200
250
Time (minutes)

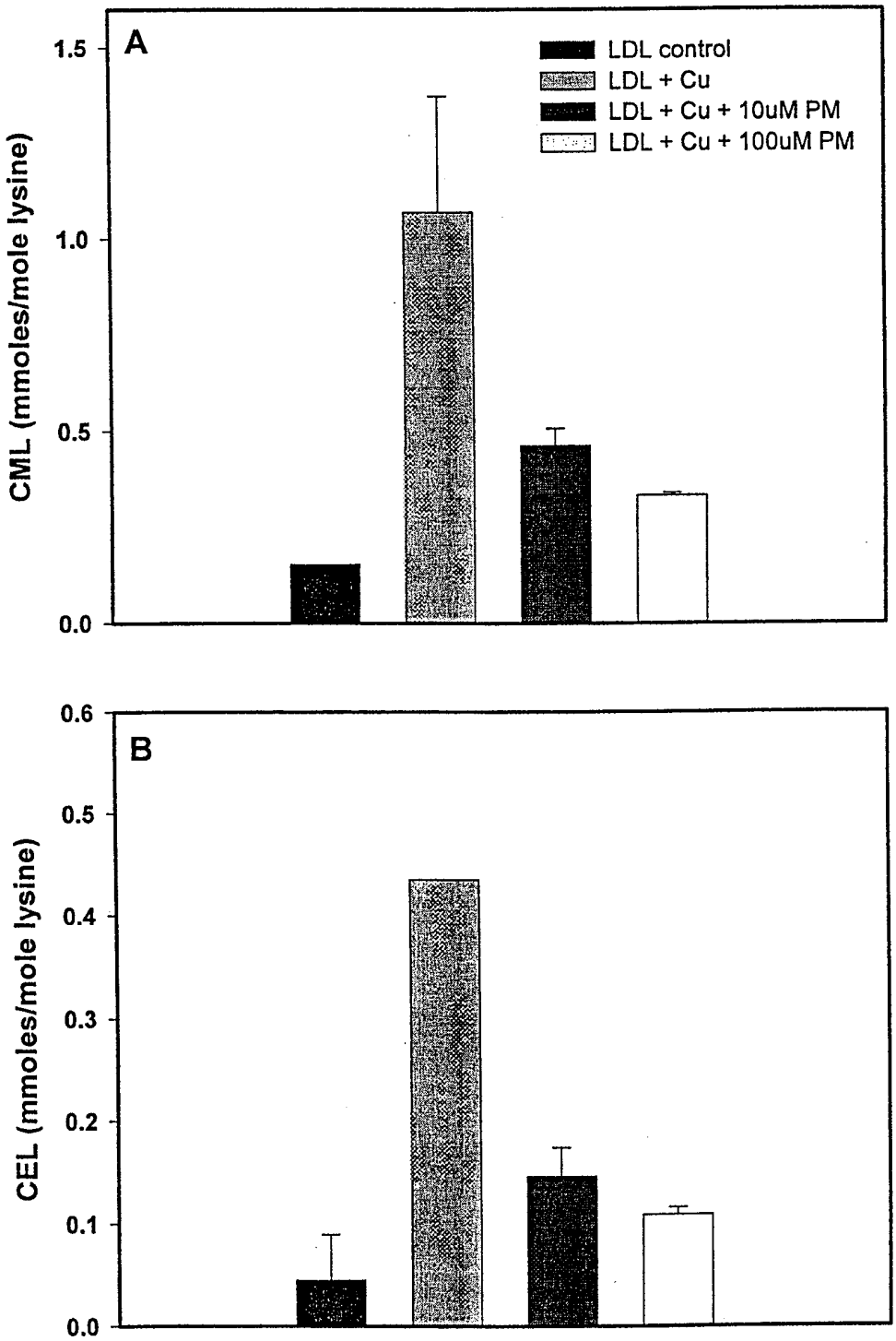
A
LDL control
LDL + Cu
LDL + Cu + 10uM PM
LDL + Cu + 100uM PM
CML (mmoles/mole lysine)
1.5
1.0
0.5
0.0
B
CEL (mmoles/mole lysine)
0.6
0.5
0.4
0.3
0.2
0.1
0.0

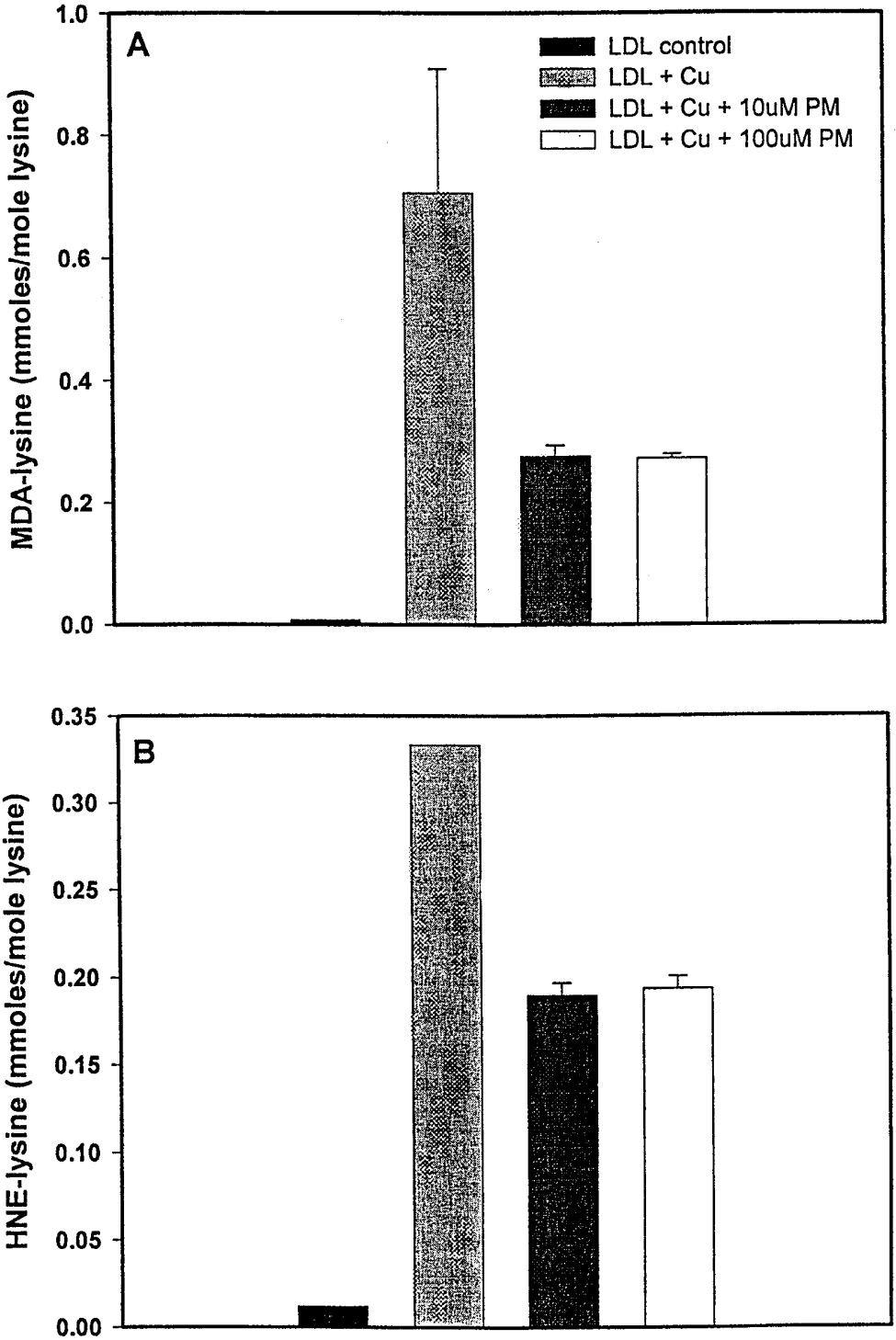
A
LDL control
LDL + Cu
LDL + Cu + 10uM PM
LDL + Cu + 100uM PM
MDA-lysine (mmoles/mole lysine)
1.0
0.8
0.6
0.4
0.2
0.0
B
HNE-lysine (mmoles/mole lysine)
0.35
0.30
0.25
0.20
0.15
0.10
0.05
0.00

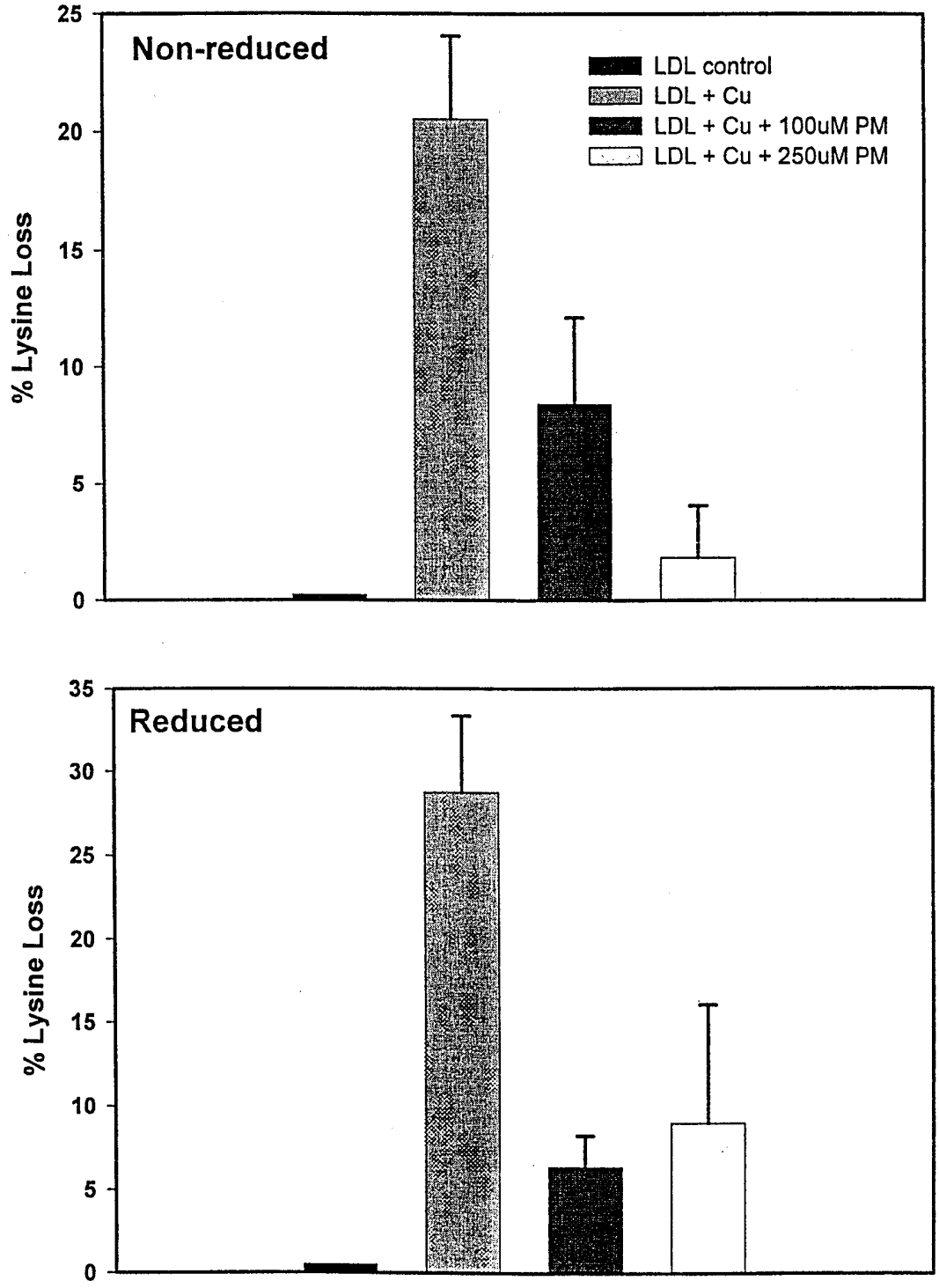
Non-reduced
LDL control
LDL + Cu
LDL + Cu + 100uM PM
LDL + Cu + 250uM PM
% Lysine Loss
0
5
10
15
20
25
Reduced
% Lysine Loss
0
5
10
15
20
25
30
35

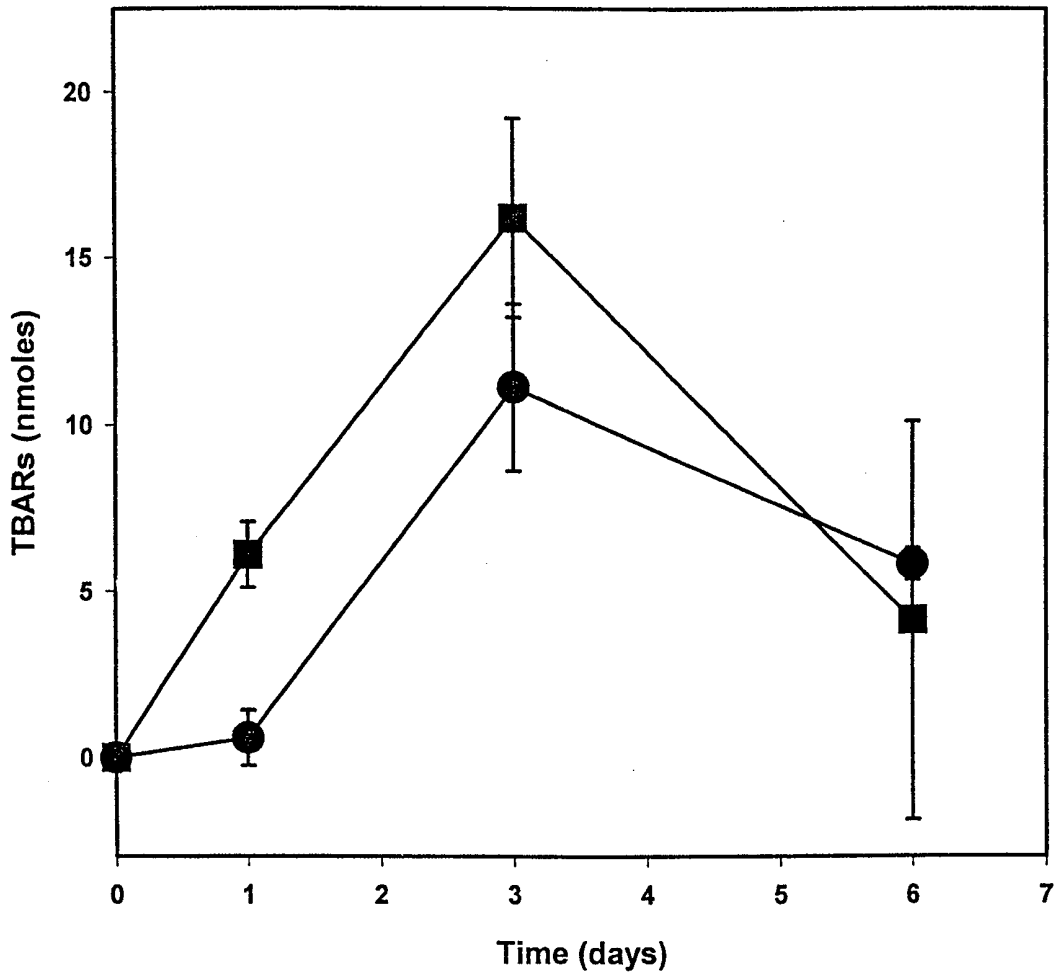
TBARs (nmoles)
20
15
10
5
0
0
1
2
3
4
5
6
7
Time (days)

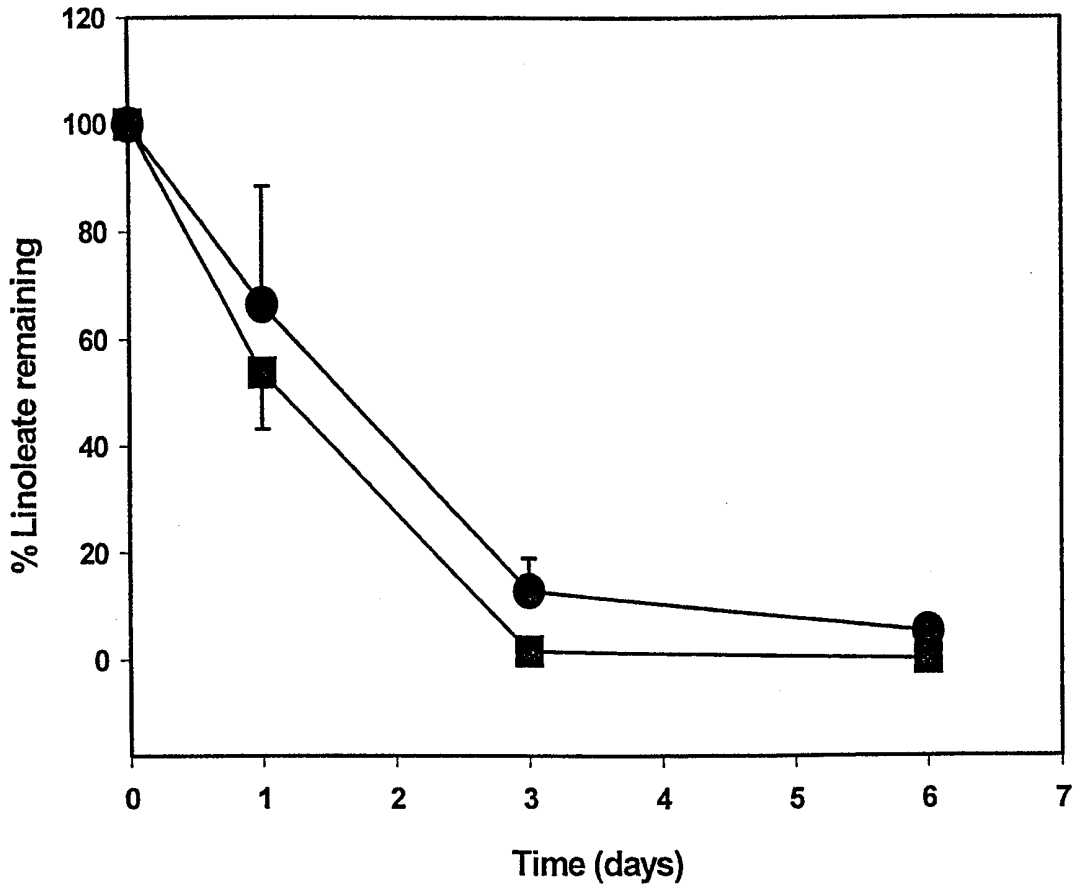
120
100
80
60
40
20
0
% Linoleate remaining
0
1
2
3
4
5
6
7
Time (days)

Initiation:

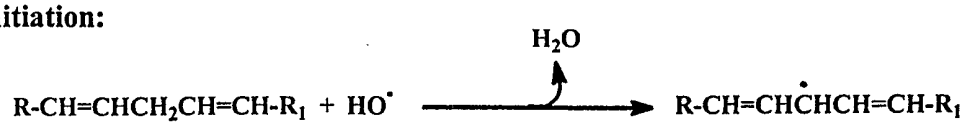

Propagation:

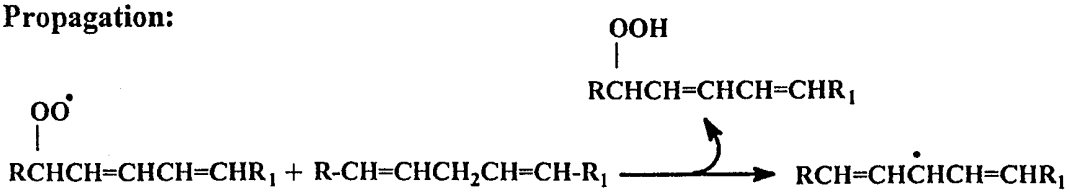

Interception by PM: